Bulletin
of
The Geological Society of America

VOLUME 70 April 1959 NUMBER 4

CONTENTS

Pages

Rock glaciers in the Alaska Range. By Clyde Wahrhaftig and Allan Cox.... 383–436

Geophysical investigation of the continental margin between Cape Henry, Virginia, and Jacksonville, Florida. By J. B. Hersey, Elizabeth T. Bunce, R. F. Wyrick, and F. T. Dietz..... 437–466

Geologic evolution of the Beartooth Mountains, Montana and Wyoming. Part 2. Fracture patterns. By Edgar Winston Spencer..... 467–508

Short Note

Pingo in the Thelon Valley, Northwest Territories: radiocarbon age and historical significance of the contained organic material. By B. G. Craig..... 509–510

Subscription $15.00 per year.
Printing Office: Mt. Royal & Guilford Aves., Baltimore 2, Md.
Communications for publications should be addressed to The Geological Society of America, Dr. H. R. Aldrich, Secretary, 419 West 117 Street, New York 27, N. Y.
Please give notice of change of address 4 weeks in advance. Claims for nonreceipt of the Bulletin of a given month must be sent to the Secretary of the Society before the end of the second succeeding month.

Second-class postage paid at Baltimore, Md.
Accepted for mailing at special rate of postage provided for in Section 1103 Act of October 3, 1917, authorized on July 8, 1918.

PAPERS IN PRESS FOR FORTHCOMING ISSUES

Overthrust Ordovician and the Nannie's Peak Intrusive, Lone Mountain, Elko County, Nevada. By Donald W. Lovejoy

Eocene Stratigraphy and Paleontology, Orocopia Mountains, Southeastern California. By John C. Crowell and Takeo Susuki

Re-evaluation of the Salt Chronology of Several Great Basin Lakes. By Wallace S. Broecker and Alan F. Walton

Optical Properties of Potassic Feldspars. By C. G. Hewlett

Chemical Composition of Argillites of the Cobalt Series (Precambrian) and the Problem of Soda-Rich Sediments. By F. J. Pettijohn and Harry Bastron

Effect of Grain Size on Strength of Mixtures of Clay, Sand, and Water. By Parker D. Trask

Geology of the Buffalo Mountain-Cherokee Mountain Area, Northeastern Tennessee. By Richard J. Ordway

Origin of the Ultramafic Complex at Union Bay, Southeastern Alaska. By John C. Ruckmick and James A. Noble

Contact Metamorphism, Crestmore, California. By C. Wayne Burnham

NEVADA.

IA. By

Broecker

BLEM OF

. Trask

EE. By

uckmick

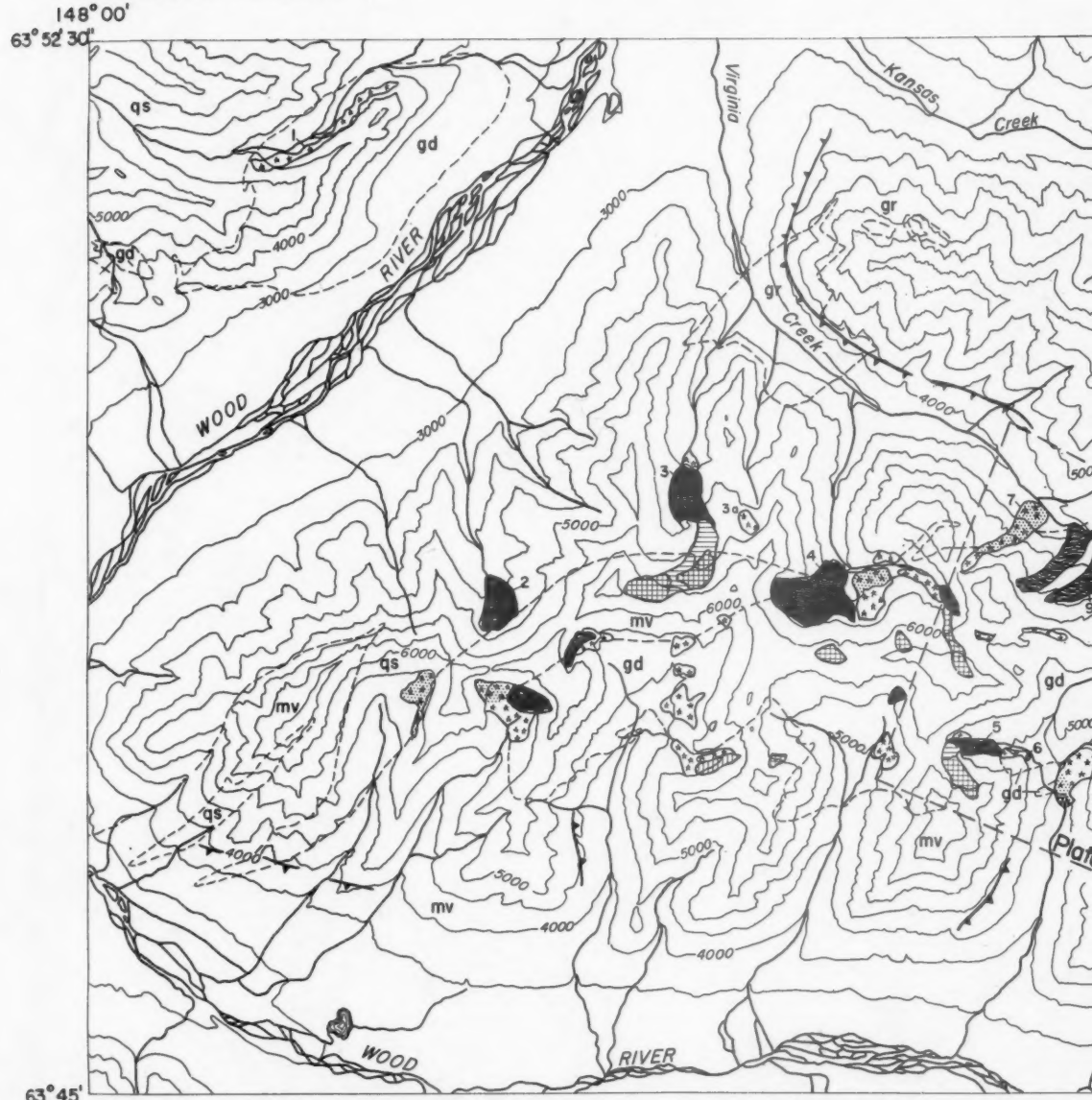

MAP OF PART OF HEALY (D-1) AND HEALY (D-2) QUA

GLACIERS AND GLACIERS, MAJOR BEDROCK T

For lo

0 1 2

CONTO
DAT

2) QUADRANGLES, ALASKA, SHOWING THE DISTRIBUT
ROCK TYPES, AND EXTENT OF LATE WISCONSIN GLAC

For location see Figure 1.

2 3 4 5 MILES

CONTOUR INTERVAL 500 FEET
DATUM IS MEAN SEA LEVEL

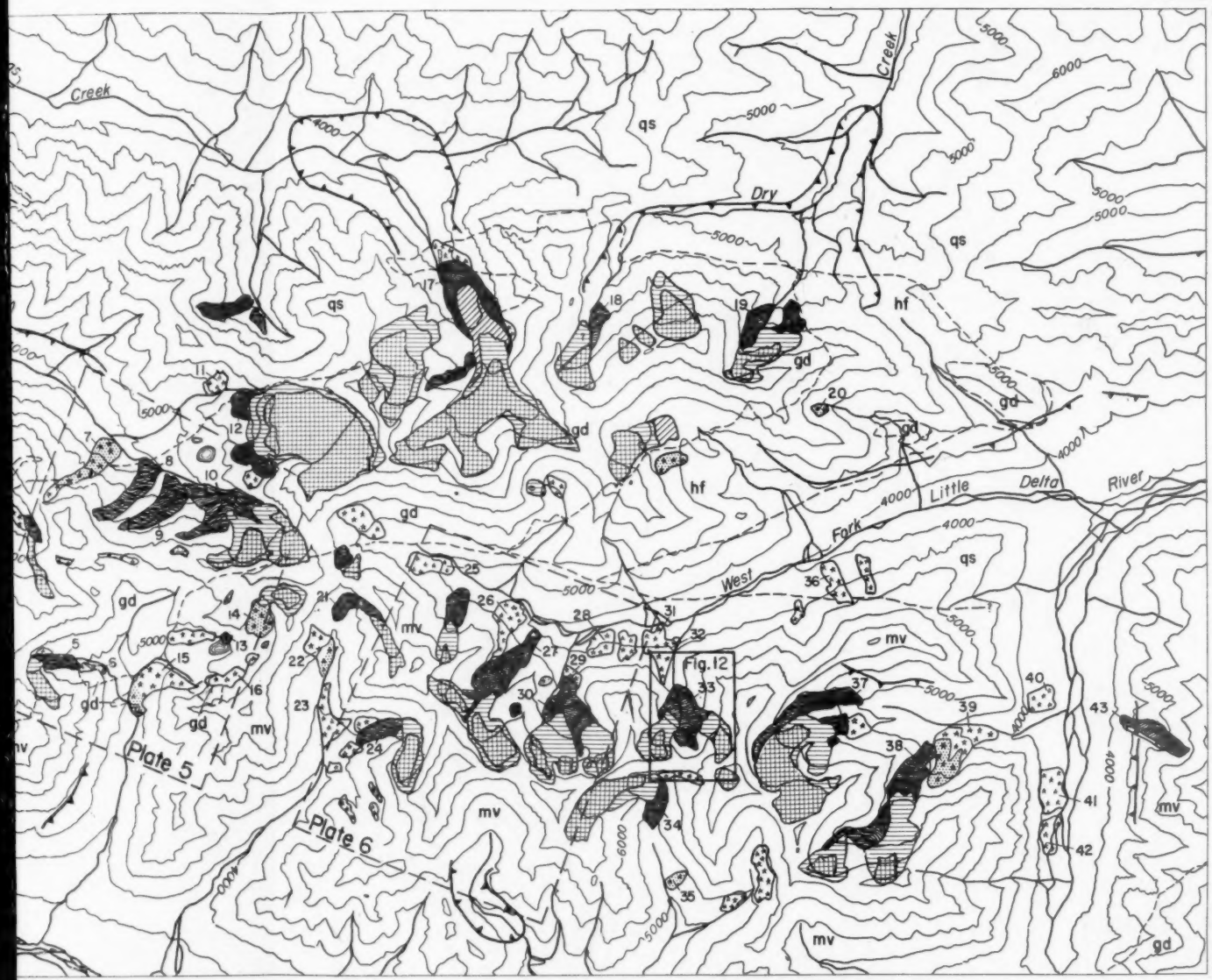

EXPLANATION

- gd — Granodiorite
- gr — Granite
- mv — Metavolcanic rocks
- qs — Quartz-sericite schist
- hf — Hornfels
- Contact between bedrock formations
- Limit of late Wisconsin Riley Creek glaciation (Culmination ca. 9000 B.C.). Hachures on the glacier side of the boundary. Shown only where morainal evidence exists
- Glacial ice in 1949-1952
- Extent of glaciers at maximum advance of ca. 1900 A.D.
- Extent of glaciers at maximum advance of ca. 1500(?) A.D. (Shown only where the earlier advance was greater than the later advance)
- Active rock glaciers
- Inactive rock glaciers
- Reactivated rock glaciers

Y (D-2) QUADRANGLES, ALASKA, SHOWING THE DISTRIBUTION OF ROCK EDROCK TYPES, AND EXTENT OF LATE WISCONSIN GLACIATION

For location see Figure 1.

1 2 3 4 5 MILES

CONTOUR INTERVAL 500 FEET
DATUM IS MEAN SEA LEVEL

BULLETIN OF THE GEOLOGICAL SOCIETY OF AMERICA
VOL. 70, PP. 383–436, 16 FIGS., 7 PLS. APRIL 1959

ROCK GLACIERS IN THE ALASKA RANGE

BY CLYDE WAHRHAFTIG AND ALLAN COX

ABSTRACT

Field studies and examination of aerial photographs of approximately 200 rock glaciers in the Healy (1:250,000) quadrangle in the central Alaska Range showed that there are three types of rock glacier in plan: lobate, in which the length is less than the width (200–3500 feet long and 300–10,000 feet wide); tongue-shaped, in which the length is greater than the width (500–5000 feet long and 200–2500 feet wide); and spatulate, tongue-shaped but with an enlargement at the front. Lobate rock glaciers line cliffs and cirque walls and probably represent an initial stage; the other two move down valley axes and represent more mature stages.

The rock glaciers are composed of coarse, blocky debris that is cemented by ice a few feet below the surface. The top quarter of the thickness is coarse rubble, below which is coarse rubble mixed with silt, sand, and fine gravel. Fronts of active (moving) rock glaciers are bare of vegetation, are generally at the angle of repose, and make a sharp angle with the upper surface. Fronts of inactive (stationary) rock glaciers are covered with lichens or other vegetation, have gentle slopes, and are rounded at the top. Active rock glaciers average 150 feet in thickness, inactive rock glaciers, 70 feet.

The upper surface of most rock glaciers is clothed with turf or lichens. Sets of parallel rounded ridges and V-shaped furrows—longitudinal near the heads of some rock glaciers and transverse, bowed downstream, on the lower parts of others—and conical pits, crevasses, and lobes mark the upper surfaces of many rock glaciers.

The upper surface of a rock glacier at the head of Clear Creek moved 2.4 feet per year between 1949 and 1957, and the front advanced 1.6 feet per year.

Heights of the upper edges of the talus aprons along the fronts of rock glaciers average 45 per cent of the heights of the fronts. Each of these observations implies that motion is not confined to thin surface layers but is distributed throughout the interiors of the rock glaciers, which in this permafrost region are probably frozen. "Viscosity" has been calculated for rock glaciers at between 10^{14} and 10^{15} poises; for glacial ice it has been estimated at between 10^{12} and 10^{14} poises. Maximum average shear stresses within active rock glaciers range from 1 to 2 bars; these values are much larger than those calculated for solifluction and creep features.

Rock glaciers occur on blocky fracturing rocks which form talus that has large interconnected voids in which ice can accumulate. They are rare on platy or schistose rocks whose talus moves rapidly by solifluction.

The rock glaciers lie in an altitudinal zone about 2000 feet thick, centered on the lower limit of existing glaciers[1]. Although the firn lines on glaciers rise 1200 feet in a distance of 25 miles northward across the Alaska Range, the lower limit of active rock glaciers rises only 800 feet. The firn line on southward-facing glaciers is 2000 feet higher than that on northward-facing glaciers, yet in any given area southward-facing rock glaciers average only 200 feet higher than northward-facing rock glaciers. Insulation by the debris cover is believed responsible for the difference in altitudinal ranges between rock glaciers and glaciers.

It is concluded that rock glaciers move as a result of the flow of interstitial ice and that they require for their formation steep cliffs, a near-glacial climate cold enough for the ground to be perennially frozen, and bedrock that is broken by frost action into coarse blocky debris with large interconnected voids. The longitudinal furrows are thought to result from the accumulation of ice-rich bands in the swales between talus cones at the head of the rock glaciers and the subsequent melting of this ice as the rock glacier moves down-valley. The transverse ridges are thought to result from shearing within the rock glacier that would occur where the thickness increases or the velocity decreases downstream.

An average of 30 feet of bedrock was removed from source areas to form the present rock glaciers, indicating an average rate of erosion of 1–3 feet per year when they are active.

[1] In this paper *glacier*, used alone, always refers to a body of ice, relatively free from debris, derived largely from compaction of snow.

The climatic history of the Alaska Range that can be deduced from the presence of active and inactive rock glaciers is: (1) deglaciation following the ice advance of 9000 B. C., leading to the thermal maximum; (2) a cold period, following the thermal maximum, during which the now-inactive rock glaciers formed; (3) a warm period; (4) a cold period, indicated by active rock glaciers, continuing to the present, with climatic amelioration during the last 50 years. The first cold period was somewhat colder and longer than the second.

CONTENTS

TEXT

	Page
Introduction	385
Acknowledgments	386
Geographic setting of the rock glaciers	387
Climate	387
General description of the rock glaciers	387
Motion of the rock glaciers	392
Introduction	392
Measurements of the motion of a rock glacier	394
Indirect indications of motion	397
Maximum shear stresses within rock glaciers	401
Deformational properties of rock glaciers and ice	403
Altitudinal distribution of active rock glaciers compared with altitudes of glaciers and firn lines	406
Composition of the rock glaciers	409
General statement	409
Debris component	409
Source	409
Structure	409
Texture of the upper surface and upper layer	412
Texture of the lower layer	412
Ice component	412
Evidence for the ice component	412
Source	413
Bedrock and the distribution of rock glaciers	414
Microrelief on the rock glaciers	415
Introduction	415
Longitudinal ridges and furrows	415
Conical pits and meandering "furrows"	418
Large pits at the heads of rock glaciers	418
Transverse ridges and furrows	418
Crevasses and landslide scarps	423
Lobes	424
Unexplained features	424
Inactive rock glaciers	424
Climatic history indicated by the rock glaciers compared with worldwide climatic events	428
Amount and rate of erosion represented by the rock glaciers	430
Rock-glacier debris as a major component of end and lateral moraines	432
Conclusions	432
Origin of rock glaciers	432
Origin of microrelief	433
Significance of rock glaciers in the geomorphology of the Alaska Range	434
References cited	434

ILLUSTRATIONS

Figure		Page
1.	Map of part of Healy (1:250,000) quadrangle, Alaska, showing areas described, existing glaciers, and extent of late Wisconsin ice	388
2.	Average monthly and annual temperatures for three stations near the Alaska Range	389
3.	Average daily maximum and minimum temperatures at McKinley Park, Alaska, showing periods of frequent daily fluctuations across the freezing point	390
4.	Photogeologic map showing rock glaciers and glaciers in the west half of the Windy area	391
5.	Photogeologic map showing rock glaciers and glaciers in the east half of the Windy area	393
6.	Sketch map showing motion of rock glacier 51 at head of Clear Creek	395
7.	Relationship between velocity of front and of upper surface of a mass that is enlarging by uniform motion of a thin surface layer over a stable interior	396
8.	Position of the top of the talus apron at the front of a rock glacier for four possible velocity distributions within the rock glacier	400
9.	Relationships of stress and strain for flow in a semi-infinite sheet on an inclined plane	401
10.	Scatter diagram of the thickness at the front of several rock glaciers plotted as a function of the cosecant of the slope of the upper surface near the front	404
11.	Altitudes of average glaciers and rock glaciers in two areas in the Alaska Range	408
12.	Map of a typical tongue-shaped rock glacier (rock glacier 33) with longitudinal ridges and furrows	416
13.	Map of rock glaciers with transverse ridges and furrows	419
14.	Profiles of rock glaciers with transverse ridges compared with profiles of rock glaciers without transverse ridges	421

Figure Page
15. Map and profiles of inactive and reactivated rock glaciers at the head of Moody Creek ... 425
16. Scatter diagram showing areas of rock glaciers plotted against size of their source areas ... 431

Plate Facing page
1. Map of part of Healy (D-1) and Healy (D-2) quadrangles, Alaska, showing distribution of rock glaciers and glaciers, major bedrock types, and extent of late Wisconsin glaciation ... 383
2. Panoramas of fronts of rock glaciers ... 398
3. Views of fronts and heads of rock glaciers ... 399

Following page
4. Microrelief on rock glaciers ...
5. Stereotriptych of an area at the head of Virginia Creek showing rock glaciers and glaciers ... 422
6. Stereotriptych of an area on the West Fork of the Little Delta River showing active and inactive rock glaciers ...
7. Vertical stereoscopic views of rock glaciers and glacially overridden rock glaciers ...

TABLES

Table Page
1. Measurements on the Clear Creek rock glacier ... 396
2. Data on height of talus at front of rock glaciers ... 399
3. Height of front, thickness, and slope angle of selected rock glaciers ... 402
4. Thicknesses and slope angles of creep and solifluction deposits on Seward Peninsula ... 403
5. Apparent viscosities of rock glaciers ... 406
6. Summary of altitude data on rock glaciers and glaciers in the Alaska Range ... 410
7. Contigency tables for the occurrence of rock glaciers in Healy D-2, D-3, D-4, and D-5 quadrangles ... 415
8. Contingency tables showing correlation between causes for downstream thickening of rock glaciers and presence of transverse ridges and furrows ... 422
9. Heights of active and inactive rock glaciers in the Wood River area ... 426

Introduction

In the half century since rock glaciers were recognized as distinct geomorphic forms they have been found in high mountains throughout the world. They were first discussed by Spencer (1900), who briefly described rock glaciers in the San Juan Mountains. Cross and Howe (1905) described the rock glaciers of the San Juan Mountains as rock streams. Rock glaciers in the Alps were described by Chaix (1919) and Cailleux (1947, p. 323–325) as *coulées de blocs*, by De Martonne (1920, p. 261–264) as *glaciers rocheux*, by Salomon (1929, p. 1–31) as *Blockglätscher*, by Domaradzki (1951) as *Blockströme*, and by Nangeroni (1954, p. 35) as *colate di pietre*. The term rock glacier was first used by Capps (1910) in his classic study of the rock glaciers in the Wrangell Mountains of Alaska.

Rock glaciers have also been reported from the Rocky Mountains by Patton (1910, p. 666); Hole (1912, p. 722); Emmons, Irving, and Loughlin (1927, p. 20); Atwood and Mather (1932, p. 162); Parsons (1939); R. L. Ives (1940); Richmond (1952); and Griffiths (1958) and from the Sierra Nevada of California (Kesseli, 1941), from the Carpathians (De Martonne, 1920), from the Altai (Matveev, 1938), and from the Andes (Lliboutry, 1953). The descriptions and photographs of these high-montane morphologic forms leave no doubt that similar phenomena have been described in widely separated places. However, theories of their origin are almost as numerous as the reports of their occurrence—evidence of the challenge that these interesting forms have presented to the imaginations of geomorphologists.[2]

Cross and Howe (1905, p. 25) advanced two theories for the two types of rock glaciers they described, considering the common streamlike ones to be unusual types of moraines. Howe (1909, p. 52) later advanced the theory that rock glaciers are the debris of violent landslides and cited the Elm landslide as a modern example.

Capps (1910, p. 364) suggested an entirely different mechanism, one anticipated by Spencer (1900). Capps thought that water from melting ice and snow and from rains sinks into the detritus at the lower edge of glaciers and freezes, gradually filling the interstices with ice up to the level where melting equals freezing. Incipient glacial movement is started by melting of the ice followed by refreezing and expansion of the water. Tyrrell

[2] After this paper went to press, we learned of two important recent discussions of rock glaciers, one by Roots (1954, p. 24–29), and the other by Flint and Denny (1958, p. 131–133).

(1910, p. 552–553) elaborated on Capps' theory, suggesting that the water which is later frozen comes from springs, and that the characteristic concentric ridges develop by the downward sliding of the rocks after melting of the ice in the spring.

Chaix (1923, p. 32) regarded rock glaciers as terminal moraines composed of blocky debris, the interstices of which are filled with mud and clay. He believed that the debris, lubricated by the interstitial mud, moves down-slope, the movement aided by freezing and thawing. Kesseli (1941, p. 226–227) similarly thought that rock glaciers are of glacial origin and that many of the smaller surface features result from deformation under the weight of overriding ice. He thought that the present motion of rock glaciers is due to a remaining core of ice or to a tendency to creep after deposition, but that creep could not have originated the rock glaciers. Richmond (1952) believed rock glaciers to be residual from small glacial advances, retaining the essential configuration and structure of the ice.

The present investigation deals with about 200 rock glaciers in the Alaska Range, all within the Healy 1:250,000 quadrangle, part of which is shown on Figure 1. Two groups of rock glaciers form the major subject of this study. One consists of about 70 rock glaciers on an eastward-trending ridge between the headwaters of the Wood River and the West Fork of the Little Delta River, called the Wood River area (Pl. 1). The other group consists of about 120 rock glaciers on the main ridge of the Alaska Range on either side of the Alaska Railroad (Figs. 4 and 5). The area shown on these figures is called the Windy area. About 10 rock glaciers occurring elsewhere, mainly at the head of Moody and Cody Creeks, near the Wood River glacier, and in the basin of Sheep Creek (Fig. 1) were examined in the field and form a part of this study.

This study is a by-product of a general geologic investigation of the central part of the Alaska Range. The rock glaciers were studied in the field from 1950 to 1957. Commonly only a few hours could be devoted to the field examination of any one rock glacier. Most of the rock glaciers studied on the ground were photographed, many in color. The photographs have proved useful for measurement of height and slope of the fronts of the rock glaciers, the microrelief, average size of fragments on the surface, and for determination of the type and extent of vegetation.

Field observations were supplemented by study of aerial photographs, at scales of 1:20,000 and 1:40,000, taken by the U. S. Air Force in 1946, 1949, and 1952. Outlines of the rock glaciers and patterns of microrelief that could be recognized on the aerial photographs were plotted on enlargements (to a scale of 1:12,000) of the multiplex manuscript of the Healy D-1, D-2, D-3, B-4, B-5, C-4, and C-5 quadrangles. All measurements of altitude, length, breadth, and area, and many of slope and height, were made on these maps at the scale of 1:12,000, contour interval 100 feet.

About three-fourths of the Wood River area rock glaciers were examined on the ground; the others were studied in aerial photographs. In the Windy area, only the rock glacier at the head of Clear Creek was studied on the ground; the others were studied by examination of aerial photographs. Field measurements of the movement of the rock glacier at the head of Clear Creek, the only one whose motion was measured, were made over a period of 8 years. A preliminary study of the rock glaciers (Wahrhaftig, 1954) was based largely on interpretation of aerial photographs. In the course of subsequent field work no major active rock glacier was discovered which had not been identified previously from photographs, and every feature previously identified from photographs as a rock glacier proved to be one when examined in the field.

Acknowledgments

The marked boulders on the Clear Creek rock glacier were established and surveyed in 1949 by the late Dr. Robert E. Fellows and the senior author. J. H. Birman assisted in resurveying the boulders in 1952, and R. E. Zartman assisted in 1957.

The manuscript has been reviewed by J. D. Sears, Troy L. Péwé, David M. Hopkins, Arthur H. Lachenbruch, John T. Hack, and Dorothy H. Radbruch of the U. S. Geological Survey, and by Prof. Robert P. Sharp of the California Institute of Technology. We thank all these for calling attention to errors of analysis and obscurities in the prose. George O. Gates, Chief of the Alaskan Geology Branch of the Geological Survey, under whose direction the work was done, encouraged and supported the investigation. Mrs. Pauline Waggoner prepared the text.

Geographic Setting of the Rock Glaciers

The rock glaciers lie in the central part of the Alaska Range (Fig. 1). This part of the Alaska Range consists of several eastward-trending ridges with crests 5000 to 8000 feet in altitude, separated by broad valleys 2000 to 3500 feet in altitude. The northern limit of the Pleistocene cordilleran ice sheet lies in the northern part of the Alaska Range, crossing the middle of the area shown in Figure 1 (Wahrhaftig, 1958, Pl. 2).

Most of the rock glaciers lie in cirques that were occupied by glaciers during the late Wisconsin ice advance. A few, however, are in places that give no sign of having been areas of accumulation of late Wisconsin ice. The maximum extent of the late Wisconsin ice in the Alaska Range is indicated on Figure 1. Carbon 14 determination on a peat sample from a terminal moraine complex near McKinley Park station has dated this advance at slightly before 8600 B.C. (Suess, 1954, p. 471, No. W-49; Wahrhaftig, 1958, p. 46). Glacial ice still covers most of the high mountains of the Alaska Range.

Climate

The Alaska Range separates two parts of Alaska with markedly different climates; climate varies abruptly, and no generalization can be made about the range as a whole. South of the range, summers are fairly cool and cloudy with heavy rainfall; winters are moderately rigorous with heavy snowfall. North of the range, summers are warm and sunny, and rainfall is fairly light; winters are severe with light snowfall. Available temperature data for the central Alaska Range are summarized in the records for McKinley Park Headquarters, Nenana, and Summit (Figs. 2 and 3). Summit lies on the Alaska Railroad south of the Alaska Range at an altitude of 2350 feet, a few hundred feet below timber line (Fig. 1). It represents the cool moist conditions of the south flank of the range. McKinley Park is in the center of the range at an altitude of 2000 feet, about 1000 feet below timber line. It is typical of the intermontane valleys of the central part of the range. Nenana lies in the Tanana flats about 26 miles north of the north edge of the range, at an altitude of 350 feet. Its records are typical of the interior region of Alaska north of the Alaska Range.

The climate of the high mountains where the rock glaciers occur probably differs considerably from that of the stations in the lowlands. The mountains are cooler in summer and probably warmer in winter; the number of cloudy days and amount of precipitation, particularly snowfall, are greater. Cliffs and outcrops in the high mountains probably remain damp during most of the cool, moist summers, particularly during the periods of diurnal freeze and thaw, and much moisture is available for freezing in cracks and joints in the rocks. Temperatures may drop to freezing in any month during the summer. All these factors contribute to greater frost riving in the high mountains of the Alaska Range than in the valleys where the weather stations are located. Weather records indicate that even in the lowlands and valley bottoms, the average annual temperature is at least 5° F. below freezing. Hence the Alaska Range is probably a region of permafrost.

General Description of the Rock Glaciers

The rock glaciers in the Alaska Range are tongue-shaped or lobate masses of poorly sorted angular debris lying at the base of cliffs or talus slopes (Fig. 3 of Pl. 2) or extending down-valley from the lower end of small glaciers (Fig. 1 of Pl. 3). They are a few hundred feet to a little more than a mile long, in the direction of flow, and a few hundred feet to nearly 2 miles wide, measured perpendicular to the direction of flow. The *front* of a rock glacier is a steep face, 30–400 feet high, that marks its down-valley end (Fig. 1 of Pl. 2, Fig. 3 of Pl. 3). The front slopes at an angle that is near the angle of repose for rockfall debris. The upper surface slopes gently toward the front of the rock glacier; it is generally marked by conspicuous microrelief. The sides of many rock glaciers rise as steep embankments, and for this reason the rock glaciers have the general appearance of very viscous lava flows. These steep embankments diminish in height upvalley and are commonly absent from the upper part of the rock glacier. The *head* is taken to be the place where the rock glacier merges with the talus cones that feed it, where it merges with a glacier, or where it ends abruptly at a pit formerly occupied by a glacier.

The rock glaciers in the Alaska Range are grouped into three types on the basis of their map pattern, the ratio of their length to breadth, and their topographic position. These types are intergradational and are believed to

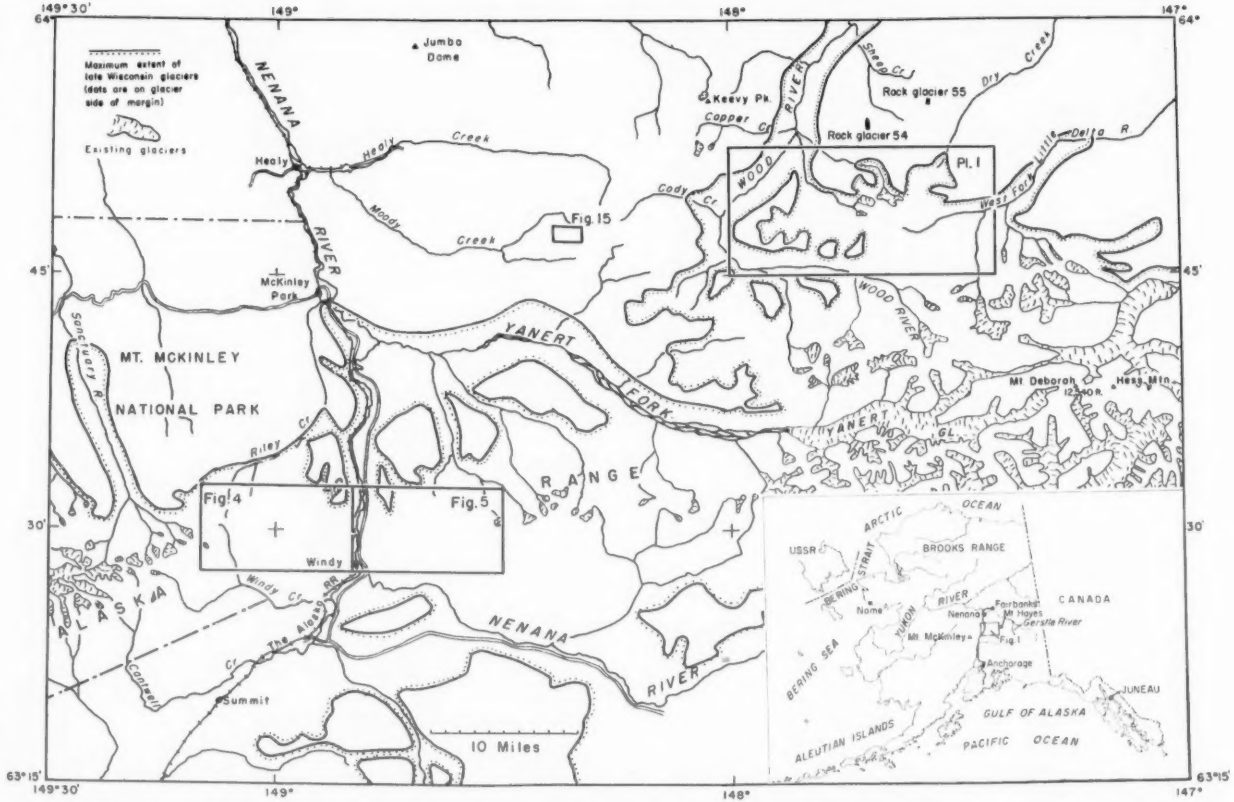

FIGURE 1.—MAP OF PART OF HEALY (1:250,000) QUADRANGLE, ALASKA, SHOWING AREAS DESCRIBED, EXISTING GLACIERS, AND EXTENT OF LATE WISCONSIN ICE

Inset map of Alaska shows location of area.

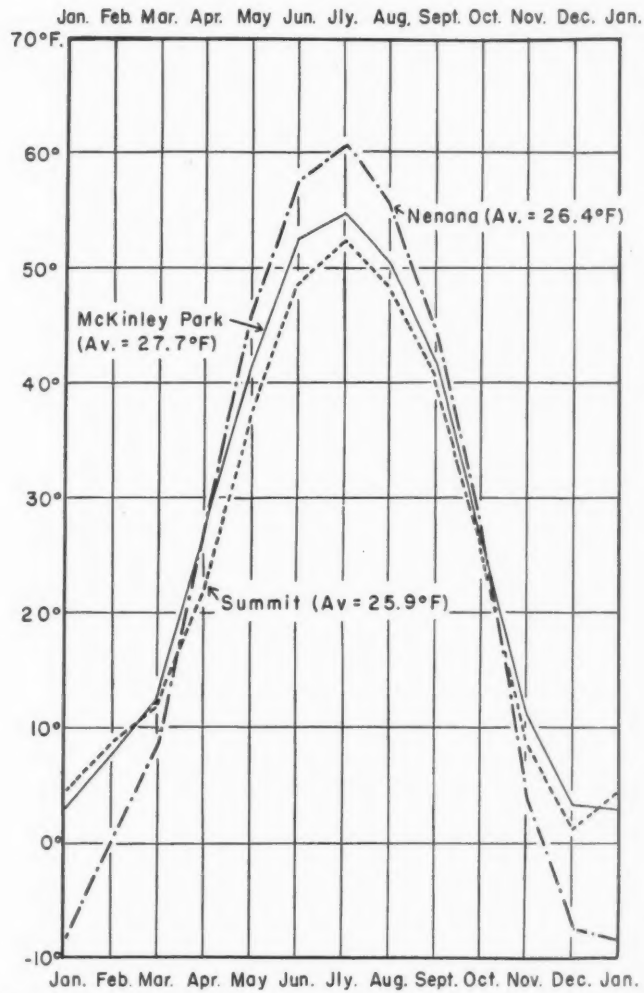

FIGURE 2.—AVERAGE MONTHLY AND ANNUAL TEMPERATURES FOR THREE STATIONS NEAR THE ALASKA RANGE

form a developmental sequence. *Lobate* rock glaciers (Fig. 3 of Pl. 2) are single or multiple lobes extending out from the bases of talus cones or talus aprons. They are characteristically as broad as or broader than they are long. Their lengths range from 200 to 3500 feet, and their widths range from 300 to 10,000 feet. More than 85 per cent of the lobate rock glaciers are less than 1500 feet long. *Tongue-shaped* rock glaciers (Figs. 1 and 2 of Pl. 3, Fig. 1 of Pl. 4) are commonly longer than they are broad. They are 500–5000 feet long and 200–2500 feet wide. More than 85 per cent of the tongue-shaped rock glaciers are more than 1500 feet long. They completely fill cirques, where they may be fed from three sides, or they extend down-valley from cirques. Tongue-shaped rock glaciers form when lobate rock glaciers from the sides and back of a cirque meet in the center, and the resulting mass flows down-valley from the cirque. *Spatulate* rock glaciers (Pl. 5, left; Fig. 13, lower) widen

FIGURE 1.—MAP OF PART OF HEALY (1:250,000) QUADRANGLE, ALASKA, SHOWING AREAS DESCRIBED, EXISTING GLACIERS, AND EXTENT OF LATE WISCONSIN ICE
Inset map of Alaska shows location of area.

abruptly near their fronts. In map pattern they are fairly long streams, similar to tongue-shaped rock glaciers, but with rounded bulges at the lower ends. The spatulate rock glaciers range in length from 3000 to 5500 feet. A spatulate rock glacier forms when a tongue-shaped rock glacier enters a trunk valley from a hanging valley or a side valley, and the debris, formerly confined in the narrow valley, can spread laterally.

Domaradzki (1951, p. 208), who first distinguished between lobate and tongue-shaped rock glaciers, has suggested that tongue-shaped rock glaciers are characteristic of sedimentary terrains, and that lobate rock glaciers are derived from crystalline rocks. However contingency tables of the rock glaciers of the Windy area, part of which is underlain by the sedimentary Cantwell formation and another part of which is underlain by greenstone and granitic rocks, failed to show any correlation between rock glacier type and rock type. The sequence of events necessary for the formation of tongue-shaped rock glaciers and spatulate rock glaciers and the probable outcome of continued growth of an apron of lobate rock glaciers lining a cirque wall indicate that these three types are probably stages in the growth of rock glaciers.

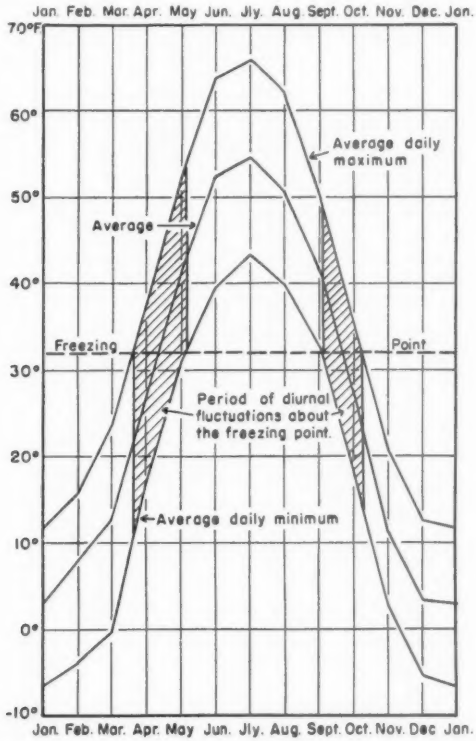

FIGURE 3.—AVERAGE DAILY MAXIMUM AND MINIMUM TEMPERATURES AT MCKINLEY PARK, ALASKA, SHOWING PERIODS OF FREQUENT DAILY FLUCTUATIONS ACROSS THE FREEZING POINT

Rock glaciers appear to consist of a thin upper layer of rubble of coarse blocks similar to the surface of the talus at the head of the rock glacier and a much thicker lower layer of debris in which similar coarse blocks are mixed with much sandy and silty material (Figs. 1 and 2 of Pl. 2). The debris is derived by rockfall from cliffs at the head of the rock glacier or at the head of the glacier upvalley from the rock glacier. Interstitial ice cements the blocks in many of the rock glaciers.

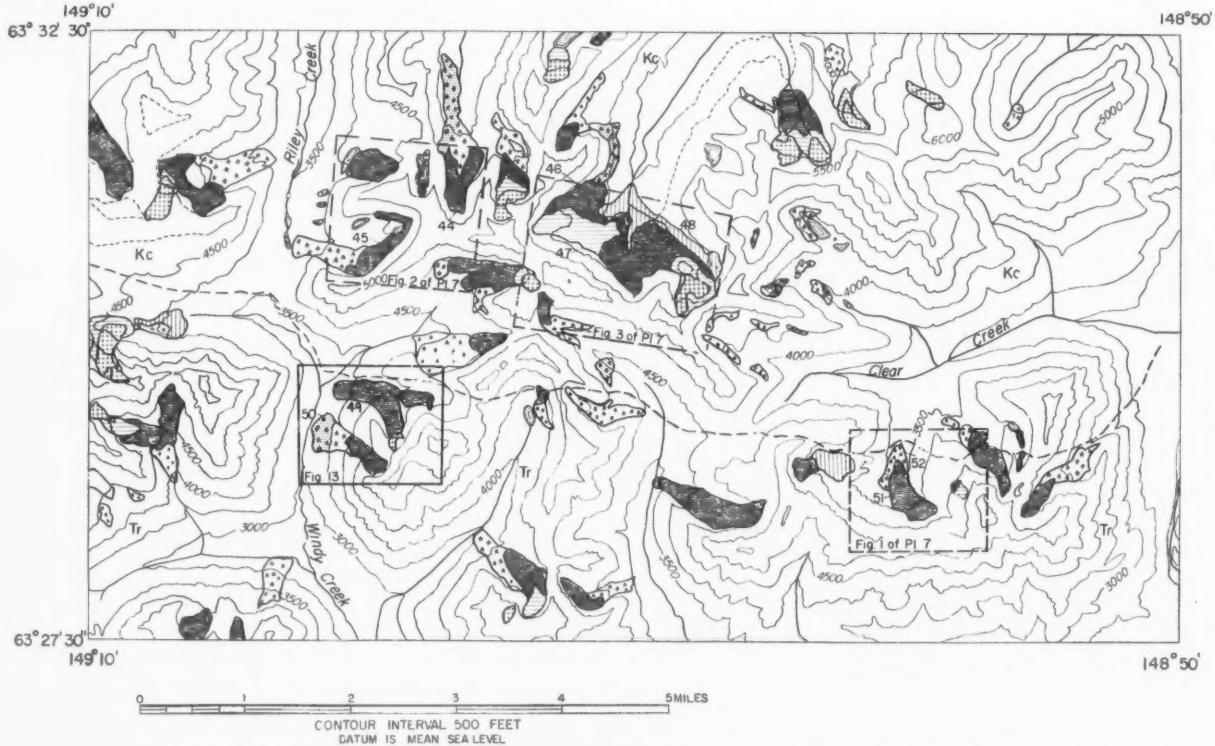
149°10'
63° 32' 30"
148°50'
63°27'30"
Kc
Tr
Piley Creek
Clear Creek
Windy Creek
Fig. 2 of Pl. 7
Fig. 3 of Pl. 7
Fig. 1 of Pl. 7
Fig. 13
EXPLANATION
Kc
Cantwell formation of Cretaceous age
Tr
Igneous and sedimentary rocks ranging in age from Devonian to Triassic
Contact between bedrock formations
Glacial ice in 1949-1952
Extent of glaciers at maximum advance of ca. 1900 A.D.
Active rock glaciers
Inactive rock glaciers
Maximum extent of glaciers during period when inactive rock glaciers were formed (Shown only where evidence of the earlier glacial advance was not covered by rock glaciers or by the later glacial advance.)
Reactivated rock glaciers
0 1 2 3 4 5 MILES
CONTOUR INTERVAL 500 FEET
DATUM IS MEAN SEA LEVEL

FIGURE 4.—PHOTOGEOLOGIC MAP SHOWING ROCK GLACIERS AND GLACIERS IN THE WEST HALF OF THE WINDY AREA
Base from parts of U. S. Geological Survey topographic maps of Healy B-4, Healy B-5, Healy C-4, and Healy C-5 quadrangles. For location see Figure 1.

Most rock glaciers are connected by smooth, graded talus slopes to the base of their source cliffs; about a third, however, are separated from their source cliffs either by a small glacier a few hundred feet to a mile and a half long, or by a large pit, steep-walled at the lower end, that marks the position of a small recently melted glacier.

All rock glaciers included in this study are above timber line. They are, however, in the zone of low tundralike vegetation, and nearly all are clothed, at least on their upper surfaces, either with nearly continuous turf consisting of low herbaceous plants and grasses or with a continuous mantle of black lichens.

The fronts of nearly half the rock glaciers are completely devoid of vegetation; these fronts are as steep as the angle of repose of their constituent debris, and the angle at the top of each front, where it joins the upper surface, is sharp. These rock glaciers give the impression that they are now moving forward over the valley floor and are called active rock glaciers. The fronts of most other rock glaciers are covered with turf or lichens. These fronts have much gentler slopes, and their tops are gently rounded and merge gradually with the upper surfaces. (Compare Fig. 3 of Pl. 3 and Fig. 3 of Pl. 2.) The fronts of these rock glaciers average about half the height of the fronts of the active rock glaciers. Rock glaciers in this second group are thought to be stable and are called inactive rock glaciers. A few rock glaciers appear to have been inactive for a period after they were formed but seem to have begun to move again recently. These are called reactivated rock glaciers. Plate 1 and Figures 4 and 5, where these three types of rock glaciers are distinguished, show that the active rock glaciers lie upvalley from the inactive rock glaciers or are in higher cirques.

Among the most striking characteristics of rock glaciers is the curious microrelief on their upper surfaces. It is this microrelief that gives the impression of slow plastic or viscous flow, remarked by earlier investigators. Not all rock glaciers show these features, but most do. Especially prominent are the sets of parallel rounded ridges separated by V-shaped furrows, 3–20 feet high and 30–150 feet apart. Some are parallel to the direction of flow of rock glaciers; these are called *longitudinal ridges and furrows* (Figs. 1 and 2 of Pl. 4). Others are approximately perpendicular to the direction of flow and are generally bowed down-valley; these are called *transverse ridges and furrows* (Figs. 4 and 5 of Pl. 4). Another type of microrelief that seems peculiar to rock glaciers appears in the air photographs as a tightly meandering incised trench extending lengthwise down the rock glacier, commonly near the middle. These are called *meandering furrows*. On the ground these were found to be irregular lines of coalescing conical pits, each pit 20–100 feet across. Less common forms of microrelief are crevasses, lobes, and irregular mounds and ridges. The crevasses are straight sharp furrows at large angles to the sets of transverse ridges and furrows.

Motion of the Rock Glaciers

Introduction

Each of the theories of the origin of the rock glaciers which have been proposed implies some particular type of motion now or in the past. Much has been learned about the movement of rock glaciers since many of these theories were presented. Direct measurements by surveying methods over considerable intervals of time have established that rock glaciers are now moving. In addition, certain morphological characteristics indicate, indirectly, the way rock glaciers move. All but a very few of the theories of origin can be rejected in the light of present knowledge of the movement of rock glaciers.

Several of the theories indicate that, except perhaps for a certain amount of settling, rock glaciers should not now be moving. The hypothesis that rock glaciers originate as sudden landslides (Howe, 1909), as accumulations of talus that have slid far out onto the floors of cirques over snow banks (Cross and Howe, 1905), or as unusual or subglacial moraines (Cross and Howe, 1905; Kesseli, 1941) all lead to this conclusion and are untenable in view of the evidence that all active rock glaciers for which accurate data are known are now moving at a fairly constant rate.

Remaining are the theory that rock glaciers move down-slope by creep or solifluction, with the movement confined to an unfrozen upper layer (Chaix, 1923), and the theory that rock glaciers are flows of debris-charged ice (Capps, 1910; Tyrrell, 1910; Richmond, 1952). So that these theories may be compared several lines of evidence will be developed that permit inference about the distribution of motion within a rock glacier; also, the known properties of ice will be utilized in an attempt to describe the

FIGURE 5.—PHOTOGEOLOGIC MAP SHOWING ROCK GLACIERS AND GLACIERS IN THE EAST HALF OF THE WINDY AREA
Base from parts of U. S. Geological Survey topographic maps of Healy B-4 and Healy C-4 quadrangles. For location see Figure 1.

distribution of motion within a flow of debris and ice.

Measurements of the Motion of a Rock Glacier

The motion of a rock glacier at the head of Clear Creek in the Windy area (Fig. 4 of Pl. 4, Fig. 1 of Pl. 7, Figs. 4 and 6) was measured over a period of 8 years.

The rock glacier is 3500 feet long and 1200 feet in maximum width and is 100–125 feet high at the front. It descends from an altitude of 4500 feet to an altitude of 3400 feet, and its upper surface has an average slope of 14½°. The rock glacier is derived from a terrain consisting largely of sedimentary and metasedimentary rocks (argillite, graywacke, slate, and limestone) with small porphyry dikes. In the lithology of its source area it is unlike most of the rock glaciers we studied; nearly all the others are derived from terrain of granodiorite, metavolcanic rocks, or blocky fracturing conglomerate—rock types that yield boulder-size talus. The material of sedimentary and metasedimentary origin on the surface of the Clear Creek rock glacier, however, averages 1–2 inches in diameter, and although the porphyry fragments are much larger, the largest porphyry boulder observed was 3 feet in diameter (Fig. 3 of Pl. 4).

The upper surface of the rock glacier has an unusually well-developed pattern of transverse roll-like ridges, convex down-valley in plan (Fig. 4 of Pl. 4). The ridges average 5 feet in height and 10–30 feet across. A fairly continuous turf was probably once present over the upper surface of this rock glacier, at least in the down-valley part. This turf cover is now represented by patches of turf, the edges of which have been freshly torn, and by areas a few feet to several tens of feet across of nearly continuous turf, broken in many places by lines of tearing. The sides, front, and upper surface of the head of the rock glacier are bare of vegetation. The front and sides are as steep as the angle of repose for debris of this sort. The talus is so unstable that climbing is difficult.

A transit station was established on an outcrop in a ravine on the concave side of a bend in the rock glacier (Fig. 6). From this station two range lines of painted boulders were established, each aligned with a target painted on a bedrock outcrop on the opposite wall of the valley. The original surveys were made on September 18, 1949. The boulders were resurveyed on August 16, 1951, and their displacement down-slope was determined by measuring their distance on the ground from a vertical plane passing through the transit station and the target. These displacements are believed to be accurate within 0.2 foot. The displacements were redetermined on August 15, 1952, and on August 15, 1957. The results of these measurements are shown in Table 1 and on Figure 6. They show that the greatest movement on the upper surface was about 2.4 feet per year along the upper line and about 2.5 feet per year along the lower line.

The rock glacier advances over turf meadows that show no signs of disturbance. Two boulders projecting through the turf formed a line in the direction of motion of the rock glacier; on September 18, 1949, the top of each boulder was painted, the distance and direction between boulders was measured, and the distance from the nearest boulder to the base of the rock glacier was measured. In 1951, 1952, and 1957 the distances and directions were again measured. The boulders and the turf around them showed no disturbance at any time. The only dimension that changed was the distance from the nearest boulder to the rock glacier, which shortened at an average rate of 1.6 feet per year—two-thirds of the rate of advance of the upper surface. Three sources of error are possible in this measurement. If the hill of debris on which the two boulders are situated is also moving—an unlikely condition in view of the unbroken turf and the stability of the line between the boulders—it would be moving down-valley, in the same direction as the rock glacier. The apparent rate of forward motion of the front in that case would be less than the true rate of motion, and the front would be advancing more rapidly than 1.6 feet per year. If the line between the boulders is not, in fact, parallel to the direction of flow, the shortening of the range line measures not the rate of advance of the front, but some factor times it. The true rate of advance would be less. This error, if present, is probably not large, for the line between the boulders is parallel to the axis of the valley.

A third source of error stems from the coarse size of debris making up the base of the front and from possible variations in the rate of falling of boulders from the front face. This debris has an average diameter between 1 and 2 inches, and boulders up to 1½ feet in diameter are common. The base of the front advances, not steadily, but in discrete increments measured by the size of the fragments that roll to the

base. The total displacement, 13.0 feet, is probably great enough so that errors introduced from this cause would not affect the conclusions.

probably decreases gradually downward from the surface. Probably, therefore, much more than two-thirds of the thickness of the rock glacier and possibly its entire thickness is in

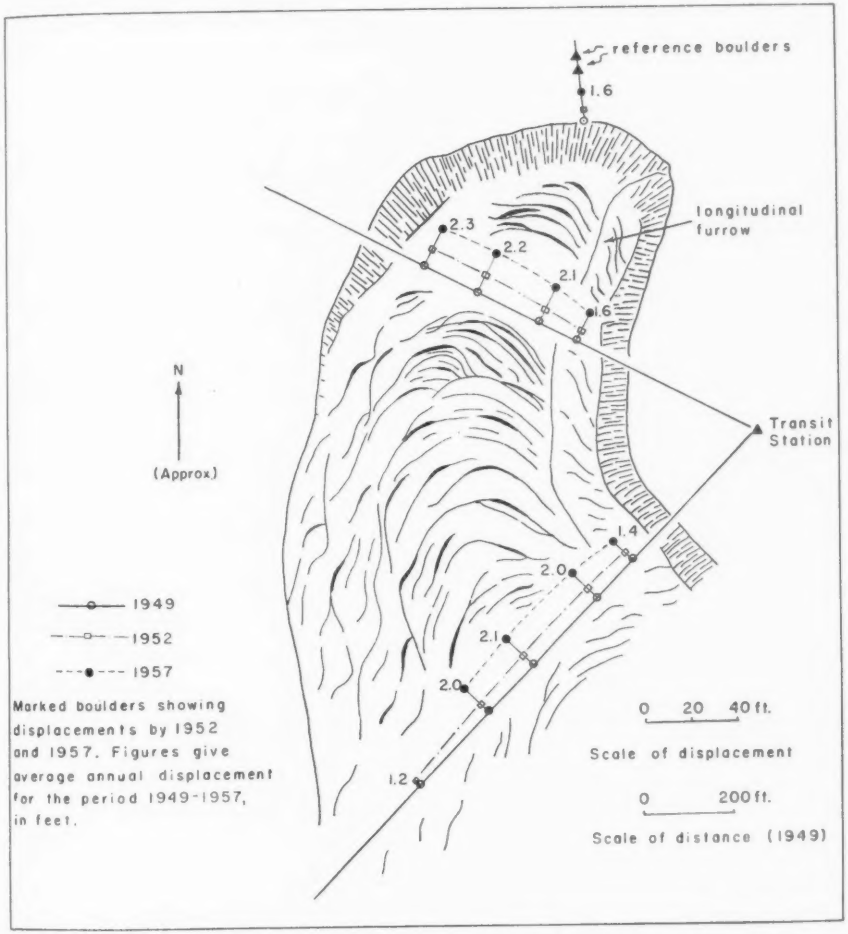

FIGURE 6.—SKETCH MAP SHOWING MOTION OF ROCK GLACIER 51 AT HEAD OF CLEAR CREEK

Pattern of fronts of transverse ridges, shown in heavy black lines, was taken from a low-altitude vertical photograph.

If the motion of the rock glacier is considered as confined to an upper layer moving with a constant velocity throughout its thickness over a lower layer that is not moving, then, as Figure 7 shows, this upper layer must be two-thirds the thickness of the rock glacier. The velocity of material within the rock glacier

motion. The rock glacier is 100–125 feet high at the front, and its thickness is presumably nearly the same. All except the upper 5 or 10 feet of its thickness should be perennially frozen. Hence frozen material is participating in the motion of the rock glacier.

The only other measurements of the motion

TABLE 1.—MEASUREMENTS ON THE CLEAR CREEK ROCK GLACIER
(In feet.)

Boulder no.	Approximate distance from transit	Displacement 8-16-51	Displacement 8-15-52	Displacement 8-15-57	Average annual displacement 1949–1952	Average annual displacement 1952–1957
Upper line						
1	390	3.2	5.1	11.5	1.7	1.3
2	500	4.3	6.4	15.7	2.2	1.9
3	700	4.8	6.9	17.0	2.4	2.0
4	840	3.7	6.0	15.9	2.0	2.0
5	1060	2.1	3.6	.....	1.3	.....
Lower line						
1	440	3.4	4.9	12.8	1.7	1.6
2	530	4.3	6.6	16.6	2.3	2.0
3	680	4.7	7.4	17.7	2.5	2.1
4	810	5.8	7.4	18.7	2.5	2.3
	Distance 9-18-49	Distance 8-16-51	Distance 8-15-52	Distance 8-15-57	Average annual displacement 1949–1952	Average annual displacement 1952–1957
Far boulder to near boulder	26	26	26	26.1	.....	.....
Near boulder to base	116	111.5	110.4	103.0	.....	.....
Motion of front	0	3.5	5.6	13.0	1.9	1.5

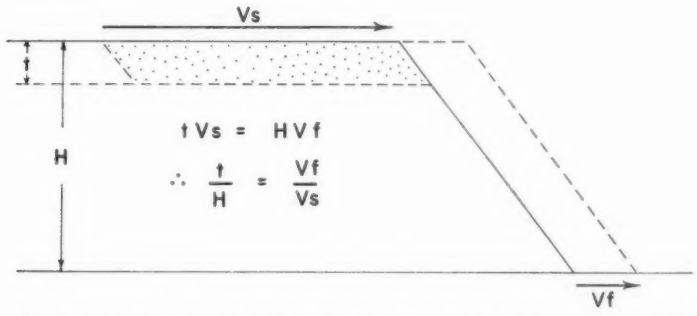

FIGURE 7.—RELATIONSHIP BETWEEN VELOCITY OF FRONT AND OF UPPER SURFACE OF A MASS THAT IS ENLARGING BY UNIFORM MOTION OF A THIN SURFACE LAYER OVER A STABLE INTERIOR

of rock glaciers reported in the literature are those by Chaix (1923, 1943) of rock glaciers of the upper Engadine, in Switzerland. The velocities measured by Chaix are of the same order of magnitude as those measured in the Alaska Range. The maximum annual surface motion, determined over an interval of 24 years, is 4.5 feet for the lower part of the Val Sassa rock glacier and 5.3 feet for the lower part of the Val dell'Acqua rock glacier (Chaix, 1943). The values determined for the 24-year period 1918–1942 agree to the second digit with those determined for the 3-year interval 1918–1921, suggesting that the rock glaciers Chaix studied have probably been moving at a constant rate for the period of measurement. The corresponding rates of advance for the bases of the fronts are 1.3 and 1.6 feet per year, re-

spectively, only one-third the velocity of the upper surface. The striking disparity between the surface and frontal velocities of the Swiss rock glaciers led Chaix and Domaradzki to conclude that their motion was due to the creep of a relatively thin surface layer over a much more slowly moving or stable interior.

Indirect Indications of Motion

Movement of many of the rock glaciers in the Alaska Range is indicated by three features: the bare fronts which slope at the angle of repose, the sharp angles at the tops of these bare fronts, and the exposures of the fine-grained lower layers of the rock glaciers on the fronts. The first two features indicate that at least some part of each rock glacier is moving, and that the upper surface is moving faster than the base; the third feature suggests that most or all of the thickness of each rock glacier is involved in the motion, not merely a thin layer on the surface. Each of these features is described in detail herein, and its significance for the motion of rock glaciers is spelled out.

The fronts of many rock glaciers are barren of vegetation (Fig. 1 of Pl. 2, Figs. 2 and 3 of Pl. 3). These same rock glaciers may have an unbroken turf extending down-valley from their bases and continuous or discontinuous vegetation on their upper surfaces. Bare boulders, apparently loosened from the front, litter the turf meadows down-valley from the rock glaciers; a few of these boulders have dead lichens on their undersides, indicating that they have rolled down recently. The barren front indicates that the rock glacier has been disturbed recently in such a way that the former front was either buried or removed. Otherwise, vegetation would have gained a foothold. Continuous removal of the upper part of the front and partial burial of the lower part would be accomplished if the upper part of the rock glacier was moving forward faster than the lower part. On the other hand, if movement was by sliding forward on a basal slipping plane, the entire front should not be disturbed. A front that is entirely barren suggests, therefore, that the rock glacier is in differential forward motion, and that the upper part is moving faster than the lower part.

The fronts of many active rock glaciers make very sharp angles with the upper surfaces, and the fronts are generally at the angle of repose (Figs. 1 and 2 of Pl. 2, Fig. 2 of Pl. 3). This again indicates that the upper part is moving forward more rapidly than the lower part, for in a climate in which mass-wasting predominates, the sharp angle at the top and the steepness of the slope can be maintained only by constant renewal. If the sharp angle was established only once in the history of the rock glacier, mass-wasting would round it off and make the slope below it more gentle, and gully erosion would carve it and obliterate its straightness.

These two features of active rock glaciers (the barren front at the angle of repose and the sharp angle at the top of the front) show that rock glaciers do not acquire all their forward velocity within a basal slipping plane, but rather that velocity increases upward. They do not indicate how the velocity increases upward. Movement might be confined to a narrow layer at the top, as is assumed in a "solifluction" or "creep" theory of motion (Chaix, 1943; Domaradzki, 1951, p. 230–231), or it might be unequally distributed throughout the body of the rock glacier according to some flow relationship such as that in ice.

Talus aprons mantle the fronts of active rock glaciers, rising from one-fourth to two-thirds of the height of the front. Since a well-defined, thick lower layer of fine-grained material crops out at the front of most active rock glaciers, the height of the apron of coarse, loose talus can usually be estimated (Figs. 1 and 2 of Pl. 2). The height of the talus was half the height of the front or less for three-fourths of the rock glaciers for which estimates could be made (Table 2). The mean height of the talus aprons is 45 per cent of the height of the front. Photographs of Swiss rock glaciers (Domaradzki, 1951) show the talus aprons of these rock glaciers usually about half the height of the front also.

The significance of this observation is seen in Figure 8. It has been noted that the fronts of all active rock glaciers are remarkably similar, with slopes within a few degrees of the angle of repose, commonly increasing somewhat toward the top. Because these fronts vary so little from one active rock glacier to the next, it may be assumed that in the steady state the profile of a single rock glacier varies little as it moves forward. Then, in Figure 8, as the front moves from *ab* to *cd* in unit time, ideally each point on the front moves forward the same distance and has, therefore, the same velocity. It is important to distinguish between the front as a form, with its constant velocity at all levels, and the actual material of the rock glacier, with a

velocity that—even at the front—is not constant but increases upward. Figure 8 shows that regardless of how the velocity of material increases upward, the velocity of the front must lie between the comparatively high velocity of material of the upper surface and the lower or zero velocity of material along the bottom. Therefore, at some level within the rock glacier (point *f* on Fig. 8) the material is moving with the same velocity (V_m) as the front. The material above this level, because it has a higher velocity, tends to project beyond the front and falls to form an apron of talus. This process is facilitated by a loose thawed zone that extends back from the front. The talus from above will cover the slower-moving portion of the front below *f*. Inasmuch as the shape of the front remains constant, as a first approximation it can be said that the material represented in section by *cef* will be equal to that of area *bdf*.

The point *f* is observed on the front of a rock glacier to mark the contract between the apron of talus and the fine-grained interior. Thus the position of this contact is the height at which the velocity within the rock glacier is the same as the velocity of the front (V_m). This velocity, multiplied by the area of cross section perpendicular to the direction of flow, is the rate of transport of material by the rock glacier. V_m is therefore also the mean velocity with respect to height. These relationships may be confirmed by noting in Figure 8 that area *aeb* equals area *acdb*.

Several ways in which the velocity might increase at different levels above the base are shown in Figure 8. The movement of a thin surface layer over a stable interior, with velocity decreasing rapidly as the depth below the surface increases, is represented in *a* of Figure 8. Chaix and Domaradzki have theorized that the Swiss rock glaciers move in this way. The flow shown in *c* of Figure 8 would exist in material having a rate of strain proportional to stress, a type of flow which will be discussed more fully. Type *b* is intermediate between *a* and *c*. Type *d* represents an even greater velocity near the base and approaches the case of slipping over a basal plane.

The effect of the vertical distribution of velocity upon the height of the talus apron should be considered. In case *b* the height will be exactly half the total height if the velocity at the base is zero. In case *a* the talus extends higher than half the height of the front, and in the case of a thin skin moving over a stable interior, the talus should extend almost to the top. For cases *c* and *d* the height of talus is correspondingly lower than half the total height, as is shown.

The observations, (1) that the average height of the talus apron is 45 per cent of the height of the front, and (2) that on three-fourths of the rock glaciers for which information could be obtained, the talus apron was half the height of the front or less suggest that motion is distributed throughout a considerable part of the rock glaciers as in *b*, *c*, or *d* of Figure 8 and is not confined to a thin surface layer as in *a* of Figure 8. Domaradzki's photographs (1951) also indicate motion is distributed throughout the total thickness in most Swiss rock glaciers. The great variation in the height of the talus apron observed is to be expected, as the lines *fb* and *fd* in Figure 8 meet at very small angles, and small irregularities in the collapse of the top of

---

PLATE 2.—PANORAMAS OF FRONTS OF ROCK GLACIERS

FIGURE 1.—Front of an active tongue-shaped rock glacier (rock glacier 17) at head of Kansas Creek. For location see Plate 1. The dark band on the front of the rock glacier is the outcrop of the fine-grained lower layer, which is mantled on the lower part of the front by a talus apron. The fine-grained lower layer appears dark because it is damp. The low mounds in the foreground are relics of an earlier, dissected rock glacier. Note the sharp angle, characteristic of active rock glaciers, between the vegetation-free front and the dark lichen-covered upper surface.

FIGURE 2.—Near view of front of an active rock glacier (rock glacier 5, looking west from upper surface of inactive rock glacier 6 in foreground; see Plate 1 for location). Note outcrop of lower layer as a fine-grained band across the front, and the apron of coarse boulders from the upper layer that now lie on the turf meadow at the base of the front. The boulder circled in black is 5 feet high. Compare the smoothly rounded front of the lichen-covered inactive rock glacier in the foreground with the sharp angle at the top of the front of the active rock glacier. Compare with Plate 5, which shows an aerial view of this rock glacier.

FIGURE 3.—An apron of inactive lichen-covered lobate rock glaciers around the base of a mountain, looking southwest from a point on the Wood River about 2 miles downstream from the present terminus of the glacier. See Figure 1 for location.

FIGURE 1

FIGURE 2

FIGURE 3

PANORAMAS OF FRONTS OF ROCK GLACIERS

FIGURE 1

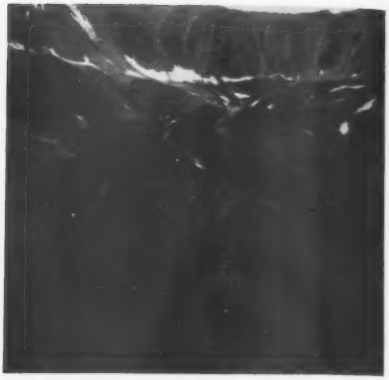

FIGURE 2

FIGURE 3

FIGURE 4

FIGURE 5

FIGURE 6

VIEWS OF FRONTS AND HEADS OF ROCK GLACIERS

TABLE 2.—DATA ON HEIGHT OF TALUS AT FRONT OF ROCK GLACIERS

Rock glacier number*	Height of front (feet)	Per cent front with interior exposed (average)	Per cent of height talus-covered (average)	Minimum height talus (per cent of total height)	Quality of observation
3	170	64	36	25	Fair for average Good for minimum
4	400	45	55	33	Good
5	160	60	40	25	Good (?)
7	100–150	72	28	17	Good
9	100	60	40	29	Good
13	270	43	57	50	Good
15	100	72	28	17	Good
17	300–400	50	50	..	Recollected
18	150–200	30	60	..	Poor
19	500 (?)	35	65	50	Fair
20	75–150	50	50	..	Fair
24	150	Considerable	..	..	..
27	325	50	50	33	Fair
30	175	50	50	..	Poor
34	125	80	20	14	Good
51	100–125	55	45	25	Good
Average		53	47		

* For location see Plate 1 and Figure 4.

the front will be reflected in large irregularities in the height of the talus.

Both lines of investigation presented indicate that motion takes place throughout a large part of the total thickness of the Alaska rock glaciers. These rock glaciers are all in a region of permafrost and are presumably composed of a mixture of debris and ice to within a few feet of

PLATE 3.—VIEWS OF FRONTS AND HEADS OF ROCK GLACIERS

FIGURE 1.—View of a tongue-shaped rock glacier descending from the lip of a hanging valley (rock glacier 27; for location see Plate 1). Note sharp angle between light-colored vegetation-free front and dark lichen-covered upper surface. Transverse ridges can be made out on the upper surface. A glacier at the head of the rock glacier is at the background. Inactive rock glacier 26 is at lower right. Compare with Plate 6.

FIGURE 2.—Front of a tongue-shaped rock glacier (rock glacier 4). Note discontinuous outcrop of dark-toned damp fine-grained lower layer along front, mantled by talus in lower part. Transverse ridges and a prominent longitudinal furrow are on upper surface. Talus cones, with snowbanks in intercone swales, lead directly from the cirque walls to the upper surface of the rock glacier. For location see Plate 1.

FIGURE 3.—Contrast between front and upper surface of an active rock glacier (rock glacier 9, looking south). The dark tone of the upper surface is due to a continuous cover of lichens on the boulders. A small turf meadow lies on the upper surface at the left just above the front. The front is bare of vegetation. An upper light-colored layer of coarse rubble rests on a lower layer of mixed sand, silt, and rubble, that crops out on the front with a somewhat darker tone. For location see Plate 1. Compare with Plate 5.

FIGURE 4.—View of head of rock glacier 9, looking south. The rock glacier is fed by talus cones that lead down from the cirque walls at its head. Note snowbanks in the intercone swales that lead downstream to longitudinal furrows.

FIGURE 5.—Interior of a rock glacier exposed in a gully wall. The coarse blocks of granodiorite are embedded in frozen sand and silt. Blocks are about 3 feet across. Pits left by detached blocks mark the face. West side of rock glacier 17, Plate 1.

FIGURE 6.—Glacier at head of rock glacier 34, looking northwest from head of rock glacier. Note the absence of debris on the ice. The glacier has melted down from a high stand of about 1900 that is marked by the base of the outcrops on its far side.

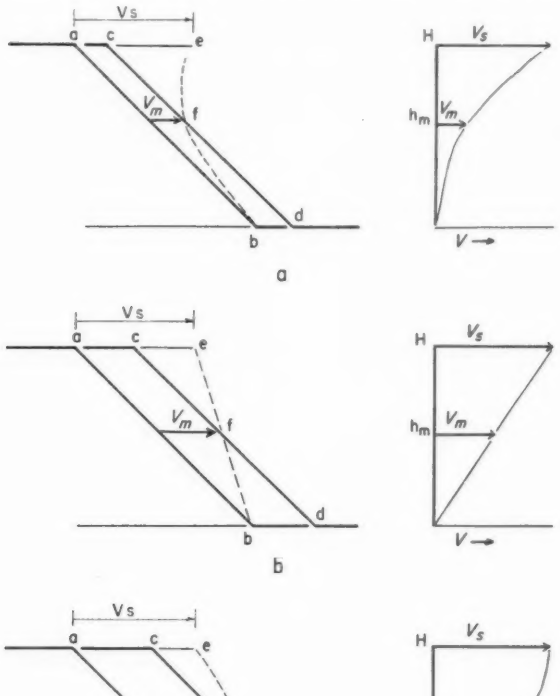

FIGURE 8.—POSITION OF THE TOP OF THE TALUS APRON AT THE FRONT OF A ROCK GLACIER FOR FOUR POSSIBLE VELOCITY DISTRIBUTIONS WITHIN THE ROCK GLACIER

Velocity distributions are shown at the right; cross sections of the rock glacier are at the left.

the surface. Interstitial ice has been observed near the surface in several of them. It is difficult to escape the conclusion that the motion of these rock glaciers is the motion of frozen rubble.

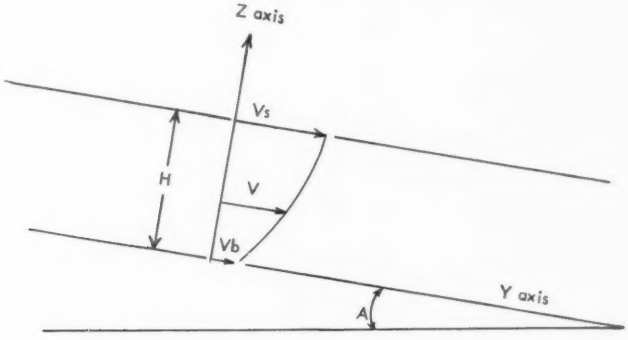

FIGURE 9.—RELATIONSHIPS OF STRESS AND STRAIN FOR FLOW IN A SEMI-INFINITE SHEET ON AN INCLINED PLANE

Maximum Shear Stresses Within Rock Glaciers

In the preceding section it was shown that the upper layers of a rock glacier move more rapidly than the lower layers. The movement of rock glaciers is thus a deformational process, rather than the thrusting or sliding forward of a rigid body. The deformation results from stresses within the rock glacier. While it would be extremely difficult to compute the stress pattern within so inhomogeneous a body as a rock glacier, it is possible to compute the distribution of stresses within a simplified conceptual model of one. This model, while representing some of the basic features of the flow of rock glaciers, is simple enough to be mathematically tractable and offers a means of estimating the average stresses at various positions within actual rock glaciers.

The simplest such model is the laminar flow of an infinite sheet of uniform thickness down an inclined plane. In this one-dimensional model (Fig. 9), the shear stress τ_{yz} acting in the direction of the y axis on a plane perpendicular to the z axis is constant at all points lying in each plane z = constant parallel to the inclined basal plane, and is given by the formula

$$\tau_{yz} = \rho g(H - z) \sin A, \qquad (1)$$

where ρ is the density of the flow, g is the acceleration of gravity, H is the thickness of the flow, z is the height above the inclined plane, and A is the slope angle. The maximum shear stress occurs at the base of the flow, where z equals 0:

$$(\tau_{yz})_{max} = \rho g H \sin A \qquad (2)$$

The shear stresses within an actual flow of finite dimensions can be estimated by means of this formula in parts of the flow where the model is a good approximation to the actual flow. This will be true for the central part of a flow if the slope remains constant, if the thickness remains uniform longitudinally and laterally, and if the flow is wide enough so that the edge effects are negligible at the center. The last condition is satisfied if the central parts of transverse features such as ridges remain geometrically similar as they move downstream.

These conditions are sufficiently well satisfied to justify the use of formula (2) in estimating the maximum shear stresses in a number of rock glaciers and other types of flows. This permits investigation of whether different types of flows, such as rock glaciers and solifluction flows, are characterized by different ranges of maximum shear stress.

The quantity most difficult to evaluate in formula (2) is H, the thickness of the flow. Fortunately, ablation does not radically thin rock glaciers near their fronts, as it does glaciers. The fronts of rock glaciers, furthermore, retain their profile due to differential flow. Therefore,

TABLE 3.—HEIGHT OF FRONT, THICKNESS, AND SLOPE ANGLE OF SELECTED ROCK GLACIERS

Designation of rock glacier (see Pl. 1)	Height of front (feet)	Slope of upper surface at front (in degrees)	Thickness (H) at front* (feet)	Cosecant of slope angle	Remarks
3	170	11	167	5.24	Active
3a	50	12½	49	4.62	Inactive
4	400	11	392	5.24	Active†
5	160	8	158	7.18	Active
7	125	8	124	7.18	Active**
8	80	9½	79	6.06	Active**
9	100	15½	96	3.74	Active
15	100	7	99	8.21	Inactive**
16	70	8	69	7.18	Inactive
17	300–400	5	300–400	11.47	Active
21	90	16½	86	3.52	Active
22	100	11	98	5.24	Active**
23	100	11	98	5.24	Inactive
24	150	12½	146	4.62	Active
27	325	22	300	2.67	Active†
29	75	14	73	4.13	Inactive
30	175	12½	171	4.62	Active
31	25–30	14	24–29	4.13	Inactive
32	40–50	15	39–48	3.86	Inactive
33	280	16	270	3.63	Active†
34	125	15	121	3.86	Active
35	125	15	121	3.86	Active
38	200	7	198	8.21	Active
40	40	7½	40	7.66	Inactive
41	60	7½	60	7.66	Inactive
43	350	16	336	3.63	Active†
51††	125	14	121	4.13	Active
55***	200	17	191	3.42	Active†
Val Sassa†††	76	8	75	7.18	Active
Val dell'Acqua†††	67	19	63	3.07	Active

* Thickness (H) equals height of front times cosecant of the slope of the upper surface.
† Spills over a steep slope; height of front and thickness abnormally large.
** Reactivated rock glacier.
†† Clear Creek rock glacier. For location see Figure 4.
*** For location see Figure 1.
††† From Chaix, 1923.

the thickness of a rock glacier may be estimated from the height of the front. If H_v is the vertical height of the front, then the thickness H to be used in formula (2) is $H = H_v \cos A$. Table 3 shows the heights of fronts and the slopes near the fronts of a number of rock glaciers. These rock glaciers were selected because they satisfy the conditions of the mathematical model, and because data on their front heights and slopes were available. Several of the rock glaciers are in the process of spilling over abrupt drops in their beds or have beds with slopes approaching the angle of repose. Loose, uncemented material cascades down the slope ahead of these rock glaciers, giving anomalously high fronts which are not a measure of the true thickness of the rock glacier. These rock glaciers are indicated in Table 3 (see footnote).

The rock glaciers designated as inactive in Table 3 are believed to be rock glaciers, formerly active, which have stopped moving. The criteria for distinguishing active from inactive rock glaciers are discussed in another section

of this paper. Briefly, these criteria are the shape of the front and the presence or absence of vegetation on the front. The classification of rock glaciers into active and inactive classes was made entirely on the basis of these criteria, before Table 3 and Figure 10 were prepared.

TABLE 4.—THICKNESSES AND SLOPE ANGLES OF CREEP AND SOLIFLUCTION DEPOSITS ON SEWARD PENINSULA
(Data from Sigafoos and Hopkins, 1952.)

Type of flow	Range of maximum thickness of individual flows (feet)	Range of slope angles (degrees)
Soil terraces	3–20	5–15
Lobate terraces	1–5	7–20
Soil lobes	1–5	20–25

The slope angles and maximum thicknesses of various types of down-slope movement of debris due to creep (*i.e.*, the action of freezing and thawing) or to solifluction, taken from Sigafoos and Hopkins (1952), are listed in Table 4.

The data in Tables 3 and 4 are plotted in Figure 10. Values of H are plotted as ordinates, values of cosecant A as abscissae. The advantage of this choice of co-ordinates is easily seen if the expression for $(\tau_{yz})_{max}$, the maximum shear stress developed in a flow of thickness H (formula 2), is rewritten in the form:

$$(\tau_{yz})_{max} = \frac{\rho g H}{\text{cosec } A} \qquad (2a)$$

The locus of points for which $(\tau_{yz})_{max}$ is equal to a constant is the straight line cosec $A = \rho g H$ which passes through the point $H = 0$, cosec $A = 0$. (There are, of course, no angles corresponding to cosec A in the range from 0 to 1.) The ordinate scale at the right of Figure 10 indicates the value of the quantity $\rho g H$, expressed in bars, which is simply a multiple of H. The term ρ is considered to be 1.8 gm/cm^3 for rock glaciers and for creep and solifluction flows. The value of $(\tau_{yz})_{max}$ along any line passing through the point $H = 0$, cosec $A = 0$, is the slope of the line, using the ordinate scale on the right. A range of stress is the sector on the diagram lying between two such lines.

Figure 10 clearly shows that the maximum shear stresses in active and inactive rock glaciers (that is, the shear stresses along their bases) lie, with few exceptions, in two distinct ranges. The maximum shear stresses in inactive rock glaciers are less than 1 bar. The maximum shear stresses in most active rock glaciers lie in the range between 1 and 2 bars. The separation of the stress fields of active and inactive rock glaciers could come about in two ways. On one hand, Figure 10 can be taken to indicate that a minimum value of 1 bar for $(\tau_{yz})_{max}$ is necessary for rock glaciers to move. If $(\tau_{yz})_{max}$ falls below this value, the rock glacier ceases to move. This could happen if the supply of debris at the head declined to a negligible amount: the rock glacier would continue to flow and spread until its thickness fell below the critical minimum, at which time motion would cease. The rate of flow would probably decrease asymptotically to zero. On the other hand, rock glaciers could become inactive for reasons not related to the value of their maximum shear stress, such as the melting out of the interstitial ice. If the cause for the cessation of motion also causes a shrinkage of volume, which the melting of ice might do, the thickness H would decrease, and the point as plotted on Figure 10 might fall below the 1-bar line. The two explanations are not mutually exclusive; however, we believe that the first process probably caused the major part of the difference; if the second process was the important one, a much greater overlap between the stress fields of active and inactive rock glaciers would be expected, for the thickness and proportion of ice would be expected to range between wide limits.

The range of stress of solifluction and creep phenomena and the range of stress of the rock glaciers are not even adjacent. This strongly suggests that these are not gradational phenomena, as some theories dealing with the movement of rock glaciers would require.

Deformational Properties of Rock Glaciers and Ice

Of the many hypotheses advanced to explain the movement of rock glaciers, one of the few which cannot be rejected in the light of information now available is the hypothesis that the movement of rock glaciers is due to interstitial ice. It has been shown that the movement of rock glaciers is a deformational process. The way in which certain types of ice are deformed when subjected to stress is known from laboratory experiments. In addition, the deformational properties of glacier ice can be estimated

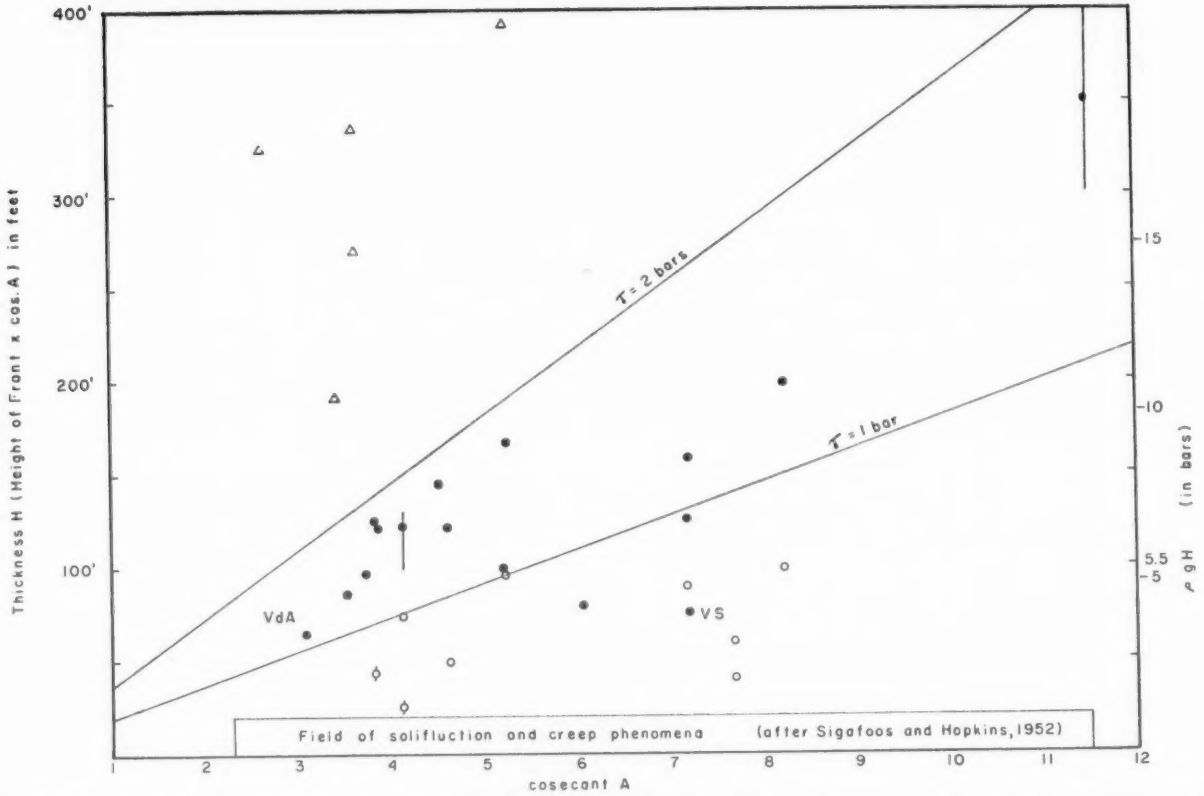

FIGURE 10.—SCATTER DIAGRAM OF THE THICKNESS AT THE FRONT OF SEVERAL ROCK GLACIERS PLOTTED AS A FUNCTION OF THE COSECANT OF THE SLOPE OF THE UPPER SURFACE NEAR THE FRONT

Lines along which basal shear stress (τ) of flows are equal to 1 bar and to 2 bars are shown. Open triangles indicate active rock glaciers spilling over steep slopes and having abnormally high fronts. Solid dots indicate active rock glaciers not spilling over steep slopes; height of front is a measure of the thickness of the rock glacier. Open circles indicate inactive rock glaciers. Vda, Val dell'Acqua; VS, Val Sassa. Data on which this figure is based are in Tables 3 and 4.

roughly from measurements of glacier flow. Similarly, the deformational properties of rock glaciers can be estimated roughly from an analysis of their rates of flow. An exact agreement between the deformational properties of ice and rock glaciers is not to be expected. Approximate agreement, however, of the sort that exists between the properties of ice as measured in the laboratory and the same properties inferred from glacier flow, would lend strong support to the interstitial ice hypothesis.

The deformational properties of ice as measured in the laboratory vary widely with the type of ice studied and with the conditions of the experiment. Glen (1952) found the following relationship between the rate of strain and stress for polycrystalline ice under compression:

$$\frac{d\epsilon}{dt} = k\sigma^n \tag{3}$$

where $d\epsilon/dt$ is the rate of strain, σ is the stress, and k and n are constants. Expressing $d\epsilon/dt$ in strain per year and σ in bars, Glen found that for the range of stress from 1.5 to 10 bars, $n = 4$ and $k = 0.0074$.

Deformation measurements within glaciers (Perutz and Gerrard, 1951; Haefeli, 1951) have been interpreted in terms of a similar functional relationship, but with n equal to 2. However Nye's evaluation of this and similar data results in a value of n equal to 3 (Nye, 1953).

The deformation of polycrystalline ice under tension has been studied by Jellinek and Brill (1956). After initial elastic deformation and transient creep phenomena lasting a few hours, the ice, when subjected to a constant stress, deformed at a constant rate. Within the range of stress of the experiment, ½ to 2½ bars, the rate of strain was found to be proportional to the stress—the familiar Newtonian viscous flow relation. This corresponds to a value of n equal to 1 in formula (3), with 1/k equal to the viscosity. The viscosity coefficients found in these experiments range from 2×10^{14} to 6×10^{14} poises for polycrystalline ice. Because the experiments were carried out with cylinders under uniaxial tension, these values should be reduced by a factor of three for comparison with shear analyses such as those to be listed herein (Jellinek and Brill, 1956, p. 1201).

It is impossible to state which, if any, of the suggested flow laws most accurately describes the over-all deformational properties of a glacier or rock glacier, since the types of ice and the conditions under which deformation occur differ from one flow to another, and even within a single flow. Since the range of maximum shear stresses within rock glaciers is between 1 and 2 bars, the viscous flow law found by Jellinek and Brill seems at least a reasonable possibility.

The rates of flow of rock glaciers are accordingly analyzed in terms of a one-parameter viscous-flow model. This analysis is not intended to imply that the authors believe that all glaciers and rock glaciers deform by viscous flow. It seems unlikely that any simple flow law such as formula (3) can describe even the gross flow characteristics of all glaciers or rock glaciers with accuracy. The viscous flow model is used, nevertheless, because it is the simplest, because it is supported as well as any other by the laboratory evidence, and because the crudity of the flow measurements does not justify a more elaborate model. The results, which will be expressed in terms of the viscosity parameter, may best be interpreted as a way of roughly comparing the rates of deformation of ice and rock glaciers within a limited range of stress.

Reference is made to Deeley (1895), Jeffreys (1925), and Nye (1952) for details of the following derivation.

In the laminar flow of an infinite plate of homogeneous viscous material down an inclined plane

$$\frac{d\epsilon}{dt} = \frac{dv}{dz} = \frac{\tau}{\eta} \tag{4}$$

where $d\epsilon/dt$ is the rate of strain, v is the velocity in the direction of the y axis, dv/dz is the velocity gradient in the direction of the z axis, τ is the shear stress, η is the viscosity, and the co-ordinate axes are as shown in Figure 9. Substituting the expression for τ in formula (1) and integrating with respect to z,

$$V - V_b = \frac{\rho g(2zH - z^2) \sin A}{2\eta} \tag{5}$$

where V is the velocity at the height z, V_b is the velocity at the base of the flow ($z = 0$), ρ is the density, g is the acceleration of gravity, H is the thickness of the flow, and A is the slope angle. The velocity at the surface is then

$$V_s = V_b + \frac{\rho g H^2 \sin A}{2\eta} \tag{6}$$

The mean velocity with respect to height is

$$V_m = \frac{1}{H}\int_0^H V\,dz = V_b + \frac{\rho g H^2 \sin A}{3\eta} \tag{7}$$

Lines along which basal shear stress (τ) of flows are equal to 1 bar and to 2 bars are shown. Open triangles indicate active rock glaciers spilling over steep slopes and having abnormally high fronts. Solid dots indicate active rock glaciers not spilling over steep slopes; height of front is a measure of the thickness of the rock glacier. Open circles indicate inactive rock glaciers. Vda, Val dell'Acqua; VS, Val Sassa. Data on which this figure is based are in Tables 3 and 4.

V_m is also the velocity of advance of the front. In applying these formulas to flows of finite width, it is assumed that the flow is sufficiently wide so that the velocity of the center is not retarded by friction of the sides.

the measurement of some of the dimensions. So that the reservations which were made at the beginning of this section may be emphasized, the value of η obtained from formula (6) is termed the apparent viscosity.

TABLE 5.—APPARENT VISCOSITIES OF ROCK GLACIERS

Name	Location	Velocity of upper surface (meters/year)	Velocity of front (meters/year)	Height of front (meters)	Slope of upper surface	Gross flow viscosity (poises)
Clear Creek	Alaska	0.7	0.58	30–40	14°	$7.5–9 \times 10^{14}$
Val Sassa	Switzerland	1.37*	0.4*	25*	7½°*	$1.6–3.7 \times 10^{14}$
Val dell'Acqua	Switzerland	1.60*	0.48*	20–25*	19½°*	$3.6–8.0 \times 10^{14}$

* From Chaix, 1923, 1943.

In a previous section the significance of the height h_m at which the velocity V of the material in the rock glacier is the same as the mean velocity, V_m, was discussed. The theoretical value of h_m for viscous flow can now be found by substituting the expression for V_m in formula (7) for V in formula (5), and solving for Z; this value of h_m is equal to 0.41 H. It was found previously that the average value of h_m for 16 rock glaciers, inferred from the heights of talus along their fronts, is approximately 0.45 H (see Table 2). If, instead of a viscous flow law, a flow law of the form given by formula (3) is used, for $n = 2$ in formula (3), $h_m = 0.37\ H$, and for $n = 4$, $h_m = 0.3\ H$. The average measured value of h_m is not in contradiction with the theoretical value based on viscous flow. The data are scattered, however, and additional measurements will be required to prove the usefulness of this type of analysis.

The motion of a number of valley glaciers was analyzed by Deeley (1908) and Deeley and Parr (1913); using formula (6) they obtained viscosities ranging from 3×10^{12} to 3×10^{14} poises. Numerous subsequent measurements of glacier flow have yielded viscosities in the range of 10^{13} to 10^{14} poises (Sharp, 1954). In view of the nature of the assumptions made in these analyses, it is surprising that the range of values is not much larger.

The measured rates of motion of the rock glaciers in Alaska and Switzerland can be treated by this formula. Using the height of the front of the rock glacier as the thickness, the slope of the upper surface near the front as the slope, assuming $V_b = 0$, and taking ρ equal to 1.8 gm per cm³, formula (6) gives the values for η shown in Table 5. The range in values of η for each rock glacier reflects uncertainties in

The range in values of η is again surprisingly low in view of the nature of the assumptions underlying the calculations. The values of the apparent viscosity of rock glaciers are somewhat higher than those found in the laboratory for polycrystalline ice and those found from glacier flow. Higher viscosities would be expected in flows of detritus cemented by interstitial ice, since the rigid detritus presumably acts as a deterrent to deformational flow. The values found for the apparent viscosity are certainly not inconsistent with the interstitial ice hypothesis and would be surprising if an entirely different process such as solifluction was the essential mechanism of rock glacier motion.

ALTITUDINAL DISTRIBUTION OF ACTIVE ROCK GLACIERS COMPARED WITH ALTITUDES OF GLACIERS AND FIRN LINES

Comparison of the altitudes of the rock glaciers with the altitude of firn lines on near-by glaciers and with the altitudes of the glaciers will indicate whether or not rock glaciers may be subject to the same climatic controls as glacial ice. Matthes (1942, p. 161) defines the firn line as

> "The highest level to which the fresh snow cover on a glacier's surface retreats during the melting season . . . on glaciers that originate in recesses carved deep in the flanks of mountains—and the vast majority of glaciers so originate—the firn line is independent of the regional snow line and lies at a considerably lower level."

In the Alaska Range, the firn line lies considerably lower on glaciers on the shaded north side of mountains than it does on glaciers on the

south side of mountains. Comparison of the altitudes of the rock glaciers with the altitudes of the firn line on both northward-facing and southward-facing glaciers seems desirable, as the two types of firn line represent different environments of ice accumulation.

The altitudes of the lowest mountains that support glaciers on their southward-facing sides have been used as an approximation for the firn line on southward-facing glaciers. In the vicinity of the Wood River area in the northern part of the range this altitude is 7800–8000 feet, and in the vicinity of the Windy area in the southern part of the range it is about 6800 feet. No mountains in either area are high enough to support southward-facing glaciers, and the firn line had to be deduced from near-by higher mountains.

The firn line on northward-facing glaciers depends heavily on the degree to which they are protected from direct sunlight as well as on the amount of snow other than direct snowfall that accumulates on these glaciers by means of wind drift and avalanches. As an approximation for the firn line on northward-facing glaciers we used the lower limit of the range of the upper end of the cirque glaciers. These lowest cirque glaciers are only a few hundred feet long, and their firn lines could be no more than 100 or 200 feet below their upper ends. The lower limit of the range of the upper ends of northward-facing cirque glaciers lies at about 6100 feet in the Wood River area (Pl. 1) and at 4700–5000 feet at the Windy area (Figs. 4 and 5). The firn line on northward-facing glaciers therefore probably lies between 5900 and 6100 feet in the Wood River area and between 4500 and 5000 feet in the Windy area.

The altitudes thus determined show that the firn lines on southward-facing and northward-facing glaciers drop about 1200 feet in 25 miles from north to south across the Alaska Range (Fig. 11). The firn line on northward-facing glaciers is 1900 to 2000 feet lower than the firn line on southward-facing glaciers. The rise of the firn lines northward, contrary to world-wide trend, is probably due to heavier precipitation and cloudier and cooler summers on the south side of the Alaska Range than along the north side, despite the fact that the average annual temperature is somewhat lower on the north side of the range than on the south side at equivalent altitudes.

To compare the altitudes of the rock glaciers with those of the cirque glaciers and of the firn lines, three features related to each rock glacier were chosen for measurement: the lower end, the upper end, and the highest point of the cirque wall behind the rock glacier or glacier. These three features were chosen because their altitudes can be determined quickly and easily from topographic maps, and because it was thought that those measurements, as much as any that are feasible, would give an idea of the altitudinal distribution of rock glaciers. Moreover, the highest point of the area upslope was chosen because the area upslope from each rock glacier or glacier can be regarded as the source of much of the debris and snow that makes up each rock glacier or glacier, and also can be regarded as a mountain wall protecting each rock glacier or glacier from direct sunlight during much of the day and much of the year. The altitudes were read directly from the maps on which Plate 1 and Figures 4 and 5 are based.

The measurements of the altitudes of the rock glaciers and glaciers are summarized in Table 6. The rock glaciers are segregated into small classes in order to isolate the factors of variation. For example, northward-facing active rock glaciers are separated from southward-facing active rock glaciers in the same area, and from northward-facing active rock glaciers in a different area, so that the influence of direction of slope and of geographical position on average altitude can be separately evaluated. Some of the information in Table 6 has been summarized graphically in Figure 11.

All statements made in this section have been tested by the Student's t test (Hoel, 1947, p. 145–146), and in all cases they are significant at a 95 level of probability; that is, there is less than one chance in 20 that the observed differences are merely chance variations rather than the effects of a real shift in average altitude. Only the northward-facing active rock glaciers are compared directly with glaciers, for all glaciers in the two areas head in northward-facing cirques. Likewise, comparison of differences in altitude from place to place, and on northward-facing and southward-facing slopes, is confined to active rock glaciers.

The active rock glaciers in the Wood River area occur in a zone between 4200 and 6200 feet in altitude; those in the Windy area occur in a zone between 3300 and 5500 feet in altitude. The rock glaciers in the Wood River area average 800–1000 feet higher in the three features measured than those in the Windy area; and in the Windy area, those east of the Nenana River average about 100 feet higher than those west of the river. No significant east-west shift in height of rock glaciers was observed along the ridge making up the Wood

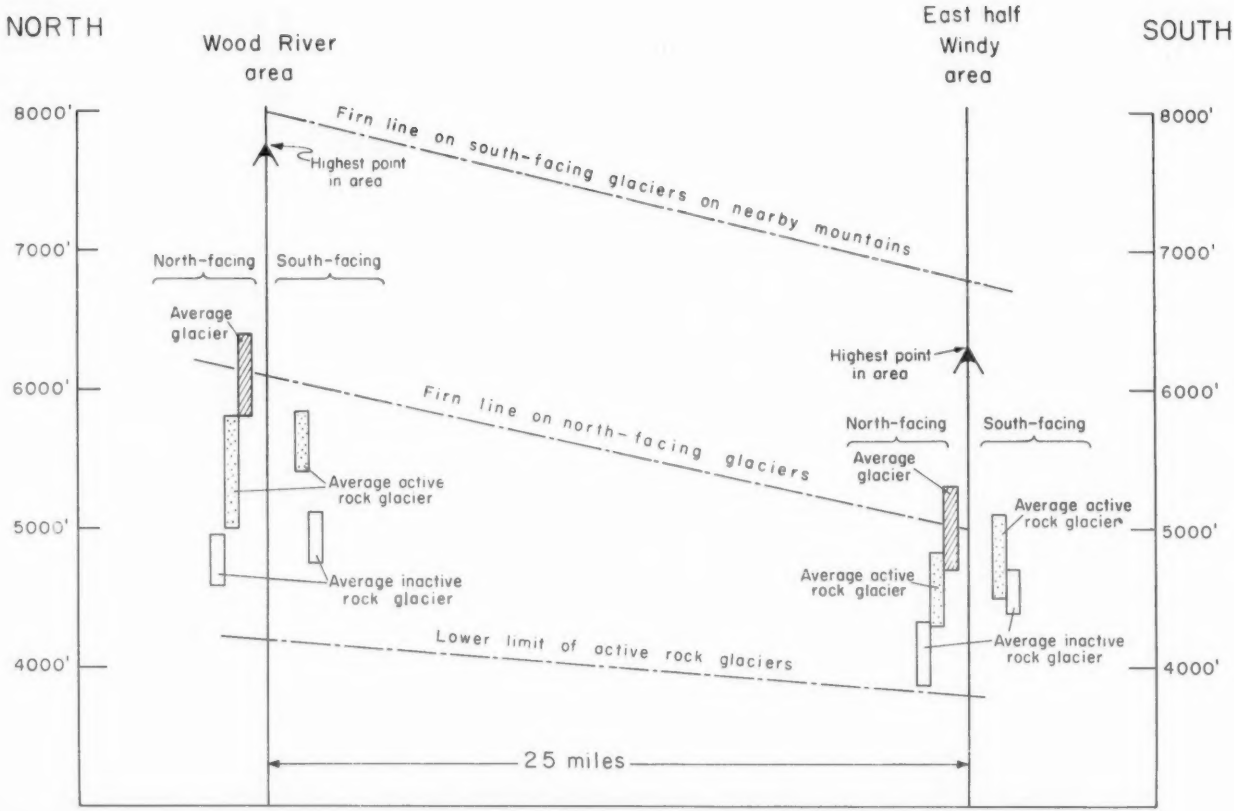

FIGURE 11.—ALTITUDES OF AVERAGE GLACIERS AND ROCK GLACIERS IN TWO AREAS IN THE ALASKA RANGE
Data on which this figure is based are summarized from Table 6.

River area. Active rock glaciers, therefore, occur in a zone about 2100 feet thick in altitude, sloping predominantly to the south but with a slight westerly component to the slope, and lying athwart the average altitude of the lower ends of cirque glaciers, which is 5700 feet in the Wood River area and 4600–4700 feet in the Windy area. The average altitudes of the upper ends of northward-facing active rock glaciers in both areas are almost equal to the average altitudes of the lower ends of glaciers in the same areas.

Comparison of the firn lines on glaciers with the upper ends of rock glaciers as measures of the lower limits of alimentation of glaciers and rock glaciers respectively reveals some interesting differences in altitudinal distribution. The firn line on southward-facing glaciers is 2000 feet higher than the firn line on northward-facing glaciers in both the Wood River area and the Windy area. On the other hand, the upper ends of southward-facing rock glaciers average only 100 feet higher than the upper ends of northward-facing rock glaciers in the Wood River area and only 200 feet higher in the Windy area.

Insolation is probably the factor affecting the preservation of firn that is most strongly affected by the direction in which the cirque wall faces, and the difference in insolation may be responsible in large part for the difference in altitude of the northward-facing and southward-facing firn lines; drifting of snow by prevailingly southerly winds may also be an important factor. The slight variation in altitude of the heads of the rock glaciers with respect to direction of slope indicates that the ice of rock glaciers, however it accumulates, is protected from both sun's rays and wind during accumulation. Presumably this protection is provided by the debris component of rock glaciers.

FIGURE 11.—ALTITUDES OF AVERAGE GLACIERS AND ROCK GLACIERS IN TWO AREAS IN THE ALASKA RANGE
Data on which this figure is based are summarized from Table 6.

COMPOSITION OF THE ROCK GLACIERS

General Statement

The composition of the rock glaciers must be largely inferred from their geographic distribution, geologic setting, morphology, and from evidence available on their surfaces. The interiors of rock glaciers are rarely exposed in nature, and we were unable to make extensive excavations. Nevertheless, it can be concluded that active rock glaciers are made almost entirely of rock debris and ice. A third, minor component, important only in that it permits turf to grow on the surface of rock glaciers, is wind-borne silt and sand.

Debris Component

Source.—The debris component of a rock glacier is derived by frost-riving and rock fall and forms talus deposits that subsequently move outward from the base of cliffs in the form of rock glaciers. The debris comes solely from the cliffs at the heads of the rock glaciers, a limited source that seems to be conclusively proved by the following evidence.

The lobate rock glaciers that extend outward from the base of cliffs at the sides of a valley are composed of material derived from those side cliffs, never of material from the valley head. This shows clearly that these masses of debris are not moraines left by retreating glaciers. Examples of such rock glaciers are those along the south wall of the West Fork of the Little Delta River and its tributaries (rock glaciers 25, 26, 28, 31, 36, 40, 41, and 42, Pl. 1), and some rock glaciers along tributaries of the Wood River (rock glaciers 1, 6, 15, 23, and 35, Pl. 1).

All rock glaciers that lie or head in cirques are composed of the debris from the cirque walls at their heads, even where they cross rocks of different lithology. For example, rock glacier 2 (Pl. 1) rests on interbedded limestone and quartz-sericite schist, yet is composed of the dark-green metavolcanic schist that makes the headwall of the cirque. Other rock glaciers that contain rocks of lithology present only in their headwalls and not on their beds are rock glaciers 24, 34, 37, and 55.

Where the walls of the cirque are crossed by a contact between two different rock types, the rock glacier is made of debris of the two different kinds of rock. Moreover, the contact between the debris derived from the two different rock types extends down the rock glacier in the direction of flow, a course that usually does not accord with the course of the bedrock contact beneath the rock glacier. Rock glaciers 4 and 5 (Pl. 1) and 55 (Fig. 1 of Pl. 4) show this feature.

Structure.—Rock glaciers appear to be made of two layers: an upper layer consisting predominantly of coarse blocky open-work rubble, and an underlying lower layer in which fine material is an abundant, and possibly the predominant, component. This double-layered structure of rock glaciers was first reported by Domaradzki (1951, p. 214). In many of the

TABLE 6.—SUMMARY OF ALTITUDE DATA ON ROCK GLACIERS AND GLACIERS IN THE ALASKA RANGE

	Number in group	Average altitude (feet)	Standard deviation (feet)	Range in altitude of group (feet)
A. LOWER END OF ROCK GLACIER AND GLACIER				
North-facing active rock glaciers, west part of Wood River area (Pl. 1)	12	4820	540	4200-5800
South-facing active rock glaciers, west part of Wood River area (Pl. 1)	4	5400	70	5300–5500
North-facing inactive rock glaciers, west part of Wood River area (Pl. 1)	11	4990	670	3500–5800
South-facing inactive rock glaciers, west part of Wood River area (Pl. 1)	6	5120	135	5000–5400
North-facing active rock glaciers, east part of Wood River area (Pl. 1)	18	5130	450	4200–5800
North-facing inactive rock glaciers, east part of Wood River area (Pl. 1)	12	4660	330	4000–5000
South-facing inactive rock glaciers, east part of Wood River area (Pl. 1)	12	4820	730	3600–5900
Glaciers, Wood River area (Pl. 1)	37	5705	375	4900–6700
North-facing active rock glaciers, west half of Windy area (Fig. 4)	30	4120	330	3300–4600
South-facing active rock glaciers, west half of Windy area (Fig. 4)	6	4400	210	4000–4700
North-facing inactive rock glaciers, west half of Windy area (Fig. 4)	21	3780	380	2800–4500
South-facing inactive rock glaciers, west half of Windy area (Fig. 4)	15	4350	180	3900–4600
North-facing active rock glaciers, east half of Windy area (Fig. 5)	14	4290	255	3800–4600
South-facing active rock glacier, east half of Windy area (Fig. 5)	8	4510	275	4100–5000
North-facing inactive rock glaciers, east half of Windy area (Fig. 5)	11	3750	285	3200–4100
South-facing inactive rock glaciers, east half of Windy area (Fig. 5)	16	4400	350	3800–4900
Glaciers, west half of Windy area (Fig. 4)	13	4590	280	4000–4900
Glaciers, east half of Windy area (Fig. 5)	7	4730	280	4200–5200
B. UPPER END OF ROCK GLACIER AND GLACIER				
North-facing active rock glaciers, west part of Wood River area (Pl. 1)	12	5600	350	4900–6000
South-facing active rock glaciers, west part of Wood River area (Pl. 1)	4	5750	50	5700–5800
North-facing inactive rock glaciers, west part of Wood River area (Pl. 1)	11	5300	540	4000–5900
South-facing inactive rock glaciers, west part of Wood River area (Pl. 1)	6	5450	205	5200–5700
North-facing active rock glaciers, east part of Wood River area (Pl. 1)	18	5755	300	5300–6200
North-facing inactive rock glaciers, east part of Wood River area (Pl. 1)	12	4960	235	4700–5400
South-facing inactive rock glaciers, east part of Wood River area (Pl. 1)	12	5185	850	3800–6500
Glaciers, Wood River area (Pl. 1)	37	6640	385	6100–7500

Glaciers, Wood River area (Pl. 1)	37	6640	385	6100–7500

North-facing active rock glaciers, west half of Windy area (Fig. 4)	30	4670	165	4400–5200
South-facing active rock glaciers, west half of Windy area (Fig. 4)	7	4740	300	4300–5200
North-facing inactive rock glaciers, west half of Windy area (Fig. 4)	17	4260	330	3700–4900
South-facing inactive rock glaciers, west half of Windy area (Fig. 4)	15	4590	300	4300–5600
North-facing active rock glaciers, east half of Windy area (Fig. 5)	14	4820	250	4400–5300
South-facing active rock glaciers, east half of Windy area (Fig. 5)	8	5090	235	4700–5500
North-facing inactive rock glaciers, east half of Windy area (Fig. 5)	10	4340	275	3700–4600
South-facing inactive rock glaciers, east half of Windy area (Fig. 5)	18	4720	390	4100–5500
Glaciers, west half of the Windy area (Fig. 4)	13	5190	345	4700–6000
Glaciers, east half of the Windy area (Fig. 5)	7	5285	260	5000–5800
C. HIGHEST POINT ON AREA UPSLOPE FROM ROCK GLACIER AND GLACIER				
North-facing active rock glacier, west part of Wood River area (Pl. 1)	12	6775	290	6300–7300
South-facing active rock glaciers, west part of Wood River area (Pl. 1)	4	6650	165	6500–6900
North-facing inactive rock glaciers, west part of Wood River area (Pl. 1)	11	6140	720	4600–7000
South facing inactive rock glaciers, west part of Wood River area (Pl. 1)	6	6135	315	5500–6500
North-facing active rock glaciers, east part of Wood River area (Pl. 1)	18	7150	380	6300–7700
North-facing inactive rock glaciers, east part of Wood River area (Pl. 1)	12	6150	525	5000–7000
South-facing inactive rock glaciers, east part of Wood River area (Pl. 1)	12	6400	675	4900–7300
Glaciers, Wood River area (Pl. 1)	37	7062	350	6400–7700
North-facing active rock glaciers, west half of Windy area (Fig. 4)	28	5630	320	5000–6500
South-facing active rock glaciers, west half of Windy area (Fig. 4)	9	5780	445	5000–6600
North-facing inactive rock glaciers, west half of Windy area (Fig. 4)	20	5285	560	4200–6400
South-facing inactive rock glaciers, west half of Windy area (Fig. 4)	15	5470	370	4900–6200
North-facing active rock glaciers, east half of Windy area (Fig. 5)	15	5890	290	5300–6300
South-facing active rock glaciers, east half of Windy area (Fig. 5)	8	5840	310	5300–6200
North-facing inactive rock glaciers, east half of Windy area (Fig. 5)	9	5565	255	5300–6000
South-facing inactive rock glaciers, east half of Windy area (Fig. 5)	17	5535	410	4900–6200
Glaciers, west half Windy area (Fig. 4)	13	6083	335	5500–6500
Glaciers, east half Windy area (Fig. 5)	7	6086	180	5700–6300

active rock glaciers examined, a sharp contact could be observed on the front between the upper layer of rubble, 20–80 feet thick, and the lower layer of debris which contains an abundance of fines, 50–320 feet thick (see Figs. 1 and 2 of Pl. 2, Figs. 1 and 2 of Pl. 3). In general, the upper layer is one-quarter to one-fifth of the thickness of the rock glacier.

Texture of the upper surface and upper layer.—The sizes of fragments in the debris have been based on visual estimates made in the field or on estimates made from ground photographs of parts of rock glaciers in which some recognizable object furnished a scale (for example, Figs. 2 and 3 of Pl. 4). Most rock glaciers are derived from blocky fracturing rocks, such as granodiorite, greenstone, metavolcanic schist, stretched conglomerate, and latite. On these rock glaciers the average fragment ranges from 1 foot to 5 feet in length with blocks 5–15 feet common and some blocks more than 20 feet long. The average fragment size on a rock glacier derived from biotite-cordierite hornfels is 6 inches, and on the upper surface of rock glacier 51, which is derived from phyllite and slate, the average fragment size is 1–2 inches; large boulders are rare.

The average fragment size varies considerably from place to place on a single rock glacier. Bands of fragments of different size alternate. Longitudinal banding appears to owe its origin to differences in the jointing of cliffs from which the rock glacier is derived. Bands of coarse debris can be traced to parts of the headwall cliff where joints are widely spaced, and bands of finer debris can be traced to parts of the headwall that are more finely jointed. The boundary between two areas of differing fragment size is in some places distinct and coincides with a longitudinal furrow. Another type of banding appears to owe its origin to some process of differential sorting or differential fragmentation, not clearly understood. In this type of banding the coarser boulders may be concentrated along the bottoms of longitudinal or transverse furrows or along the crests of longitudinal or transverse ridges, or in both places. Fine material is most common along ridge crests, and along the down-valley sides of transverse ridges.

Originally observations were confined to estimates of the average size of the coarser material on the surface and the maximum size of the blocks. Toward the end of the 1954 season, we became aware that the upper layer of many rock glaciers has a bimodal fragment-size distribution. On rock glacier 37, for instance, the surface consists of large boulders averaging 3 feet in diameter, mingled with material with an average diameter of about 3 inches; material between 6 inches and 1½ feet in diameter is not common. To what degree this is true of all rock glaciers we cannot say.

Texture of the lower layer.—The nature of the lower layer can be deduced from exposures on the fronts of the rock glaciers. There the lower layer has much more fine material than the upper layer, as Figure 2 of Plate 2 and Figure 3 of Plate 3 show; in fact, the fine material so covers the front that the lower layer appears to contain very little coarse material, particularly near its top. A 4-foot deep excavation into an apparently very sandy part of the front of rock glacier 5 (Fig. 2 of Pl. 2, Pl. 5) made on July 26, 1954 disclosed that about 50 per cent of the lower layer, by volume, consists of blocks and fragments greater than 4 inches in diameter—some blocks are as much as 1 foot in diameter—and that the rest is small pebbles, interstitial sand and silt. No ice was seen.

In a few places, parts of the interior of rock glaciers are exposed in stream cuts and landslide scars. The material thus exposed consists of large and small angular blocks embedded in a matrix of solidly frozen mud (for example, on rock glacier 17, Fig. 5 of Pl. 3, and on rock glaciers 4, 30, and 52, Pl. 1 and Fig. 4).

Therefore, the lower layer probably contains just as many coarse blocks as the upper layer, but in the lower layer the interstices are filled with fine material, whereas in the upper layer they are open or filled with ice. The double-layered structure develops probably because (1) fine material sifts downward through coarse blocks to accumulate in the lower levels of the rock glacier, (2) meltwater moving along the top of the ice within the rock glacier washes fine material into the nearest cracks and moulins, and (3) abrasion of the coarser blocks in the lower parts of the rock glacier, where differential motion is greatest, produces fine-grained debris.

Ice Component

Evidence for the ice component.—Ice has been observed at a number of places on several rock glaciers. It has been found most commonly near the heads of the rock glaciers but has also been observed at the front. Clear ice was observed in interstices between boulders 1–3 feet

below the surface of rock glaciers 5, 30, 14, 22, and 23 (Pl. 1). All the observations were made within a few hundred feet of the heads of the rock glaciers. The dates of observation were July 19 and 23, 1954, for rock glaciers 14, 22, and 23, July 26, 1954, for rock glacier 5, and August 5, 1954, for rock glacier 30. Only two of these rock glaciers, 5 and 30, head in glaciers, and one, rock glacier 23, appears to be inactive.

Exposures of debris solidly cemented by interstitial ice were observed on the walls of gullies cut into the fronts of rock glaciers 4, 17, and 19 (Fig. 5 of Pl. 3). On the other hand, a 4 foot excavation into the front of rock glacier 5 disclosed no ice. Presumably, ice near the front of a rock glacier is buried by several feet of debris.

Our observations agree with those of Capps (1910, p. 362), who reported that he was able to reach ice in excavations a foot or two in depth near the heads of seven rock glaciers but was unable to reach it in shallow excavations near the fronts. According to Capps, all the ice was interstitial, cementing the debris of the rock glaciers. Domaradzki (1951) described many ice masses 6–9 feet thick and 3–6 feet below the surface near the heads of many of the Swiss rock glaciers.

Brown (1925) described a tunnel driven the length of a rock glacier in the San Juan Mountains of Colorado. This tunnel penetrated a few feet of ice-free rubble at the front, then 300 feet of rubble cemented by ice, and finally 100 feet of clean ice, before reaching solid bedrock at the head of the rock glacier.

Permafrost is common throughout the Alaska Range. It has been found in mines in the Nenana coal field and in most excavations for railroads and roads across the Alaska Range down to the lowest altitudes in the range. The depth to permafrost in these excavations ranged from 2 to 20 feet. Permafrost-free areas, if present, lie only beneath southward-facing slopes. However, even mines beneath southward-facing slopes have penetrated permafrost. Permafrost is in areas that were glaciated as recently as late Wisconsin time and in areas that were never glaciated. As has been indicated, the average annual temperature in lowland valleys in the Alaska Range is 5° F. below freezing; permafrost is therefore probably in equilibrium with the climate under most conditions. Conditions would be even more favorable to permafrost at high altitudes, where the climate is colder, and in northward-facing valley heads and on northward-facing walls of valleys, the sites of most rock glaciers. The cold springs emerging at the toes of many rock glaciers show that the rock glaciers contain water, but most of the water in them must be in the form of ice.

Source.—The ice in rock glaciers can form (1) from compacted snow, as does most glacier ice; (2) by the freezing of water derived from melting snow or rain; or (3) from ground water that rises beneath the talus and freezes on contact with cold air. Probably all three processes form the ice of most rock glaciers, although at some times in the history of a rock glacier one process will predominate.

The heads and feeding talus cones of most of the rock glaciers of the Alaska Range are nearly free of snow by the end of summer (Fig. 4 of Pl. 3, Pls. 6 and 7); hence it appears that compaction of snow is not today an important process in the formation of interstitial ice of rock glaciers. However, the climate was more rigorous during the nineteenth century than it is now, and at that time snowbanks could have persisted from year to year at the heads of many of the rock glaciers. The rock glaciers probably grew several hundred feet in length during that period; consequently, parts of many of them may today consist of mixtures of debris and névé-born ice.

Water from rain and from melting snow trickles down through the interstices of rubble on a rock glacier, where it can freeze. From time to time snow may drift into the interstices. The process by which meltwater ice could accumulate is analogous to the formation of some blue bands in glaciers (Journal of Glaciology, 1953). In the spring especially, meltwater trickling down through the snow and rubble would freeze upon reaching the top of the frozen layer of the year before.

Ground water in some permafrost regions is known to flow all winter. Where it emerges as springs, thick deposits of ice known as icings (Muller, 1945, p. 76) are built up in the winter. If a spring emerges in talus, the icing will form in the interstices. It will be insulated from melting during the following summer by rubble or debris, and an additional flow of ground water each winter will add new ice to the new talus. Eventually the thickness of ice-cemented talus would be great enough to cause it to flow as a rock glacier. Tyrrell (1910) has used the concept of icings in talus, which he calls "chrystocrenes", to explain a rock glacier on the outskirts of the city of Dawson, Yukon Territory, a locality outside the limits of Pleistocene

glaciation and several thousand feet below the theoretical firn line on northward-facing glaciers, yet in a region of climate favorable to permafrost.

Bedrock and the Distribution of Rock Glaciers

The bedrock formations of the Alaska Range are in roughly parallel bands that trend east and west, parallel to the range. These formations vary greatly in their behavior under frost weathering. The mountains of the northern part of the range, from the latitude of McKinley Park station northward, consist of metamorphic rocks locally intruded by granodiorite, granite, and fine-grained igneous rocks ranging in composition from rhyolite to basalt (Capps, 1912; Wahrhaftig, 1958, Pl. 1). Poorly consolidated Tertiary sedimentary rocks are present locally in low-lying areas but are not present within the zone of the rock glaciers. The metamorphic rocks of the northern part of the Alaska Range are of two types. The first type includes micaceous schists, probably of sedimentary origin, such as quartz-sericite schist, sericite schist, phyllite, and carbonaceous schist. Frost action weathers rocks of this type into slabs, plates, and flakes, and eventually into a great quantity of sand and silt consisting of grains of quartz and sericite. The second type includes metamorphic rocks, presumably of volcanic origin, which are for the most part free of sericite, and a quartzose gneiss that is a stretched conglomerate. Rocks of the second type as well as the igneous rocks intruding this area break down into approximately equidimensional blocks, fragments, and grains. The rocks of the Wood River area (Pl. 1) include representatives of most of these rocks.

The predominant rock units of the Windy area (Figs. 4 and 5) are massive greenstone and gabbro of Triassic age (Moxham *et al.*, 1953, p. 13–15) and the Cantwell formation, of Cretaceous age, consisting of conglomerate and sandstone. The greenstone and gabbro intrude or are interbedded with argillite, slate, graywacke, limestone, and phyllite and are intruded in turn by granodiorite in large stocks. Most of these rocks, except for the argillite, slate, limestone, and phyllite, weather by frost action into roughly equidimensional blocks and fragments.

The rock glaciers are predominantly derived from the blocky weathering rocks. A very few, including the Clear Creek rock glacier, are made of platy weathering sedimentary rocks. In the area shown in Plate 1 only three rock glaciers are derived from quartz-sericite schists, although quartz-sericite schists underlie almost half the area shown. The relative suitability of rock types is strikingly shown at rock glacier 1 in the small canyon in the northwest corner of the area shown in Plate 1. The south wall of the lower part of this canyon, composed of granodiorite, is flanked by an apron of lobate rock glaciers. The rock glaciers end abruptly where the contact between the granodiorite and the Birch Creek schist crosses the south wall of the canyon, and there are no rock glaciers in the higher parts of the canyon where the walls are made of quartz-sericite schist.

All the aerial photographs of the north side of the Alaska Range between the Nenana River on the west and the Gerstle River on the east (Fig. 1, inset) were examined stereoscopically for rock glaciers. The area investigated is 130 miles long and 10–30 miles wide and ranges in altitude from 2000 to 13,000 feet. Mountains of quartz-sericite schist as high as 9000 feet, well above the regional snow line, are included. Although the geology of this area is imperfectly known, the distribution of the major bedrock formations has been broadly determined by Capps (1912, Pl. 2) and Moffit (1954, Pl. 7), and the western part of the area has been mapped in detail by the senior author. There are very few rock glaciers in the areas mapped as Birch Creek schist (and none identifiable with certainty in the area east of the Little Delta River). However, rock glaciers are abundant in areas of greenstone and granodiorite on the Little Delta River and in an area of granite between the Delta River and the Gerstle River, as well as in all other outcrop areas of blocky weathering rocks sufficiently high to be in the zone of rock glaciers.

A quantitative study was made of four quadrangles of the Geological Survey 1:63,360 series (Healy D-2, D-3, D-4, D-5) for which detailed field investigations of the bedrock geology had just been completed by the senior author. Aerial photographs covering these four quadrangles were carefully examined for rock glaciers that might have been missed in field mapping. The valley heads were classified on the basis of the highest point of the watershed around each valley head, the direction in which the valley head faces, the rock type in the valley head, and whether or not it contains rock glaciers. The results of this study are shown in contingency tables (Table 7). The

rocks are grouped under two classes: blocky fracturing rocks and platy fracturing rocks. Blocky fracturing rocks include metavolcanic rocks, conglomerate, granodiorite, and hypabysal intrusive rocks. Platy fracturing rocks include various types of sericite and quartz-sericite schists.

TABLE 7.—CONTINGENCY TABLES FOR THE OCCURRENCE OF ROCK GLACIERS IN HEALY D-2, D-3, D-4, AND D-5 QUADRANGLES

	Blocky fracturing rocks*	Platy fracturing rocks†
A. Northward-facing valley heads with divides reaching 6500 feet or more in altitude		
Contain rock glaciers	31	3
Do not contain rock glaciers	10	15
B. Northward-facing valley heads with divides reaching altitudes between 5500 and 6500 feet		
Contain rock glaciers	13	0
Do not contain rock glaciers	7	44
C. Southward-facing, eastward-facing, and westward-facing valley heads with divides reaching altitudes between 6000 and 7000 feet		
Contain rock glaciers	11	1
Do not contain rock glaciers	2	10

* Includes granodiorite, metavolcanic schist (meta-rhyolite and meta-andesite), andesite, latite, and conglomerate.

† Birch Creek schist.

The technique of the use of the contingency tables is described by Hoel (1947, p. 191–193). The probability that the distribution shown in these tables could arise by chance is less than 1 in 1000. We have eliminated the bias caused by the tendency of schist mountains in general to have lower altitudes than mountains of other rock types by showing that this relationship holds regardless of altitude and direction of slope. Table 7 demonstrates quantitatively that micaceous schists are unfavorable for the development of rock glaciers, whereas blocky weathering rock types are favorable.

Talus slopes derived from the micaceous schists, especially in the region of active creep and solifluction above the upper limit of vegetation, consist of a mixture of large and small platy fragments of schist mixed with micaceous mud and sand derived from the schist. During most of the summer, and especially immediately after the spring thaw, this material is saturated with water and is a plastic mass into which one sinks a few inches at every step. Solifluction and creep are extremely active at these times. If solifluction or some other mass-wasting process that operated within the layer subject to annual freezing and thawing were instrumental in producing rock glaciers, the micaceous schist terrain would be an ideal place for their occurrence.

The blocky fracturing rocks, on the other hand, provide talus that does not move noticeably by solifluction during the spring thaw. Such talus is equigranular and open, and water drains quickly through it. However, it has an abundance of interconnected voids, in which interstitial ice could accumulate. Thus the tendency of rock glaciers to be composed of debris that provides for the greatest interstitial accumulation of ice, without itself possessing any tendency toward mobility, supports the belief that rock glaciers owe their origin to interstitial ice.

MICRORELIEF ON THE ROCK GLACIERS

Introduction

The upper surfaces of most rock glaciers are covered wholly or in part by striking and characteristic microrelief. This microrelief was probably caused by two kinds of processes: one involves the accumulation and wasting away of ice; the other involves variations in the rate of flow of rock glaciers. Microrelief caused by processes of the first kind includes most longitudinal ridges and furrows, all conical pits, and the large pits at the heads of some rock glaciers. Microrelief caused by processes of the second kind includes transverse ridges and furrows, some of the longitudinal ridges and furrows, especially the "lateral moraines" that border some rock glaciers, and crevasses and lobes.

Longitudinal Ridges and Furrows

Longitudinal ridges and furrows are present on most of the larger rock glaciers. In the Wood River area they are on nearly all tongue-

shaped and spatulate rock glaciers but are on less than half of the lobate rock glaciers.

The ridges are rounded in cross section, and the furrows are, in general, V-shaped. Ridge crests are spaced 25–300 feet apart, spacings of 50–150 feet being most common. Relief of the longitudinal ridges of nine rock glaciers as determined in the field ranges from 3 to 40 feet but is generally 5 to 20 feet. Most longitudinal ridges and furrows extend the greater part of the length of the rock glacier; these ridges and furrows range from about 200 to 3000 feet in length. Lengths of 1000 to 2000 feet are most common (see Pl. 5, rock glaciers 5 and 9, Figs. 1 and 2 of Pl. 4, Fig. 3 of Pl. 7 (rock glacier 46), and Fig. 12). Generally each ridge heads at or near the base of a talus cone that feeds the rock glacier, and each furrow heads at an intercone swale (Fig. 4 of Pl. 3). In general the furrows line up more closely with the intercone swales than ridges do with the talus cones. Snowbanks were observed in the intercone swales and in the upper parts of most longitudinal furrows late in August and early in September, both in the field and on aerial photographs taken at that time of the year (Fig. 4 of Pl. 3, Pls. 5, 6, and 7). Some snowbanks probably persist from year to year.

On some rock glaciers, longitudinal ridges and furrows extend to the front (Fig. 1 of Pl. 4; Fig. 12), and each ridge behaves like a separate rock glacier. On other rock glaciers the furrows join down-valley, ending the intervening ridges where they join. On most rock glaciers the longitudinal ridges and furrows die out near the front. On lobate rock glaciers the

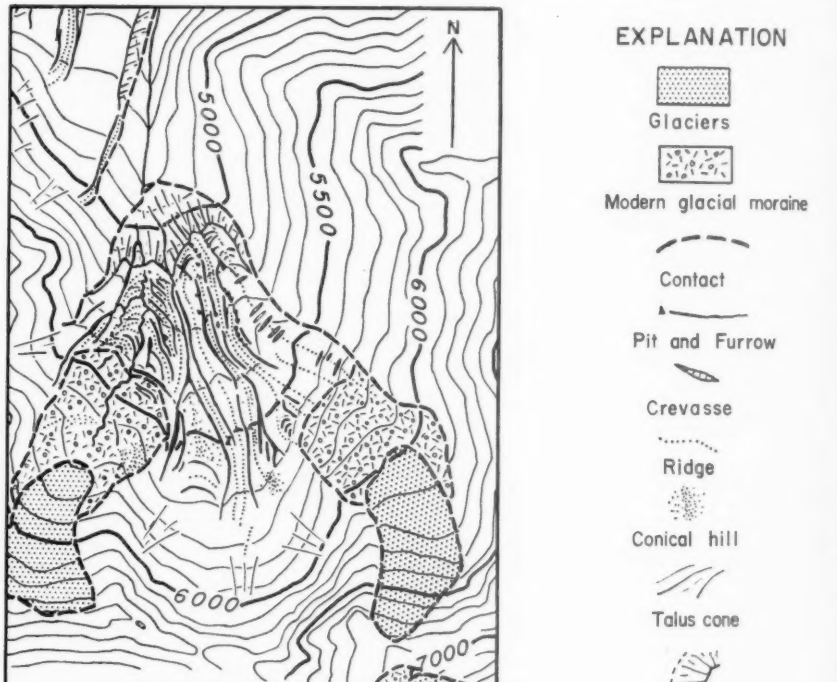

FIGURE 12.—MAP OF A TYPICAL TONGUE-SHAPED ROCK GLACIER (ROCK GLACIER 33) WITH LONGITUDINAL RIDGES AND FURROWS

For location see Plate 1. Base enlarged from U. S. Geological Survey topographic map of Healy D-2 quadrangle.

furrows die out before they reach the front, and the ridges tend to merge with a low frontal ridge.

Many rock glaciers are bordered on one or both sides by prominent ridges that could be likened to the lateral moraines of glaciers. Some of these "lateral moraine" ridges stand slightly higher than the surface of the rock glaciers and die out toward the front. Others are at the same level as the rest of the upper surface of the rock glacier but are separated from it by a sharp furrow; such ridges do not die out but extend to the front. Transverse ridges if present on the same rock glacier die out against these lateral ridges or bend sharply to merge with them.

Where talus cones stem from bedrock of differing lithology, each longitudinal ridge is composed of bedrock fragments of the talus cone at its head, and the contacts on the rock glacier of rubble from different bedrock sources generally coincide with the furrows (Figs. 1 and 2 of Pl. 4). Similarly, some ridges on a rock glacier have much coarser debris on their surfaces than others; this reflects differences in the coarseness of debris on the talus cones at their heads. The lithology of the ridges indicates, therefore, that the longitudinal ridges and furrows develop at the head of the rock glacier and maintain their identity during its forward movement.

On a few rock glaciers, including rock glaciers 23 and 55 (Fig. 2 of Pl. 4), the coarse rubble is on the tops of the ridges, whereas the fine rubble is on the sides; on rock glacier 37, on the other hand, the coarse rubble is in the furrows. Platy boulders in the furrows commonly have a preferred orientation parallel to the length of the furrows and are almost vertical. This orientation may be due to lateral thrust by frost action from the sides of the furrows (R. P. Sharp, 1958, personal communication).

Commonly, the tops of the ridges bear lichens and other vegetation, whereas the sides and bottoms of the furrows are free of vegetation (note especially rock glacier 46, Fig. 3 of Pl. 7; also Fig. 4). This could be attributed to the adverse effect of lingering snowbanks on vegetation growth or may be due to the collapse of the sides into the furrows.

Most of the longitudinal ridges and furrows can be explained if one assumes that mixtures of névé and talus accumulate beneath the swales between the talus cones at the head of the rock glaciers. Talus cones increase in volume by addition of material onto their surfaces; for the rock glaciers to be fed by these talus cones, the material within the cone must flow downward and outward. In this respect a rock glacier would behave like the cirque glacier described by McCall (1952). The snowbanks filling the intercone swales would likewise be drawn down and forward by the motion of the rock glacier. During winter and spring, when much debris is being supplied to the talus, snow drifts into the swales, filling the snowbanks up to the level of the surface of the talus cones. As the surfaces of the talus cones rise by accumulation of debris, the surfaces of the snowbanks would rise with them. The intercone areas at the head of the rock glacier would then consist of névé in which rock fragments are suspended, and the talus cones would consist of rubble and debris with interstitial ice. As a given segment of the rock glacier moves away from the shade of the cliff, the snowbanks would be exposed to more and more sunlight. They would melt, leaving furrows, meltwater running down the furrows would further deepen them by thawing the ice protected from the sun by the cover of debris. Mass wasting of material into each furrow from the sides would round the intervening ridges.

Longitudinal ridges and furrows may also be enlarged and possibly caused by variations in the rate of flow within a rock glacier. The surface velocity of rock glaciers is observed to be greatest in the center, decreasing toward each side. Longitudinal shear movement would probably be concentrated along any longitudinal zones of weakness between the center and sides. Transverse ridges and furrows on some rock glaciers are interrupted by and apparently displaced along longitudinal furrows. This suggests that shear takes place along some longitudinal furrows. The zones of weakness along which shear movement occurs could be the ice-rich bands on which the furrows are forming. A bedrock ridge projecting up into the body of the rock glacier may also develop a zone of weakness downstream along which longitudinal shear movement could take place. Longitudinal shear planes may develop near the sides of a rock glacier owing to an increase in "viscosity" as the sides become less ice-rich. This might be especially true in a rock glacier confined in a valley, for in such a rock glacier the frictional resistance of the rock glacier against the valley wall might be greater than the friction along some longitudinal planes within the rock glacier, and longitudinal shear might take place

along these planes. The shear planes would appear as furrows on the surface of the rock glacier. The material in the lateral portion of the rock glacier between the shear plane and the side would be moving more slowly than the material in the center of the rock glacier; if material is supplied to these lateral portions at the same rate per unit of width as it is to the central portion of the rock glacier, these more slowly moving lateral portions would have to be thicker than the center. They would stand up above it as ridges, separated from the central portion by sharp furrows. The "lateral moraine" ridges of rock glaciers might be formed in this way. Krauskopf (1948) has observed the actual formation of such "lateral moraines" on lava flows. Mudflow levees (Sharp, 1942) are somewhat similar.

Conical Pits and Meandering "Furrows"

Steep-sided pits are common on some rock glaciers and rare on others. Generally the walls of these pits come together in a point or line at the bottom and are at the angle of repose (Fig. 3 of Pl. 4). The pits are commonly bare of vegetation and show evidence of recent collapse, particularly near the heads of the rock glaciers. Some pits have ponds; others contain thin deposits of silt and abandoned shore lines of temporary ponds marked by coatings of silt on pebbles and blocks.

On many rock glaciers, particularly those that extend down-valley from small glaciers, there is an irregular row of conical pits that join down-valley to form what appears in the aerial photographs to be an irregular furrow (note especially rock glacier 10 and 15 in Pl. 5, rock glacier 24 in Pl. 6). The collective feature is called herein a meandering furrow; these generally extend down-valley from the point of discharge of meltwater from the glacier. Generally the meltwater stream flows on the surface of the rock glacier as far as the uppermost pit, into which it disappears. Water can be heard running beneath the furrows immediately upstream from some of the pits, but never immediately downstream from them.

Conical pits, both isolated and in rows as meandering furrows, occur also along longitudinal furrows. It seems likely that they are formed solely by thawing of ice and removal of fines by water that descends into the depths of a rock glacier through a crack. Collapse of the debris into the moulin so formed gives the conical pit its characteristic shape. The presence of conical pits and meandering furrows along longitudinal furrows supports the idea that the longitudinal furrows mark concentrations of ice within the rock glacier.

Large Pits at the Heads of Rock Glaciers

Large pits occur at the heads of many rock glaciers (*cf.* rock glacier 5, Pl. 5; rock glaciers 27 and 30, Pl. 6). These are not properly called microrelief, as their dimensions approach those of the rock glaciers themselves. They are believed to be due to the melting of ice, in this case the clear ice of a glacier at the head of the rock glacier. The down-valley wall of each pit is a steep embankment 50–150 feet high of stagnant ice veneered with debris. Presumably this stagnant ice grades abruptly down-valley into material which is typically found in rock glaciers. The upvalley side of most pits is the surface of the small cirque glacier, relatively free of debris. For example, the surface of the glacier at the head of rock glacier 5 (Pl. 5) is 25 per cent bare ice at its lower end and 75 per cent bare ice at its upper end. Figure 6 of Plate 3 shows the glacier which is nearly free of debris at the head of rock glacier 34.

The glaciers of the Alaska Range have been retreating from a maximum stand attained sometime within the last hundred years. This maximum stand is marked by a trim line of lichens on most of the cirque walls around the glaciers. Where rock glaciers lie down-valley from the glaciers, this trim line coincides with the top of the down-valley wall of the large pit at the head of the rock glacier, indicating that when the glaciers were at their maximum stand, they filled the pits, and the surface of ice and debris sloped continuously from the head of the glacier to the front of the rock glacier. The pits exist today because the bare glacial ice has wasted away much more rapidly than the interstitial ice within the rock glacier.

Transverse Ridges and Furrows

Transverse ridges and furrows are present on about half the rock glaciers. They are perhaps the most striking microrelief features of the rock glaciers and are the ones that convey most strongly the impression of glacierlike or lavalike flow. From 2 to 35 or more parallel ridges occur on the upper surface of a rock glacier. They commonly extend across the entire width of the rock glacier or else join prominent lateral ridges along one or both of its sides, either at a sharp

FIGURE 13.—MAP OF ROCK GLACIERS WITH TRANSVERSE RIDGES AND FURROWS

Note effect of bend in rock glacier 49, near top, on pattern of transverse ridges and furrows. Rock glacier 50 is a typical spatulate rock glacier. Base enlarged from U. S. Geological Survey topographic map of Healy B-5 quadrangle. Geology by interpretation of aerial photographs. For location see Figure 4.

angle or by gradually bending around, parallel to the sides. (See rock glaciers 51, Fig. 1 of Pl. 7; 7 and 15, Pl. 5; 24 and 27, Pl. 6; Figs. 13 and 15.) Ridge crests are 15–200 feet apart and stand 5–20 feet above the furrows on their down-valley sides and 3–10 feet above the furrows on their upvalley sides (Fig. 4 of Pl. 4). The ridges are broadly convex in cross profile, and the furrows are V-shaped (Figs. 4 and 5 of Pl. 4). The down-valley side of each ridge is fairly steep, although rarely as steep as the angle of repose, and on many ridges it is bare of vegetation. The upvalley side of each ridge slopes more gently, and the top and upvalley side of each ridge are commonly covered with a continuous mat of vegetation, either turf or lichens. There is commonly no variation in the lithology or average size of the fragments making up the surface rubble from ridge to ridge. On the other hand, the fragments appear to be larger on the tops and upvalley sides of the ridges than on down-valley sides, possibly because slumping on the down-valley side uncovers fine material that has disappeared from the surface of the rock glacier by sifting down between the larger fragments (R. P. Sharp, 1958, personal communication). Some ridges show by the torn turf, moss, or lichens strewn about their down-valley base that they have moved over their down-valley furrows. Locally, tabular blocks in the furrows are oriented parallel to the furrows and stand vertically.

Transverse ridges and furrows are generally bowed downstream in plan; some are nearly straight, and the radius of curvature on others may be as short as a few hundred feet along the midline of the rock glacier. They are never concave downstream in ground plan. At the point where transverse ridges join "lateral moraine" ridges, the radius of curvature ranges from less than 20 feet for nearly straight transverse ridges to more than 200 feet for transverse ridges that are continuously arcuate across the rock glacier.

The convex side of an active rock glacier that bends in its course is mantled by a lichen and turf cover which is continuous with the vegetation on the upper surface and with the turf meadow at the base. The concave side and the front are barren. Transverse ridges on such a rock glacier are spaced closely on the convex side and diverge toward the concave side (see rock glacier 15, Pl. 5 and rock glacier 49, Fig. 13). The ridges bend to become tangent to the convex side and merge there into one or several ridges parallel to the side. On the concave side, either the transverse ridges and furrows extend to the side, meeting it at an angle of about 90°, or the furrows die out abruptly where the ridges join a "lateral moraine" ridge at right angles to them. The impression given by such a rock glacier is that the concave side is in motion, whereas the convex side apparently is not moving, or at most is moving very slowly.

In a rapidly moving stream, particularly if it is turbulent, motion is "inertial", and the maximum velocity tends to be on the convex side of a bend. The motion of a rock glacier, on the other hand, is laminar and noninertial, and the maximum velocity will be along the steepest slope, regardless of its position. Generally the steepest slope is on the concave side of a bend. Similar behavior has been observed on extremely slow-flowing rivers (Rubey, 1952, p. 129).

On the concave side of a bend, then, the transverse ridges and furrows would draw apart, whereas on the convex side they would be forced together. Because of the change in direction at a bend, amounting in some cases to 90° or more, the transverse ridges and furrows on the convex side would appear to be longitudinal ridges and furrows farther downstream.

Transverse ridges and furrows on rock glaciers resemble the transverse ridges and furrows that develop on parts of many other nonturbulent flows such as lava and glaciers (Anderson, 1941, Pl. 6; Haefeli, 1951, p. 498; Ives and King, 1954; Leighton, 1951; Washburn, 1935, p. 1885–1889; Williams, 1944, Pl. 12). Most of those on lava flows and glaciers appear to be associated with a downstream decrease in velocity.

A downstream decrease in velocity must be accompanied by an increase in cross-sectional area perpendicular to the direction of flow, provided that the material is incompressible and provided that no matter is removed from the flow, as occurs in ablation of a glacier. The cross-sectional area can be increased by either thickening or widening the flow. If the width is restricted, the flow must thicken, and the average distance along the direction of flow between two particles must decrease in proportion to the decrease in velocity. The development of transverse ridges and furrows on rock glaciers commonly appears to be related to such an increase in thickness. Photographs of glaciers and lava flows suggest a similar relationship.

An increase in thickness and contraction in the direction of flow might produce transverse ridges in several ways. Folds or wrinkles on the

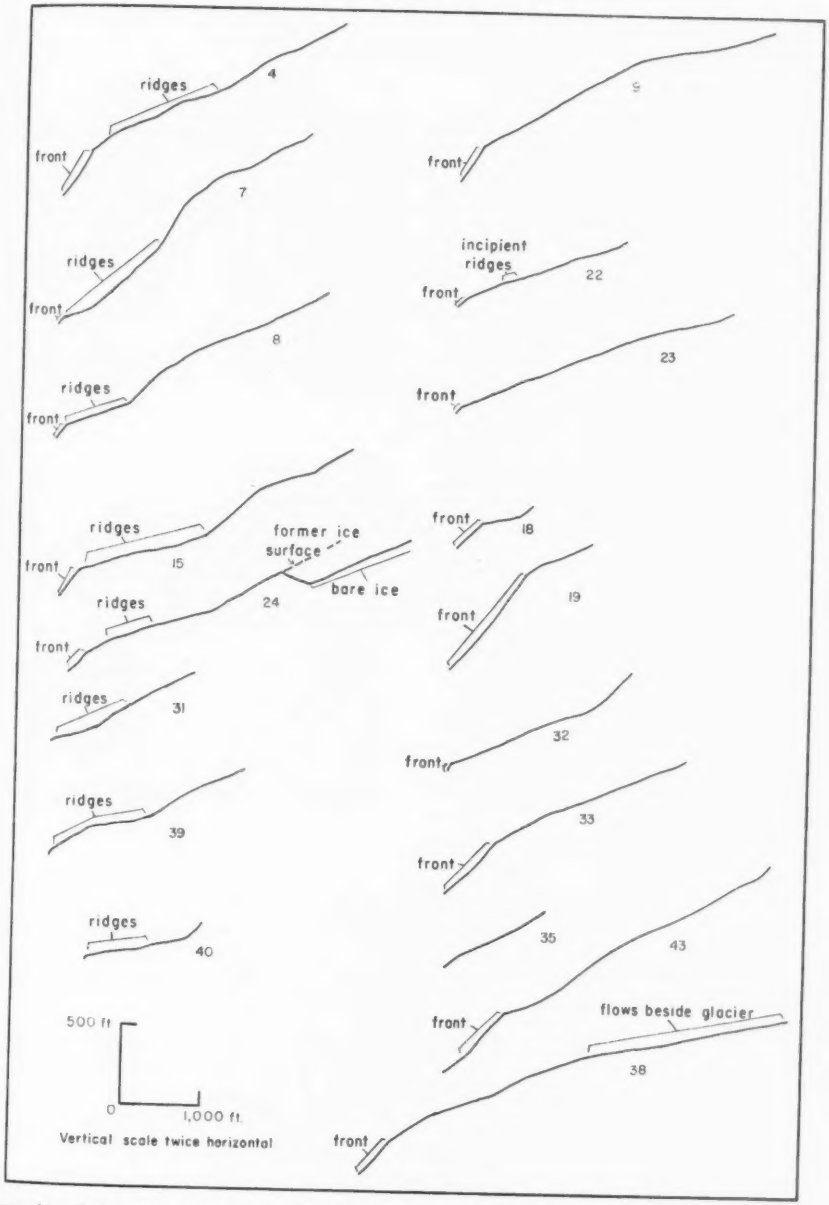

FIGURE 14.—PROFILES OF ROCK GLACIERS WITH TRANSVERSE RIDGES COMPARED WITH PROFILES OF ROCK GLACIERS WITHOUT TRANSVERSE RIDGES

Numbers beside profiles indicate designation of rock glaciers in accordance with numbering on Plate 1.

TABLE 8.—CONTINGENCY TABLES SHOWING CORRELATION BETWEEN CAUSES FOR DOWNSTREAM THICKENING OF ROCK GLACIERS AND PRESENCE OF TRANSVERSE RIDGES AND FURROWS

	Transverse ridges and furrows present	Transverse ridges and furrows absent
A. Wood River area		
Cause for thickening recognized	24	4
Cause for thickening not recognized	1	21
B. Windy area		
Cause for thickening recognized	19	3
Cause for thickening not recognized	1	15

upper surface would be expected if the upper layers of the flow were more resistant to deformational stresses than the lower layers. This is probably the mechanism linking an increase in thickness with the development of ridges on lava flows. A second possibility is that overthrusting along closely spaced fault surfaces produces the thickening and contraction in the direction of flow; on rock glaciers, the ridges formed by overthrusting would be rounded by slumping and mass wasting of loose surface material as they formed. An observation supporting this mechanism is that the lichen cover on the downstream sides of ridges is occasionally disrupted. Nye (1951) predicted such overthrusting accompanying a decrease in slope in the plastic flow of ice, and such overthrusting has been observed on some glaciers. From theoretical considerations Hubbert (1951) predicted low-angle overthrusting in a situation similar to the thickening due to a restriction in the width of a channel, and he produced such overthrusts in sand, with a surface expression similar to the transverse ridges of rock glaciers. A third possibility is that the ridges correspond to annual cycles of growth, as has been suggested for ogives on glaciers. The great difference between the amount of annual movement of rock glaciers and the distance between successive ridges makes this explanation unlikely.

The hypothesis that transverse ridges and furrows are associated with a downstream decrease in velocity and increase in thickness cannot be tested directly, since the necessary velocity and thickness data are not available. However, transverse ridges and furrows are not present on all rock glaciers, and their presence or absence can be compared with the occurrence of circumstances that probably cause a downstream thickening and decrease in velocity. The following five types of circumstances that could have such an effect have been observed in the Wood River and Windy areas.

(1) A downstream decrease in velocity would be produced by a downstream decrease in the slope of the flow. Figure 14 compares the slopes

PLATE 4.—MICRORELIEF ON ROCK GLACIERS

FIGURE 1.—View of rock glacier 55, looking south, showing longitudinal ridges and furrows. For location see Figure 1.

FIGURE 2.—Detail of longitudinal ridges and furrows on rock glacier 55, looking south from upper surface near front. Man standing at edge of snowbank in lower right corner of picture is 6 feet tall. Compare with Figure 1 of Plate 4.

FIGURE 3.—Conical pit on longitudinal furrow. Looking north from Boulder Number 4 of upper line, Clear Creek rock glacier (rock glacier 51). The stadia rod is 13 feet long. Note transverse ridges descending to a longitudinal furrow in background.

FIGURE 4.—View of upper surface of Clear Creek rock glacier (rock glacier 51) looking west from transit station, showing roll-like transverse ridges and furrows on its upper surface. For location see Figure 4. Compare with Figure 1 of Plate 7 and Figure 3 of Plate 4.

FIGURE 5.—View south on the surface of rock glacier 15 (see Pl. 1). Large south-trending transverse ridges end on the far side of a meandering furrow in the foreground. Compare the appearance on the ground with the appearance in aerial photographs of Plate 5.

PLATE 5.—STEREOTRIPTYCH OF AN AREA AT THE HEAD OF VIRGINIA CREEK SHOWING ROCK GLACIERS AND GLACIERS

For location and designation of rock glaciers see Plate 1. North arrow approximately 3500 feet long. Photographs by U. S. Air Force.

FIGURE 1

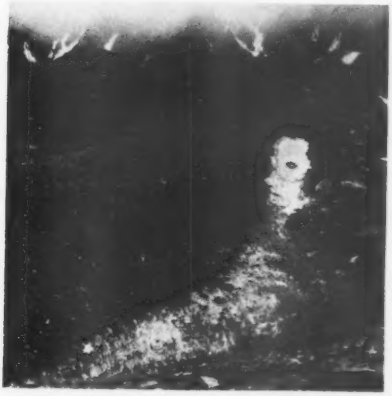

FIGURE 2

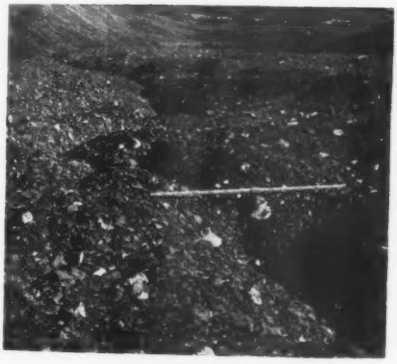

FIGURE 3

FIGURE 4

FIGURE 5

MICRORELIEF ON ROCK GLACIERS

STEREOTRIPTYCH OF AN AREA AT THE HEAD OF VIRGINIA CREEK SHOWING ROCK GLACIERS AND GLACIERS

STEREOTRIPTYCH OF AN AREA ON THE WEST FORK OF THE LITTLE DELTA RIVER
SHOWING ACTIVE AND INACTIVE ROCK GLACIERS

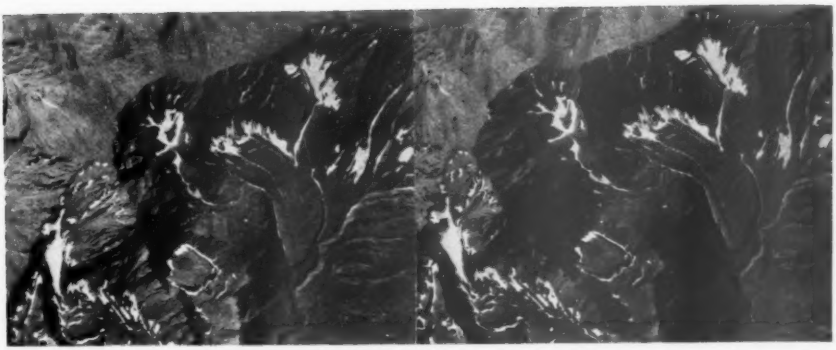

FIGURE 1

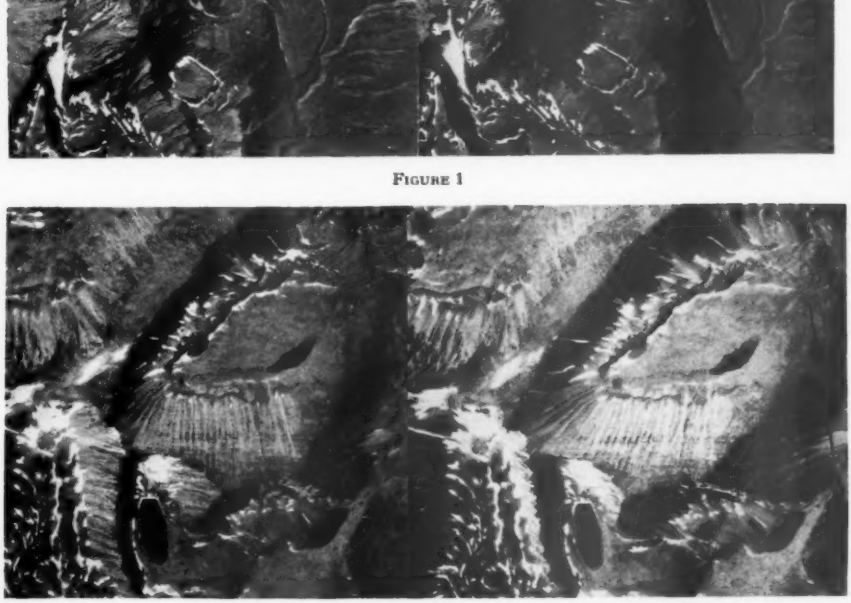

FIGURE 2

FIGURE 3

VERTICAL STEREOSCOPIC VIEWS OF ROCK GLACIERS
AND GLACIALLY OVERRIDDEN ROCK GLACIERS

of several rock glaciers that have transverse furrows with the slopes of several that do not. Every rock glacier with transverse ridges and furrows has a concave break in slope immediately above the ridges; with few exceptions, the rock glaciers that lack transverse ridges and furrows have straight or convex longitudinal profiles.

(2) If the slope and width of a flow remain constant but the resistance of the material to deformational stresses increases downstream (as, for example, by a downstream increase in viscosity) the velocity must decrease and the thickness increase. Where a glacier lies at the head of a rock glacier, the apparent viscosity of the rock glacier is probably greater than that in the glacier, and there should be a downstream thickening of the flow, even though the slope is uniform. Examples of rock glaciers with glaciers at their heads are rock glaciers 10 (Pl. 5), 17 (Pl. 1 and Fig. 1 of Pl. 2), and 48 (Fig. 4 and Fig. 3 of Pl. 7).

(3) The stress necessary to cause a rock glacier to flow across a flat surface is provided by the pressure gradient that is produced by the slope of its upper surface (Nye, 1952). After the front of a rock glacier that is advancing across a flat valley floor passes any point in its path, the thickness of the rock glacier at that point must continually increase in order for the slope of the upper surface to be maintained as the front advances away from that point. The thickness may be increased by shearing within the rock glacier, which would result in transverse ridges and furrows on the upper surface.

(4) A decrease in the width of the rock glacier caused by a constriction in its course would require an increase in thickness. Parts of rock glacier 33 (Pl. 1) and rock glacier 10 (Pl. 5) exemplify this situation.

(5) A sharp bend in the valley occupied by a rock glacier, by stopping its flow in one direction and redirecting it, may cause transverse ridges and furrows to be produced (Fig. 13).

Table 8 is a contingency table showing the results of a study grouping each of 50 rock glaciers in the Wood River area and 38 rock glaciers in the Windy area on the basis of the presence of one of the five causes listed and also on the basis of the presence of transverse ridges and furrows. For a large number of these rock glaciers, two or more causes were present. On each rock glacier, the transverse ridges and furrows appeared near or downstream from the cause that was farthest upstream on the rock glacier. The table indicates a very strong correlation between the causes that could lead to thickening of the rock glacier and the presence of transverse ridges and furrows.

Crevasses and Landslide Scarps

Crevasses are straight narrow trenches 1–10 feet deep, 3–30 feet wide, and as much as a few hundred feet along. Their sides are at the angle of repose and meet with a sharp angle along the bottom. The crevasses cross transverse ridges at a large angle, usually nearly 90°. Commonly the crevasses make angles of 45° with the sides and trend down-valley and outward from the axis

PLATE 6.—STEREOTRIPTYCH OF AN AREA ON THE WEST FORK OF THE LITTLE DELTA RIVER SHOWING ACTIVE AND INACTIVE ROCK GLACIERS

For location and designation of rock glaciers see Plate 1. North arrow is approximately 3000 feet long. Photographs by U. S. Air Force.

PLATE 7.—VERTICAL STEREOSCOPIC VIEWS OF ROCK GLACIERS AND GLACIALLY OVERRIDDEN ROCK GLACIERS

FIGURE 1.—Stereoscopic view of rock glaciers 51 and 52 at the head of Clear Creek. Left-hand margin trends due south and covers approximately 6000 feet. North is to the bottom. The younger rock glacier (51) in its advance is filling gullies carved into the older rock glacier (52). Note transverse ridges and furrows on rock glacier 51. The motion of this rock glacier has been measured. For location see Figure 4. Compare with Figure 6. Photographs by U. S. Air Force.

FIGURE 2.—Stereoscopic view of an area at the head of Riley Creek, showing an apron of lobate rock glaciers lining the walls of a cirque. Arrow points north and is approximately 3500 feet long. Note that the rock glaciers at the base of northward-facing cliffs are much larger than those at the base of southward-facing cliffs. For location see Figure 4. Photographs by U. S. Air Force.

FIGURE 3.—Stereoscopic view of the head of a fork of Riley Creek, showing rock glacier 46, an active rock glacier with exceptionally deep longitudinal furrows; rock glacier 47, a rock glacier that has been overridden by a glacier; and rock glacier 48, a rock glacier with a pit at its head from which a glacier has melted. Arrow points north and is approximately 3500 feet long. For location of rock glaciers see Figure 4. Photographs by U. S. Air Force.

(rock glacier 10, Pl. 5). The rare crevasses that extend across rock glaciers are concave down-valley (Fig. 13). Crevasses are most common on rock glaciers that have arcuate transverse ridges and that are expanding laterally downstream (rock glacier 27, Pl. 6). They are common on rock glaciers that are down-valley from glaciers and are rare on rock glaciers without glaciers at their heads. Rock glaciers 3, 10, and 27 (Pls. 1, 5, and 6), for example, have many crevasses. The general appearance and location of the crevasses support the idea that they are tension cracks. If a rock glacier enters a wide part of a valley, where it spreads laterally, or if the central part moves rapidly past the sides, tension results. Tension cracks open in most cases parallel to the direction of maximum shortening—in other words, nearly normal to the transverse ridges. These cracks are similar to the crevasses on glaciers. They are quickly filled by debris sliding in from the sides and are consequently marked by sharp straight trenches.

Features somewhat related to crevasses are small imperfect scarps, concave down-valley, that can be detected in the aerial photographs across the steeper parts of rock glaciers that have a steepening in their course approaching the angle of repose (*e.g.* rock glacier 50, Fig. 13). These are regarded as incipient landslide scarps. Locally, rock glaciers descending a steep slope may disintegrate. For example, rock glacier 30 (Pl. 6) has broken into several rotational shear-slip landslide blocks where it descends a steep part of its valley.

Lobes

Lobes are rounded tonguelike mounds that rise sharply on their down-valley and lateral margins and merge gradually upvalley with the upper surface of the rock glacier. They are 5–50 feet high on their down-valley sides, and 100–400 feet across. They resemble small rock glaciers perched on the backs of larger ones.

Lobes are present only on rock glaciers that appear to have been reactivated (Fig. 3 of Pl. 2, Fig. 15). They are generally near the heads of rock glaciers that have turf-covered or lichen-covered fronts. The fronts and sides of the lobes are free of turf and lichens, and the lobes appear to have advanced forward over the surface of the rock glaciers down-valley from them. Hence a line of lobes marks the boundary between the down-valley segment of the rock glacier that is inactive and an upvalley part that shows signs of activity. They are thought, therefore, to result from the incomplete reactivation of a rock glacier. The alternative explanation that they are small debris flows seems unlikely because (1) there are no gullies or scars upvalley from which they could have come, and (2) their upper surfaces slope gradually upward to the talus cones at the head of the rock glacier and resemble in every other respect the upper surfaces of rock glaciers without lobes.

Unexplained Features

In addition to the microrelief described, there are some rare features that cannot be explained satisfactorily. Most common of these are small isolated conical or ridgelike hills that are generally near the heads of rock glaciers, especially just down-valley from the lower ends of cirque glaciers. They may be a product of melting ice and could be ice-cored debris cones. Two of these hills on rock glacier 4 (Pl. 1) are sharp-crested zigzag ridges extending down the length of the rock glacier, 150 and 400 feet long. Explanation of these as debris cones contradicts the hypotheses which explained the longitudinal and transverse ridges on the same rock glacier.

Other unexplained features are shallow depressions at the heads of some rock glaciers. Many lobate rock glaciers, for instance, have broad depressions 10–15 feet deep along their heads. On some, such as rock glacier 16 (Pl. 5), these depressions have a steep wall on the down-valley side. These depressions may mark the positions occupied during the latter half of the nineteenth century by perennial snowbanks, or they might mark areas that once had more interstitial ice and névé.

Inactive Rock Glaciers

Less than half the rock glaciers we studied have the steep bare fronts and the angle between the front and the upper surface that indicate that they are active. Most of the others do not appear to be in motion. The fronts of these other rock glaciers slope at angles of 20°–35° and are convex upward, joining the upper surface in a smooth curve (Fig. 2 (foreground) and Fig. 3 of Pl. 2, Fig. 15). The fronts are clothed with turf or lichens which form a cover of vegetation continuous with the vegetation on the upper surface of the rock glacier and with the vegetation on the valley floor down-valley from the front. Generally

there are no fresh breaks or tears in the mantle of vegetation. Lichens mantle the upper and outward-facing surfaces of the boulders, giving the rock glacier a somber aspect, and comphotographs (compare especially Pl. 6 with Pl. 1). Bare fronts are markedly lighter in tone in the aerial photographs than lichen-covered fronts, and rounded fronts can be distinguished

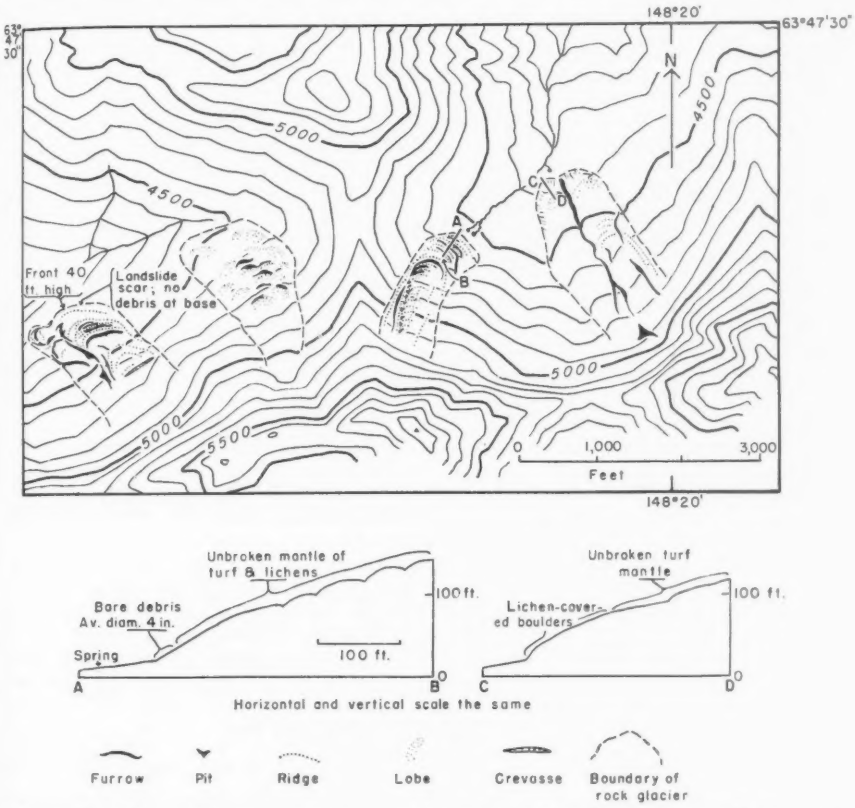

FIGURE 15.—MAP AND PROFILES OF INACTIVE AND REACTIVATED ROCK GLACIERS AT THE HEAD OF MOODY CREEK

The rock glaciers at the extreme west and east are reactivated; the two in the center are inactive. Base enlarged from U. S. Geological Survey topographic map of Healy D-3 quadrangle. For location see Figure 1.

monly lichens from neighboring boulders intertwine. The undersides of boulders, even where exposed to air, are completely devoid of vegetation.

Any motion within the rock glacier would tip or dislodge the boulders on the front and would disturb the turf and lichens. Therefore the rock glaciers with such a mantle on their fronts cannot have moved forward for at least the length of time necessary for its accumulation. Active and inactive rock glaciers are easily distinguished in stereoscopic study of aerial from fronts that are straight in cross profile and have a sharp angle at the top. On the basis of field investigation, study of colored and black-and-white ground photographs, and study of aerial photographs, the rock glaciers in the Wood River area (Pl. 1) have been mapped as active rock glaciers, inactive rock glaciers, and reactivated rock glaciers; the same distinctions were made in the Windy area (Figs. 4 and 5) on the basis of study of air photographs only.

The active rock glaciers appear to be thicker than the inactive rock glaciers, and their fronts

are higher. Height of front of many rock glaciers in the Wood River area was determined by several methods, including direct measurements with a hand level in the field, measurements by comparison with known distances in ground photographs, parallax measurements on aerial photographs, and estimation from the topographic map. For most rock glaciers, two or more methods were used, and agreement was usually within 20 or 30 feet. The average height, range, and standard deviation of height of the fronts of active and inactive rock glaciers are shown in Table 9. Some active rock glaciers have abnormally high fronts because they are spilling down steep slopes (Fig. 10). These were not included in the computations leading to Table 9. A Student's t test of the differences between means shows that there is a 95 per cent probability on the basis of these small samples that the inactive rock glaciers average at least 40 feet (or 25 per cent) thinner than the active rock glaciers. In spite of the difference in height, the microrelief on many inactive rock glaciers is perfectly preserved, and the ridges are comparable in height to those on active rock glaciers.

TABLE 9.—HEIGHTS OF ACTIVE AND INACTIVE ROCK GLACIERS IN THE WOOD RIVER AREA

	Active rock glaciers	Inactive rock glaciers
Average height of front	170 feet	74 feet
Range in height of front	90–350 feet	30–125 feet
Standard deviation $(s^2)^{1/2}$	79 feet	24 feet
Number in sample	10	13

This disparity in height suggests that rock glaciers decrease in thickness when they become inactive. The decrease may be caused in large part by continued flow of the rock glacier at a diminished rate after the supply of talus ceases. The rock glacier would spread and thin, much as masses of tar do. Apparently motion does not occur when the shear stress at the base of the rock glacier falls to a value of approximately 1 bar, judging from Figure 10. The decrease in height may also be partly due to the melting out of interstitial ice and washing out of fine material. This can contribute significantly to the decrease in thickness of only those rock glaciers that contain ice in proportions considerably greater than that necessary to fill the interstices in the debris.

Table 6, which summarizes altitudinal data on the rock glaciers of the Alaska Range, shows that the altitudes of lower ends, upper ends, and source areas of inactive rock glaciers average about 300 feet lower than do those of the active rock glaciers. If rock glaciers require a near-glacial climate, then the period during which the now-inactive rock glaciers were formed was more "glacial" than the present by an amount sufficient to bring the isoclimatic surfaces roughly 300 feet lower than they now are.

Only one-eighth of the active rock glaciers in the Wood River area and only one-quarter of those in the Windy area are overriding inactive rock glaciers. Most active and inactive rock glaciers descend from wholly different parts of cirque or valley walls, even where they are contiguous (Pl. 1; Figs. 4 and 5).

Where the active rock glaciers advance over inactive rock glaciers, there is conclusive evidence that there have been two periods of rock glacier activity, separated by a period of inactivity. For example, active rock glacier 51 at the head of Clear Creek, whose motion was measured, advances over flat-topped hills about 50 feet high, separated by steep-walled gullies. The gullies were cut by streams that flow from the active rock glacier and from the valleys on either side of it (Fig. 1 of Pl. 7). Exposures on the gully walls show that the hills consist of porous till-like material with about the same size distribution as the active rock glacier. The aerial photographs show that the hills are dissected remnants of an ancient rock glacier (52) that once extended 1000 feet farther down the valley than rock glacier 51. After rock glacier 52 had advanced to its present position and ceased moving, a turf mat developed on its upper surface, and either then or shortly thereafter streams dissected the rock glacier into flat-topped hills. Subsequent to its dissection rock glacier 51 advanced down the valley, filling the gullies and partially burying rock glacier 52. A similar relationship between active and inactive rock glaciers occurs at the head of Kansas Creek (Pl. 1; Fig. 1 of Pl. 2) and on the west fork of Virginia Creek (Pl. 1).

The history deduced for these localities cannot be applied with certainty to all the inactive rock glaciers; in most other localities inactive rock glaciers still possess the typical surface

microrelief and are undissected. They have probably been preserved at these other localities because they line the walls of valleys and are away from valley axes and stream courses.

The time necessary for the growth of a lichen or turf mantle is the minimum length of time that the inactive rock glaciers have been stable (Beschel, 1950, 1957). The work of Faegri (1933) in Norway and Frey (1922) in Switzerland shows that such factors as availability of moisture, chemical composition of the rocks, and roughness of the surface influence the rate of colonization and growth of lichens (Frey, 1922, p. 189–192). Beschel (1950, 1957) shows that for certain species of lichen, the rate of growth increases tenfold for a fourfold increase in the ratio of precipitation to altitude. Unfortunately, Beschel's papers were brought to our attention when this report was in a late stage of revision, and after field work had been completed; we were unable therefore to apply his method of diameter measurement of critical species of lichens, which would give much more reliable information than that quoted in following sections.

The studies of Faegri (1933, p. 137–142) and of Frey indicate that the rough surface of a fresh block or boulder remains essentially free of lichens for at least 20 years after exposure. A smooth surface will remain free of lichens much longer. Beschel (1950, p. 159) found that moraines in Switzerland and Austria abandoned 30 years had practically no lichen colonies, and moraines abandoned since 1895, or for 55 years, showed only minor colonization. Faegri found that single large blocks resting on the floor of a valley were entirely covered with crustose lichens after about 60–70 years of exposure, and that a continuous cover of dark *Gyrophora*, which appears to be the most common genus on the rock glaciers of the Alaska Range, is completed somewhat later. Beschel (1950, p. 160) on the other hand, found that moraines abandoned for 100 years had only moderate colonization and that on these moraines, boulders covered as much as 50 per cent by lichens were uncommon.

Evidence that the lichens of the Alaska Range are at least as slow-growing as those of Norway and Switzerland was found in a riprap quarry along the Alaska Railroad north of Clear Creek (Fig. 5), visited by the senior author in 1949, 1950, and 1957. The riprap quarry is in a talus cone of well-cemented conglomerate that breaks into large equidimensional blocks along joints. This conglomerate is the source formation of many of the rock glaciers shown in Figures 4 and 5. The upper surface of the talus cone was covered with black lichens; the undersides of boulders on the talus cone were completely barren of lichens. Riprap was obtained from the talus cone in the period 1920–1922, and the quarry was abandoned about 1922. Although the boulders of the quarry wall and quarry floor had not been disturbed since 1922, the boulders were still bare of lichens, and the quarry wall as a consequence was light gray.

The studies of Faegri, Frey, and Beschel and observations in the Alaska Range indicate that the development of a continuous growth of *Gyrophora* and *Parmelia* which not only covers the exposed surfaces of the boulders but also joins boulders together by intertwining of thalli probably takes at least 100, and possibly 200–300, years. The inactive rock glaciers have not moved for at least 100 years and probably for much longer. Conditions for the growth of the active rock glaciers were probably as favorable during the latter half of the nineteenth century, when glaciers reached their greatest extent in central and southern Alaska in modern times, as they have been at any time within the past several centuries. Therefore the inactive rock glaciers are probably not a product of the latest period of climatic deterioration.

About 15–20 per cent of the total number of rock glaciers are apparently beginning to readvance after a long period of inactivity. Two types of these reactivated rock glaciers have been observed. One type shows the morphologic features of an inactive rock glacier: it has the characteristic "deflated" look; its front slopes 20°–30° and joins the upper surface with a gentle curve, and the front is less than 75 feet high and is largely clothed with vegetation. However, in most cases for 10 to 20 feet of height along the base, the front is free of vegetation, and fresh debris—a mixture of silt, sand, and blocks—is exposed. The lower edge of the turf above this bare strip is freshly torn, and pieces of green turf lying overturned could be found buried behind the front for at least 3 or 4 inches. Two of the four rock glaciers at the head of Moody Creek (Fig. 15) are of this type. They are clearly advancing, but the disruptive differential motion appears to be concentrated near the base. They appear to be advancing by shear along the basal surface of the rock glacier rather than by differential plastic flow within it. This basal shear is characteristic of some

landslides and probably does not require interstitial ice.

The second reactivated type has the morphologic features of an active rock glacier. However, certain aspects of vegetation cover suggest strongly that these have advanced little, if at all, for a long period. This type of reactivated rock glacier characteristically occurs high within the zone of active rock glaciers. Examples are rock glaciers 18 and 39 (Pl. 1). These rock glaciers have steep fronts which make a sharp angle with the upper surface and are as high as the fronts of the active rock glaciers. The upper part of the front consists of exposed fresh debris which is completely or partially bare of vegetation. The lower part of the front is partially clothed with lichens that extend a short distance up from the base of the front. Because the lichens require about 100 years for their growth, the lower part of the front cannot have moved for at least that length of time, nor could it have been buried by debris rolling down from the upper part of the front. The bare upper part has apparently just begun to move forward and has begun to destroy the lichen cover on the lower part, leaving undestroyed streaks extending upward from the base. The velocity distribution within this type of reactivated rock glacier is similar to that within the active rock glaciers and probably depends on interstitial ice.

Reactivated rock glaciers that appear exactly like the active rock glaciers suggest that perhaps all the active ones may also have had a period of inactivity between two periods of growth. Such a history would explain the cover of turf and lichens on the upper surfaces of nearly all active rock glaciers. In many of the active rock glaciers this otherwise continuous cover is torn by tension rents and by shearlike cracks. Along the borders of these rock glaciers the upper surface is barren, except for a few patches of turf whose torn sides indicate that they are remnants of a once more continuous turf cover. Probably this cover developed when the rock glaciers were inactive or were moving much more slowly than they are now, and the vegetation cover is torn in places and destroyed in others because the rock glaciers have resumed or increased their forward motion. Such a history for the active rock glaciers—that they were active, inactive, and subsequently reactivated—would explain the absence of inactive rock glaciers below most of the now-active rock glaciers. The "inactive" rock glaciers that should be there are the active rock glaciers themselves.

Climatic History Indicated by the Rock Glaciers Compared With Worldwide Climatic Events

Most of the rock glaciers are in cirques formerly occupied by ice that reached a maximum advance 3–40 miles downstream from the cirques a little more than 10,600 years ago (ca. 8600 B.C.) (Wahrhaftig, 1958, p. 45–56). The rock glaciers could not have been in existence when ice filled the cirques, or they would have been swept out of the cirques by the glaciers. They have developed since that ice disappeared. If the rock glaciers had grown, even in part, during the deglaciation of this region after the ice maximum of 8600 B.C., they would represent part of a process that accompanied the deglaciation, and it would be reasonable to expect that, wherever the ice fronts stood during deglaciation, at least on the smaller glaciers, there would be a zone of rock-glacier activity. As the ice retreated, the zone of active rock glaciers would have risen. Rock glaciers no longer in the zone of active rock glaciers would remain as inactive rock glaciers, for the debris of which they are composed is not washed away when they become inactive. The walls of the glaciated valleys should now be lined with ancient, inactive rock glaciers to altitudes at least 1000 feet lower than the present lower limit of active rock glaciers, for the snow line during the glaciation of 8600 B.C. was about 1000 feet lower than the present snow line (Wahrhaftig, 1958, p. 56). However, except for a few talus deposits, the walls of the valleys downstream from the active rock glaciers are relatively free of debris. Except for a few rare rock glaciers such as those on the southwest side of Panorama Mountain (Fig. 5), and a questionable rock glacier (which may have formed at the glacial maximum) on the east side of the Wood River just north of the mouth of Sheep Creek, the lowest inactive rock glaciers are about 500 feet lower than the lowest active ones.

This suggests that, except in a few places, the retreat of late Wisconsin ice was not accompanied by the formation of rock glaciers. The rock glaciers probably grew during periods of renewed cold after the thermal maximum. Relationships at the head of Clear Creek, on Kansas Creek, and on Virginia Creek indicate that at least two cold periods followed the

thermal maximum, and that the climate is still favorable for the growth of the rock glaciers of the last cold period.

An alternative explanation is that rock glaciers can form only in certain topographic situations, and that these are limited in distribution. Rock glaciers need for their formation an oversteepened slope fronting a flat or gently sloping area that is distant from streams. Such topographic conditions are common in recently glaciated terraines, particularly in cirques but are uncommon beyond the limits of glaciation. The restriction of rock glaciers to cirque headwalls and the upper parts of glaciated canyons could be due to the absence of suitably located cliffs elsewhere. Although suitably located cliffs are rare at low altitudes in this part of the Alaska Range, they are present along the flanks of some of the anticlinal mountains in the northern foothills and along the walls of glaciated valleys crossing the foothills, for example, the valleys of the Wood River and Dry Creek. Rock glaciers are not present in these localities. The only rock glaciers observed in the foothills, besides the one north of the mouth of Sheep Creek mentioned previously, are on the north side of Jumbo Dome (Wahrhaftig, 1949) and are apparently of Wisconsin age and older. In the glaciated region south of the Alaska Range between the Nenana River and the Richardson Highway, and in Yosemite National Park in the Sierra Nevada of California, are extensive cliffs favorably located for rock glaciers throughout a wide range of altitude. In both regions rock glaciers are found only in the highest ice-free cirques or along cliffs less than a thousand feet below the northward-facing firn line. These observations in the Alaska Range and elsewhere show that the alternative explanation is insufficient to account for the distribution of rock glaciers.

Some indication of the length of the last cold period can be gained from the active Clear Creek rock glacier (No. 51), whose length is 3500 feet, and whose front advanced 1.5–2 feet per year from 1949 to 1952. If the rate of advance of the front before that time was constant at that rate, it would have taken the rock glacier between 1750 and 2250 years to reach its present length. However, the rate of advance for the period 1952–1957 is a little less than 1.5 feet, indicating that the rock glacier is slowing; it is likely that its motion before 1949 was greater than 2 feet per year. The actual time of formation of the rock glacier might have been anywhere from less than half to more than twice the time determined, and the likelihood is great that it is much less than 1750 years.

The older, inactive rock glacier at Clear Creek must have taken somewhat longer to form, unless its motion was accelerated by the growth of a glacier at its head. Probably there was a glacier in this cirque when the older rock glacier was forming, because the isoclimatic surfaces were about 300 feet lower when the inactive rock glaciers were formed than they now are. Hence the rock glaciers indicate the following history:

(1) General deglaciation, following an ice advance that culminated about 8600 B.C.
(2) A period too warm for rock glaciers to develop (the thermal maximum).
(3) A cold period, during which rock glaciers developed in the Alaska Range.
(4) A period of inactivity and dissection of rock glaciers, probably marking a warm period.
(5) A cold period with growth of rock glaciers, continuing to the present.

A similar history, with two post-Pleistocene warm periods, each followed by a cold period, has been indicated by a number of other lines of evidence (Wahrhaftig, 1958, p. 64). The two cold periods together, judging from the evidence at the head of Clear Creek, lasted between 1500 and 5000 years.

The evidence for post-Wisconsin glacial and climatic fluctuations has been summarized by Ahlmann (1953, p. 37–41). According to Ahlmann there was general deglaciation from 8000 to 5000 B.C.; a thermal maximum from 5000 to 1000 B.C.; change to glacial conditions similar to those of the eighteenth and nineteenth centuries A.D., that began about 1000 B.C. and reached a climax between 500 B.C. and A.D. 1; a warm period from A.D. 1 to A.D. 400; a period somewhat cooler than the preceding, but milder than at present, from A.D. 400 to A.D. 1300; and cooling beginning in A.D. 1300 with glacial conditions from A.D. 1600 to the present. Zumberge and Potzger (1955) place the end of the thermal maximum at 1500 B.C. rather than 1000 B.C.; Matthes (1941) and Antevs (1955) both place it at about 2000 B.C.; and Karlstrom (1955) would put it as far back as 3000 B.C. If the minimum figures given by Ahlmann are used, there were two periods of glacial climate, each about 500 years long, giving a total of 1000 years as the minimum period during which rock glaciers were active. This seems much too short a time for them to

have formed. If rock glaciers were active during the periods of climatic deterioration, as well as during the coldest periods since the end of the Pleistocene, or if Zumberge and Potzger's, Matthes', Antevs', or Karlstrom's figures give a more accurate date for the beginning of the climatic deterioration, the time during which rock glaciers could have been active would be as much as 1500 or 3000 years long. This would include a period of activity 1000 to more than 2000 years long immediately preceding the Christian era, and a period 600 to possibly 1000 years long within the last millenium. These periods are of the magnitude indicated by the rate of growth of the Clear Creek rock glacier.

Amount and Rate of Erosion Represented by the Rock Glaciers

The amount of debris in a rock glacier is the amount of material removed from its source. Divided by the area of the source, it gives the average vertical thickness of bedrock removed from the source area. Thus rock glaciers can be used as a measure of the amount and rate of post-glacial erosion in the areas where they occur.

The vertical thickness of bedrock removed is greater than the thickness normal to the surface by a factor equal to the secant of the average slope angle; where the slope is steep, this factor is large. The vertical thickness removed is given by

$$T_{vs} = T_{rg} \times R \qquad (8)$$

where T_{vs} is the vertical thickness of bedrock worn from the source area; T_{rg} is the thickness of debris in the rock glacier, corrected for increase in volume due to formation of voids, and R is the ratio of the area of the rock glacier to the area of its source. Areas of rock glaciers and source areas were measured on 1:12,000 enlargements of the multiplex manuscript for the topographic map of Healy D-2 quadrangle. The source area is the area upslope from the talus cones at the head of a rock glacier as far as the crest of the ridge; that is, all the area from which any fragment, once dislodged, must eventually find its way to the rock glacier. In Figure 16 the areas of 40 rock glaciers in the Wood River area are plotted against the size of their source areas. The regression line determined for the points in Figure 16 has a slope of 1.36 and passes very nearly through the origin. Hence the average ratio of the source area to the area of the rock glacier is probably close to 1.36, and its reciprocal can be used in equation (8). If the difference in thickness between the active and inactive rock glaciers is assumed to be largely due to the loss of interstitial ice, the average thickness of inactive rock glaciers, approximately 70 feet, would give the thickness of debris with voids. Use of this assumption has probably resulted in an underestimation, rather than overestimation, of the amount of debris in active rock glaciers. According to Peele's Handbook of Mining Engineering (1948, p. 3–03) the porosity of gravel is Between 37 and 42 per cent. No figures are available for the porosity of rubble such as that in rock glaciers, and it undoubtedly varies widely from place to place within a rock glacier. If Peele's average value of 0.4 is used, the vertical thickness eroded is no less than $70 \times 0.6/1.36$, or about 30 feet. This figure indicates little more than the order of magnitude of the erosion involved. The average erosion that produced a particular rock glacier may be one-fifth or 5 times this figure, depending on the size of the rock glacier, its thickness, and how much of it is debris.

A minimum figure for the rate of erosion is given by the time since ice last occupied these cirques, no more than 10,000 years. This gives a rate of erosion of about 3 feet per 1000 years. However, the period of time during which the rock glaciers have been active is probably no more than 3000 years, and many of them have been active for only 1000 or 2000 years. Most of the erosion to produce rock glaciers occurred at the time of formation; hence an average rate of erosion of at least 1 foot per century, and probably 2 or 3 feet per century, is indicated for the relatively short periods of accelerated frost riving and growth of rock glaciers.

Erosion in an individual source area is not uniform. Frost prying of rock fragments, the chief mechanism whereby talus accumulates in the Alaska Range, depends on abundant moisture. It is more rapid in gullies and couloirs, which are kept damp by late-lying snow, than on projecting ridges, spines, and pinnacles, which are generally dry. Fragments falling from a cliff loosen other fragments in their path, and these in turn loosen others. Because the fall of rock fragments is channeled through the couloirs, their erosive effect is concentrated along the couloir walls. The processes that erode the cirque walls therefore tend to accentuate any irregularities that might exist in these walls. As a consequence the source areas of the rock glaciers are masses of sharp ridges and pin-

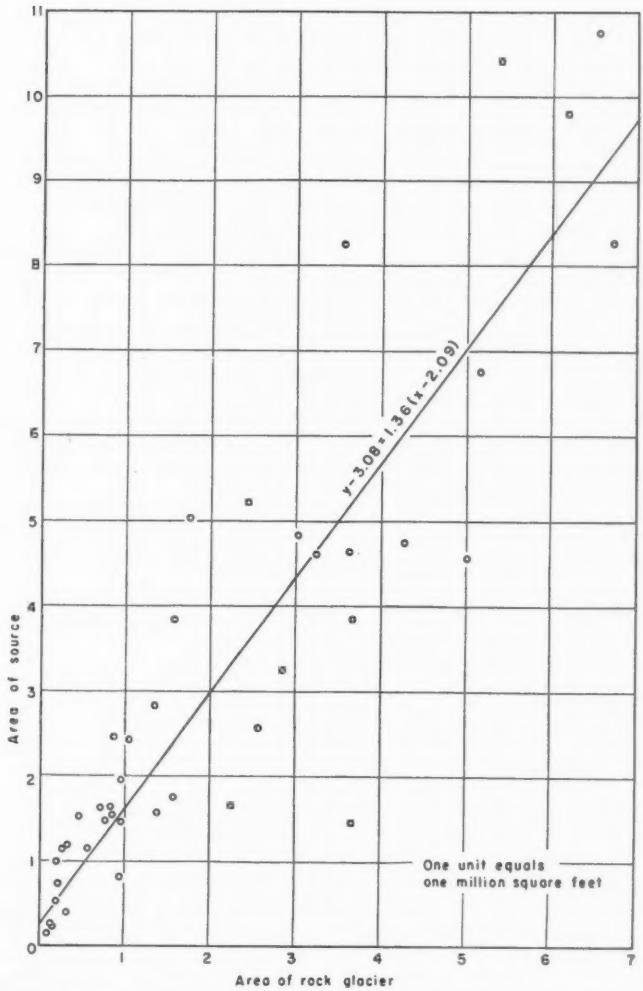

FIGURE 16.—SCATTER DIAGRAM SHOWING AREAS OF ROCK GLACIERS PLOTTED AGAINST SIZE OF THEIR SOURCE AREAS

Regression line derived by least-squares methods from these points.

nacles separated by narrow gullies and steep couloirs. Elsewhere along the cirque and valley walls, where frost action has not significantly worn the cliffs since ice left these valleys, the cliffs are fairly smooth.

The source areas of the rock glaciers are the areas of blocky weathering rocks which are being eroded most actively. Only 7 per cent of the area shown in Plate 1 and 15 per cent of the area shown in Figure 5 are source areas of the rock glaciers, although blocky weathering rocks amount to 50 per cent of the area shown on Plate 1, and the entire area of Figure 5 is blocky weathering rocks. If the rate of erosion for the remainder of these areas of blocky weathering rocks was zero, the average rate of erosion on blocky weathering rocks at the altitudes of the areas shown in Plate 1 and Figures 4 and 5 would be about 1 foot in 1000 years, during periods when rock glaciers are active.

For all post-Wisconsin time it would be about 1 foot in 4000 years. However, erosion does occur elsewhere in these areas. Rock falls are feeding other talus cones at small increments a year, and various forms of solifluction and creep continually move material down-slope, exposing more bedrock to be broken by frost action. Hence, for blocky weathering rocks at these altitudes the average rate of erosion in post-Wisconsin time might lie between 1 foot in 4000 years and 1 foot in 1000 years.

This rate of erosion is a measure oft the rat at which bedrock is being destroyed. I is note directly a measure of the lowering of the land surface. Many rock glaciers are beyond the reach of streams capable of transporting their coarse fragments. Probably, in order for the coarse debris of these rock glaciers to be brought within reach of streams large enough to handle it, the rock glaciers must be incorporated into the till of a glacier and carried to the lower reaches of a large stream system.

Rock-Glacier Debris as a Major Component of End and Lateral Moraines

If the climate in a region where rock glaciers abound should become more glacial, the rock glaciers will be overwhelmed by the advancing ice of a new glaciation and will be incorporated into the debris borne along at the front and sides of a glacier, to be deposited as part of the terminal and end moraines. In the southwest part of the area shown in the stereoscopic view of Figure 3 of Plate 7, a typical cirque glacier has advanced over the rock glacier down-valley from it and subsequently retreated (rock glacier 47). The microrelief on the rock glacier has been smeared out into a series of sharp-crested dunelike forms, with short steep lee slopes and long gentle stoss slopes. Longitudinal groove marks scoured by the glacier are also visible. The difference between the overridden surface of this rock glacier and the surfaces of other rock glaciers in this cirque (e.g. rock glaciers 46 and 48) that were not overridden by ice is readily apparent.

A more advanced stage in the transition of a rock glacier to morainal material is represented by the east lateral moraine of the glacier at the head of the northward-flowing tributary of the Wood River about 5 miles west of the Wood River glacier (Fig. 1). This glacier has melted back half a mile from its maximum recent stand. The abandoned terminal moraine in the west half of the valley consists of two low parallel ridges, about 15 feet high and 100 feet apart. The west lateral moraine above them is likewise very low. Behind the terminal moraines is an alluvial flat, which extends back to rolling ground moraine, beyond which is partly till-covered and partly bare ice. A collapse pit at the lower end of the alluvial flat indicates that ice lies beneath the alluvium.

The eastern third of the valley is filled with a long, narrow, flat-topped mound about 60 feet high and about 500 feet wide, which is the east lateral moraine of the glacier. This mound has a front typical of those of rock glaciers and both longitudinal and transverse ridges on its upper surface. This terracelike lateral moraine probably developed from a rock glacier that entered the main valley from the east side, or that formed along the east valley wall. It has been drawn out alongside the glacier to form the massive lateral moraine. Other massive lateral moraines with longitudinal ridges and furrows are near the head of this glacier as well as on the Wood River glacier and on other glaciers in this region.

An apron of lobate rock glaciers around the base of a mountain approximately 1 mile downstream from the foot of the Wood River glacier (Fig. 3 of Pl. 2) was overridden on its upstream side during the nineteenth century by the Wood River glacier, which has since retreated about half a mile. Where the rock glacier was overridden by ice, the rock-glacier topography has been obliterated, and the surface resembles that of till recently exposed by ice and modified slightly by mass wasting.

Lobate rock glacier aprons just downstream from the lower ends of glaciers have been observed on some forks of the Little Delta River. If the onset of glaciation is slow enough, the advance of glaciers down-valley might be preceded by rapid frost spalling of the valley walls and the development of rock glacier aprons downstream from the glacier snout. Such rock-glacier aprons would provide large quantities of debris to the lateral and ground moraines of glaciers and would be a significant factor in valley widening by glacial erosion.

Conclusions

Origin of Rock Glaciers

Active rock glaciers are masses of debris and interstitial ice and owe their motion to the flow of the ice. Relationships between the velocity,

thickness, slope, and surface features of the rock glaciers are consistent with the known physical properties of ice. Rock glaciers, then, are essentially a type of glacier, and hypothetically all gradations between rock glaciers and glaciers would be possible. Because of the manner in which their ice is formed and preserved, the climatic conditions under which rock glaciers occur differ slightly from those under which glacial ice accumulates. Consequently, their geographic distribution is different, and intermediate forms are rare.

The conditions necessary for the growth of rock glaciers are an abundant supply of coarse blocky debris and a climate conducive to the accumulation of ice in its interstices. The amounts of debris necessary for the formation of rock glaciers are commonly found only at the bases of high steep cliffs, such as the walls of cirques and glacial valleys. The average annual temperature must be below freezing in order for interstitial ice to accumulate. Where such temperatures prevail, frost riving of bedrock to form talus is most rapid in the cloudy moist regions around areas of glacial accumulation where bedrock is kept moist during freezing weather; a near-glacial permafrost climate, but without the net accumulation of snow necessary for the formation of glaciers is required.

The talus must have large interconnected interstices. Generally rocks which break into equidimensional blocks, such as granite or greenstone, provide such talus. Highly fissile schistose or platy weathering rocks do not. Ice accumulates within the interstices of the talus, either from snow drifting among the blocks or from freezing of water. When the talus reaches a certain thickness, the weight of the superincumbent debris causes the ice to flow. As the mass flows outward from the base of the cliff, its front is a talus slope 100–300 feet high.

Initially rock glaciers are in the form of lobes at the bases of cliffs or lining the walls of cirques (lobate rock glaciers). When lobate rock glaciers coalesce in the center of a cirque, the resulting mass flows down-valley as a tongue (forming a tongue-shaped rock glacier). If a tongue-shaped rock glacier enters a large valley, it spreads laterally and forms a terminal lobe. In glaciated regions tributary valleys are commonly hanging valleys, and the rock glacier, on reaching the larger valley, cascades down its side as a great talus slide. As the lobe at the base of the talus slide grows, the slope of the talus is reduced until material no longer rolls down it, but flows down the slope as a rock glacier. Such a rock glacier, with a terminal lobe, is a spatulate rock glacier.

When the climate changes in a direction favoring the formation of glaciers, névé fields and glaciers accumulate at the heads of many rock glaciers. The growth of these glaciers in most cases is slow enough so that the rock glaciers maintain their characteristic form as they move down-valley ahead of the advancing glaciers. The upper surfaces of the glacier and the rock glacier slope continuously from the head of the glacier to the front of the rock glacier, and the two are parts of a single dynamic system. During the last 50 years the climate in these glacier-filled cirques has become less favorable for the accumulation of glacial ice, and the glaciers have melted down and back, leaving large depressions at the heads of many rock glaciers.

In some mountain ranges an interval of rock-glacier formation, separated from other intervals of activity by inactivity and dissection, may be equivalent to a glacial advance elsewhere, where snow accumulated from year to year. If the difference in altitude between the lower limit of rock glaciers and that of glaciers can be established in higher mountain ranges near by, it should be possible to determine, for mountain ranges where only rock glaciers exist, the approximate height of snow line at the time the rock glaciers were formed.

Origin of Microrelief

Most longitudinal ridges and furrows on the surface of a rock glacier are believed to be formed by differential accumulation of talus and snow at the head of a rock glacier. Snow drifts into the swales between talus cones at the head of a rock glacier and may persist from season to season on northward-facing slopes. If these snowbanks fill the swales to the level of the cones, the resulting surface slopes directly away from the base of the cliff, rather than radially outward from the head of the talus cones, as it would if no snow were present. Fragments falling to the heads of the cones would roll outward rather than to the sides of the cones, and the swales would not receive as much debris as they would have if no snow were present. As this snow sinks downward and outward during the growth of the rock glacier, it would be converted to ice, and the rock glacier as a consequence would consist of longitudinal bands of debris with interstitial ice alternating with ice containing embedded debris. It is postulated

that the ice-rich bands melt as they leave the shade of the cliff, and a pattern of longitudinal ridges and furrows results. Creep of material from the ridges into the furrows would keep the ridges rounded and the furrows sharp.

Transverse ridges and furrows are believed to result where the motion of the rock glacier is impeded, or where its thickness increases downstream. Downstream decrease in velocity and thickening of the rock glacier both involve shortening in the direction of flow. This appears to be accomplished by overthrusting along closely spaced shear surfaces within the rock glacier. The transverse ridges and furrows are the surface expression of this overthrusting. Because of the manner in which they form, and because of subsequent deformation, transverse ridges and furrows are commonly convex downstream in plan.

Crevasses, which are short straight widely spaced V-shaped furrows trending nearly perpendicular to the trends of transverse ridges and furrows, are believed to be tension cracks, developed either where rock glaciers are spreading laterally, or where there is a convex change in slope. Under these conditions tension cracks develop which are similar to those on glaciers; debris sliding into these cracks converts them to sharp V-shaped trenches.

Conical pits, either single or closely spaced in lines, are formed where running water melts vertical tubes within the ice of the rock glacier. Debris collapses into these tubes as they are formed producing the conical pits. The closely spaced conical pits generally form irregular lines along the lower ends of longitudinal furrows, because these are the natural channels for water running down the surface of the rock glacier and also contain the greatest concentrations of ice.

Lobes on the surface of a rock glacier are thought to result from renewed activity after a period of inactivity. The renewed activity starts at the head of the rock glacier and takes the form of lobes, which are essentially small rock glaciers forming on the back of a large one. Several periods of renewed activity can produce on the surface of a rock glacier a very complex pattern of lobes.

Significance of Rock Glaciers in the Geomorphology of the Alaska Range

Both active and inactive rock glaciers are present in the areas studied and occur in cirques that were filled with ice during Wisconsin time. The inactive rock glaciers are completely covered with a mantle of turf or lichens, and their fronts are rounded in profile; the fronts of active rock glaciers are barren of vegetation and have a straight profile which intersects the upper surface at a sharp angle. After cessation of activity, some of the inactive rock glaciers were dissected by gullies into which the active rock glaciers have flowed. The active and inactive rock glaciers are therefore interpreted as the products of two different periods of rigorous climate, separated by a period of less rigorous climate, all within the latter part of post-Wisconsin time. The inactive rock glaciers are somewhat lower in average altitude than the active rock glaciers and descend in part from slightly lower mountains. Therefore the earlier cold period was probably somewhat more rigorous than the later one. The rock glaciers indicate the following history for the Alaska Range since Wisconsin time.

(1) General deglaciation.

(2) A period too warm for formation of rock glaciers (the thermal maximum).

(3) A period somewhat colder than the cold period of 1850–1900, lasting at least 1000 and possibly 2000 years. This is tentatively correlated with the cold period of 1000 B.C. to A.D. 1 (Ahlmann, 1953, p. 38).

(4) A period too warm for formation of rock glaciers.

(5) A period cold enough for rock glaciers to form, lasting at least 600 and possibly 1000 years, and continuing to the early twentieth century.

(6) Gradual deglaciation for the last 25 years.

Rock glaciers are a significant factor in erosion of the Alaska Range. Those present today represent an average of 30 feet of bedrock eroded from the areas from which their debris was derived. This material was eroded certainly in the last 10,000 years, and probably during a total of only 2000 or 3000 years. Rock glaciers therefore represent a rate of denudation of bedrock walls amounting to 1–3 feet per century. The average rate of erosion throughout post-Wisconsin time, in the areas that are favorable to rock glaciers, is between 1 foot and 4 feet per 1000 years.

References Cited

Ahlmann, H. W: son, 1953, Glacier variations and climatic fluctuations: Bowman Memorial Lectures, ser. 3, Am. Geog. Soc., 51 p.

Anderson, C. A., 1941, Volcanoes of the Medicine

Lake highland, California: Calif. Univ. Dept. Geol. Sci. Bull., v. 25, no. 7, p. 347–422, 6 pls.

Antevs, Ernst, 1955, Geologic-climatic dating in the west: Am. Antiquity, v. 20, no. 4, p. 317–335

Atwood, W. W., and Mather, K. F., 1932, Physiography and Quaternary geology of the San Juan Mountains, Colorado: U. S. Geol. Survey Prof. Paper 166, 176 p.

Beschel, Roland, 1950, Flechten als Altersmassstab rezenter Moränen: Zeitschr. Gletscherk. Glazialgeol., Bd. 1, H. 2, p. 152–161

—— 1957, Lichenometrie im Gletschervorfeld: Jahrbuch des Ver. zum Schutze der Alpenpflanzen und -Tiere München für 1957, preprint, 22 p.

Brown, W. H., 1925, A probable fossil glacier: Jour. Geology, v. 33, no. 4, p. 464–466

Cailleux, André, 1947, Caractères distinctifs des coulées de blocailles liées au gel intense: Soc. Géol. France, Compte rendu Sommaire des seances, no. 16, p. 323–325

Capps, S. R., 1910, Rock glaciers in Alaska: Jour. Geology, v. 18, p. 359–375

—— 1912, The Bonnifield region, Alaska: U. S. Geol. Survey Bull. 501, 63 p.

Chaix, André, 1919, Coulées de blocs (rock-glaciers, rock-streams) in the Swiss National Park of the lower Engadine: Soc. Physique et d'Histoire Naturelle de Genève, Compte rendu des seances, v. 36, no. 1, p. 12–15

—— 1923, Les coulées de blocs du Parc National Suisse d'Engadine (note preliminaire): Le Globe (Organe de la Societé de Géographie de Genève), v. 62, p. 1–34

—— 1943, Les coulées de blocs du Parc National Suisse, Nouvelles mesures et comparison avec les "rock streams" de la Sierra Nevada de Californie: Le Globe (Organe de la Societé de Géographie de Genève), v. 82, p. 121–128

Cross, Whitman, and Howe, Ernest, 1905, Geography and general geology of the quadrangle *in* Silverton Folio: U. S. Geol. Survey Geologic Folio no. 120, Silverton Folio, p. 1–25

Deeley, R. M., 1895, The viscous flow of glacier ice: Geol. Mag., v. 32, p. 408–415

—— 1908, The viscosity of ice: Royal Society of London Proc., ser. A, v. 81, p. 250–259

Deeley, R. M., and Parr, P. H., 1913, The viscosity of glacier ice: Philos. Mag., 6th ser., v. 26, p. 255–267

Domaradzki, Josef, 1951, Blockströme im Kanton Graubünden: Ergebnisse Wiss. Untersuchungen Schweiz. Nationalparks Bd. 3, no. 23 (Arb. Geogr. Inst. d. Univ. Zurich, ser. A, no. 54, p. 173–235

Emmons, S. F., Irving, J. D., and Loughlin, G. F., 1927, Geology and ore deposits of the Leadville mining district, Colorado: U. S. Geol. Survey Prof. Paper 148, 368 p.

Faegri, Knut, 1933, Ueber die Längenvariationen einiger Gletscher des Jostedalsbre und die dadurch bedingten Pflanzensukzessionen: Bergens Mus. Årb., 1933, Naturvidens. rekke., H. 2, no. 7, 255 p., 47 text figs.

Flint, R. F., and Denny, C. S., 1958, Quaternary geology of Boulder Mountain, Aquarius Plateau, Utah: U. S. Geol. Survey Bull. 1061-D, p. 103–164

Frey, Ed., 1922, Die Vegetationsverhältnisse der Grimselgegend im Gebiet der sukünftigen Stausseen: Mitt. der Naturf. Gesell. in Bern Jahre 1921, p. 85–265

Glen, J. W., 1952, Experiments on the deformation of ice: Jour. Glaciology, v. 2, p. 111–114

Griffiths, Thomas M., 1958, A theory of rock-stream morphology (Abstract); Assoc. Am. Geographers Annals, v. 48, p. 265–266

Haefeli, R., 1951, Some observations on glacier flow: Jour. Glaciology, v. 1, p. 496–500

Hoel, P. G., 1947, Introduction to mathematical statistics: N. Y., John Wiley and Sons, Inc., 258 p.

Hole, A. D., 1912, Glaciation in the Telluride quadrangle, Colorado: Jour. Geology, v. 20, p. 502–529, 605–639, 710–737

Howe, Ernest, 1909, Landslides in the San Juan Mountains, Colorado: U. S. Geol. Survey Prof. Paper 67, 58 p., 20 pls.

Hubbert, M. K., 1951, Mechanical basis for certain familiar geologic structures: Geol. Soc. America Bull., v. 62, p. 355–372

Ives, J. D., and King, Cuchlaine A. M., 1954, Glaciological observations on Morsarjökull, S. W. Vatnajökull, Part I: The ogive banding: Jour. Glaciology, v. 2, p. 423–428

Ives, R. L., 1940, Rock glaciers in the Colorado Front Range: Geol. Soc. America Bull., v. 51, p. 1271–1294

Jeffreys, Harold, 1925, The flow of water in an inclined channel of rectangular section: Philos. Mag., 6th ser., v. 49, p. 793–807

Jellinek, H. H. G., and Brill, R., 1956, Viscoelastic properties of ice: Jour. Applied Physics, v. 27, no. 10, p. 1198–1209

Journal of Glaciology, 1953, Conference on terminology: v. 2, p. 229–232

Karlstrom, T. N. V., 1955, Late Pleistocene and Recent glacial chronology of south-central Alaska (Abstract): Geol. Soc. America Bull., v. 66, p. 1581

Kesseli, J. E., 1941, Rock streams in the Sierra Nevada: Geog. Rev., v. 31, p. 203–227

Krauskopf, K. B., 1948, Lava movement at Paricutin volcano, Mexico: Geol. Soc. America Bull., v. 59, p. 1267–1284

Leighton, F. B., 1951, Ogives of the East Twin Glacier, Alaska; their nature and origin: Jour. Geology, v. 59, p. 578–589

Lliboutry, Louis, 1953, Internal moraines and rock glaciers: Jour. Glaciology, v. 2, p. 296

Matthes, F. E., 1941, Rebirth of the glaciers of the Sierra Nevada during late post-Pleistocene time (Abstract): Geol. Soc. America Bull., v. 52, p. 2030

—— 1942, Glaciers, p. 149–219 *in* Meinzer, O. E., *Editor*, Physics of the earth, Part 9, Hydrology: N. Y., McGraw Hill Book Co., reprinted 1949, Dover Publications, Inc., New York

Matveev, S. N., 1938, Les coulées de pierres (rock streams): Problemy Fizicheskoi Geografii, v. 6, p. 91–124, Russ. with Fr. Summ., p. 122–124

McCall, J. G., 1952, The internal structure of a cirque glacier, Report on studies of the englacial movements and temperature: Jour. Glaciology, v. 2, p. 122–130

Moffit, F. H., 1954, Geology of the eastern part of the Alaska Range and adjacent area: U. S. Geol. Survey Bull. 989-D, p. 65–218

Moxham, R. M., Eckhart, R. A., Cobb, E. H.,

West, W. S., and Nelson, A. E., 1953, Geology and cement raw materials of the Windy Creek area, Alaska: U. S. Geol. Survey open-file rept., 49 p.

Muller, S. W., 1945, Permafrost or permanently frozen ground and related engineering problems: U. S. Army Engineers, Strategic Eng. Study, Special Rept. no. 62, 231 p. (Reprinted by J. W. Edwards, Inc., Ann Arbor, Mich., 1947)

Nangeroni, Giuseppe, 1954, Neve-acqua-ghiaccio; fenomeni crionivali delle regioni periglaciali nelle Alpi Italiane: Como, Italy, Antonio Noseda, publisher, 43 p.

Nye, J. F., 1951, The flow of glaciers and ice sheets as a problem in plasticity: Royal Soc. London Proc., v. 207, p. 554–572

—— 1952, The mechanics of glacier flow: Jour. Glaciology, v. 2, no. 12, p. 82–93

—— 1953, The flow law of ice from measurements in glacier tunnels, laboratory experiments, and the Jungfraufirn borehole experiments: Royal Soc. London Proc., v. 219, p. 477–489

Parsons, W. H., 1939, Glacial Geology of the Sunlight area, Park County, Wyoming: Jour. Geology, v. 47, p. 737–748

Patton, H. B., 1910, Rock streams of Veta Peak, Colorado: Geol. Soc. America Bull., v. 21, p. 663–676, pls. 48–52

Peele, R., 1948, Mining engineers' handbook: 3d ed., v. 1, N. Y., John Wiley and Sons, Inc.

Perutz, M. F., and Gerrard, J. A. F., 1951, Determination of the velocity distribution in a vertical profile through a glacier: Internat. Geod. Geophys. Union, Assoc. Sci. Hydrology, General Assembly Brussels Proc., 1951, v. 1, p. 214

Richmond, G. M., 1952, Comparison of rock glaciers and block streams in the La Sal Mountains, Utah (Abstract): Geol. Soc. America Bull., v. 63, p. 1292–1293

Roots, E. F., 1954, Geology and mineral deposits of Aiken Lake map-area, British Columbia: Geol. Survey Canada Mem. 274, 246 p.

Rubey, William W., 1952, Geology and mineral resources of the Hardin and Brussels quadrangles (in Illinois): U. S. Geol. Survey Prof. Paper 218, 179 p.

Salomon, Wilhelm, 1929, Arktische bodenformen in den Alpen: Heidelberger Akad. Wiss., Math-natur. Kl., Sitzungsber. Jahrg. 1929, Abh. 5, p. 1–51

Sharp, Robert P., 1942, Mudflow levees: Jour. Geomorphology, v. 5, p. 222–227

—— 1954, Glacier flow, a review: Geol. Soc. America Bull., v. 65, p. 821–838

Sigafoos, R. S., and Hopkins, D. M., 1952, Soil instability in regions of perennially frozen ground, p. 176–192 *in* Frost action in soils; a symposium: Natl. Research Council, Highway Research Board Special Rept. No. 2

Spencer, A. C., 1900, A peculiar form of talus (Abstract): Science, v. 11, p. 188

Suess, Hans, 1954, U. S. Geological Survey radiocarbon dates I: Science, v. 120, no. 3117, p. 467–473

Tyrrell, J. B., 1910, "Rock glaciers" or chrystocrenes: Jour. Geology, v. 28, p. 549–553

Wahrhaftig, Clyde, 1949, The frost-moved rubbles of Jumbo Dome and their significance in the Pleistocene chronology of Alaska: Jour. Geology, v. 57, p. 216–231

—— 1954, Observations on rock glaciers in the Alaska Range (Abstract): Geol. Soc. America Bull., v. 65, p. 1353

—— 1958, Quaternary geology of the Nenana River and adjacent parts of the Alaska Range, Alaska: U. S. Geol. Survey Prof. Paper 293A, 68 p.

Washburn, Bradford, 1935, Morainic banding of Malaspina and other Alaskan glaciers: Geol. Soc. America Bull., v. 46, p. 1879–1890

Williams, Howel, 1944, Volcanoes of the Three Sisters region, Oregon Cascades: Calif. Univ. Dept. Geol. Sci. Bull., v. 27, no. 3, p. 37–84

Zumberge, J. H., and Potzger, J. E., 1955, Late Wisconsin chronology of the Lake Michigan basin correlated with pollen studies (Abstract): Geol. Soc. America Bull., v. 66, p. 1640

Alaskan Geology Branch, U. S. Geological Survey, Menlo Park, California; Bacon Hall, University of California, Berkeley, California

Manuscript Received by the Secretary of the Society, May 20, 1958

Publication Authorized by the Director, U. S. Geological Survey

Wiss.,
. 1929,

s: Jour.

. Amer-

52, Soil
frozen
in soils;
l, High-
2
of talus

y radio-
3117, p.

chrysto-
3
rubbles
e in the
ır. Geol-

s in the
America

Nenana
a Range,
er 293A,

nding of
rs: Geol.
0
ıe Three
if. Univ.
p. 37–84
55, Late
Michigan
bstract):
0

OLOGICAL
BACON
ERKELEY,

Y OF THE

OR, U. S.

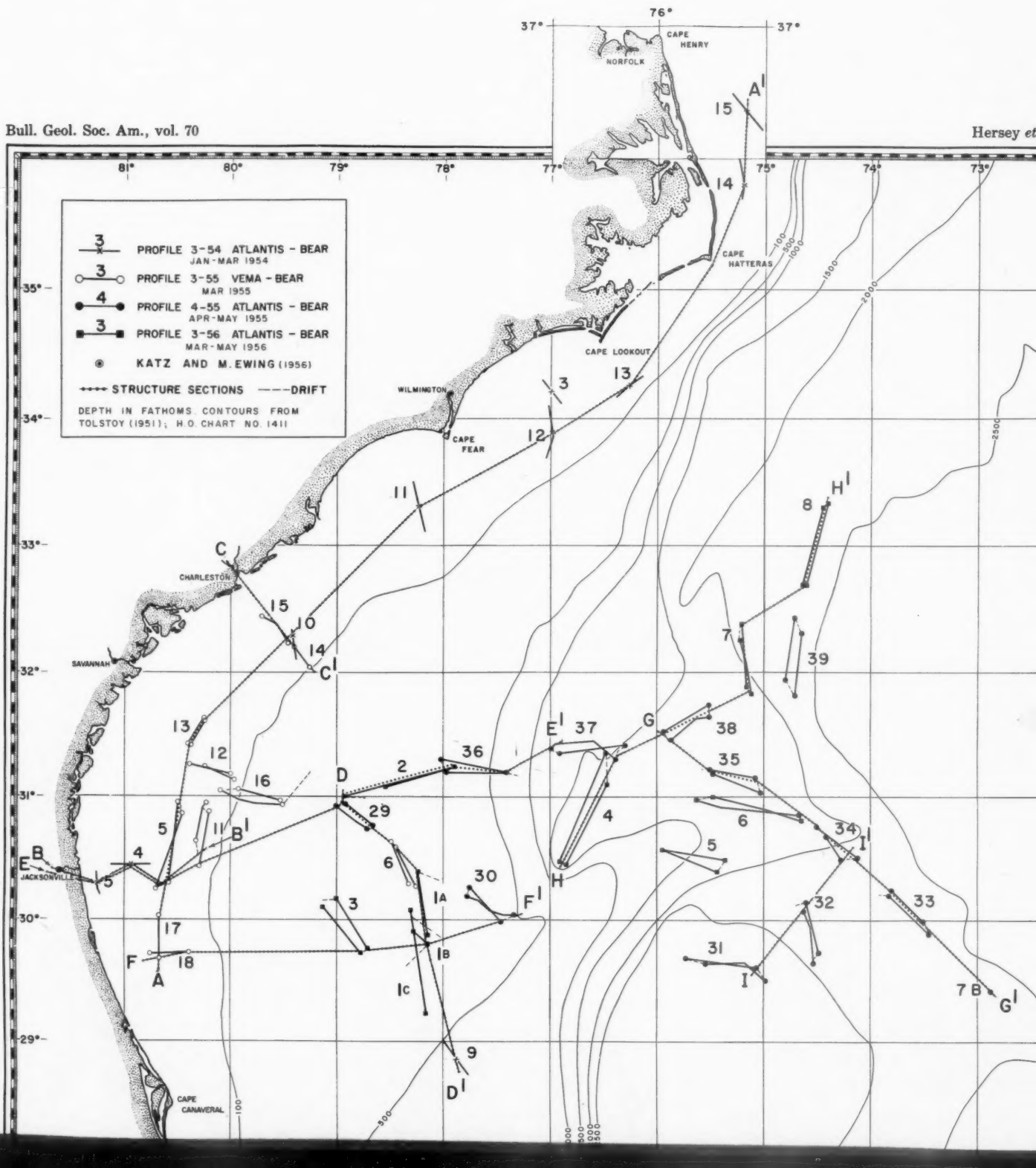
3 PROFILE 3-54 ATLANTIS - BEAR JAN-MAR 1954
3 PROFILE 3-55 VEMA - BEAR MAR 1955
4 PROFILE 4-55 ATLANTIS - BEAR APR-MAY 1955
3 PROFILE 3-56 ATLANTIS - BEAR MAR-MAY 1956
KATZ AND M. EWING (1956)
STRUCTURE SECTIONS ---DRIFT
DEPTH IN FATHOMS. CONTOURS FROM TOLSTOY (1951); H.O. CHART NO. 1411
76°
37°
81°
80°
79°
78°
77°
75°
74°
73°
35°
34°
33°
32°
31°
30°
29°
NORFOLK
CAPE HENRY
CAPE HATTERAS
CAPE LOOKOUT
WILMINGTON
CAPE FEAR
CHARLESTON
SAVANNAH
JACKSONVILLE
CAPE CANAVERAL
100
500
1000
1500
2000
2500
A
A'
B
B'
C
C'
D
D'
E
E'
F
F'
G
G'
H
H'
I
I'
1A
1B
1C
7B

Hersey *et al.*, Pl. 1

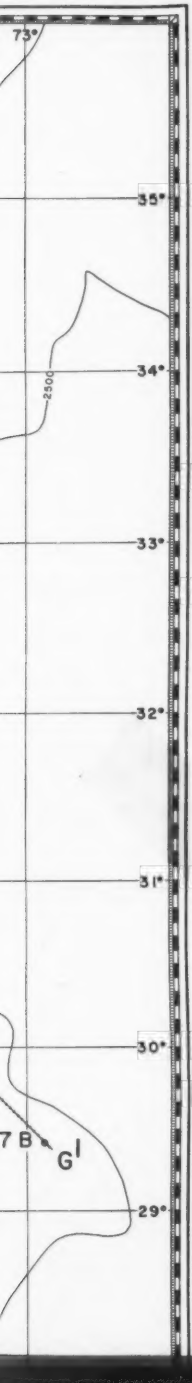

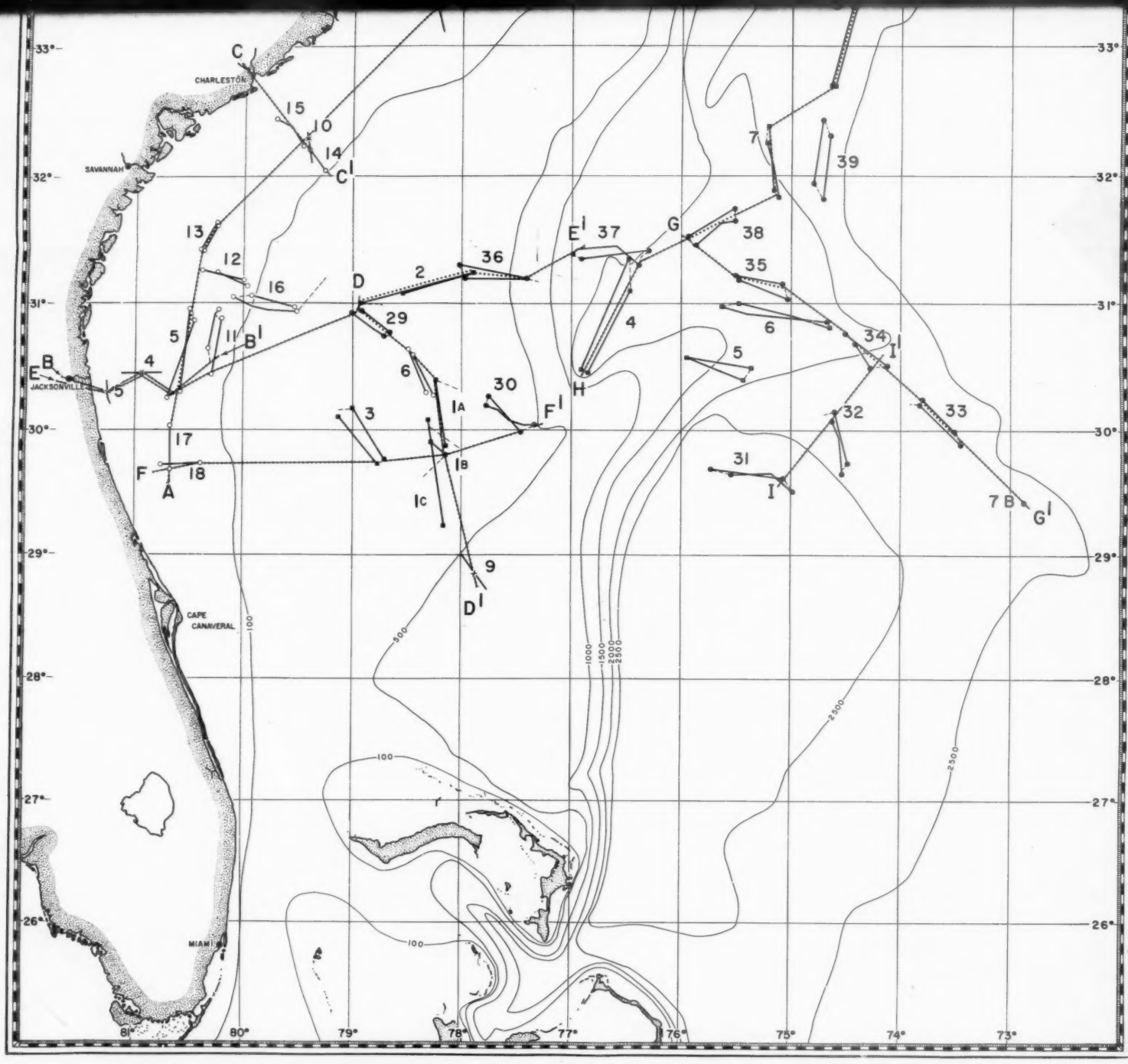

PROFILE AND STRUCTURE-SECTION LOCATIONS AND BATHYMETRY

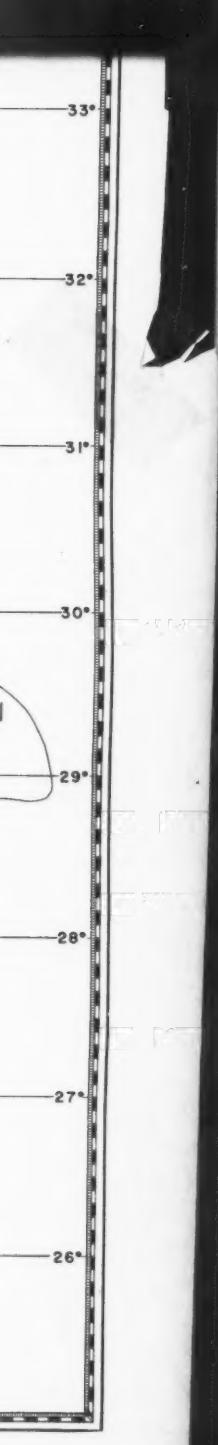
33°
32°
31°
30°
29°
28°
27°
26°

Intr
Ack
Obs
G
M

BULLETIN OF THE GEOLOGICAL SOCIETY OF AMERICA
VOL. 70, PP. 437–468, 13 FIGS., 2 PLS. APRIL 1959

GEOPHYSICAL INVESTIGATION OF THE CONTINENTAL MARGIN BETWEEN CAPE HENRY, VIRGINIA, AND JACKSONVILLE, FLORIDA

BY J. B. HERSEY, ELIZABETH T. BUNCE, R. F. WYRICK, AND F. T. DIETZ

ABSTRACT

Forty seismic-refraction and reflection profiles on the eastern continental shelf and adjacent deep-water areas of the Atlantic Ocean, from 29°39′ to 36°30′ N. Lat. and 73°30′ to 81°10′ W. Long. trace the transition from deep-oceanic to continental-type structures. The transitional area divides naturally into three parts: the continental shelf, the Blake Plateau, and the adjoining deep-water area.

The results on the continental shelf are correlated with adjacent continental geology. The deepest horizon traced along the shelf is interpreted as granitic basement, which has compressional velocities of 5.82–6.1 km/sec. At the southern extremity it is at a dept of 6 km, shoals to 0.86 km near Cape Fear, and deepens north of Cape Hatteras to more than 3 km. North of Charleston, South Carolina, there is excellent depth correlation with granitic basement in coastal wells; to the south all deep wells are inland. Age correlations are based on well data near the coast, which indicate to us that most of the observed section is Cretaceous.

On the Blake Plateau, several layers (1.83–4.5 km/sec.) are interpreted as sedimentary. A 5.5-km/sec. layer is found only south of a line from 30°30′N., 78°W. to Cape Canaveral. Velocities higher than 5.5 km/sec. have been measured on six profiles on the Blake Plateau. The 5.5-km/sec. layer and a 6.2-km/sec. layer appear to form a positive feature to the south of the above-mentioned line. Higher velocities, 8.0 km/sec. and 7.28 and 7.3 km/sec., which are probably not the same horizon, are found at markedly different depths. Possibly these represent the M layer and ultrabasic material, depending on relations not now known.

The deep-water area is a continental slope and rise modified by the Blake Plateau and by a ridge trending southeastward from Cape Fear and deepening from about the 1500-fathom contour to more than 2000 fathoms (3657 m). The ridge is underlain by thick low-velocity layers (1.83–2.96 km/sec.), interpreted as sediments, and higher-velocity layers which form a distinct linear structure having the same general trend as the ridge. At its northwestern end this trend terminates against a thick lower-velocity section interpreted as a sediment-filled trough. South of the ridge profiles are similar to those of the ocean basins. Excellent seismic-refraction evidence of faulting indicates subsidence of the ridge relative to its surroundings. A hypothesis interprets the ridge as a former chain of islands and reefs on a structural trend colinear with the Cape Fear Arch.

The structural pattern formed by the Piedmont crystallines and the Peninsular Arch of Florida and the Cape Fear Arch and the ridge resembles that formed by the Japanese archipelago, the Ryukyus, and the Bonin ridge. The pattern of the trough of the Blake Plateau and the deep-water area is somewhat similar to such modern features as Exuma Sound and the Tongue of the Ocean in the Bahamas. Such comparisons should not be regarded as strictly homologous but are suggested as possibly reflecting similarities in deep-lying tectonic activity. Similarly it would seem fruitful to consider similarities of deep structure beneath isolated seamounts, chains of seamounts, submerged ridges, island arcs, and mature mountain ranges.

CONTENTS

TEXT

	Page
Introduction	438
Acknowledgments	439
Observations	440
General description	440
Methods	441
Reduction and interpretation of data	444
Discussion	445
Continental shelf profiles	445
Blake Plateau profiles	448
Deep-water profiles	455
Relationship of adjoining structures	460
Relation to the ocean basins	460

Page
Relation to other continental slope structures 461
Relation to continental structures 461
Comparison with other regions 461
References cited 462
Appendix: Discussion of data 463
Continental shelf 463
Blake Plateau 463
Outer continental slope and ridge area 464

ILLUSTRATIONS

Figure Page
1. Layers of Tables 2, 3, and 4 444
2. Depths of layer boundaries, continental shelf 446
3. Continental shelf: 29°50′N. to 36°50′N. 449
4. Continental shelf: Jacksonville, Florida, section 450
5. Continental shelf: Charleston, South Carolina, section 451
6. Blake Plateau: 28°90′N. to 31°00′N 452
7. Blake Plateau: 77°W to 81°30′W 453
8. Blake Plateau: 77°30′W to 80°35′W 454
9. Deep-water section along the ridge 455
10. Deep-water section paralleling continental slope 456
11. Deep-water section: Interior basin to ridge 457
12. Speculative history of the ridge 459
13. Comparison of Piedmont, coastal plain, and oceanic structure with western Pacific island arcs 460

Plate Facing page
1. Profile and structure section locations and bathymetry 437
2. Travel-time graphs 466

TABLES

Table Page
1. Receiving positions for seismic-refraction profiles 440
2. Layer velocities and layer thicknesses, continental shelf 441
3. Layer velocities and layer thicknesses, Blake Plateau 442
4. Layer velocities and layer thicknesses, deep-water section 443

Introduction

A geophysical study of the transitional structures between an ocean basin and a continent is presented in this paper. The area studied lies between Cape Henry, Virginia, and Jacksonville, Florida, and extends from the coast to the 73rd meridian. Primary reliance has been placed on the seismic-refraction method, although bathymetric and seismic-reflection evidence has been considered as well. The observations reported form one of several sets taken within the area since Hersey and M. Ewing (1949) reported a bathymetric and seismic and reflection study, and Katz and M. Ewing (1956) reported a reconnaissance seismic-refraction study, each of larger areas which include part of this one. Woollard, Bonini, and Meyer (In preparation) have made a study of continental structures in Georgia, North Carolina, and South Carolina which overlaps ours on the continental shelf, and Nafe and Hennion (In preparation) have studied the ocean area south of the latitude of Jacksonville.

Seismic-refraction investigations made by at least four separate groups of geophysicists since World War II have led to a general picture of the structure of the earth's crust beneath the broad deep areas of the oceans. There is general agreement that the simplest oceanic crustal structure consists of (1) about 5 km of sea water overlying about 1 km of sediments whose compressional wave velocity approximates 1.8 km/sec. near the top of the column, and (2) 4.0–5 km of rock below, which has a compressional wave velocity of about 6.5 km/sec. and overlies the Mohorovic discontinuity (M layer). At the M layer, compressional wave velocities ranging from about 7.8 to 8.2 km/sec. were measured (M. Ewing and Press, 1955). In the vicinity of oceanic islands such as the Bermudas this simple picture appears to be altered by structures resulting from the volcanic activity in the area (Officer, 1955), and in the vicinity of relatively young island-arc structures, such as the Lesser Antilles, even more complicated alterations are found (Officer *et al.*, 1957; J. Ewing *et al.*, 1957). M. Ewing and his coworkers have established several lines of seismic-refraction profiles (M. Ewing *et al.*, 1937; 1939; 1940; 1950; Officer and M. Ewing, 1954; Oliver and Drake, 1951) from North America Basin to the shallow water of the eastern continental shelf of North America north of Cape Hatteras to study the nature and structural arrangement of the changes that take place between the simple, thin crustal section of the ocean basin and the much more complicated, thicker, and deeper continental crust. In all these last studies, the M-layer arrivals that are readily measured in deep water are lost beneath a thick section, which has velocities

suggesting thick sediments laid down in a trough more or less parallel to the edge of the continental shelf (*e.g.*, Officer and M. Ewing, 1954; Drake *et al.*, 1957).

The bathymetry of the deep-water area south of Cape Hatteras (Pl. 1) suggests different and more complicated underlying structures than those discussed by Drake *et al.* (1957) for the continental margin to the north. The continental slope is interrupted at 450 fms. by the Blake Plateau, a remarkably smooth and nearly flat area extending north from the Bahamas to Cape Hatteras. The plateau is bounded on the east by a steep escarpment more than a mile high in the southern half, and, within the area of the present study, by irregular slopes dominated by a ridge trending southeastward from Cape Fear. This ridge appears to protrude from below the northern Blake Plateau at a depth of about 1500 fms. To the southeast it deepens irregularly, turns abruptly southwestward toward the Bahamas, and joins Eleuthera at about 2500 fms. It was suspected that here might be a continental-type structure that gradually changes into ocean-basin structure. The trend of the topographic ridge coincides with a prominent continental structure, the Cape Fear Arch, or the Great Carolina Ridge or Carolina Arch. One of the objectives in the present study has been to find out whether a structural connection exists between the Cape Fear Arch and this topographic ridge. Another objective has been to learn what we could about the structures underlying the Blake Plateau and their relationship with known structures both on the continent and under the ocean to the east and north.

In addition to seismic-refraction, seismic-reflection, and echo-sounding studies, we have attempted some core sampling, but this program has not yet been productive; coring should be continued and supplemented by rock dredging. A few dredgings and bottom photographs were made during a recent cruise and will be reported in another paper. J. L. Worzel and his co-workers at the Lamont Geological Observatory have made numerous gravity observations within this area (M. Ewing *et al.*, 1957; Worzel, unpublished data), and M. Davidson has made some magnetic observations there. We have had access to these data during preparation of this paper, but the gravity and magnetic data have not been analyzed entirely at present writing and hence are principally useful as a qualitative guide.

Acknowledgments

Woods Hole Oceanographic Institution ships participating were Atlantis and Bear with masters W. S. Bray and E. J. Mysona, respectively. Their helpful co-operation throughout is greatly appreciated.

Staff members of the institution who contributed to the observations at sea were: A. C. Vine, R. S. Edwards, and H. R. Johnson as chief scientists, and as members of the scientific party: R. H. Backus, S. W. Bergstrom, H. A. Cain, A. L. Carter, L. C. Davis, W. M. Dunkle, G. Duys, Jr., M. E. Edwards, C. S. Innis, S. T. Knott, D. E. Maddux, M. S. Rutstein, H. Small, G. W. Wheeler, W. E. Witzell.

The following technical assistants helped in reducing the data: J. Dragonette, R. S. Singsaas, N. C. Hickman, R. V. Olson, C. M. Dixon, S. J. Klein, and E. H. Rogers. Charles Innis, J. W. Stimpson, and C. E. Spooner prepared the plates and figures for publication. Peter J. Westervelt of Brown University, J. L. Northrop of Hudson Laboratories, Clifford Parker and J. B. Duchene of the Marine Division, Sperry Rand Corporation, assisted in part of the work at sea.

The co-operative effort at sea in 1955 with Nafe and Hennion on R/V Vema made possible much of the shallow-water work. The continued co-operation of Nafe and Hennion throughout the analysis of the sea data has contributed much to this study through repeated exchange of ideas. We are most grateful to J. L. Worzel for the opportunity to consult his unpublished gravity data and to Maurice Davidson for his efforts to make his magnetic program as useful as possible in the area of our research. We are grateful to the Bureau of Ships (Contract NObsr-43270) and the Office of Naval Research (Contract Nonr-1367) for support of this work and to the Bureau of Ordnance and the Naval Ammunition Depot, Charleston, South Carolina, for assistance with explosives.

All authors contributed to analysis of the data. Final interpretation and preparation of the manuscript are the responsibility of the first two authors, and the geological speculation was made by the first author.

The base map for Figure 13 is AMS1101 (The World), Army Map Service (SN) Dept. of the Army, Washington, D. C.

TABLE 1.—RECEIVING POSITIONS FOR SEISMIC-REFRACTION PROFILES

Profile Number	Latitude (N.)	Longitude (W.)
ATLANTIS 196—BEAR 89		
3–54	34°11′	76°59.5′
4–54	30°27.1′	81°00.4′
5–54	30°16′	81°14.8′
9–54	28°48′	77°51′
10–54	32°12.4′	79°24′
11–54	33°14′	78°12′
12–54	33°52′	76°58′
13–54	34°16′	76°15′
14–54	35°47′	75°12′
15–54	36°22′	75°11.5′
VEMA 6—BEAR 113		
5–55 N.	30°52.5′	80°28′
5–55 S.	30°17′	80°32.8′
6–55 N.	30°37′	78°28′
6–55 S.	30°21.9′	78°19.8′
11–55 N.	30°52.8′	80°13.8′
11–55 S.	30°34.5′	80°18.5′
12–55 E.	31°09.5′	79°57.8′
12–55 W.	31°14.0′	80°16.5′
13–55 N.	31°35.7′	80°15.0′
13–55 S.	31°24.8′	80°21.8′
14–55 E.	32°04.5′	79°16.2′
14–55 W.	32°13.08′	79°24.5′
15–55 E.	32°14.5′	79°27.8′
15–55 W.	32°26′	79°39.5′
17–55 N.	29°58.5′	80°39.7
17–55 S.	29°41.6′	80°40′
18–55 E.	29°43.9′	80°25.6′
18–55 W.	29°41′	80°41.5
ATLANTIS 213—BEAR 113		
29–55 N.	30°56′	78°57.8′
29–55 S.	30°45′	78°40.1′
30–55 N.	30°14′	77°46.5′
30–55 S.	30°01′	77°25′
31–55 E.	29°33.5′	75°01′
31–55 W.	29°40.2′	75°40.6
32–55 N.	30°08.3′	74°39.5′
32–55 S.	29°43′	74°30.6′
33–55 N.	30°13′	73°53′
33–55 S.	29°56′	73°28′

Table 1.—*Continued*

Profile Number	Latitude (N.)	Longitude (W.)
ATLANTIS 213—BEAR 113—*Continued*		
34–55 N.	30°45′	74°33′
34–55 S.	30°30.7	74°11.8′
35–55 E.	31°05.7′	75°03.3′
35–55 W.	31°11.5′	75°30′
36–55 E.	31°11′	77°21′
36–55 W.	31°15.5	78°00′
37–55 E.	31°22′	76°22′
37–55 W.	31°21′	76°57.3′
38–55 E.	31°39.2′	75°30′
38–55 W.	31°29′	75°53′
39–55 N.	32°22.2′	74°41′
39–55 S.	31°52′	74°46′
ATLANTIS 223—BEAR 140		
1A–56	30°22.5′	78°10′
1B–56	29°42.5′	78°14.8′
1C–56	29°56.6′	78°10′
2–56 E.	31°13.5′	77°56.5′
2–56 W.	30°59.4′	78°50′
3–56 N.	30°10.4′	79°04′
3–56 S.	29°44.7′	78°45′
4–56 N.	31°12.3′	76°28.1′
4–56 S.	30°28.0′	76°53.5′
5–56 E.	30°26.5′	75°24.5′
5–56 W.	30°35.4′	75°58.2′
6–56 E.	30°49.8′	74°39′
6–56 W.	30°59.5′	75°44′
7–56 N.	32°18.6′	75°13.2′
7–56 S.	31°50.8′	75°08.2′
8–56 N.	33°19′	74°25′
8–56 S.	32°41.5′	74°36.9′

OBSERVATIONS

General Description

The seismic-refraction program commenced in 1954 when Dietz and Hersey made a series of 15 end-to-end profiles on the continental shelf with ATLANTIS and BEAR. Most of these are in the area of the present study (Pl. 1). In 1955 R. F. Wyrick on BEAR and J. E. Nafe of the Lamont Geological Observatory on VEMA shot 24 refraction profiles on the con-

tinental shelf and the Blake Plateau. Nafe and Hennion are preparing for publication the profiles south of 30°N.Lat.; the more northerly stations are included in the present study (Pl. 1). Later in 1955, Hersey and others made 15 additional stations with ATLANTIS and BEAR, some on the northern part of the Blake Plateau, but most over the ridge and its surroundings (Pl. 1). Finally, in 1956 Hersey and others made 8 profiles with ATLANTIS and BEAR on the Blake Plateau and over the outer continental slope and ridge area (Pl. 1). Receiving positions for the profiles are listed in Table 1.

Seismic-reflection studies were made concurrently with most of the deep-water refraction profiles of the 1955 and 1956 cruises. Echo-sounding data were taken routinely during all the cruises, but inasmuch as all this work had to be accommodated to other programs, we had limited opportunity to exploit fully the echo sounder as a geological tool; one exception is a brief study of a fault zone in this area, (Hersey and Knott, in preparation).

TABLE 2.—LAYER VELOCITIES AND LAYER THICKNESSES, CONTINENTAL SHELF

(In km and km/sec.) N., S., E., W.: locations of receiving positions relative to each other

	LAYER VELOCITY									LAYER THICKNESS						
PROFILE	WATER	A	B	C	D	E	F	G		WATER	A	B	C	D	E	F
3-54	1.50	1.86		2.48			5.49			0.03	0.22		0.91			
4-54	1.51	1.77			3.25		5.38			0.03	0.20			1.50		
5-54	1.51		1.96	2.66	3.67					0.02		0.13	0.23			
10-54	1.52	1.86		2.71				6.04		0.03	0.47		1.28			
11-54	1.51		2.05	2.26				5.89		0.03		0.06	0.77			
12-54	1.51	1.88		2.46				5.90		0.04	0.36		1.07			
13-54	1.51	1.84		2.41	3.88					0.03	0.50		0.79			
14-54	1.49	1.69		2.85		4.30		6.14		0.03	0.58		1.32		1.31	
15-54	1.48	1.75	1.98	2.79	3.27		5.32			0.02	0.26	0.63	0.59	2.09		
5-55	1.52	1.68		2.57	3.65		5.16	5.82	N	0.03	0.23		0.72	1.32		1.44
									S	0.03	0.11		0.34	1.99		2.45
11-55	1.52		1.92	2.34/2.85	3.43			5.96	N	0.04		0.10	0.41/0.46	2.04		
									S	0.04		0.22	0.29/0.51	2.04		
12-55	1.52		1.95	2.88				6.30	NW	0.04		0.30	2.45			
									SE	0.04		0.40	2.27			
13-55	1.51	1.83		2.56	3.45			5.95	NE	0.03	0.22		0.84	1.18		
									SW	0.03	0.28		0.42	1.86		
14-55	1.51	1.77		2.65				5.96	NW	0.05	0.57		1.53			
									SE	0.05	0.56		1.79			
15-55	1.51	1.90		2.44				5.98	NW	0.03	0.32		0.93			
									SE	0.03	0.45		1.29			
17-55	1.52	1.76		2.42	3.16	4.26	5.35	6.06	N	0.03	0.08		0.19	0.94	1.40	3.48
									S	0.03	0.08		0.21	0.42	2.95	2.22
18-55	1.52	1.69		2.25	3.21	4.36	5.52		E	0.04	0.13		0.19	0.91	2.56	
									W	0.03	0.05		0.28	0.66	3.09	

Methods

The seismic-refraction observational techniques were basically similar to those that have been described in many papers on deep-sea explosion seismology (M. Ewing *et al.*, 1937; 1939; 1950; Officer *et al.*, 1952). We were able to drop very closely spaced charges (about 0.25 mile apart) and paid special attention to doing so at short range on most of the profiles. This practice frequently revealed shallow and intermediate depth layers which could not have been demonstrated without such close spacing.

In the seismic-reflection studies, we followed the method described by Officer (1955) except that we alternated shallow changes (no bubble

TABLE 3.—LAYER VELOCITIES AND LAYER THICKNESSES, BLAKE PLATEAU

(In km and km/sec.) N., S., E., W.: locations of receiving positions relative to each other. Overbar indicates unreversed velocities.

	LAYER VELOCITY												LAYER THICKNESS								
PROFILE	WATER	A	B	C	D	E	F	G	H	I	J		WATER	A	B	C	D	E	F	G	H	I
9-54	1.51	1.83				4.11	5.52						1.01	0.38				1.72				
6-55	1.52	1.83		2.77	3.80	4.54						N	0.84	0.49		0.02	1.01					
												S	0.83	0.52		0.07	0.59					
29-55	1.51	1.83			3.87	4.81		$\overline{6.18}$				NW	0.84	0.55			2.39					
												SE	0.85	0.58			0.75	7.33				
30-55	1.51	1.83				4.30	4.99			$\overline{7.20}$		NW	0.83	0.59				0.90	0.50			
												SE	0.83	0.52				0.94	0.40[a]			
36-55	1.50	1.83			3.61	4.55		$\overline{5.77}$		$\overline{7.28}$		E	0.88	0.66			0.53					
												W	0.84	0.58			1.01	4.45[b]		7.31[b]		
1A-56	1.51	1.83		$\overline{2.61}$		$\overline{4.04}$	$\overline{5.50}$		$\overline{6.70}$			N	0.90	0.31		1.14		0.85	3.04			
1B-56	1.51	1.83		$\overline{2.27}/\overline{2.80}$		$\overline{4.63}$	$\overline{5.22}$		$\overline{6.96}$			NW[1]	0.81	0.09		0.04/1.30		1.01	3.22			
1C-56	1.51	1.83		$\overline{3.15}$		$\overline{4.45}$	$\overline{5.50}$	$\overline{5.85}$				N	0.81	0.26		1.04		1.31	3.88			
2-56	1.51	1.74			3.84	4.62			6.38		$\overline{8.04}$	E	0.79	0.77			0.52	0.45				
												W	0.77	0.66			1.04	5.91			5.82	
3-56	1.51	1.77				4.36	4.96					NW	0.82	0.69				1.15				
												SE	0.79	0.64				1.38				

[1] *See* Appendix

[a] Velocity line associated with this thickness not observed; assumed from correct reverse point

[b] Thickness obtained by a complex interpretation

TABLE 4.—LAYER VELOCITIES AND LAYER THICKNESSES, DEEP-WATER SECTION

(In km and km/sec.) N., S., E., W.: locations of receiving positions relative to each other. Overbar indicates unreversed velocities.

		LAYER VELOCITY											LAYER THICKNESS								
PROFILE	WATER	A	B	C	D	E	F	G	H	I	J		WATER	A	B	C	D	E	F	G	H	I
31-55	1.51	1.89							6.70	7.65		E	4.50	2.39							4.44	
												W	4.57	2.52							3.89	
32-55	1.51	1.83	2.06						6.55	7.34		N	4.49	0.16	2.46						2.61	
												S	4.49	0.16	2.46						4.20	
33-55	1.51	1.83		2.44			5.67		$\overline{6.90}$		$\overline{8.10}$	NW	3.80	1.12		2.20			1.54		4.90[a]	
												SE	3.80	1.24		2.15			1.10[a]		4.90	
34-55	1.51	1.83	2.20	2.96			5.20		6.33	$\overline{7.36}$		NW	3.69	0.41	1.67	1.39			1.00		3.79[a]	
												SE	3.69	0.41	1.76	1.43			1.14		2.92	
35-55	1.51	1.83	2.17	2.57			5.24		6.69	7.20	$\overline{8.40}$	E	3.43	1.07	0.49	1.97			2.90		0.37	8.00
												W	3.43	1.07	0.63	1.85			1.85		2.55	7.01
37-55	1.50	1.83		2.77	3.88			6.10		7.42		E	2.90	0.93		2.18	3.48			3.21		
												W	2.45	1.32		1.34	5.55			5.01		
38-55	1.51	1.83		2.38	3.98				6.36	7.73		NE	3.05	1.13		1.78	4.16				1.38	
												SW	2.81	1.79		1.55	3.10				5.08	
39-55	1.51	1.83		2.64	3.84				6.45	7.12	$\overline{7.95}$	N	4.17	1.12		1.32	3.53				2.05	
												S	4.11	1.44		1.38	2.08				3.34	8.98
4-56	1.51	1.88		2.43	3.75	4.46			6.70	$\overline{7.64}$		N	2.78	0.83		2.17	1.58	3.55			3.55	
												S	2.90	0.57		1.64	0.62	6.23				
5-56	1.51	1.83	$\overline{2.26}$ / 2.22		$\overline{3.94}$		$\overline{5.37}$		$\overline{6.51}$	$\overline{7.16}$ / 7.31	$\overline{8.60}$	E	4.06	0.22	2.31				1.66			
												W	3.83	0.75	1.57		2.52				1.29	3.78
6-56	1.51	1.83	$\overline{2.20}$ / 2.15	$\overline{2.78}$ / 2.73	$\overline{3.99}$ / 3.80			$\overline{6.00}$ / 6.00		$\overline{7.37}$ / 7.55		E	3.56	1.12	0.65	0.99	2.40			2.14		
												W	3.55	0.53	0.51	2.18	1.96			1.58		
7-56	1.51	1.83			3.20	4.26		6.15		7.54		N	3.94	1.09			2.30	3.17		2.71		
												S	3.42	1.46			1.64	2.25		2.71		
8-56	1.51	1.77		2.35	3.71			6.24		7.10	8.43	N	4.34	0.80		1.54	2.31			4.25		4.27
												S	4.45	1.19		0.76	3.10			1.31		4.27

[a] Velocity line associated with this thickness not observed; assumed from correct reverse point

pulse) with deeper charges in order to take advantage of the enhanced low-frequency radiation from the deep charge for very deep reflections. Alternate deep and shallow charges make it possible to trace adequately both the deep and shallow reflecting horizons simply by adjusting appropriately the spacing between charges.

Throughout all these cruises, ATLANTIS and BEAR were equipped with Edo Corporation UQN-1B echo sounders and Woods Hole precision graphic recorders (PGR) (Knott and Hersey, 1956) for echo sounding. This combination can resolve depth differences of 1 fm in any depth of water; its usefulness in submarine geologic and topographic studies has already been demonstrated (Hersey and Rutstein, 1958). Regrettably the weather was generally so bad that the full potentialities of precision depth recording were not realized most of the time.

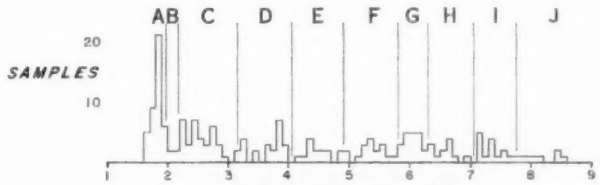

FIGURE 1.—LAYERS OF TABLES 2, 3, AND 4

Reduction and Interpretation of Data

Reduction of the seismic data was done by the same general method described by Officer and Wuenschel (1951) and Sutton and Bentley (1953). This includes a correction for the time taken for the sound to travel from the shot to the shooting ship (shot-instant correction); a correction reducing the travel times to a surface of reference, taken as sea level; and a correction necessitated by the irregular bottom topography underlying a number of the stations.

Certain departures from the standard procedures were made necessary by gaps in the recorded data. During computation of the shot-instant correction for profiles 4-56 to 8-56, BEAR receiving, it was found that sinking times (time from the moment the charge is thrown over the side to detonation) had not been recorded for the majority of the M-2 shots. Since bubble-pulse intervals (and hence charge depths) from the two ships for the same charge size and fuse length were nearly identical, it was possible to infer an average value for the sinking time from data taken by the other ship at the same range. The error thus introduced into the determination of shot-instant correction has been determined as no more than .01 sec. In a few cases, no echo-sounding records were available for both ends of the profile owing to malfunctions of the equipment. In these cases water depths were determined on the basis of the bottom-reflection record taken by the shooting ship. Good agreement was obtained between these and the available echo-sounder records.

Determination of compressional wave velocities and layer thicknesses followed the methods of M. Ewing *et al.* (1939). Individual profiles are discussed in the Appendix, and the refracted-wave travel-time graphs for the three principal regions are reproduced in Plate 2. Layer velocities and layer thicknesses are presented in Table 2, 3, and 4 in km/sec. and km respectively. Layer designations of A, B, C—J are arbitrary and based principally on grouping of the velocities (Fig. 1). These groupings are based on velocity only and do not imply identical horizons.

We have made only a preliminary examination of the reflection data from the 1955 and 1956 deep-water profiles. The results indicate that reflections can be identified from several of the low-velocity layers. The computed layer thicknesses are slightly less than the corresponding ones determined by refraction data. The velocities, however, are closely comparable, and there is only one instance throughout the analysis of a large discrepancy in layer thickness. Deepest reflection penetration was on profile 7–56 where at least a portion of layer E (4.26 km/sec.) was penetrated. There is considerable reflection evidence of multiple layering. Hence it is possible that we have picked travel times of layers with

slight velocity contrast lying above the boundaries along which the refracted waves are transmitted.

Discussion

Continental Shelf Profiles

Continental structures buried beneath the Atlantic Coastal Plain sediments are dominated by two major positive features, the Cape Fear Arch in North Carolina and Peninsular Arch in Florida. These same structures extend beneath the continental shelf. The Cape Fear Arch trends southeastward from the Piedmont Upland to Cape Fear on the southern North Carolina coast. The Peninsular Arch similarly trends southeastward underlying and conforming in shape generally to the Florida peninsula. The principal structural trends have been discussed by Mansfield (1936), Richards (1945), Spangler (1950), and Stephenson (1926; 1928) for North Carolina and South Carolina and by Applin and Applin (1944), Applin (1951), and Stephenson (1926; 1928) for Georgia and Florida. The structure contours are shown for the top of Cretaceous over this whole region and on Ocala limestone (Eocene) in Florida on the Tectonic Map of the United States (Longwell *et al.*, 1944). Oil exploration and other geophysical studies along the coastal areas have provided considerable structural data, especially on the depth of crystalline basement. Published material is discussed by Skeels (1950) and Spangler (1950), Applin (1951), Applin and Applin (1944), Mansfield (1936), King (1950), and Richards (1945). Other excellent data from seismic studies in shallow water and on the coastal plain were presented at the New Orleans meeting (1955) of The Geological Society of America (Meyer, 1955; Bonini, 1955).

The refraction results from the shelf profiles are summarized in Figure 2*a*, *b*, *c*, and *d* for the four principal higher velocities. Depths are given in km, and velocities (in parentheses) are in km/sec. We suggest that the velocities shown together in each division of the figure are correlated over the shelf southwest of Cape Fear. These are also to be correlated with the results of Nafe and Hennion (In preparation) south of 30°N. Lat. Correlations of the more northerly structures are discussed below.

Several dry holes near shore reached granitic basement, the depth of which is shown on Figure 2*d*. These depths, together with the structural trends suggested by Spangler's map (1950), indicate that the horizon having velocity near 6.0 km/sec. is granitic basement, where the wells are close by. This velocity (layer G) is found on all but four profiles; thus we interpret its depths as depths to granitic basement. The possibility that it might be a high-velocity limestone cannot be disproved, but the correlation with the well logs supports the granitic-basement interpretation, and under the Blake Plateau, where there is much more likelihood of a thick limestone section, the velocities at these depths are all appreciably lower. Meyer (Personal communication) found velocities well above granitic which he supposes may be intrusive basalts. We may have a similar instance in the unreversed 6.3 km/sec. of profile 12-55 to the southwest. To the north a 6.0-km/sec.-type layer appears to be replaced by 5.49 and 5.32 km/sec. at 3-54 and 15-54 respectively. M. Ewing *et al.* (1937; 1939; 1950) presented strong arguments for such a low-velocity basement in Virginia and New Jersey. These may be used to explain both 3-54 and 15-54. If so, 12-54 may indicate local variation. We know from good evidence that 5.2 to 5.5 km/sec. onlaps 6.0 km/sec. in the south. This may also be the case near Cape Hatteras. Only closer control in this area can provide proof.

Both north and south of the Cape Fear Arch a lower-velocity, 5.16- to 5.5-km/sec., layer is found on a few stations (Fig. 2*c*). The southern group appear well correlated; they reflect the Peninsular Arch toward Jacksonville and deepen with basement to the south and to the east. This trend is to be seen also in the results of Nafe and Hennion (In preparation) south of 29°30'N. Lat. Thus, this layer appears to onlap the Cape Fear structure to the north. Worzel and Ewing (1948) found this layer at depths in essential agreement with ours in their Jacksonville deep and shoal profiles. They interpreted it as basement. However, it seems clear now that their profiles were too short to bring out the higher velocity (6.06 km/sec.) of 17-55 which is now correlated with other granitic basement-layer velocities. Nafe and Hennion (Personal communication) present evidence for identifying this velocity with the top of lower Cretaceous from its correlation with Big Pine Key (Applin 1951). The northern profiles, 3–54, 12–54, and 15–54 appear to present a different picture, as outlined above.

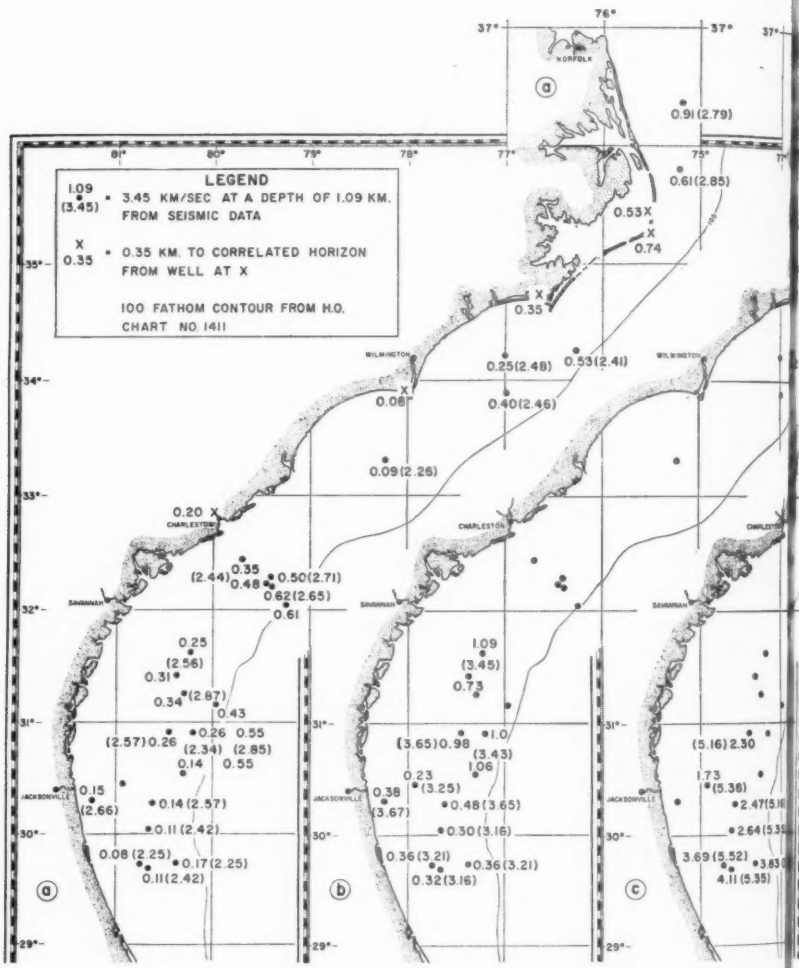

FIGURE 2.—DEPTHS OF [illegible] BOUNDARIES, [illegible] GEORGIA;

(a) 2.26–2.85 km/sec. (top of Upper Cretaceous) (b) 3.0–3.9 km/sec. (top of Taylor formation, [illegible] of Lower Cretaceous, Nafe *et al.*, unpublished) (d) 5.89–6.1 km/sec. (top of granitic basement)

The next lower velocity group lying between 4.26 and 4.36 km/sec. were found on only three profiles: in the north on 14-54 and south on 17-55 and 18-55. More detail is required for the interpretation of these profiles, although their location suggests another onlap to the Cape Fear Arch from both north and south. Nafe and Hennion correlate similar velocities to the south with well data, indicating that this layer may be approximately top of Upper Cretaceous.

The layer (Fig. 2*b*) that has velocities from 3.2–3.9 km/sec. is also missing from the crest of the Cape Fear Arch between Savannah and Cape Lookout. It shoals from Georgia to Florida toward the Peninsular Arch and locally forms a positive feature along a north-northwest south-southeast trend including 4-54, 17-55, and 18-55. Its absence over the Cape Fear Arch and its presence on two stations to the north suggest that it is a sedimentary onlap there. However, it may be present farther

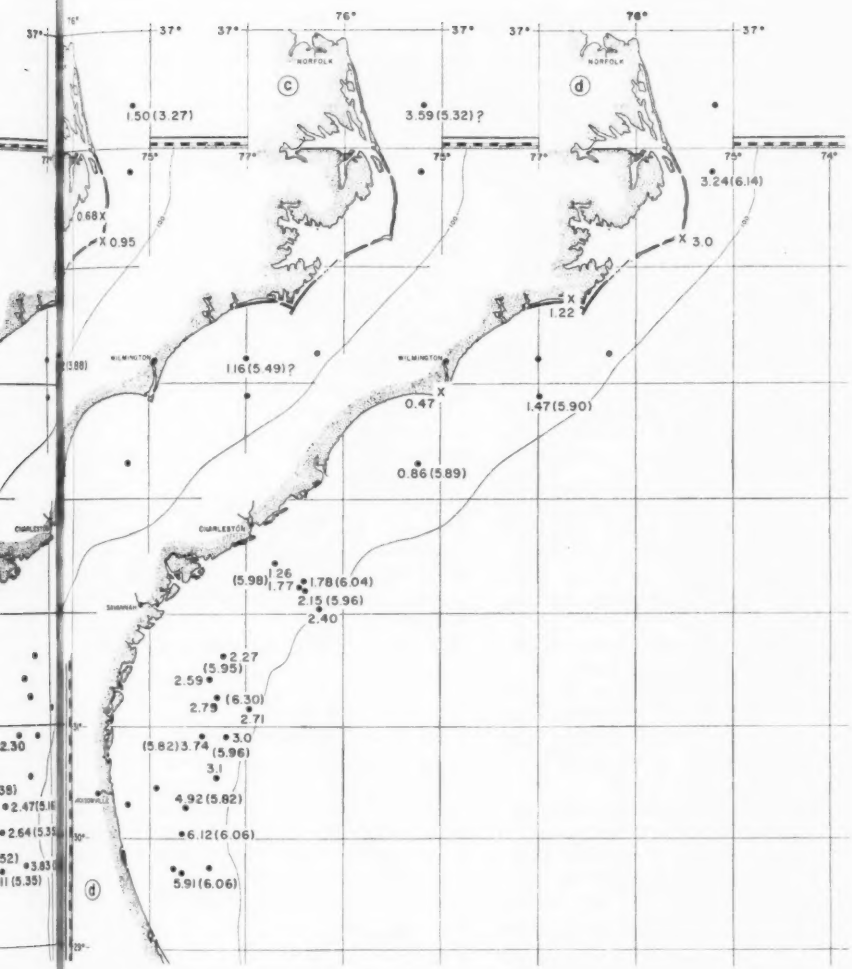

PTHS OF IDARIES, CONTINENTAL SHELF

rmation, eorgia; top of Black Creek formation, North Carolina and South Carolina) (c) 5.0–5.5 km/sec. (top

ient)

from crest nnah gia to ocally north- 4-54, Cape ons to ntary arther

up the flanks of the Cape Fear Arch but is a masked arrival on some of the stations there.

A layer of 2.26–2.85 km/sec is found on all profiles along the shelf (Fig. 2*a*). Its depth reflects both major arches and shows an offshore crest slightly farther east than the 3.5-km/sec. layer. It deepens northeast of Cape Fear, deepens gradually southeast of Charleston, and shows a depth minimum southeast of Jacksonville; Nafe and Hennion's results (In preparation) show that it deepens south of 29°30′N. On profile 11-55 velocities of 2.34 and 2.85 km/sec. are found on the same profile; otherwise the seismic data indicate that we are dealing with a single extensive layer. Comparison of the depths of this layer with well logs taken at various points near the coast shows that it agrees well with the depths to the top of Upper Cretaceous from Charleston northeast. Near Jacksonville the only well control is the Hilliard Turpentine Co. No. 1 mentioned in several studies of the region.

(*Cf.* Applin, 1951, well 67.) There the top of Upper Cretaceous is at a depth of 0.8 km, which is considerably deeper than these velocities on the shelf. We have adequate control to indicate correlation of this layer from profile to profile along the shelf south of Charleston but not northeast where well-log correlation is good. Nevertheless we suggest that this layer represents the top of Cretaceous over the entire area because of the depth correspondence with coastal Carolina well data. Applin and Applin (1944) show thickening of Eocene and some Cretaceous formations toward the sea in southeastern Georgia. If the above correlation be true, the shallow-layer depths along the shelf and the greater depth inland imply a partially closed basin for Eocene sediments and for part of Upper Cretaceous as well. A further possible implication of these results is that the presence of the ridge trending from Charleston toward Cape Canaveral may be the reason for the broadening of the continental shelf there. More information is needed both east and west of the present profiles, and detailed information about shallower formations would be needed to assess the effect of the structure on the shelf topography.

Above the 2.5-km/sec. layer we found only one layer, which had velocities from 1.66 to 2.05 km/sec. and lay very close to, if not quite at, the sea bottom. The 2.05 km/sec. layer was measured 25 miles south of Cape Fear at 11-54. Other bottom velocities are all lower, ranging from 1.66 to 1.95 km/sec. We have not studied the bottom sediments along the shelf here except by means of these measurements and by a few scattered reflection measurements made to test the combination of the precision graphic recorder (PGR) and a spark-sound source discussed by Knott and Hersey (1956). From the latter, we know that considerable local variation occurs in the first 10–30 meters below the bottom; some sediments have velocities not exceeding that of sea water by more than 1 per cent. Hence it seems useless to speculate about the possible significance of the refraction measurements of bottom velocity until much more detailed information is available.

SUMMARY OF CONTINENTAL SHELF PROFILES: The foregoing discussion of the shelf profiles is summarized by the sections in Figures 3, 4, and 5. The section of Figure 3, taken along line *A-A′* (Pl. 1), shows the granitic basement continuously traced (except at 13-54) from south of Jacksonville to north of Cape Hatteras. The onlapping 5.3-km/sec. layer, possibly the top of Lower Cretaceous, is traced north of Jacksonville to 31°N. Similarly, the 4.3-km/sec. layer appears to onlap from the south and possibly from the north as well. To the south Nafe and Hennion (In preparation) correlate it approximately with the top of Upper Cretaceous. The 3.3-km/sec. layer has been correlated tentatively with Black Creek near Cape Hatteras but is not satisfactorily correlated with well data to the south. The apparent inconsistency with Nafe and Hennion's correlation cannot now be resolved. The 2.5-km/sec. layer is present throughout the section and is thought to correspond with or lie close to the top of Cretaceous throughout. Both these latter surfaces show the structural high east of Jacksonville, whereas the older surfaces do not.

East-west structural trends are indicated by the section roughly east-northeast from Jacksonville along line *B-B′* (Fig. 4; Pl. 1), which shows the high in the Cretaceous rocks and an apparently reverse trend in the basement. A third section, *C-C′* (Fig. 5; Pl. 1), southeast from Charleston shows a seaward deepening of all formations. Thus the high, which appears to trend north-northeast from the offing of Jacksonville, must trend somewhat west of 15-55, probably toward Charleston.

Blake Plateau Profiles

The floor of the central portion of the Blake Plateau is grossly smooth at about 800 meters depth. To the west, it becomes somewhat rough and irregular toward the continental slope, while to the north the smooth topography is interrupted by depressions and ridges with many fluctuations in depth of as much as 100 meters. We know little about the details of the topography, but some consistent trends, which appear to be evidence of faulting, have been found among these apparently irregular features. Between 27° and 30°N. the plateau gradually deepens eastward to its lip at a depth of about 1280 meters, where depths then increase suddenly to the small deep basin in the central part. To the northeast it deepens, as shown in Plate 1, approximately over the submerged ridge and into North America Basin. The topographic forms in this northeastern region suggest complicated underlying structures; this suggestion is borne out in the refraction profiles.

The 11 profiles discussed below are located on the northern part of the central smooth area, on the southern part of the rough terrain, and on the irregular northeastern slope. One

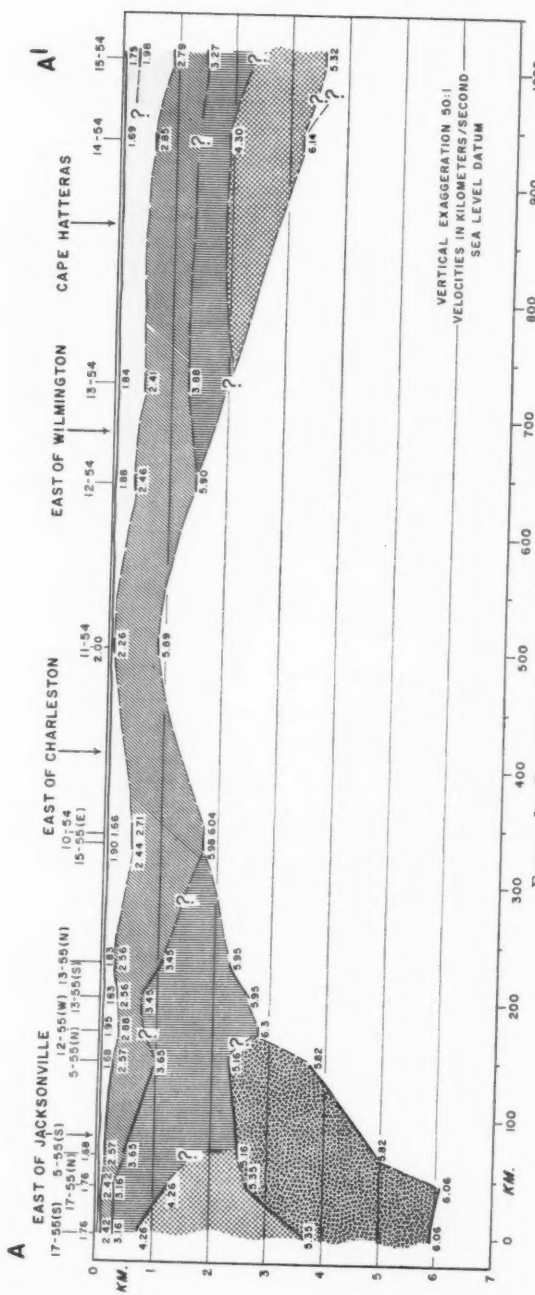

FIGURE 3.—CONTINENTAL SHELF: 29°50′N. to 36°50′N.
Structure section *A-A′* (Pl. 1)

profile, 16-55, on the continental slope could not be interpreted because of drift in the Gulf Stream. The remaining profiles vary in quality because of rough weather that plagued much of the observational program.

and tunicates. Photographs indicate that this bottom composition is widespread at least on the northern half of the plateau.

Seismically we have had only modest success in measuring apparent bottom velocities and

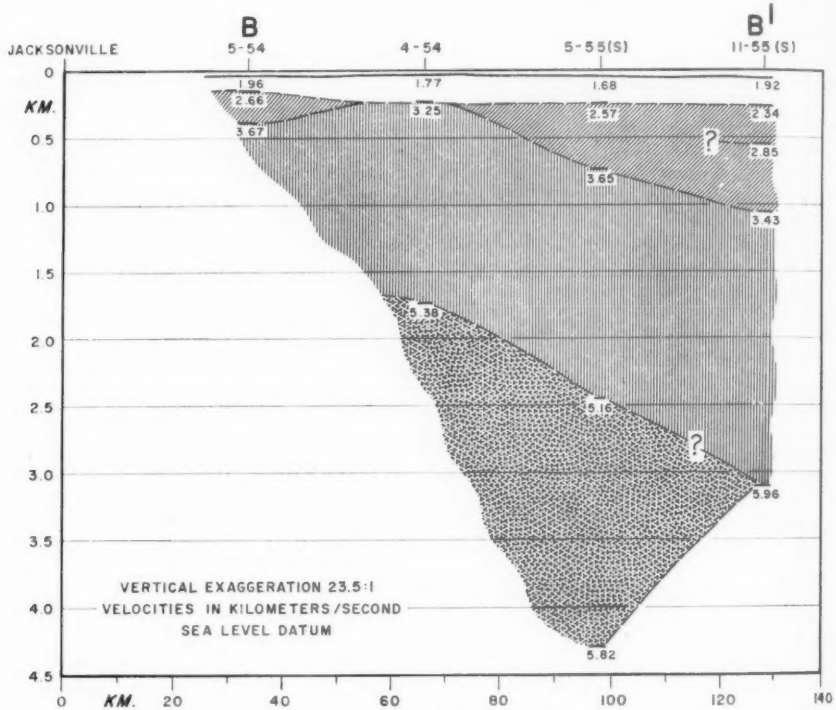

FIGURE 4.—CONTINENTAL SHELF: JACKSONVILLE, FLORIDA, SECTION
Structure section *B-B'* (Pl. 1)

The structures of the Blake Plateau are simplest at shallowest depth and therefore are described from top to bottom.

The surface of the Blake Plateau has been sampled by coring and dredging and has been photographed in a few places. Manganese nodules have been recovered in cores taken on cruises of ATLANTIS by Edwards and Rutstein (Unpublished) and of VEMA by Heezen (Personal communication). Calcareous samples have been recovered from scrapings on the core barrel, bottom cameras, and dredges. In August 1957, Edwards, Graham, and others dredged a considerable sampling of manganese nodules and a friable breccia of coral fragments, Globigerina, pteropods, barnacles, and similar calcareous remains, as well as living bryozoans

have assumed 1.83 km/sec. for many of the refraction profiles. Some of these assumptions are taken from the accompanying reflection data. On two profiles 1.77 and 1.74 km/sec. were measured.

The second-layer velocity ranges from 2.27 to 4.6 km/sec., obviously representing different rock surfaces in different places. The slowest velocities, 2.27–3.16 km/sec., are found in a group comprised of 6-55 and 1A-56, 1B-56, 1C-56, all of which are in the central part of the plateau where the bottom is "smooth".

The higher velocities found as the second layer are also found as the third or fourth layers (or are missing) on other stations; thus a layer 3.6-3.87 km/sec. is found at 29-55, 36-55, 2-56, and at 6-55 but not anywhere south of 6-55. A

4.1- to 4.68-km/sec. layer is found on all profiles, whereas velocities from 4.96 to 5.5 km/sec. are found at comparable depths south of 1A-56 and are tentatively regarded as corresponding. the 7.28-km/sec. layer as 14 km, but since the profile is otherwise complicated and is unreversed for this layer, both velocity and depth are at best merely indications. However, the

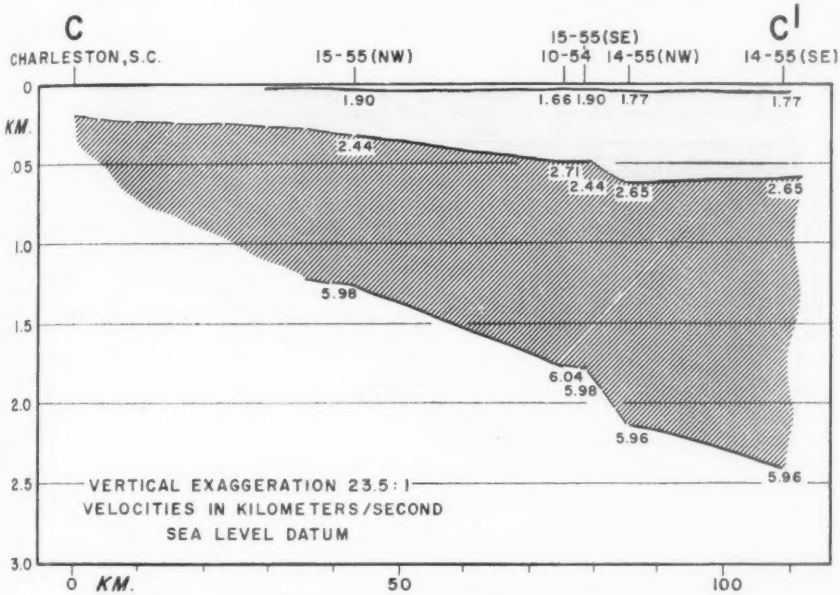

FIGURE 5.—CONTINENTAL SHELF: CHARLESTON SOUTH CAROLINA, SECTION
Structure section *C-C'* (Pl. 1)

The structures indicated by these layers are all gently sloping, except for local faulting.

Velocities higher than 5.5 km/sec. were measured on comparatively few profiles because of the aforementioned weather difficulties and are available in many instances only as unreversed velocity lines. However, with appropriate reservations, their characteristics are helpful in speculating about deep crustal structure beneath the plateau. One velocity group ranges from 6.18 (one profile of poor quality) to 6.33 and 6.7 km/sec. (one good, two poor) which, if they are correlated, indicate considerable relief in the horizon from a possible depth of 5.7 km at 1B-56 to 9.4 km at 2-56. The latter profile is reversed and of good quality, whereas all the others are unreversed for this velocity. Higher-velocity lines were obtained on one side only of two profiles: 36-55 and 2-56 with apparent velocities of 7.28 and 8.0 km/sec., respectively. The former profile is near the edge of the plateau and was made over an irregular surface in an overlying layer. We have shown the depth of profile 2-56 was placed with considerably more knowledge of probable structure, and its shallower layers show very small slopes. Hence, the unreversed velocity of 8.0 km/sec., depth of 14.5 km, must be given correspondingly more weight. The thickness of 5 km for the 6.3-km/sec. layer is comparable to the corresponding layer in the ocean basins.

GEOLOGICAL INTERPRETATION: The structure of the northern half of the Blake Plateau can be sketched in a tentative way from the available results, but from our own data no age identifications can be made. Coring data reported by Nafe, Hennion, and Ericson (Unpublished) on the steep eastern slope separating the plateau from the deep ocean have led them to deduce that the top of Cretaceous probably corresponds to their 4.2-km/sec. layer there. The character of their coring evidence is such that the layers of 2.3-3.8 km/sec. might also be Cretaceous. This view has some support from comparison with the age correlations on the continental shelf discussed above.

STRUCTURE: Three structure sections (Figs. 6, 7, 8) summarize what we have deduced about the northern half of the plateau.

In Figure 6 (Pl. 1, *D-D'*), the 3.8-km/sec. layer, which immediately underlies the surface layer, is markedly thinner than for near-by 29-55 and 36-55 to the south and east. The shallow trench found by Hersey and Knott (In preparation) lies just south of 2-56 and trends roughly parallel to it. Because of this relationship we have shown a fault at this point in the section. Farther south the 3.8-km/sec. layer is replaced by layers of lower velocity. From 6-55 we suppose that the 3.8-km/sec. layer extends beneath the lower-velocity layers and may be present but masked to the south.

The interpretation of the low velocities is reasonably based on first arrivals and clearly correlated second arrivals. However, on profiles where, for example, the 3.8-km/sec. layer does not form a first arrival and hence does not appear, the layer should not be regarded as necessarily absent. The same can be said of still lower velocities which generally appear as second arrivals. We have tested the effect on the apparent structure of supposing these intermediate velocities to be present but masked at profiles 2-56, 3-56, and 30-55, which are critical profiles in which the low velocities are missing.

It is wholly on the absence of low velocities in 3-56 and 30-55 that one might interpret the synclinal profile shown in Figure 8. We have tested these interpretations by supposing that a 3.8-km/sec. layer is present but just barely masked on the three profiles. On 2-56 possibly second arrivals of about 2.5 km/sec., similar to those observed elsewhere on the plateau, are present. A similar assumption would make similar changes in 29-55 and 36-55 (Fig. 7), so that the same interpretation of faulting here would be justified, but the low velocity would be thickened. With respect to the synclinal section shown in Figure 8, the 3.8-km/sec. layer cannot be present on 3-56 and 30-55, but velocities of about 2.5 km/sec. can be assumed, which at most would deepen the 4.4-km/sec. horizon by about 250 meters. Hence a synclinal section there is established.

Below the lower-velocity layers the 4.11- to 4.89-km/sec. layer shoals gradually to the south as does the next deeper one of 5.2 to 5.5 km/sec. This latter layer is well established on

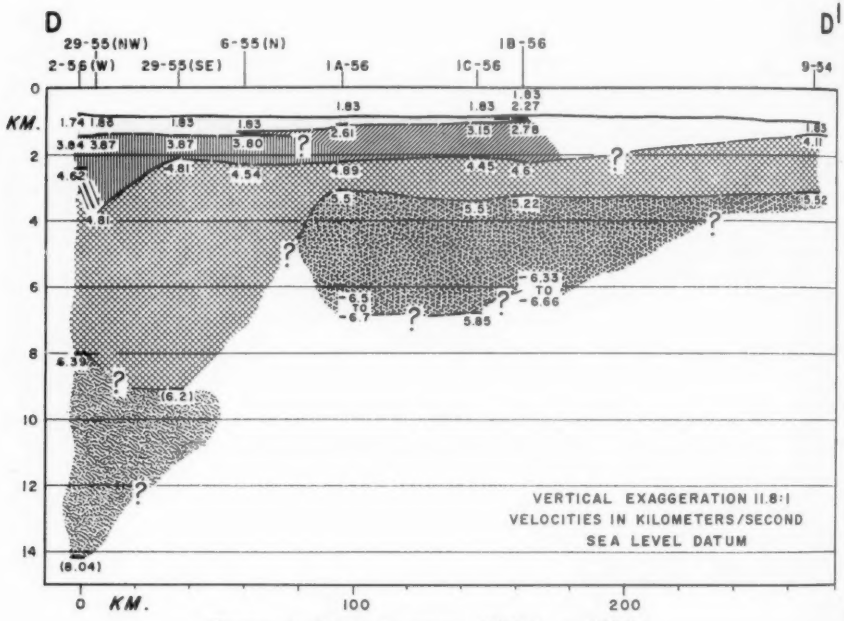

FIGURE 6.—BLAKE PLATEAU: 28°90'N. to 31°00'N.
Structure section *D-D'* (Pl. 1)

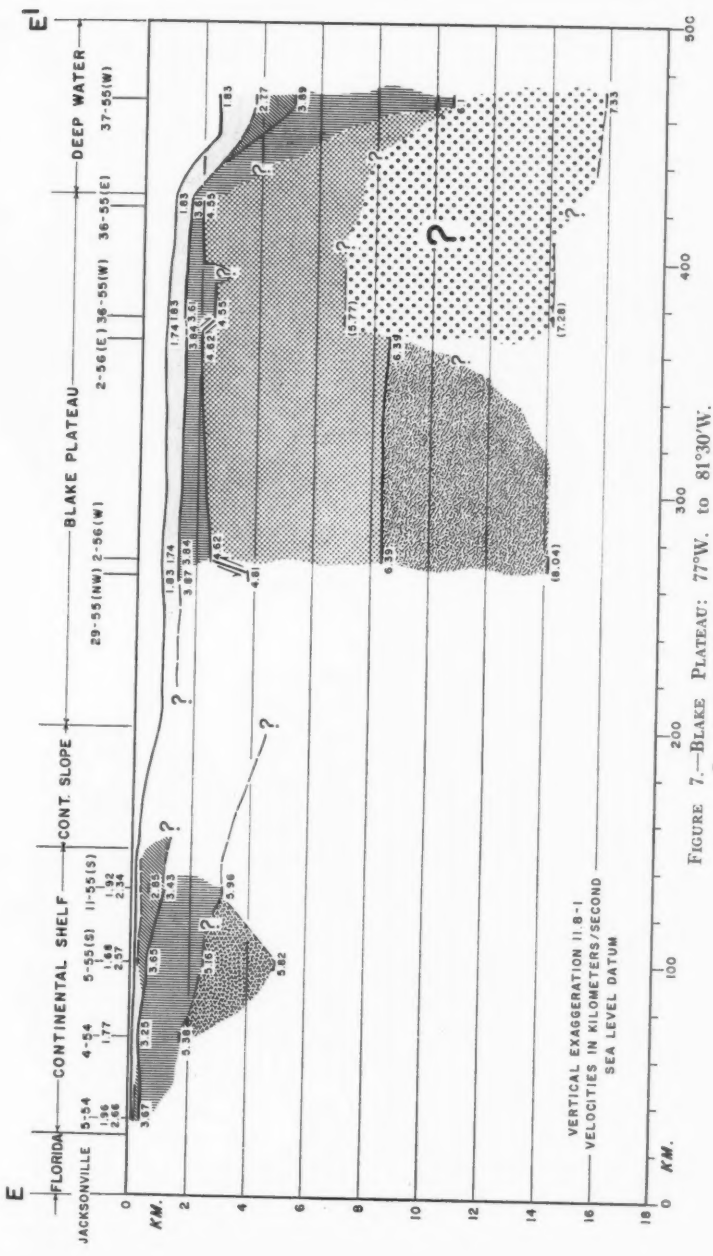

FIGURE 7.—BLAKE PLATEAU: 77°W. to 81°30'W. Structure section *E-E'* (Pl. 1)

9-54, an end-to-end profile, and on 1A-56, 1B-56, 1C-56, all unreversed. On 2-56, the absence of the 5.2-km/sec. layer is based on inadequate travel-time evidence; it is apparently excellent evidence of local depression, possibly faulting, in the 4.55-km/sec. layer as shown. North and northwest of the general vicinity of 2-56 the plateau loses its smooth character and

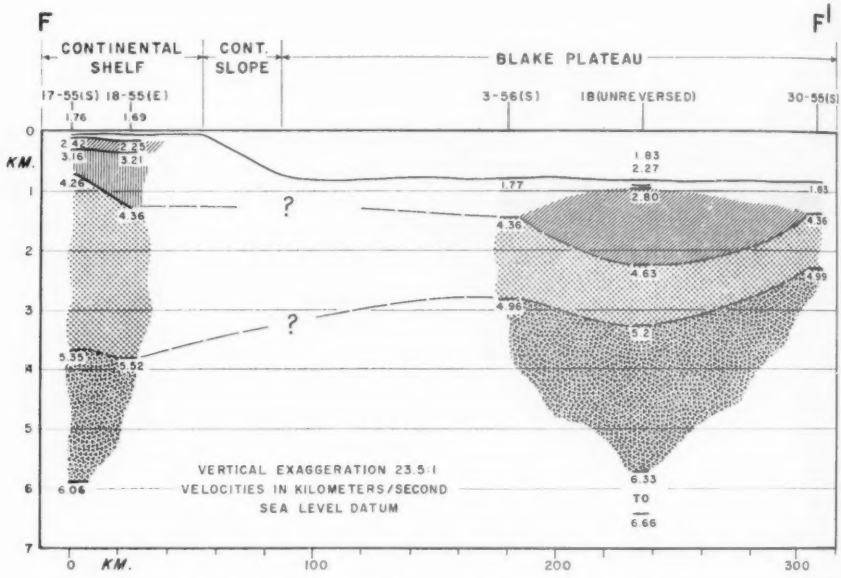

FIGURE 8.—BLAKE PLATEAU: 77°30'W. to 80°35'W. Structure section *F-F'* (Pl. 1)

absent on 29-55 and 36-55 as well. Hence we suggest that there is probably a considerable thickness of the 4.4-km/sec. layer beneath these profiles. Test calculations indicate the same beneath 6-55, indicating a major trough structure which, on evidence to be discussed, we suppose trends east-northeast.

Four profiles, three unreversed, show a high velocity, mostly 6.3–6.7 km/sec.; three south of the trough are shallow compared with the fourth, which is over it. The greater depth is the reversed profile (2-56). This large difference in depth corroborates the trough structure discussed above.

The structure section *E-E'* (Fig. 7) crosses and recrosses the fault zone south of 2-56. Recent topographic studies by Hersey and others (Unpublished) have shown that the east-west trench south of 2-56 curves northward near the eastern end of 2-56 and the western end of 36-55, as is also indicated by the occurrence of the 3.8-km/sec. layer and the change in depth of the 4.4-km/sec. layer. Profile 36-55 contains shows complicated relief as the bottom shoals to the continental shelf. From this admittedly scanty evidence we suggest that structures similar to those shown in Figure 7 form the pattern of adjustment between the southern flank of the Cape Fear Arch, the northern wedge of the Blake Plateau, and the deeper ocean area to the east.

The deeper horizons of 2-56, 36-55, and 37-55 are based on data of variable quality, but there can be little doubt that high-velocity layers are present. On 2-56, 6.3 km/sec. is well established, as is 6.1 km/sec. on 37-55, but 5.77 km/sec. on 36-55 is unreversed. It seems plausible that these represent the same horizon. If so, they show much less marked change in depth here than the lower-velocity layers. However, the high relief in the 6.3 km/sec. indicated on section *D-D'* (Fig. 6) and the uniformly great depth on section *E-E'* (Fig. 7) and on profile 30-55 reveal a major depression of this layer trending east-northeast, north of 1A-56. The topographic nose trending east-northeast (Pl. 1)

might represent the extension of the southern flank of this depression, but we were not able to investigate this possibility. On 2-56, 8.0 km/sec. is unreversed but is based on high quality data. On 36-55, 7.28 km/sec. is unreversed, whereas 7.4 km/sec. on 37-55 is reversed and shows considerable slope at this interface. If these represent the same interface, it must have considerable relief. We have not measured velocities higher than 7 km/sec. elsewhere on the Blake Plateau. These high velocities could represent either the M layer or possibly partially differentiated ultrabasic material; we suggest that either may be the case, depending on locality. In order to determine the depth and velocity of this layer beneath the Blake Plateau, several critically located long profiles with heavy charges will be needed.

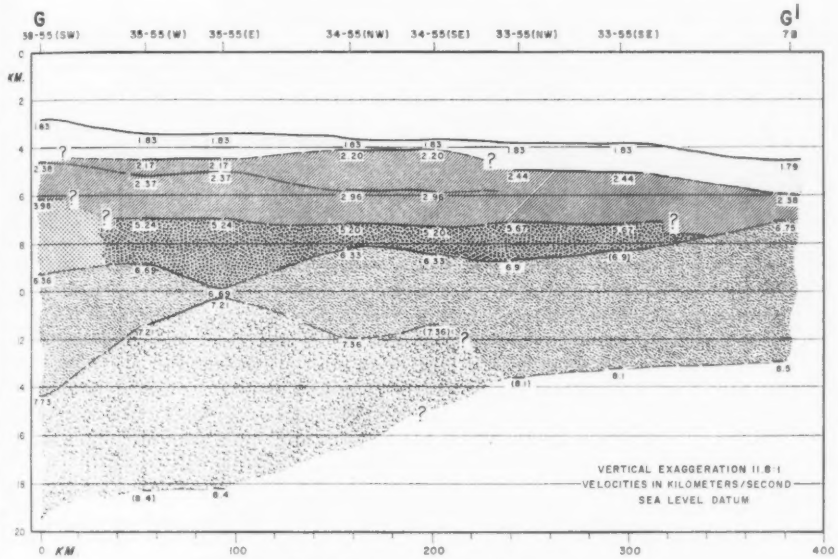

FIGURE 9.—DEEP-WATER SECTION ALONG THE RIDGE
Structure section *G-G'* (Pl. 1)

Deep-Water Profiles

East of the northern part of the Blake Plateau 13 profiles were established in water depths from 2800 to 4500 meters with the intention of studying the structures underlying the topographic ridge extending on a line roughly southeast from Cape Fear. With a few exceptions the locations and orientation of the profiles were determined by weather rather than the problems to be solved. Nevertheless we were able to gather fair to excellent data giving velocities as high as 7.5–8.4 km/sec. on nearly all profiles.

The sections of Figures 9–11 summarize the results. In Figure 9 (Pl. 1, *G-G'*) a section is shown approximately along the crest of the ridge. At the southeastern end is one end of profile 7 of Katz and Ewing (1956) where the section is rather like those representative of deep ocean basins (Ewing and Press, 1955) except that a 2.38-km/sec. layer is shown overlying the layer commonly identified as basaltic. Proceeding northwestward, a 2.5-km/sec. layer is underlain by 5.3 km/sec. which, in turn, overlies 6.6 km/sec., 7.3 km/sec., and 8.4 km/sec. in more or less similar sequences through 35-55. Here the section thickens and the 8.4-km/sec. interface deepens to the northwest. Between 35-55 and 38-55 the section changes abruptly and the 5.3-km/sec. layer is replaced by 3.98 km/sec. Other notable features are the very thick section of low velocities 1.79–2.96 km/sec. and considerable variation in thickness of the 5.3- and 6.6-km/sec. layers.

The sections shown in Figures 10 and 11 are transverse to *G-G'*. Section *H-H'* (Fig. 10) to the northwest indicates that a section some-

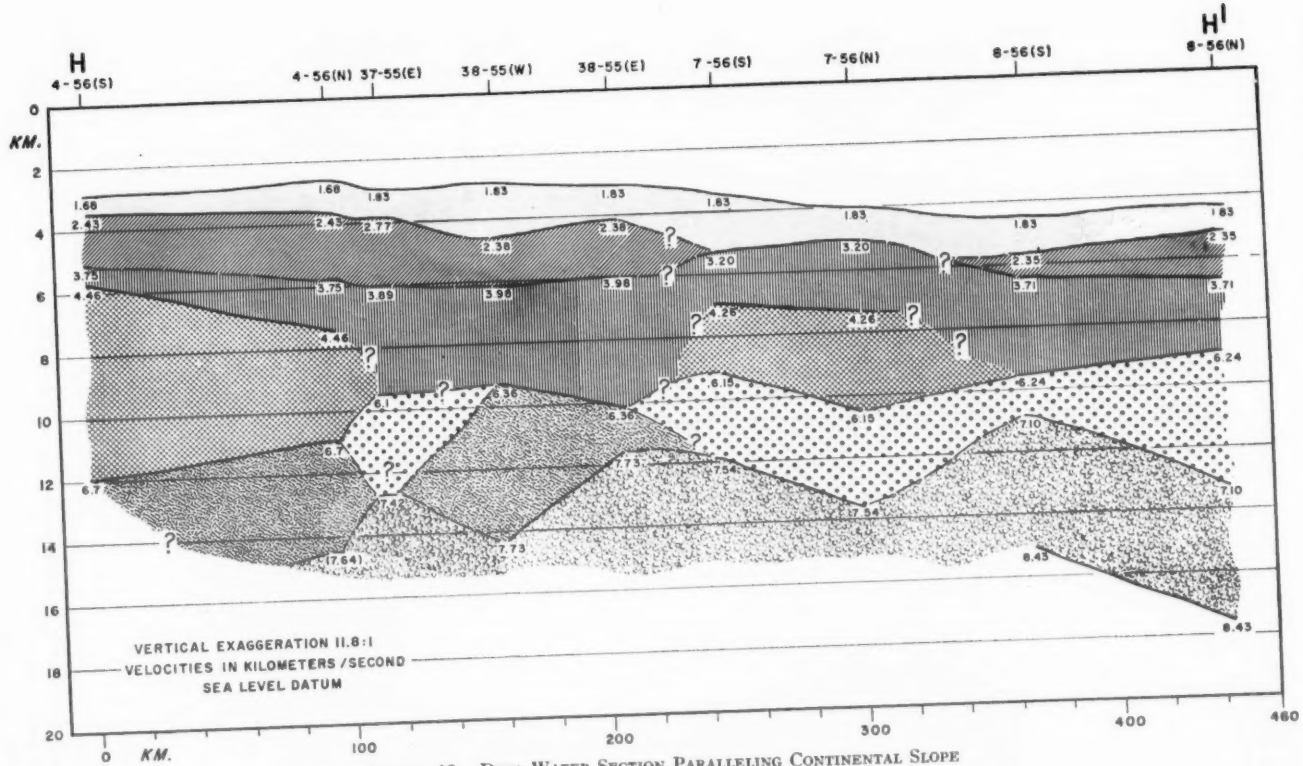

FIGURE 10.—DEEP-WATER SECTION PARALLELING CONTINENTAL SLOPE
Structure section *H-H'* (Pl. 1)

what like that of 38-55 persists along this trend, and that the velocities above 10-km depth are rather similar to those in the structural trough of the Blake Plateau and could be an extension of it. Notable in contrast to section *G-G'* is the absence of any velocity close to 5.3 km/sec. and the variable thickness and velocity of the group lying between 6.1 and 6.7 km/sec. Profile 39-55 is essentially similar to section *H-H'*.

Profiles 5-56 and 6-56 which lie southwest of the ridge are complicated by evidence of faulting which appears as displacement of the highest-velocity line. Both lie over structures that are partly like those of section *H-H'* and partly like the ridge; this indicates that the trough mentioned in connection with section *H-H'* extends southeastward from profile 37-55 between the ridge and the edge of the Blake Plateau (Fig. 13). The faulting shown in 6-56 is downthrown on the ridge side. We cannot reconcile the displacement of the high-velocity line because of the difficulty with the low velocities discussed in the evaluation of the profile (Appendix). Maximum possible vertical fault throw is 2 km. Profile 5-56 is downthrown to the northwest and appears to overlie different shallow structures at either end; it is like the trough section to the northwest and like the ridge to the southeast.

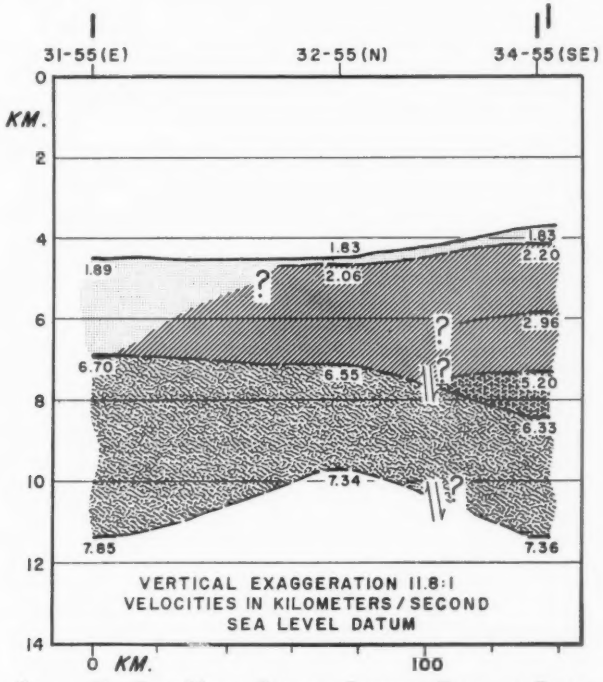

FIGURE 11.—DEEP-WATER SECTION: INTERIOR BASIN TO RIDGE
Structure section *I-I'* (Pl. 1)

The final section *I-I'* (Fig. 11) shows the transition from the nearly ocean-basin type of 31-55 through the slightly more complicated section of 32-55 to the typical ridge section of 34-55. Katz and Ewing's (1956) station 13 (A-164, not shown) lies about halfway between 32-55 and the ridge but is similar to 32-55, which indicates that the change to the ridge section is abrupt on its southwest side.

Gravity measurements were made by J. L. Worzel and his co-workers (1957) on the Blake Plateau and over the deep-water area. Free-air anomalies over the Blake Plateau section of the trough are as great as −47 milligals, compared with 0 to about −20 milligals in the area south of the trough. The thick section of 4.5 km/sec. in the trough compared with 6.2 km/sec. at the

Structure section *H-H'* (Pl. 1)

same depths to the south results in about this gravity difference using the density/P-wave velocity relationships recently compiled from various sources by Nafe and Drake (Personal communication). The ridge has free-air anomalies from about 0 to 8 milligals compared with about −30 to −50 milligals in surrounding near-by ocean-basin areas. Roughly a 40-milligal gravity excess can be found on the ridge by comparing a velocity section down to the base of the 5.4-km/sec. layer with an assumed ocean-basin section of 5 km of water, 1 km of sediment, and 5 km of 6.5 km/sec. above the M layer. The spread of the density-velocity relations allows considerable choice throughout this section without having an overwhelming effect on the anomaly. However, below the 5.4-km/sec. layer the layer thicknesses are so much greater that slight differences in density choice have a large effect on the computed gravity effect. Hence it seems useless now to speculate about the gravitational effects of the deeper structures.

Air-borne magnetometer observations were made over the area by M. Davidson. These have not been reduced at this writing, but some of their obvious qualitative features indicate that further magnetic observations will be valuable in continued study of this whole area.

GEOLOGIC HISTORY OF THE DEEP-WATER AREA: Even though additional profiles are needed both north and south of the ridge, there are adequate data for a coherent hypothesis about the structure and geologic history. In this section, we present a hypothesis about the structural history of the deep-water area and its relation to the Blake Plateau structures based on our results there.

The structure sections in the deep-water area suggest that three main divisions in the area can be treated as units: (1) the interior-basin type comprising profiles 31-55 and 32-55, (2) the ridge, comprising 33-55, 34-55, 35-55, parts of 5-56 and 6-56, and 7B of Katz and Ewing (1956), and (3) the slope comprising section *H-H'* and parts of 5-56 and 6-56.

(1) The interior-basin-area profiles are somewhat similar to typical deep-ocean-basin sections with low-velocity sediment layers and two higher-velocity layers. The thickness of low-velocity material, thought to be of unconsolidated sediments, is about 2.5 km, or considerably thicker than the 1 km or less of the oceanic section. The basaltic layer taken as 6.4–6.8 km/sec. is somewhat less thick than that of the ocean basins and is underlain by a velocity somewhat lower than the expected 8.0 km/sec. for the M layer, particularly at 32-55. The thicker sedimentary section there is reasonable because of its nearness to the continental slope. The 7.5- to 7.8-km/sec.-layer depths in this area and beneath the ridge suggest a deep-seated structural high just to the southwest of the ridge and parallel to it. Such a velocity at this depth might be due to interaction between the mantle and the basaltic layer which resulted in a material of intermediate composition, as suggested by Officer *et al.* (1957) for portions of the Caribbean. On this supposition, it is reasonable to account for structures restricted to the ridge as consequent to this deep-seated activity.

(2) The ridge structures differ from all others here by containing an appreciable thickness of 5.3 km/sec. overlying the basaltic layer (6.4-6.8 km/sec.) and the intermediate layer (7.3 km/sec.) discussed above. Velocity lines of the M layer, recorded on two profiles beneath the ridge, indicate that the M layer deepens there to the northwest; this is a wholly reasonable expectation. If we suppose it to be igneous rock, the 5.3-km/sec. layer, occurring near the apparent crest of the high in the intermediate layer (7.3 km/sec.), suggests further differentiation which might be consequent to that producing the intermediate layer. Its velocity is low for granite but agrees with oceanic volcanic rocks reported by Raitt *et al.* (1955) west of the Tonga trench.

The top of the 5.3-km/sec. layer under the ridge is at about the same depth as the top of the basaltic layer to the southwest but appreciably shoaler than basaltic velocities everywhere in the slope section. However, profile 6-56 on the southwest flank of the ridge shows a fault downthrown on the ridge side possibly by as much as 2 km. This indicates that the ridge area is one of relative subsidence. The indicated movement may not be the whole subsidence, and thus we suggest that the ridge may once have been as much as 2 km higher; another 2-km elevation would readily allow it to have been a shallow reef or a land area.

(3) The slope structures are distinguished principally by the great thickness of layers having 3.8- to 4.4-km/sec. velocity, by apparently unsystematic variations in the depth of the intermediate layer (7.3 km/sec.), by evidence of faulting on several profiles, and by the persistent occurrence of material with 6.0- to 6.24-km/sec. velocity, apparently in place of adjoining masses which have velocities of 6.34–6.7 km/sec.

Profiles 36-55, on the edge of the Blake Plateau, and 5-56 and 6-56 contain evidence of faulting; *i.e.*, they contain two velocity lines of identical slope but displaced in intercept on the same end of the profile. The faults of 36-55 and 5-56 and the abrupt contrast between the ridge section and structures in near-by 6-56 and 38-55 are consistent with the notion that a fault-bounded trough was formed roughly along the trend of section *H-H'* (Fig. 10) before and during the formation of the layers which have velocities 3.8–4.5 km/sec. However, as discussed above, the fault in 6-56 has the opposite throw; *i.e.*, the ridge area has moved downward perhaps as much or more than 2 km relative to the adjoining depression.

In light of the facts discussed above we suggest the following speculative hypothesis about the geologic history of the trough and ridge area. The history of the ridge according to this hypothesis is sketched in Figure 12. The horizontal dimensions of the structures are outlined in Figure 13.

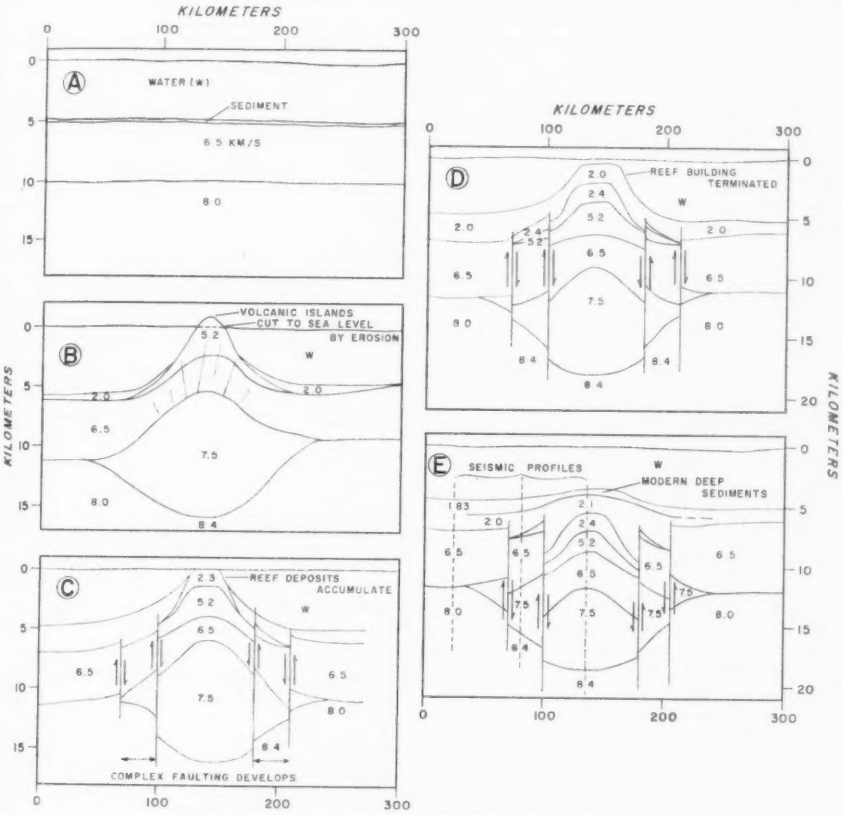

FIGURE 12.—SPECULATIVE HISTORY OF THE RIDGE
Section is southwest–northeast across ridge.

If we suppose that all velocities from 1.7 to 4.5 km/sec. represent sediments, then the depths and thicknesses of the corresponding layers can be accounted for by the following sequence: (1) normal ocean structure (Fig. 12*A*); (2) formation of the material of 7.5-km/sec. velocity from interaction between the mantle and the basaltic layer, and accompanying formation of the lower-velocity 5.2 km/sec. above the basaltic layer by extrusion and separation of the lighter materials; during this period the ridge structures may have formed a continuous land area, or a chain of islands and

reefs (Fig. 12*B*); (3) downwarping and faulting of the irregular area where the trough structures of the slope are found (outlined in Figure 13), accompanied by deposition of material, the part of a structure that has irregular relief but trends beneath the Blake Plateau toward Cape Canaveral. Nafe and Hennion were able to map the 5.2- to 5.8-km/sec. layer extensively south

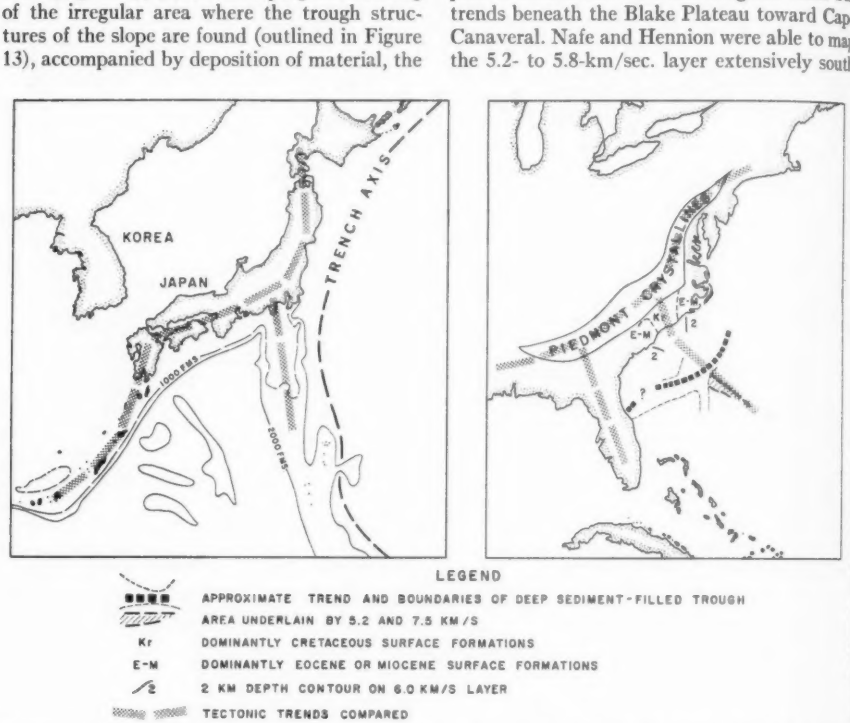

FIGURE 13.—COMPARISON OF PIEDMONT, COASTAL PLAIN, AND OCEANIC STRUCTURE WITH WESTERN PACIFIC ISLAND ARCS

velocity of which is now 3.8–4.5 km/sec; (4) deposition of 2.1- 2.4-km/sec. material accompanied by downward movement of the ridge with accommodation along bordering fault zones (Fig. 12*C*, *D*); (5) downward movement of the whole area relative to the continent accompanied by deposition of the unconsolidated sediments forming the top layer (Fig. 12*E*).

The Blake Plateau structures are consistent with this hypothesis, if one imagines that the considerable thickness of material having velocities of 4.5 km/sec. and less at and north of profiles 6-55 forms a southwesterly extension of the trough interpreted to occupy the slope section. There appear to be far greater thicknesses of material with velocities in the 5.2–5.8 range beneath the Blake Plateau than on the ridge. Nafe and Hennion (In preparation) present evidence that the shallow 6.7-km/sec. layer at 1A-56, 1B-56, and 1C-56 together with the overlying 5.2- to 5.8-km/sec. layer are of this trend. It is tempting to suppose that this 5.2- to 5.5-km/sec. layer is found only on this trend and south of it. In any event there is no other evidence for such a velocity north of 1A-56 except on the ridge.

Relationship of Adjoining Structures

Relation to the ocean basins.—The nearest seismic-refraction profiles in North America basin are those of Katz and Ewing (1956), one of which is reproduced here in part (Fig. 9, profile 7B). They are essentially typical ocean-basin profiles with a thin basaltic crust overlain by one or two thin layers of low-velocity sediments. A profound change has occurred between them and the easternmost profiles in deep water here. Assuming the ridge to be an ancient volcanic-island structure, by analogy with modern structures one might expect to find evidence of an ancient foredeep in the deeper water northeast of the ridge. The struc-

ture of this area must be known to understand the region as a whole. Similarly, the apparent extension of the topographic ridge toward Eleuthera (Pl. 1) and the structure of the interior basin west of it must be better known.

Relation to other continental slope structures.—Drake *et al.* (1957) presented an interpretation of the findings of the Lamont Geological Observatory group beneath the continental shelf and slope north of Cape Hatteras to the Grand Banks. They found two roughly parallel sediment-filled trenches of probable Mesozoic age paralleling the coast. Possibly the trench of the slope section in this area is continuous with the eastern one to the north. Again, additional seismic observations should provide the answer.

Relation to continental structures.—The work of Nafe and Hennion (In preparation) on the southern part of the Blake Plateau indicates that the layers of 5.2–5.6 km/sec. and 4.2–4.5 km/sec. are of Cretaceous age; similarly Upper Cretaceous age is indicated for the 2.5-km/sec. layer in the depth relations between the outermost profiles on the shelf off Jacksonville and profile 29-55 on the Blake Plateau. This implies Cretaceous age for the layers 2.8 through 4.5 km/sec. throughout the area. This further implies Cretaceous as the age of the sediment-filled trough that we have interpreted above as cutting across the northern Blake Plateau and along the slope section. This would imply a pre-Upper Cretaceous period of tectonic activity as the time of formation of the deep-water ridge and the positive feature from profile 1A-56 south.

The Cape Fear Arch, a positive feature, is a basement structure which has been traced southeast from the Piedmont nearly to the edge of the continental shelf. It seems unlikely that it ends abruptly there, and from a very early stage in the present study we supposed that the deep-water ridge might be an extension of it. We have been unable to make observations in the obvious gap between the shelf and the 1500-fm (2745 m) contour here, but some facts support such an interpretation: (1) The ridge has the same trend as the arch and is approximately aligned with it. (2) The ridge is the surface expression of a deep-lying structure traceable to activity of the mantle, which has the same trend. (3) In several profiles of the slope area there are thin and variable thicknesses of 6.0- to 6.2-km/sec. velocity. Supposing this material to be granitic, it seems likely that here is the edge of continental granitic material. Hence the Cape Fear Arch may persist in some form this far from the shelf.

In any event the gap in seismic results between the shelf and 1500 fathoms (2745 m) must be an area of structural adjustment. There are many superficial suggestions of complicated structure in the known topography here, but the topographic picture is not detailed enough to further our understanding at present.

Comparison with Other Regions

The tectonic lineaments suggested by this line of speculation are similar to those of the western Pacific. Thus, the Appalachian Piedmont of late Paleozoic time may be compared with the modern Japanese archipelago, the Cape Fear Arch and ridge structure with the Bonin-Marianas arc, and the Peninsular Arch of Florida described by Applin (1951) with the Ryukyu island chain extending southwestward from Japan (Fig. 13). This comparison rests primarily on the similarity between western Pacific topography and southeastern United States structures. The Cape Fear Arch trends southward from a sharp northward bend in the Piedmont, as do the Honshu-Mariana ridges from a similar northward bend of Honshu; the Peninsular Arch trends sharply away from the Piedmont much as the Ryukyu arc does from Japan. However, there is another point of similarity in the relative ages of the component parts of the two systems: the Japanese and Ryukyu arc structures are thought to be mid-Mesozoic and the Honshu-Mariana ridges Cretaceous to Tertiary (Hess, 1948); Kay (1951, p. 57–60) favors a mid-Paleozoic age for the development of Piedmont structures, and structures on the seaward trend from the Cape Fear Arch appear to have been formed much more recently, possibly in late Mesozoic. The American structures are older than those of the western Pacific, and seismic activity in the former is much less than the latter, thus eliminating present-day dynamics as a means of comparison. Comparative studies in the two regions including seismic and other geophysical exploration techniques are needed for testing further any ideas of tectonic similarity.

The conjectured Cretaceous aspect of the plateau and slope region is strikingly similar to modern land forms in the Bahamas; the plateau-slope trench has a probable shape (not yet completely defined) somewhat similar to the Tongue of the Ocean or Exuma Sound. The latter comparison is consistent with what is known of the Bahamas, where great thicknesses of limestone have been found by drilling, with our hypothesis about the region as a whole, and with modern

Blake Plateau topography. For example, imagine a Cretaceous aspect of the plateau similar to the modern Bahamas. Then during the later history of the trough erosional action, possibly in part by the Gulf Stream and in part by subaerial processes, may have planed the central portion of the Blake Plateau to nearly its present smoothness near sea level. Subsequent subsidence and continued erosion by Gulf Stream-driven currents might then produce the modern aspect of the plateau. Possibly the pattern of Gulf Stream flow may have been deflected easterly and southerly by the ridge when it was partially emerged or at least much shoaler than now. In this event the latter stage of purely submarine erosion was probably most marked to the south and progressed northerly across the plateau as the submarine topography permitted the Gulf Stream thus to alter its course. Such an account of the history of the region would imply that this erosional process continues. This is consistent with what is known of the area and the behavior of the Gulf Stream as far north as Cape Hatteras.

These large-scale comparisons contain obvious pitfalls. However, we have become increasingly convinced in the course of this study that much new understanding of crustal tectonics may be found by comparative study of smaller and probably simpler oceanic structures, such as individual seamounts and their environs, connected chains of seamounts, and relatively minor ridge-like topographic features such as that of the present study. Just as the studies of the Caribbean Island arcs by M. Ewing and Worzel (1954), Officer *et al.* (1957), and J. Ewing *et al.* (1957), and the studies of the Bermuda area (Officer *et al.*, 1952) have suggested large-scale interactions between crust and mantle, it appears likely that lesser oceanic topographic features which probably have simpler structures may be the key to understanding the elements of the larger structures and the antecedent geodynamics.

References Cited

Applin, P. L., 1951, Preliminary report on buried pre-Mesozoic rocks in Florida and adjacent States: U. S. Geol. Survey Circ. 91, 28 p.

Applin, P. L., and Applin, E. R., 1944, Regional subsurface stratigraphy and structure of Florida and southern Georgia: Am. Assoc. Petroleum Geologists Bull., v. 28, p. 1673–1753

Bonini, W. E., 1955, Seismic-refraction studies of geologic structure in North Carolina and South Carolina (Abstract): Geol. Soc. America Bull., v. 66, p. 1552

Drake, C. L., Sutton, G. H., and Ewing, M., 1957, Continental margins and geosynclines, east coast of North America north of Cape Hatteras (Abstract): Geol. Soc. America Bull., v. 68, p. 1718

Ewing, J. I., Officer, C. B., Johnson, H. R., and Edwards, R. S., 1957, Geophysical investigations in the Eastern Caribbean and Trinidad Shelf, Tobago trough, Barbados Ridge, Atlantic Ocean: Geol. Soc. America Bull., v. 68, p. 897–912

Ewing, M., and Press, F., 1955, Geophysical contrasts between continents and ocean basins, p. 1–6 *in* Poldervaart, Arie, *Editor*, Crust of the Earth: Geol. Soc. America Special Paper 62, 762 p.

Ewing, M., and Worzel, J. L., 1954, Gravity anomalies and structure of the West Indies, Parts I and II: Geol. Soc. America Bull., v. 65, p. 165–174, 195–200

Ewing, M., Crary, A. P., and Rutherford, H. W., 1937, Geophysical investigations in the emerged and submerged Atlantic Coastal Plain, Part I: Methods and results: Geol. Soc. America Bull., v. 48, p. 753–802

Ewing, M., Woollard, G. P., and Vine, A. C., 1939, Geophysical investigations in the emerged and submerged Atlantic Coastal Plain, Part III: Barnegat Bay, New Jersey, section: Geol. Soc. America Bull., v. 50, p. 257–296

—— 1940, Geophysical investigations in the emerged and submerged Atlantic Coastal Plain, Part IV: Cape May, New Jersey, section: Geol. Soc. America Bull., v. 51, p. 1821–1840

Ewing, M., Worzel, J. L., and Shurbet, G. L., 1957, Gravity observations at sea in U. S. submarines Barracuda, Tusk, Conger, Argonaut, and Medregal, p. 50–115 *in* Jubilee Volume in honor of F. A. Vening Meinesz: The Hague, Royal Netherlands Geol. and Min. Soc.

Ewing, M., Worzel, J. L., Steenland, N. C., and Press, F., 1950, Geophysical investigations in the emerged and submerged Atlantic Coastal Plain, Part V: Woods Hole, New York, and Cape May section: Geol. Soc. America Bull., v. 61, p. 877–892

Hersey, J. B., and Ewing, M., 1949, Seismic reflections from beneath the ocean floor: Am. Geophys. Union Trans., v. 30, p. 5–14

Hersey, J. B., and Rutstein, M., 1958, A reconnaissance survey of the Oriente Deep with a precision echo sounder: Geol. Soc. America Bull., v. 69, p. 1297–1304

Hess, H. H., 1948, Major structural features of the western North Pacific; an interpretation of H. O. 5485, bathymetric chart, Korea to New Guinea: Geol. Soc. America Bull., v. 59, p. 417–445

Katz, S., and Ewing, M., 1956, Seismic-refraction measurements in the Atlantic Ocean, Part VII: Atlantic Ocean Basin, west of Bermuda: Geol. Soc. America Bull., v. 67, p. 475–510

Kay, Marshall, 1951, North American geosynclines: Geol. Soc. America Mem. 48, 143 p.

King, P. B., 1950, Tectonic framework of southeastern United States: Am. Assoc. Petroleum Geologists Bull., v. 34, p. 635–671

Knott, S. T., and Hersey, J. B., 1956, Interpretation of high-resolution echo sounding techniques and their use in bathymetry, marine

geophysics, and biology: Deep Sea Research, v. 4, p. 36–44
Longwell, C. R., *et al.*, 1944, Tectonic map of the United States: Am. Assoc. Petroleum Geologists
Mansfield, W. C., 1936, Some deep wells near the Atlantic coast in Virginia and the Carolinas: U. S. Geol. Survey Prof. Paper 186-I, p. 159–161
Meyer, R. P., 1955, Seismic studies of offshore geologic structure between Charleston, South Carolina, and Cape Fear, North Carolina (Abstract): Geol. Soc. America Bull., v. 66, p. 1597
Officer, C. B., 1955, A deep-sea seismic reflection profile: Geophysics, v. 20, p. 270–282
Officer, C. B., and Ewing, M., 1954, Geophysical investigations in the emerged and submerged Atlantic Coastal Plain, Part VII: Continental shelf, continental slope, and continental rise south of Nova Scotia: Geol. Soc. America Bull., v. 65, p. 653–670
Officer, C. B., and Wuenschel, P. C., 1951, Reduction of deep-sea refraction data: Palisades, N. Y., Lamont Geol. Observatory Tech. Rept. 1, 12 p.
Officer, C. B., Ewing, M., and Wuenschel, P. C., 1952, Seismic refraction measurements in the Atlantic Ocean, Part IV: Bermuda, Bermuda Rise, and Nares Basin: Geol. Soc. America Bull., v. 63, p. 777–808
Officer, C. B., Ewing, J. I., Edwards, R. S., and Johnson, H. R., 1957, Geophysical investigations in the eastern Caribbean: Venezuelan basin, Antilles island arc, and Puerto Rico trench: Geol. Soc. America Bull., v. 68, p. 359–378
Oliver, J. E., and Drake, C. L., 1951, Geophysical investigations in the emerged and submerged Atlantic Coastal Plain, Part VI: The Long Island area: Geol. Soc. America Bull., v. 62, p. 1287–1296
Raitt, R. W., Fisher, R. L., and Mason, R. G., 1955, Tonga Trench, p. 237–254 *in* Poldervaart, Arie, *Editor*, Crust of the earth: Geol. Soc. America Special Paper 62, 762 p.
Richards, H. G., 1945, Subsurface stratigraphy of Atlantic Coastal Plain between New Jersey and Georgia: Am. Assoc. Petroleum Geologists Bull., v. 29, p. 885–955
Skeels, D. C., 1950, Geophysical data in the North Carolina Coastal Plain: Geophysics, v. 15, p. 409–425
Spangler, W. B., 1950, Subsurface geology of Atlantic Coastal Plain of North Carolina: Am. Assoc. Petroleum Geologists Bull., v. 34, p. 100–132
Stephenson, L. W., 1926, Major features in the geology of the Atlantic and Gulf coastal plain: Wash. Acad. Sci. Jour., v. 16, p. 460–480
—— 1928, Major marine transgressions and regressions and structural features of the Gulf Coastal Plain: Am. Jour. Sci., ser. 5, v. 16, p. 281–298
Sutton, G. H., and Bentley, C. R., 1953, Topographic correction curves: Palisades, N. Y., Lamont Geol. Observatory Tech. Rept. 3, 5 p.
Tolstoy, I., 1951, Submarine topography in the North Atlantic: Geol. Soc. America Bull., v. 62, p. 440–451
U. S. Hydrographic Office, 1948, North America, East Coast and West Indies: Halifax to Hispaniola including the Bahamas and Greater Antilles: H. O. Chart No. 1411
Worzel, J. L., and Ewing, M., 1948, Explosion sounds in shallow water, p. 1–53 *in* Ewing, M., Worzel, J. L., and Pekeris, C. L., Propagation of sound in the ocean: Geol. Soc. America Mem. 27, 205 p.

Woods Hole Oceanographic Institution, Woods Hole, Mass.; Woods Hole Oceanographic Institution, Woods Hole, Mass.; General Electric Company, Syracuse, N. Y.; University of Rhode Island, Kingston, R. I.
Manuscript Received by the Secretary of the Society, April 24, 1958
Woods Hole Oceanographic Institution Contribution No. 973

Appendix: Discussion of Data

I. *Continental Shelf—Plate 2A*

Profiles 3-54 to 5-54 and 10-54 to 15-54

(a) Atlantis 196—Bear 89

Bear acted throughout as receiving ship, while Atlantis closed and opened range, using Bear as center. The velocity and layer-thickness determinations based on these data are reasonable interpretations of the profiles obtained and will not be discussed in detail. Comparatively small charges (up to 20 pounds) were used, the profiles were short, and the depth of penetration modest.

Profiles 5-55 and 11-55 to 18-55

(b) Vema 6—Bear 113

With the exception of the profiles discussed in more detail below, all the reversed data are in good agreement. Velocities that range from 1.68 to 1.92 km/sec. (indicative of sediments) are found on almost all the travel-time plots as second and third arrivals and at short range as first arrivals.

Profile 17-55:

All the lower velocities are relatively well established. The 5.35 km/sec. horizon has few points because of the relatively wide shot spacing in this range. The 6.06 km/sec. horizon occurs as strong first arrivals over the last three seconds on Vema and last 4.5 seconds on Bear.

Profile 18-55:

Vema receiving end of this profile indicates a velocity of 1.69 km/sec. which is apparently masked by 2.25-km/sec. arrivals on Bear. It has been assumed present on Bear from Vema evidence and an equivalent velocity on Profile 17. Vema has only slight substantiation of the 4.36-km/sec. velocity found on Bear. Some evidence suggests a horizon of velocity 5.55 km/sec. on Bear only.

II. *Blake Plateau—Plate 2B*

Profiles 9-54, 6-55, 29-55, 30-55, 36-55; 1A-56, 1B-56, 1C-56, 2-56, and 3-56

(a) ATLANTIS 196—BEAR 89

Profile 9-54: The velocities determined on this profile are well established by the data. There is no refraction evidence for any horizon of velocity higher than 4.11 km/sec., but the profile is short, and 20 pounds was the largest charge used.

(b) VEMA 6—BEAR 113

Profile 6-55: These velocities are well established. There is no evidence for any horizon of velocity higher than 4.54 km/sec. This is a short profile with 20-pound maximum charge.

(c) ATLANTIS 213—BEAR 113 (Profiles 29-55, 30-55, and 36-55)

Profile 29-55: This profile station was made before the structure of the area was known. The travel-time data suggest a complicated structural problem. The determination of the 3.8-km/sec. velocity is excellent. On the southeast end (ATLANTIS), there is strong evidence for a layer of 4.81 km/sec. velocity which overlies one of 6.18 km/sec. A few arrivals on the northwest (BEAR) end of the profile substantiate this 4.81-km/sec. layer. A horizon with compressional velocity of greater than 4.68 km/sec. is suggested but not established by some arrivals received at distances greater than 9 seconds on the BEAR end.

Profile 30-55: The determination of 4.30- and 4.99-km/sec. horizons is straightforward. A few poor arrivals at distances greater than 15 seconds on ATLANTIS end indicate a higher-velocity horizon but do not determine it. On BEAR end there is evidence (indicated by the dashed line) for a high-velocity horizon. This can be interpreted as 6.9 km/sec., at 8.5 km below sea level or as high as 7.2 km/sec., 8.8 km below sea level. Possibly the 5.5-km/sec. horizon found throughout this region of the Blake Plateau is present but masked by the BEAR high velocity and by poor data on the reverse.

Profile 36-55: The 3.61-km/sec. horizon is well established. The lines having approximately 4.5 km/sec. indicate that it is deeper at the northwest end than at the southeast end, but that in between it is depressed still farther, possibly by local faulting, over about 12 km. The depression amounts to about 0.5 km relative to the southeast end (Fig. 7). An excellent line with an apparent velocity of 7.33 km/sec. is found on the BEAR profile (northwest); no data on ATLANTIS end.

(d) ATLANTIS 223—BEAR 140 (Profiles 1A-56 1B-56, 1C-56, 2-56, and 3-56)

Refraction arrivals on Profiles 1A-56, 1B-56, 1C-56, and 3-56 substantiate the reflection evidence for sedimentary horizons varying in velocity from 1.6 to 1.9 km/sec. In computing velocities for the profiles having no refraction evidence for these sedimentary horizons a value of 1.83 km/sec. obtained from reflection data has been used.

Profiles 1A-56, 1B-56, and 1C-56: These three unreversed profiles are from the same general vicinity (Pl. 1). Their geographic direction is approximately north-south. The receiving locations for 1A-56 and 1C-56 are indicated as north (N); the shooting-ship track is south in each case. Profile 1B-56 is indicated as northwest (NW) since the shot line is northwest of the receiving-ship position. All show approximately the same velocity horizons through 5.2–5.5 km/sec. Evidence for a higher velocity can be found on all three. The dashed line on 1A shows the highest velocity that can be determined, 6.7 km/sec. at 6.9 km below sea level. The lowest value possible from these data is 6.5 km/sec., 6.33 km below sea level. On profile 1B the highest determination is 6.6 km/sec., 6.4 km deep. The lowest determination possible is 6.3 km/sec., at 5.73 km depth. Profile 1C shows 5.85 km/sec. at a depth of 6.8 km. No significantly different alternative velocity can be measured.

Profile 2-56: This was unreversed over the range 38-55 seconds on BEAR (east) end. The 3.84-km/sec. layer is determined on first arrivals on ATLANTIS end (west) only. Comparable observations were taken on BEAR so that this layer must be regarded as masked there. The 4.62-km/sec. horizon is well established on both ends of the profile. The 6.39-km/sec. horizon is strongly shown on both ends. On the ATLANTIS end the 4.62-km/sec. arrivals became undetectable at about 17 seconds water-travel time, although they should normally have continued as the first arrival until about 25 seconds. In this interval the 6.39-km/sec. arrival was evident. The same range interval for BEAR is too sparsely shot to make this effect evident. However, if this gap were due to inadequate gain or some other shortcoming in the observations arrivals of intermediate velocity might have been found. We decided on the interpretation shown, since (1) no such arrivals were observed here, and (2) no such velocities were found either on near-by 29-55 or 36-55. A very well-defined 8.04-km/sec. horizon is indicated by the unreversed ATLANTIS data in the range 50-80 km.

Profile 3-56: Velocities of 4.36 and 4.96 km/sec. are determinable in the refraction data. Although data were recorded beyond the range indicated in the 4.96-km/sec. region, the records are so poor that no higher velocities can be determined.

III. *Outer Continental Slope and Ridge Area—Plate 2C*

Profiles 31-55 to 35-55, and 37-55 to 39-55; 4-56 to 8-56

(a) ATLANTIS 213—BEAR 113
ATLANTIS 223—BEAR 140

On profile 37-55 there is refraction evidence for the 1.83-km/sec. horizon. On all other stations in this general region, reflection evidence has been used for the 1.83-km/sec. velocity.

Profiles 31-55 and 32-55 are more like oceanic structure than are the stations to the north and east. There is strong second-arrival refraction evidence on BEAR (north) end of 32-55 for 2.06 km/sec. velocity. A few second arrivals on ATLANTIS (south) end indicate the same velocity but are not adequate to establish it. Profile 31-55 shows weak arrivals

indicating a velocity in the region of 1.89 km/sec., but these data are not adequate for deriving precise values. Velocities of 6.70 km/sec. (31-55) and 6.55 km/sec. (32-55) are relatively well determined. On profile 31-55 6.70 km/sec. overlies 7.85 km/sec. Profile 32-55 shows 7.34 km/sec. as its highest velocity, which is equivalent in depth (10–11 km) to the 7.5 km/sec. layer found on adjacent profiles.

Profile 33-55: There is evidence here for a 2.44-km/sec. layer above one of 5.67 km/sec. which appears only on ATLANTIS (northwest) but has been assumed present across the profile and probably masked on BEAR by the 8.1-km/sec. layer which does not show on ATLANTIS.

Profile 34-55: There is fair evidence for layers of 2.2 km/sec. and 2.96 km/sec., followed by 5.20 km/sec. and a higher-velocity layer of 6.33 km/sec. The 7.36-km/sec. layer is observed on BEAR (southeast) but is not apparent on ATLANTIS (northwest).

Profile 35-55: There is fair evidence for 2.17-km/sec. and 2.57-km/sec. layers above 5.24 km/sec. The BEAR (east) travel-time curve for the 5.24 km/sec. is sigmoid with a maximum excursion of approximately 0.04 sec. The ATLANTIS (west) travel-time plot indicates horizons of 6.69 km/sec. and 7.20 km/sec. BEAR records show 6.69 km/sec. weakly. Weak evidence for 7.20 km/sec. on BEAR has enabled computation of the thickness on this end of the profile. Also, a few arrivals occurring as later events on the refraction trace indicate the possible presence of 8-km/sec. velocity. Since this appears as a first arrival at the very end of the travel-time plot, possibly a longer profile would have established the presence of this horizon.

Profile 37-55: Velocity lines 2.77, 3.89, and 6.1 km/sec. are shown. A velocity of 7.42 km/sec. is well founded on good evidence from ATLANTIS (east), and although it appears on the BEAR travel-time plot in a region of rather poor records, it can be identified there.

Profile 38-55: This profile has second-arrival evidence for a layer of 2.38 km/sec. velocity, overlying one of 3.98 km/sec. The 6.36-km/sec. layer is well supported by arrivals on BEAR (southwest) but is weak on the ATLANTIS (northeast) travel-time plot. The 7.73-km/sec. layer is well established on BEAR, but there is scatter of about 0.05 sec. on the ATLANTIS travel-time plot.

Profile 39-55: There is good second-arrival evidence, on BEAR (south), for a 2.64-km/sec. horizon. A set of widely spaced (because of shot spacing) second and third arrivals on ATLANTIS (north) gives uncertain indications of this velocity. The 3.84-km/sec. layer is based on first arrivals on the BEAR end of the profile, but there is only second-arrival evidence on ATLANTIS, mainly because of lack of shots in the critical range. The 6.45- and 7.12-km/sec. layers are evident on the two ends of the profiles. The 7.95-km/sec. horizon occurs only on BEAR, at the end of the profile, and is indicated as very deep (21 km). A computation that assumes the presence of this horizon at the ATLANTIS end gives a tentative depth of 20 km.

(b) ATLANTIS 223—BEAR 140 (Profiles 4-56 to 8-56)

Profile 4-56: Reflection data indicate the 1.68-km/sec. velocity. The 2.43-km/sec. has strong refraction arrivals on both ends of the profile. We have assumed a masked 3.75-km/sec. velocity, indicated by dashed lines on the travel-time plot, from good evidence for such a layer on adjacent profiles. The higher velocities, 4.46, 6.7, and 7.63 km/sec., are very well established by BEAR (northeast) data but are less evident on ATLANTIS (southwest), showing some scatter because of low recording gain and slow paper speed throughout the station. The 7.63-km/sec. horizon does not appear on ATLANTIS.

Profile 5-56: This profile was reversed but was located over such complicated structure that it could not be so computed. Hence the data have been interpreted and computed as two unreversed profiles. The 1.83-km/sec. layer has been assumed present on both ends. The 2.26-km/sec. (east) and 2.24-km/sec. (west) horizons are measured on second-arrival evidence. Apparent velocities of 5.37 and 7.16 km/sec. are measured on the east end, with indicated fault in the 7.16-km/sec. layer. On the west the apparent deeper velocities are 3.94, 6.51, 7.31, and 8.60 km/sec.

Profile 6-56: This is a reversed profile which has similar velocity lines for first arrivals. However, two low-velocity horizons (apparent velocity 2.20 and 2.78 km/sec.) were measured by refraction data on the ATLANTIS (east) end but only from reflection data on the BEAR (west) end (Table 4). The resulting apparent velocities agree well. However, we lack proper data for computing velocities, slopes, and thicknesses for these layers. Hence we have preferred to treat the two ends separately as unreversed profiles. The 7.55-km/sec. line on the west end shows a well-defined fault displacement.

Profile 7-56: All the velocities shown on the travel-time plot are well established.

Profile 8-56: The 2.35-km/sec. horizon is established by second arrivals on both BEAR (south) and ATLANTIS (north), and by good sub-bottom reflections on BEAR. The 3.71-km/sec. layer occurs on ATLANTIS as first arrivals in the range 9–10 sec. There are no refraction arrivals in the range on BEAR, but the layer has been assumed to exist across the station area from ATLANTIS data and evidence on adjacent profiles. The 6.24-, 7.10-, and 8.43-km/sec. horizons are well determined on both ends.

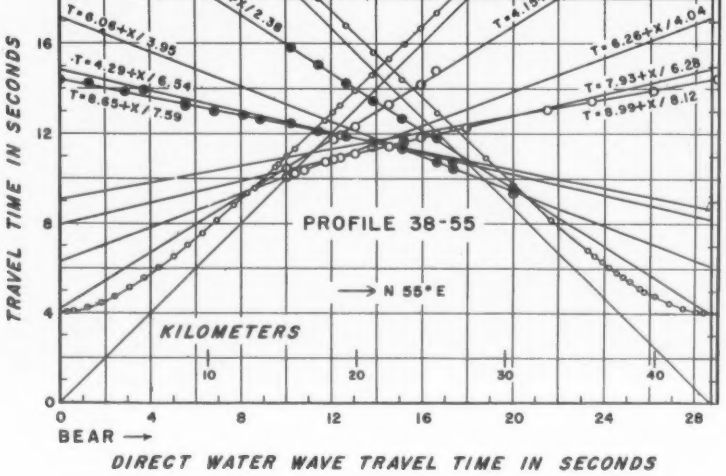

DIRECT WATER WAVE TRAVEL TIME IN SECONDS

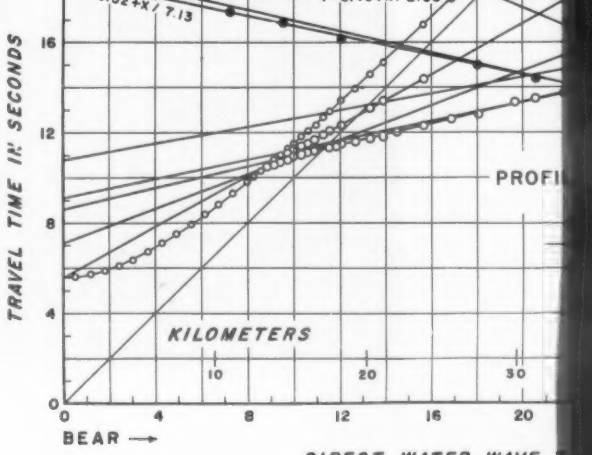

DIRECT WATER WAVE

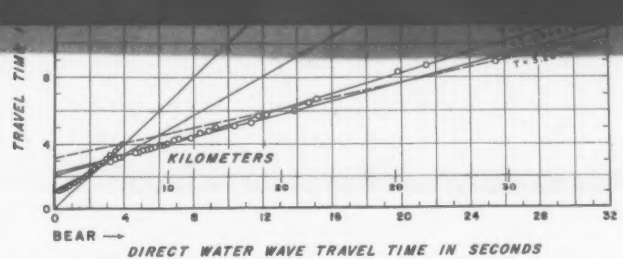

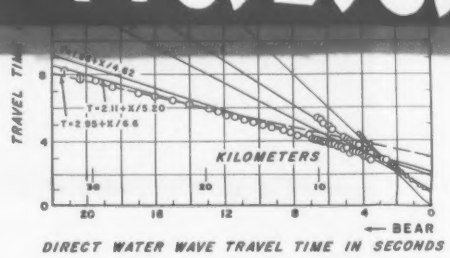

DEEP-WATER AREA

C

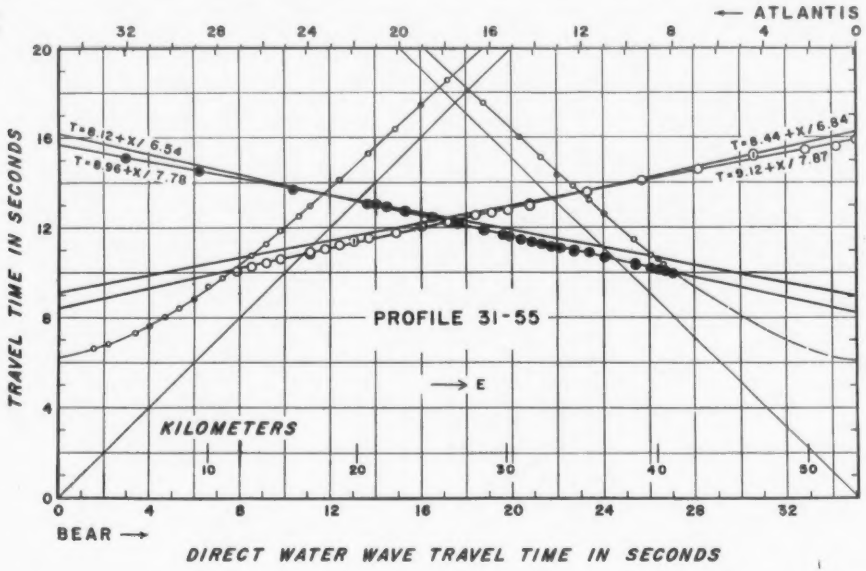

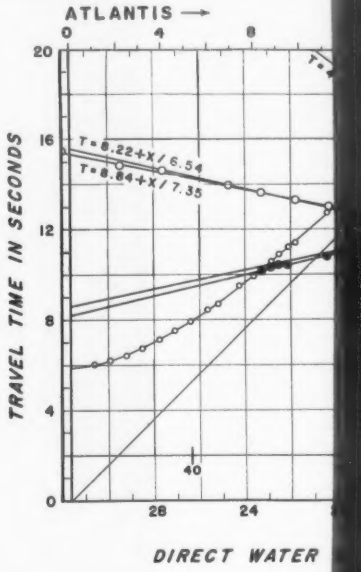

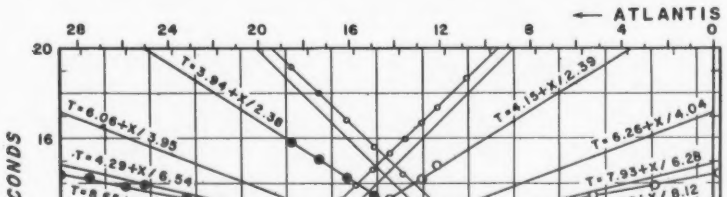

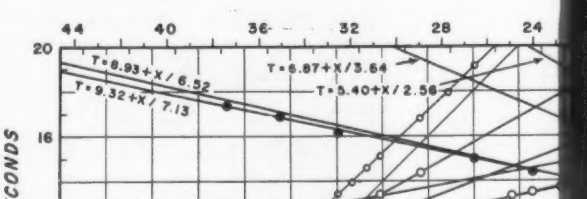

BLAKE PLATEAU

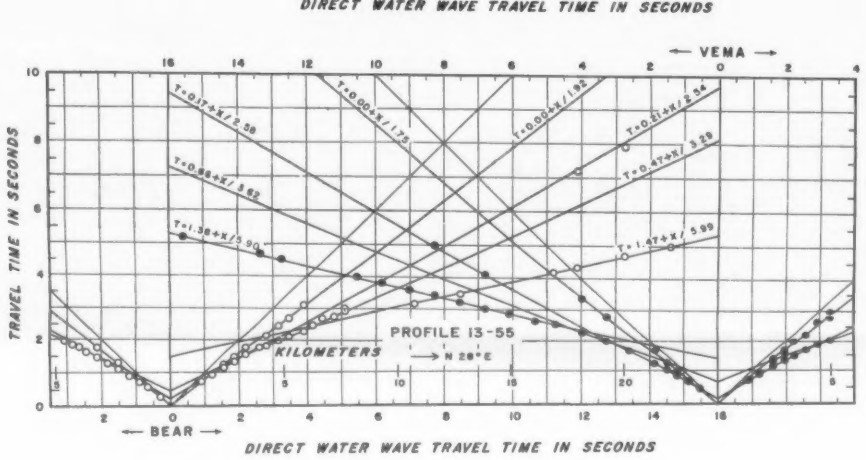

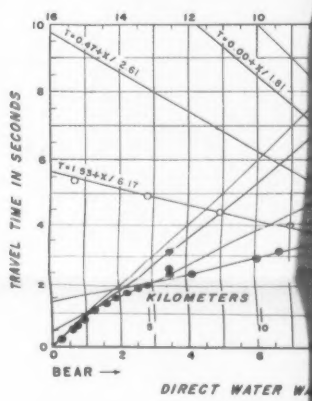

B

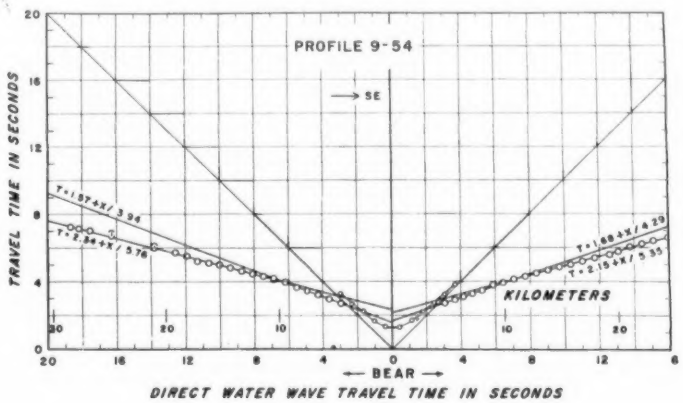

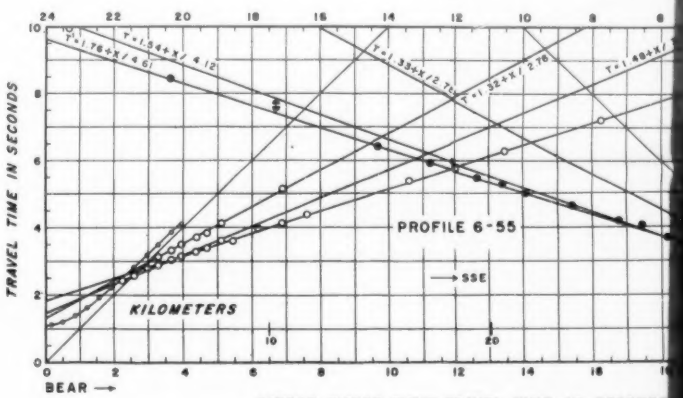

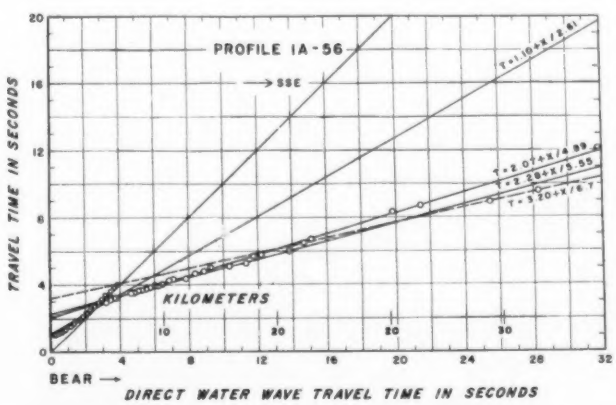

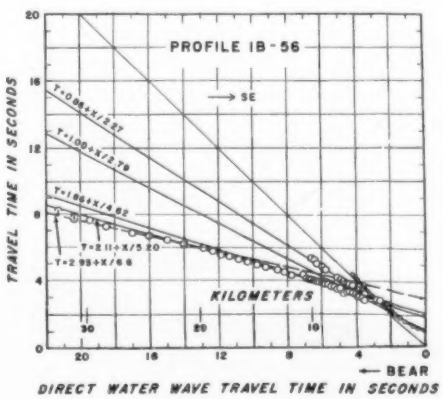

C

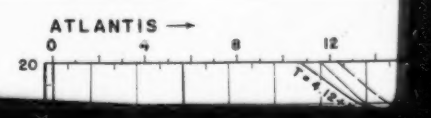

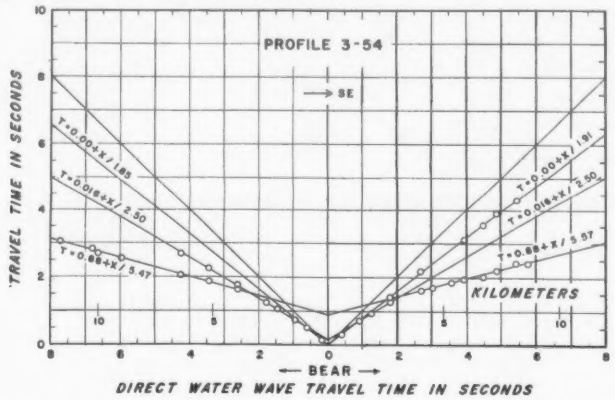

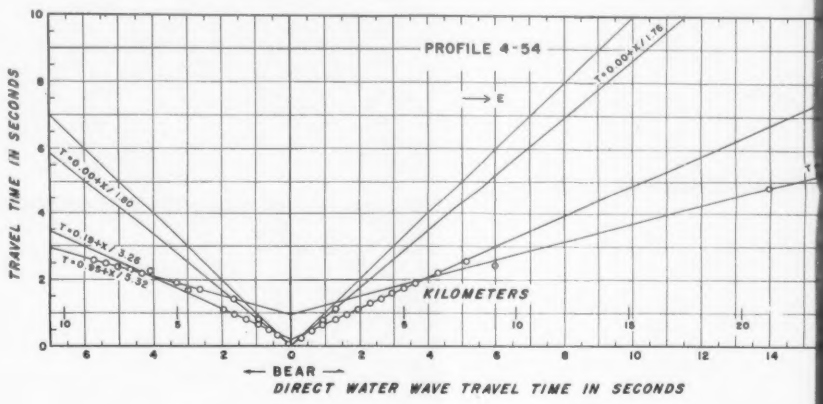

CONTINENTAL SHELF

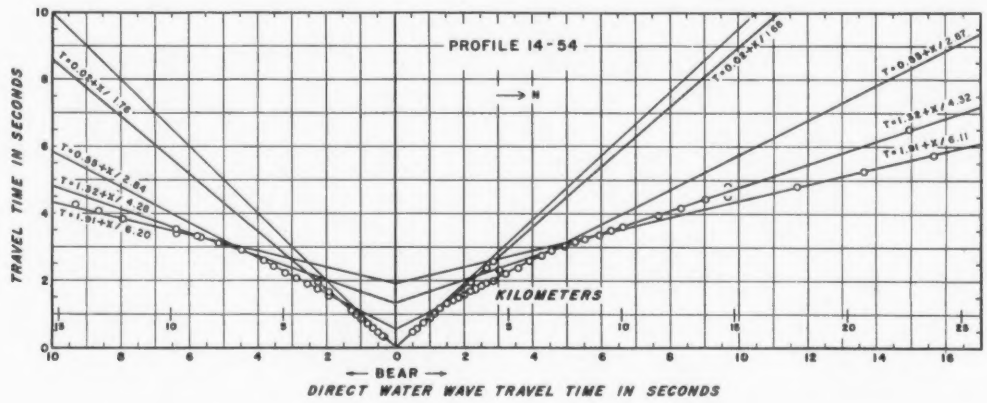

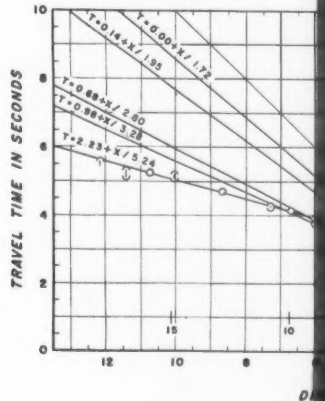

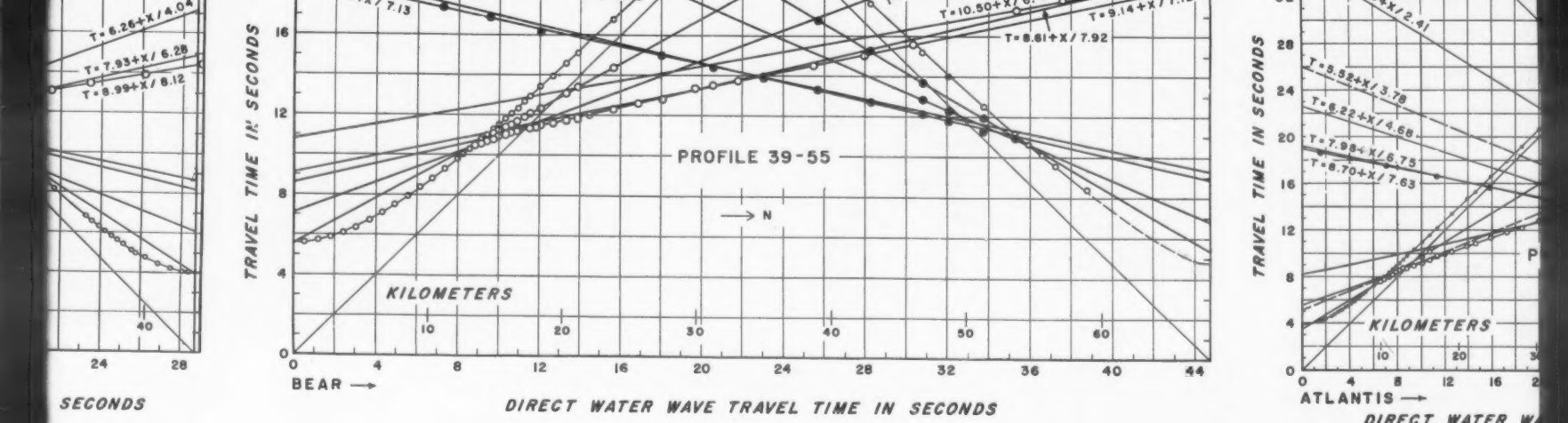
T = 6.26 + X / 4.04
T = 7.93 + X / 6.28
T = 8.99 + X / 8.12
T = 7.13
T = 10.50 + X / 8.
T = 9.14 + X / 7.
T = 8.61 + X / 7.92
T = 8.52 + X / 2.41
T = 8.52 + X / 3.78
T = 8.22 + X / 4.68
T = 7.98 + X / 6.75
T = 8.70 + X / 7.63
PROFILE 39-55
→ N
KILOMETERS
TRAVEL TIME IN SECONDS
BEAR →
ATLANTIS →
SECONDS
DIRECT WATER WAVE TRAVEL TIME IN SECONDS
DIRECT WATER WA

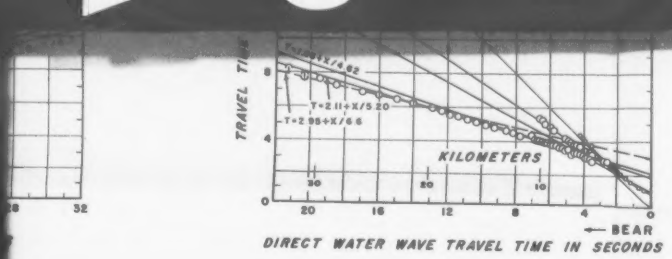
T=2.11+X/5.20
T=2.95+X/6.6
KILOMETERS
BEAR
DIRECT WATER WAVE TRAVEL TIME IN SECONDS

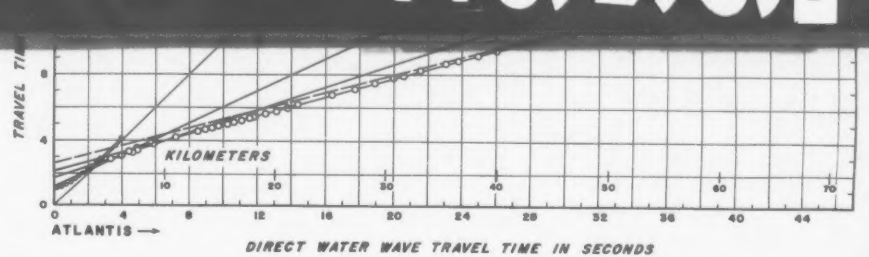
KILOMETERS
ATLANTIS
DIRECT WATER WAVE TRAVEL TIME IN SECONDS

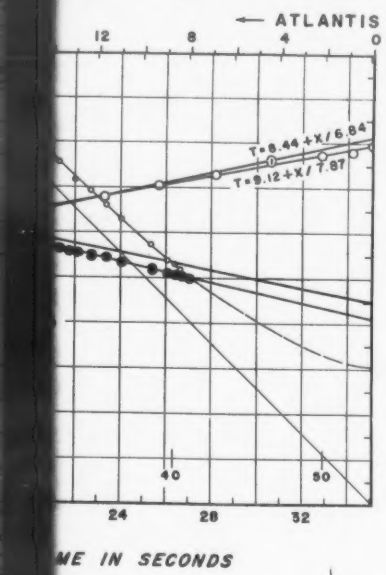
ATLANTIS
T=8.44+X/6.84
T=9.12+X/7.87
ME IN SECONDS

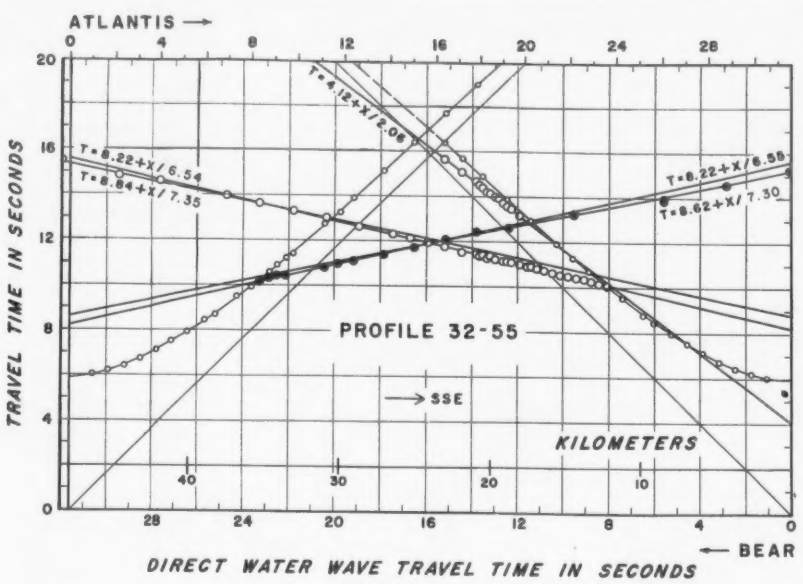
ATLANTIS
T=4.12+X/2.06
T=8.22+X/6.54
T=8.84+X/7.35
T=8.22+X/8.58
T=8.62+X/7.30
PROFILE 32-55
SSE
KILOMETERS
BEAR
TRAVEL TIME IN SECONDS
DIRECT WATER WAVE TRAVEL TIME IN SECONDS

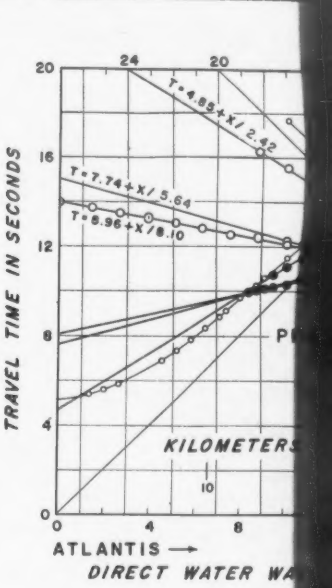
T=4.85+X/2.42
T=7.74+X/5.64
T=8.96+X/8.10
KILOMETERS
ATLANTIS
TRAVEL TIME IN SECONDS
DIRECT WATER WA

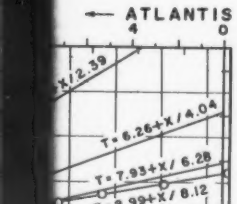
ATLANTIS
T=8.26+X/4.04
T=7.93+X/6.28

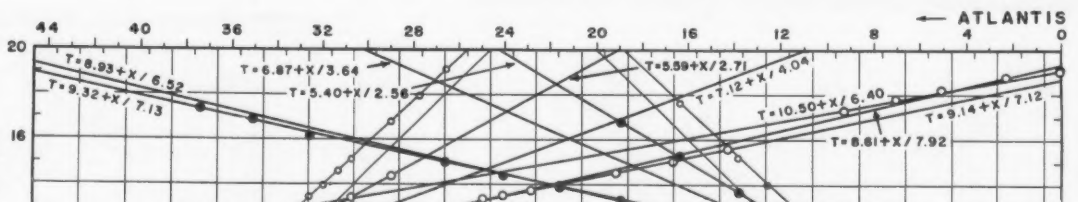
ATLANTIS
T=8.93+X/6.52
T=9.32+X/7.13
T=6.87+X/3.64
T=5.40+X/2.56
T=5.59+X/2.71
T=7.12+X/4.04
T=10.50+X/6.40
T=9.14+X/7.12
T=8.61+X/7.92

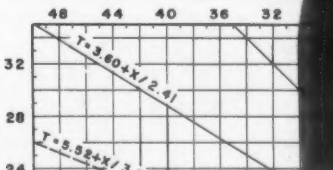
T=3.60+X/2.41

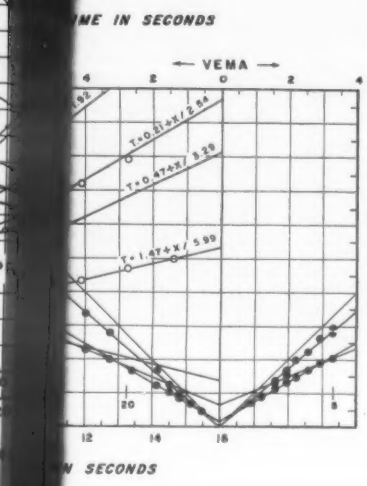
VEMA
T=0.21+X/2.84
T=0.47+X/3.29
T=1.47+X/5.99
20
8
12
14
16
N SECONDS

ME IN SECONDS

BEAR
DIRECT WATER WAVE TRAVEL TIME IN SECONDS

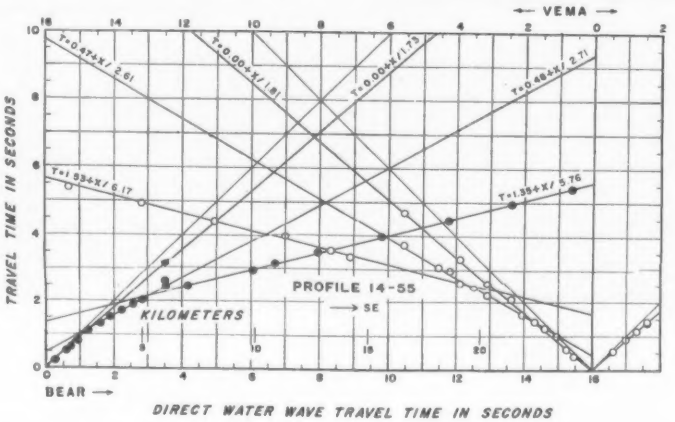
VEMA
T=0.47+X/2.61
T=0.00+X/1.81
T=0.00+X/1.73
T=0.46+X/2.71
T=1.53+X/6.17
T=1.39+X/5.76
PROFILE 14-55
SE
KILOMETERS
TRAVEL TIME IN SECONDS
BEAR
DIRECT WATER WAVE TRAVEL TIME IN SECONDS

TRAVEL TIME IN SECONDS

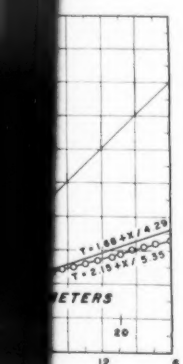
T=1.88+X/4.29
T=2.18+X/5.35
ETERS
20
12
6

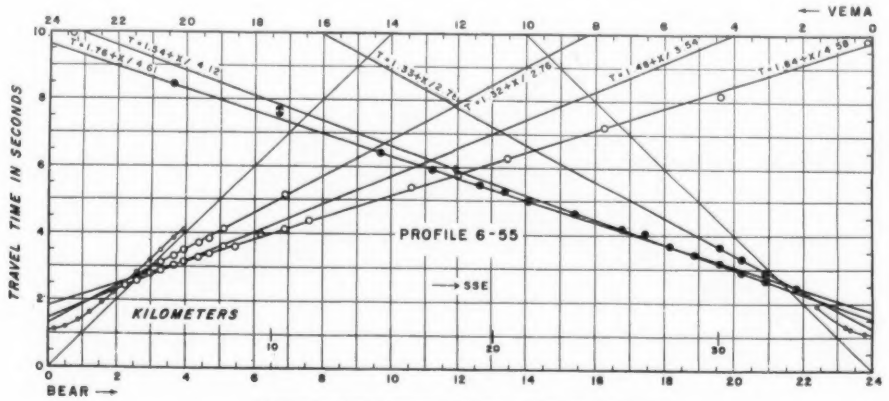
VEMA
T=1.76+X/4.61
T=1.54+X/4.12
T=1.33+X/2.76
T=1.32+X/2.76
T=1.46+X/3.54
T=1.64+X/4.58
PROFILE 6-55
SSE
KILOMETERS
TRAVEL TIME IN SECONDS
BEAR
DIRECT WATER WAVE TRAVEL TIME IN SECONDS

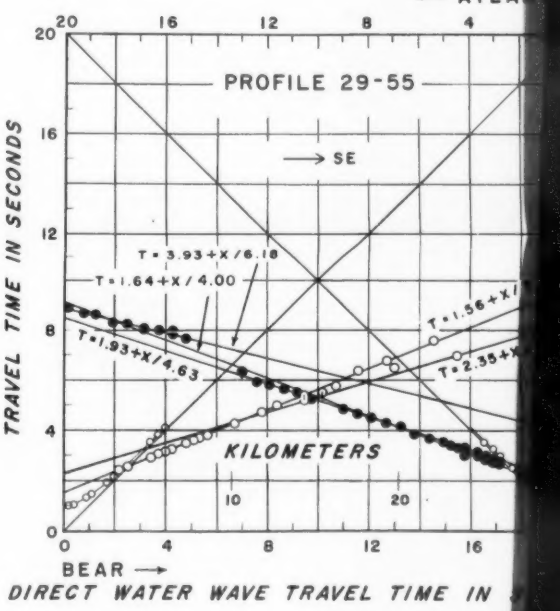
ATLA
PROFILE 29-55
SE
T = 3.93+X/6.18
T=1.64+X/4.00
T=1.93+X/4.63
T=1.56+X/
T=2.35+X
KILOMETERS
TRAVEL TIME IN SECONDS
BEAR
DIRECT WATER WAVE TRAVEL TIME IN

32

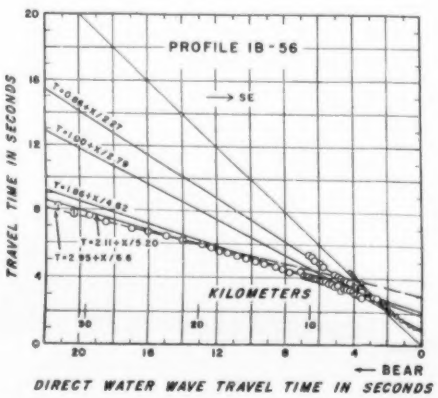
PROFILE 1B-56
SE
T=0.84+X/2.67
T=1.00+X/2.79
T=1.86+X/4.82
T=2.11+X/5.20
T=2.95+X/5.6
KILOMETERS
TRAVEL TIME IN SECONDS
BEAR
DIRECT WATER WAVE TRAVEL TIME IN SECONDS

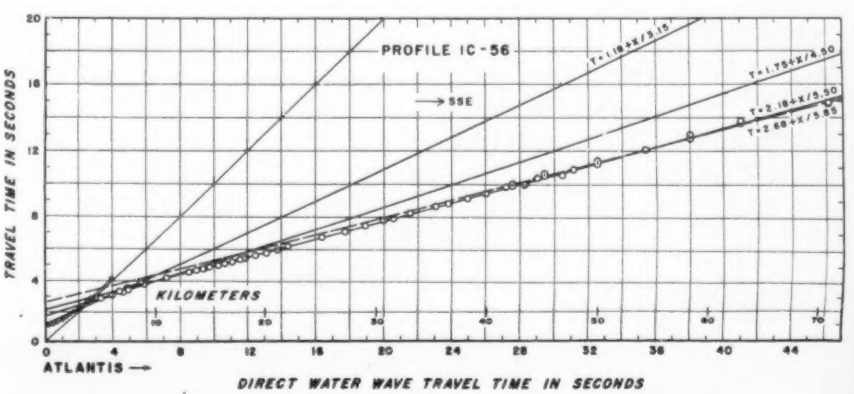
PROFILE 1C-56
SSE
T=1.19+X/3.15
T=1.75+X/4.50
T=2.18+X/5.50
T=2.60+X/5.85
KILOMETERS
TRAVEL TIME IN SECONDS
ATLANTIS
DIRECT WATER WAVE TRAVEL TIME IN SECONDS

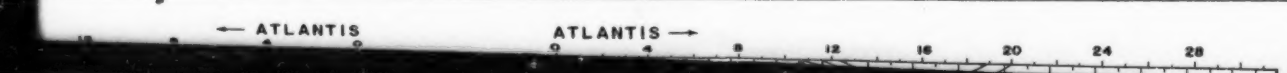
ATLANTIS
ATLANTIS
0
4
8
12
16
20
24
28

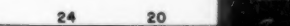
20
24
20

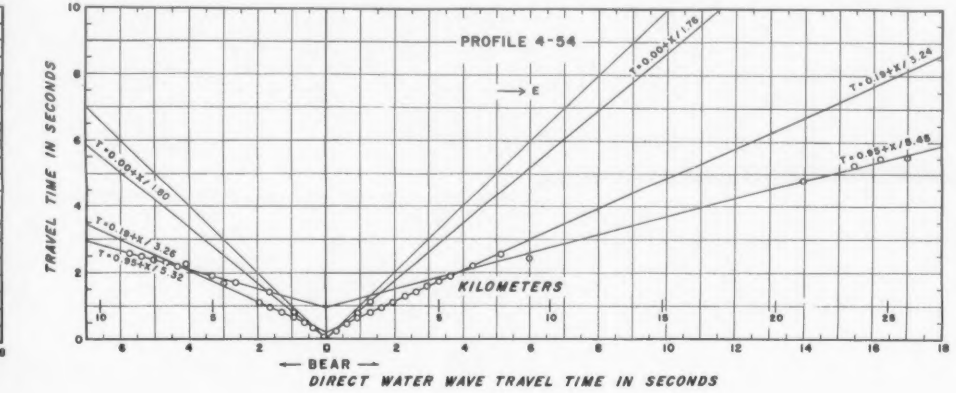
PROFILE 4-54
→ E
T=0.00+X/1.80
T=0.00+X/1.79
T=0.19+X/3.24
T=0.19+X/3.26
T=0.95+X/5.32
T=0.95+X/8.48
TRAVEL TIME IN SECONDS
KILOMETERS
← BEAR →
DIRECT WATER WAVE TRAVEL TIME IN SECONDS

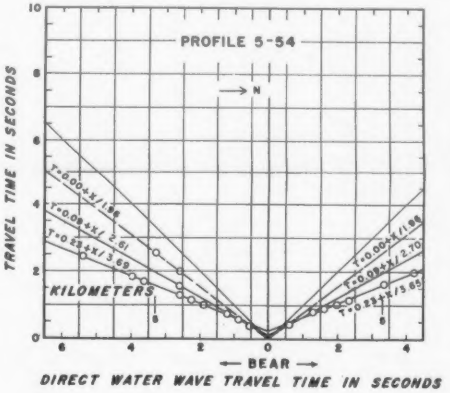
PROFILE 5-54
→ N
T=0.00+X/1.86
T=0.08+X/2.81
T=0.23+X/3.69
T=0.00+X/1.84
T=0.00+X/2.70
T=0.23+X/3.69
TRAVEL TIME IN SECONDS
KILOMETERS
← BEAR →
DIRECT WATER WAVE TRAVEL TIME IN SECONDS

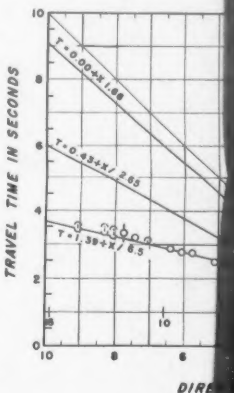
T=0.00+X/1.68
T=0.43+X/2.65
T=1.39+X/6.5
TRAVEL TIME IN SECONDS

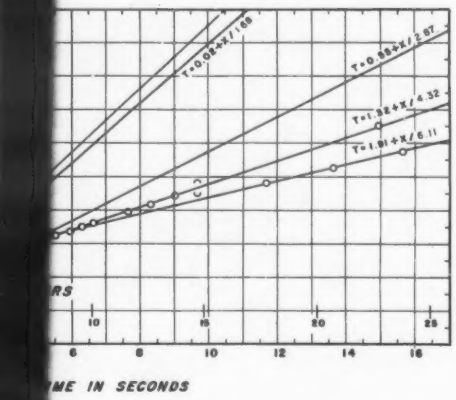
T=0.08+X/1.68
T=0.58+X/2.87
T=1.32+X/4.32
T=1.91+X/6.11

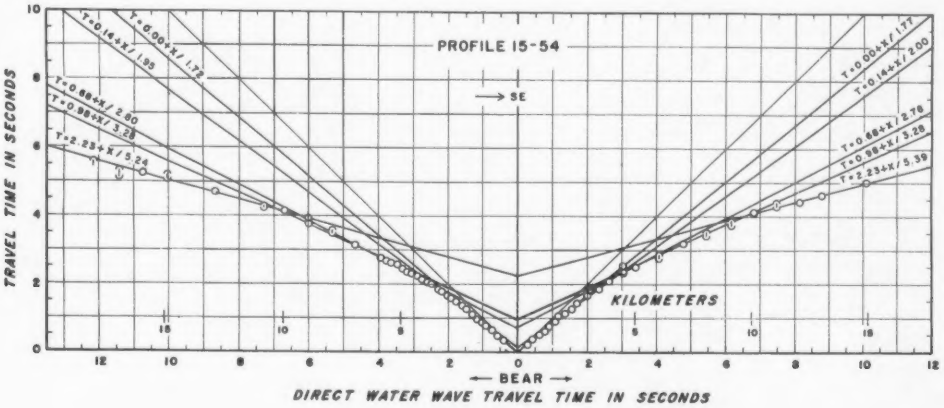
PROFILE 15-54
→ SE
T=0.14+X/1.95
T=0.00+X/1.77
T=0.00+X/1.78
T=0.14+X/2.00
T=0.68+X/2.50
T=0.68+X/2.76
T=0.98+X/3.28
T=0.98+X/3.28
T=2.23+X/5.24
T=2.23+X/5.39
TRAVEL TIME IN SECONDS
KILOMETERS
← BEAR →
DIRECT WATER WAVE TRAVEL TIME IN SECONDS

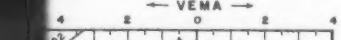
← VEMA →

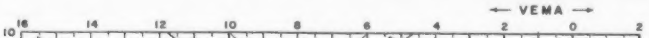
← VEMA →

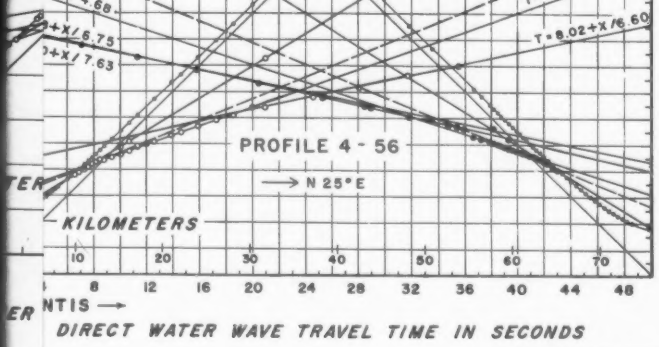
T = 8.02 + X/6.60
PROFILE 4 - 56
→ N 25° E
KILOMETERS
10 20 30 40 50 60 70
0 4 8 12 16 20 24 28 32 36 40 44 48
NTIS →
DIRECT WATER WAVE TRAVEL TIME IN SECONDS

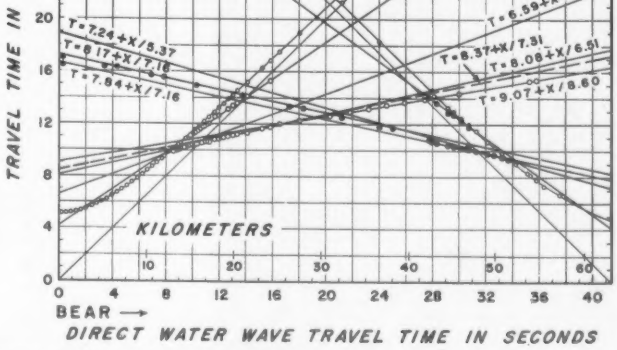

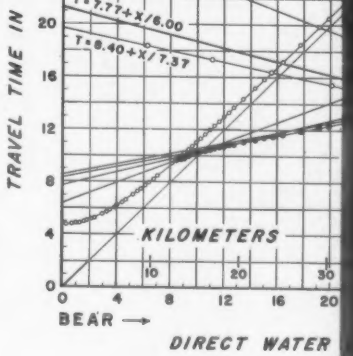

TRAVEL-TIME GRAPHS

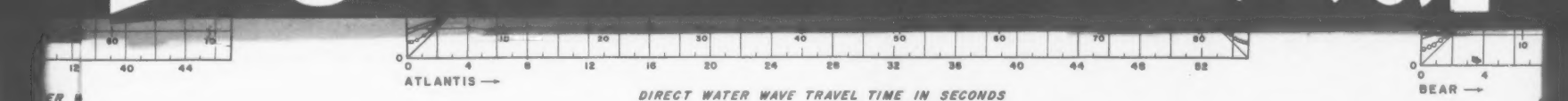
ATLANTIS →
DIRECT WATER WAVE TRAVEL TIME IN SECONDS
BEAR →

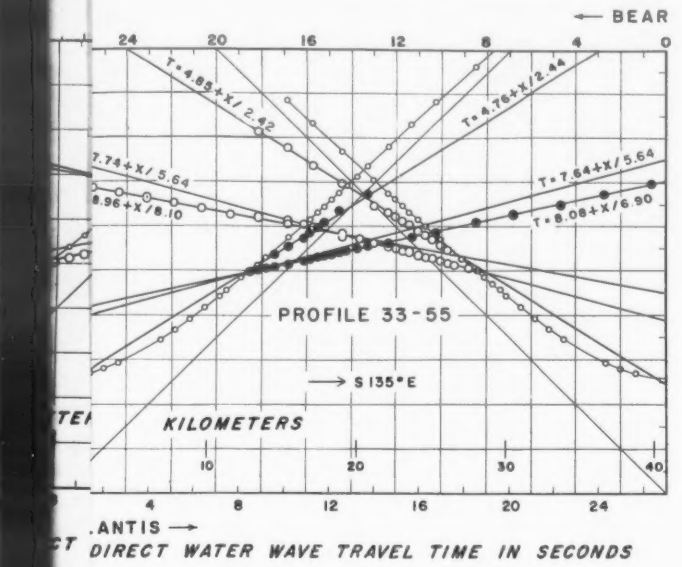
← BEAR
T = 4.83 + X / 2.42
T = 4.76 + X / 2.44
T = 7.74 + X / 5.64
T = 8.96 + X / 8.10
T = 7.64 + X / 5.64
T = 8.08 + X / 6.90
PROFILE 33 - 55
→ S 135° E
KILOMETERS
10
20
30
40
ANTIS →
DIRECT WATER WAVE TRAVEL TIME IN SECONDS

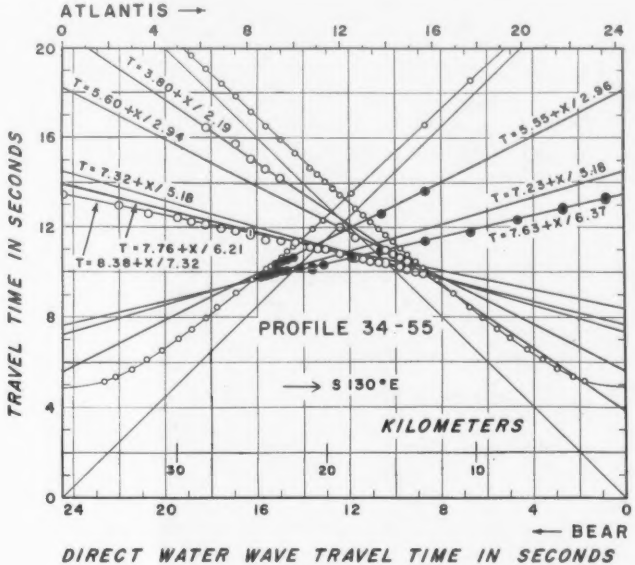
ATLANTIS →
TRAVEL TIME IN SECONDS
T = 3.80 + X / 2.19
T = 5.60 + X / 2.94
T = 5.55 + X / 2.96
T = 7.32 + X / 5.18
T = 7.23 + X / 5.18
T = 7.76 + X / 6.21
T = 8.38 + X / 7.32
T = 7.63 + X / 6.37
PROFILE 34 - 55
→ S 130° E
KILOMETERS
30
20
10
← BEAR
DIRECT WATER WAVE TRAVEL TIME IN SECONDS

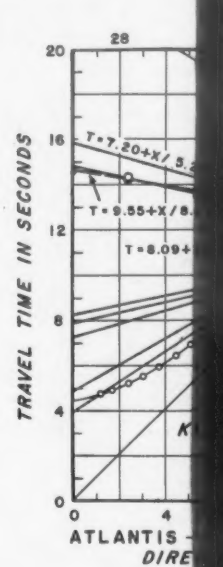
TRAVEL TIME IN SECONDS
T = 7.20 + X /
T = 9.55 + X /
T = 8.09 +
ATLANTIS →
DIRE

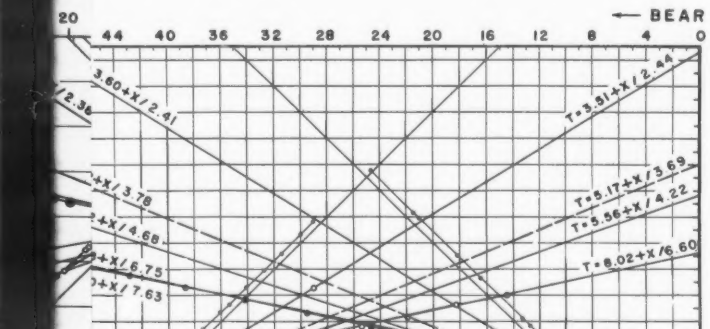
← BEAR
T = 3.60 + X / 2.41
T = 3.31 + X / 2.44
T = 5.17 + X / 3.69
T = 5.56 + X / 4.22
T = 8.02 + X / 6.60

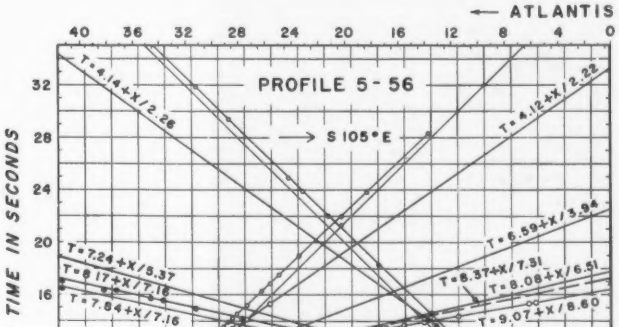
← ATLANTIS
TIME IN SECONDS
PROFILE 5 - 56
→ S 105° E
T = 4.14 + X / 2.26
T = 4.12 + X / 2.22
T = 7.24 + X / 5.37
T = 8.17 + X / 7.16
T = 7.84 + X / 7.16
T = 6.59 + X / 3.94
T = 8.37 + X / 7.31
T = 8.08 + X / 6.51
T = 9.07 + X / 8.60

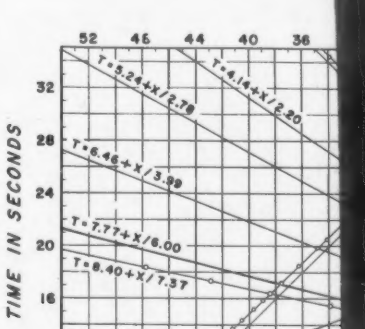
TIME IN SECONDS
T = 5.24 + X / 2.78
T = 4.14 + X / 2.20
T = 6.46 + X / 3.99
T = 7.77 + X / 6.00
T = 8.40 + X / 7.37

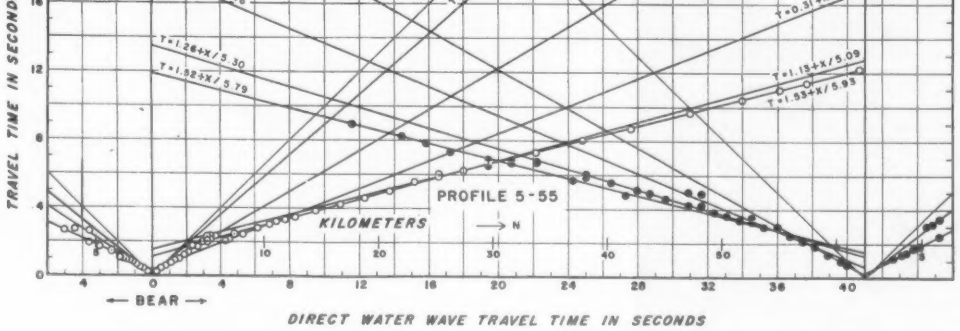

DIRECT WATER WAVE TRAVEL TIME IN SECONDS

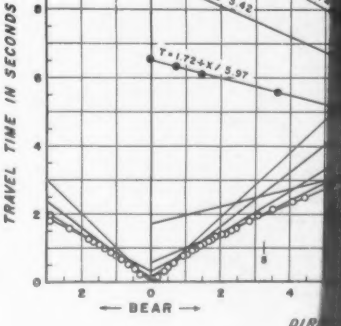

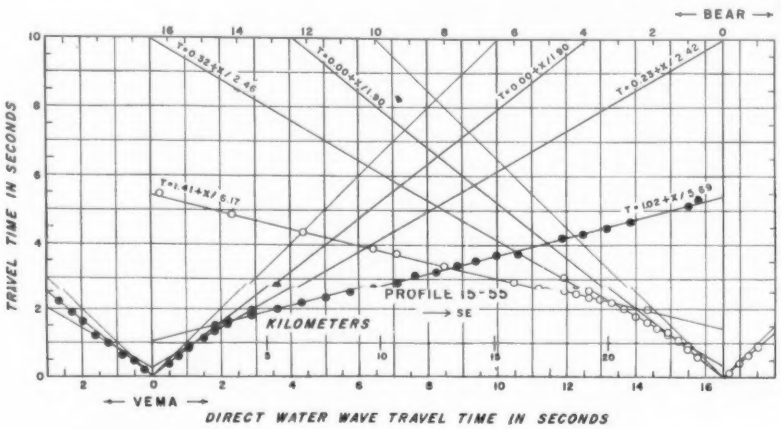

DIRECT WATER WAVE TRAVEL TIME IN SECONDS

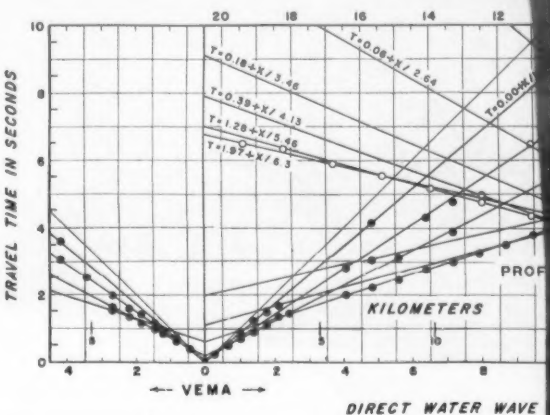

DIRECT WATER WAVE

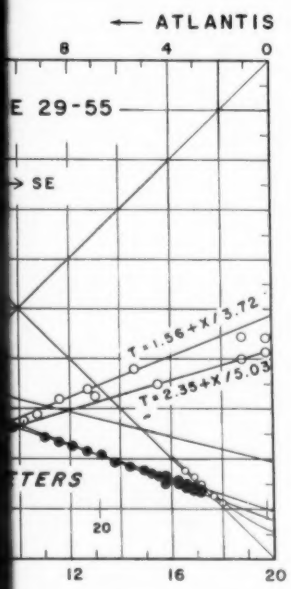

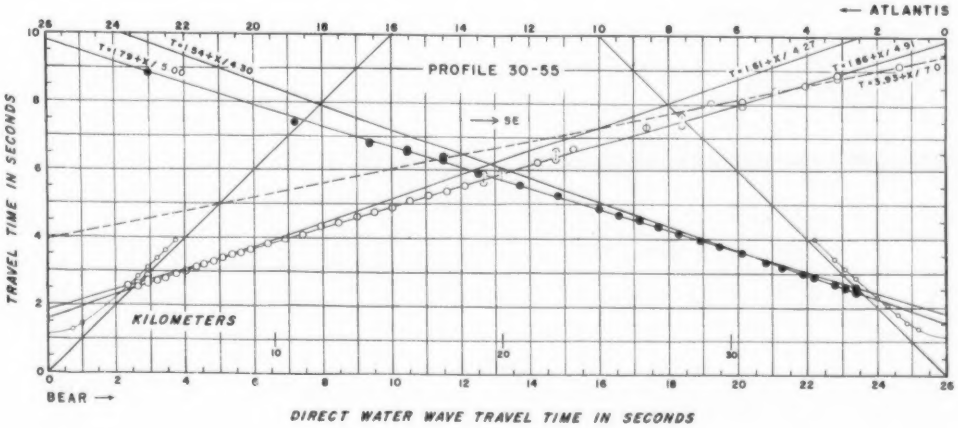

DIRECT WATER WAVE TRAVEL TIME IN SECONDS

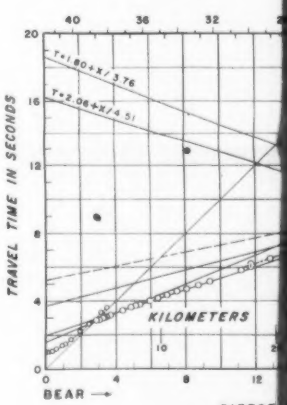

DIRECT

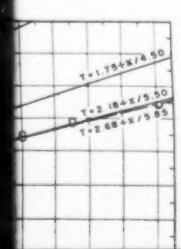

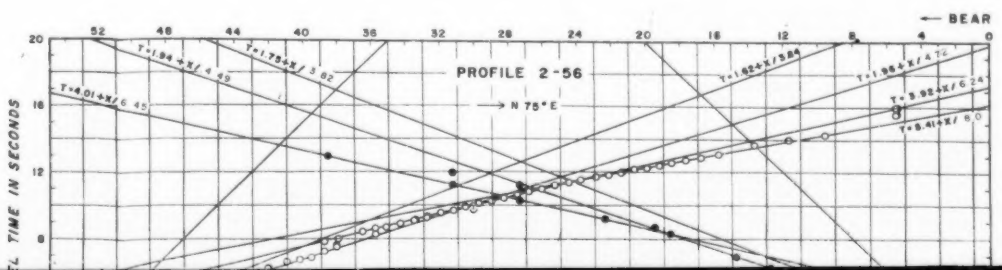

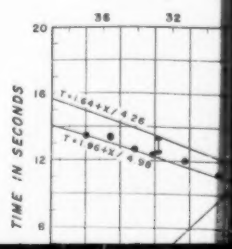

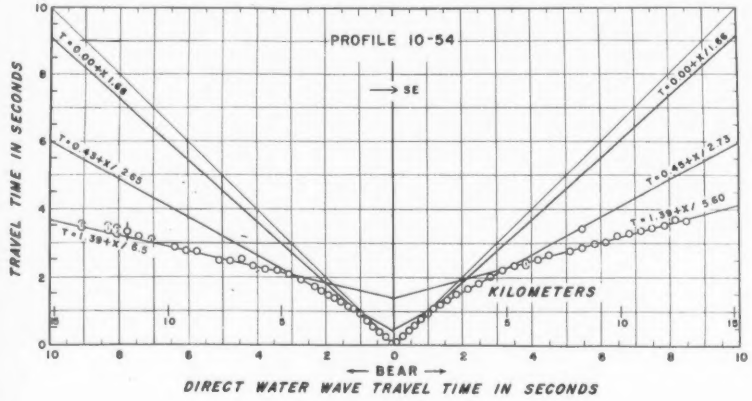
PROFILE 10-54
→ SE
T=0.00+X/1.68
T=0.00+X/1.68
T=0.43+X/2.65
T=0.48+X/2.73
T=1.39+X/5.60
T=1.39+X/6.5
KILOMETERS
TRAVEL TIME IN SECONDS
← BEAR →
DIRECT WATER WAVE TRAVEL TIME IN SECONDS

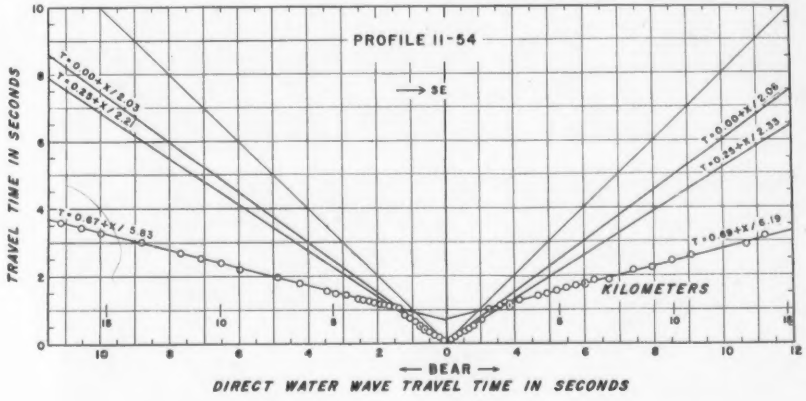
PROFILE 11-54
→ SE
T=0.00+X/8.03
T=0.83+X/2.21
T=0.00+X/2.06
T=0.25+X/2.33
T=0.87+X/5.83
T=0.69+X/6.19
KILOMETERS
TRAVEL TIME IN SECONDS
← BEAR →
DIRECT WATER WAVE TRAVEL TIME IN SECONDS

TRAVEL TIME IN SECONDS

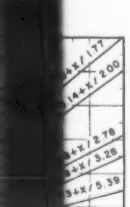

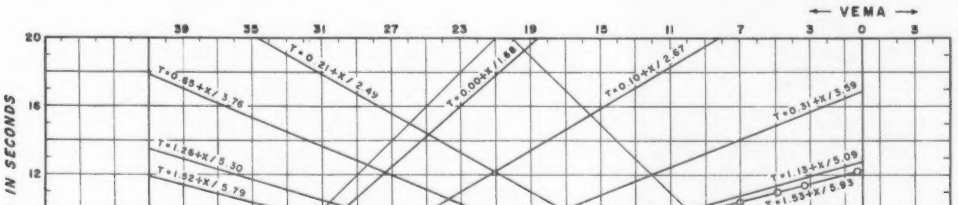
← VEMA →
T=0.69+X/3.76
T=0.21+X/2.49
T=0.00+X/1.68
T=0.10+X/2.67
T=0.31+X/3.59
T=1.26+X/5.30
T=1.52+X/5.79
T=1.13+X/5.09
T=1.59+X/5.93
TRAVEL TIME IN SECONDS

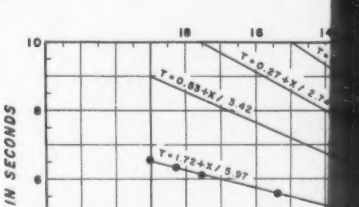
T=0.27+X/3.42
T=0.89+X/5.42
T=1.72+X/5.97
TRAVEL TIME IN SECONDS

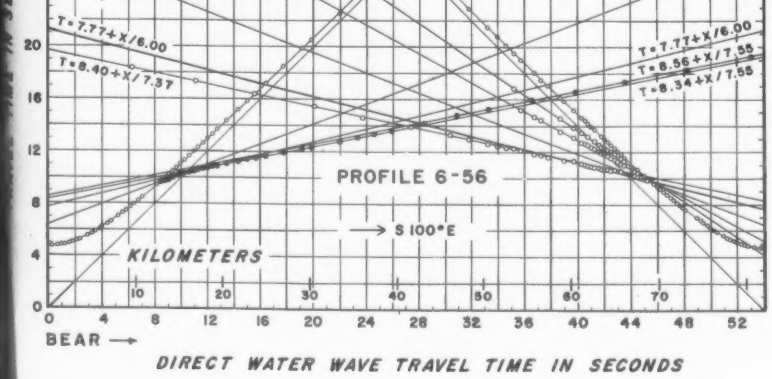
T=7.77+X/6.00
T=8.40+X/7.37
T=7.77+X/6.00
T=8.56+X/7.55
T=8.34+X/7.55
PROFILE 6-56
→ S 100°E
KILOMETERS
BEAR →
DIRECT WATER WAVE TRAVEL TIME IN SECONDS

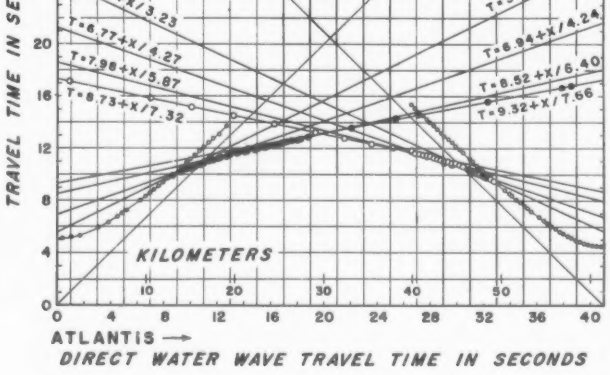
TRAVEL TIME IN SE
T=8.77+X/4.27
T=7.98+X/5.87
T=8.73+X/7.32
T=6.94+X/4.24
T=8.52+X/6.40
T=9.32+X/7.66
KILOMETERS
ATLANTIS →
DIRECT WATER WAVE TRAVEL TIME IN SECONDS

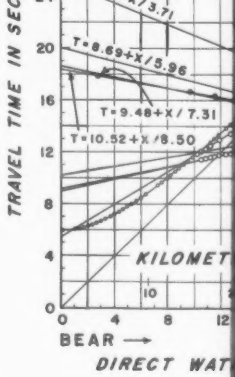
TRAVEL TIME IN SEC
T=8.69+X/5.96
T=9.48+X/7.31
T=10.52+X/8.50
KILOMET
BEAR →
DIRECT WAT

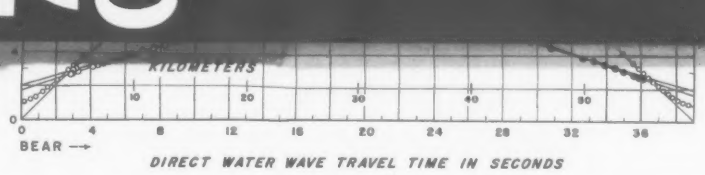
KILOMETERS
BEAR →
DIRECT WATER WAVE TRAVEL TIME IN SECONDS

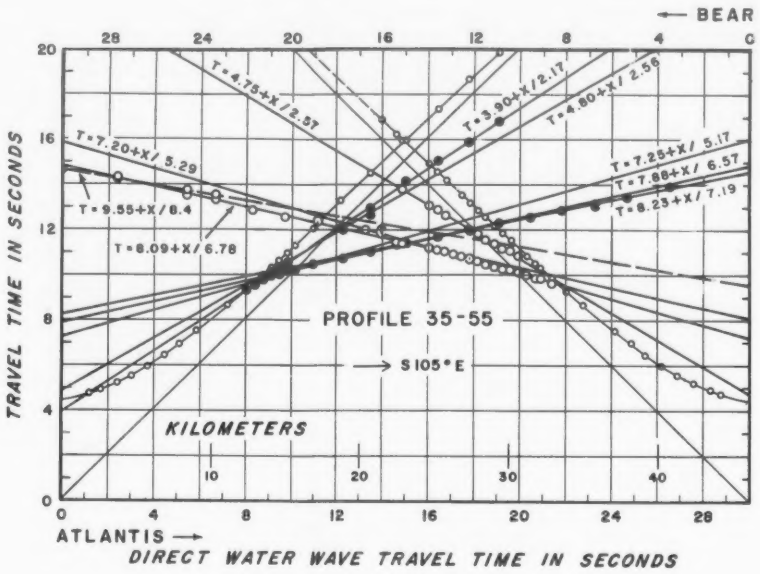
← BEAR
T = 4.78+X/2.57
T = 3.90+X/2.17
T = 4.80+X/2.56
T = 7.20+X/5.29
T = 7.25+X/5.17
T = 7.86+X/6.57
T = 8.23+X/7.19
T = 9.55+X/8.4
T = 8.09+X/6.78
PROFILE 35-55
→ S105°E
TRAVEL TIME IN SECONDS
KILOMETERS
ATLANTIS →
DIRECT WATER WAVE TRAVEL TIME IN SECONDS

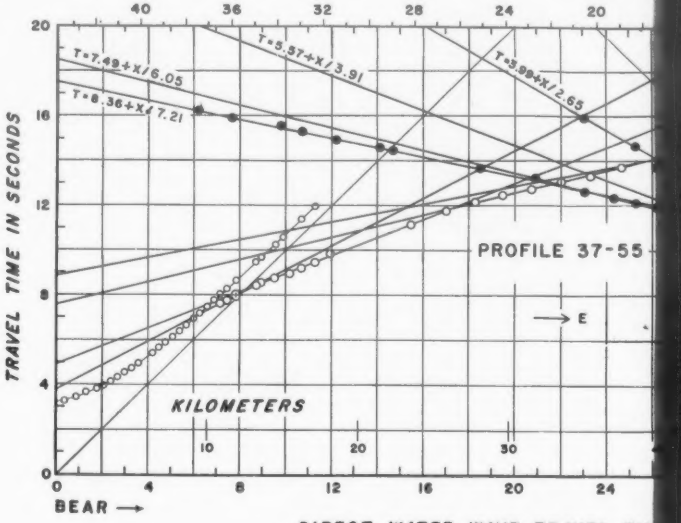
T = 7.49+X/6.05
T = 5.37+X/3.91
T = 8.36+X/7.21
T = 3.95+X/2.65
PROFILE 37-55
→ E
TRAVEL TIME IN SECONDS
KILOMETERS
BEAR →
DIRECT WATER WAVE TRAVEL TIM

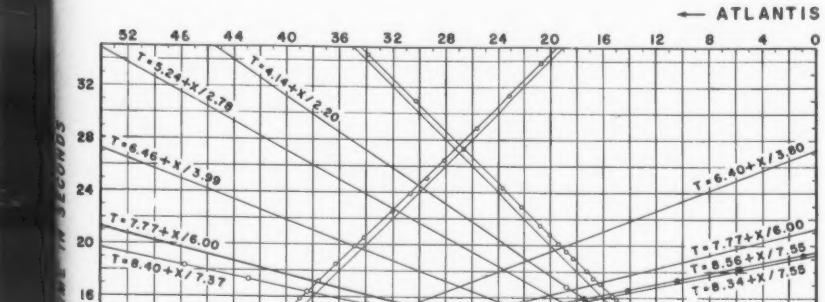
← ATLANTIS
T = 5.24+X/2.78
T = 4.14+X/2.20
T = 6.46+X/3.99
T = 6.40+X/3.80
T = 7.77+X/6.00
T = 8.40+X/7.37
T = 7.77+X/6.00
T = 8.56+X/7.55
T = 8.34+X/7.55

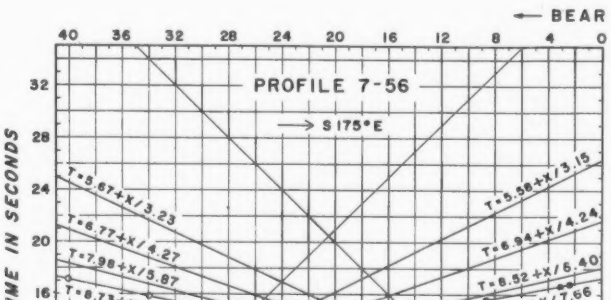
← BEAR
PROFILE 7-56
→ S175°E
T = 5.67+X/3.23
T = 5.56+X/3.15
T = 6.77+X/4.27
T = 6.94+X/4.24
T = 7.98+X/5.87
T = 6.52+X/6.40
TIME IN SECONDS

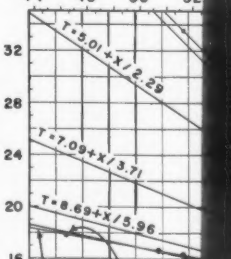
T = 5.01+X/2.29
T = 7.09+X/3.71
T = 8.69+X/5.96

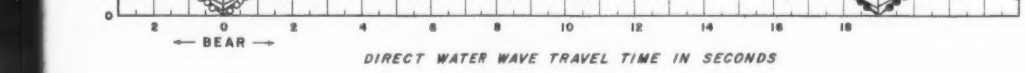

DIRECT WATER WAVE TRAVEL TIME IN SECONDS

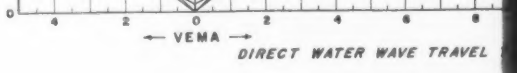

DIRECT WATER WAVE TRAVEL

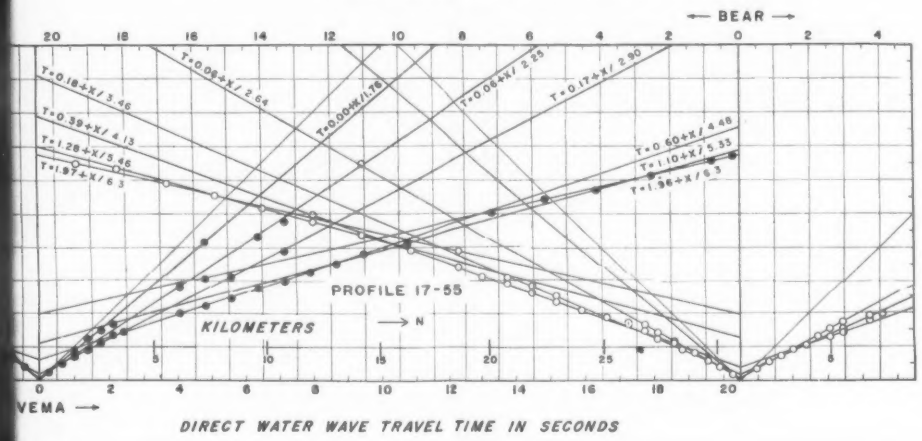

DIRECT WATER WAVE TRAVEL TIME IN SECONDS

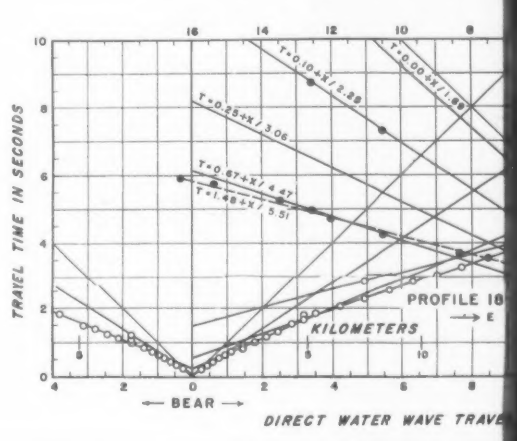

DIRECT WATER WAVE TRAVE

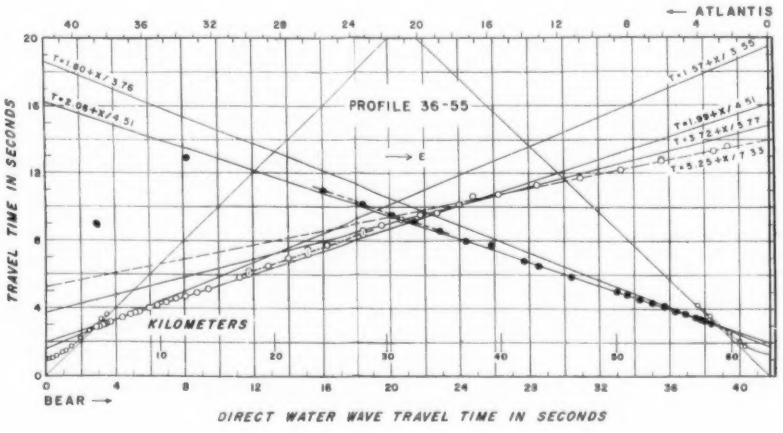

DIRECT WATER WAVE TRAVEL TIME IN SECONDS

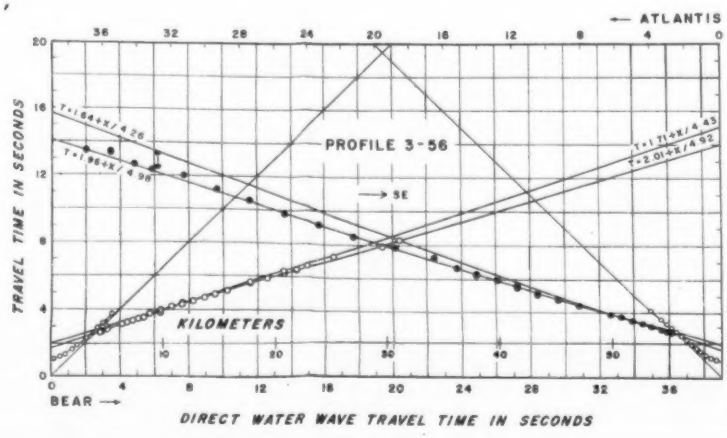

DIRECT WATER WAVE TRAVEL TIME IN SECONDS

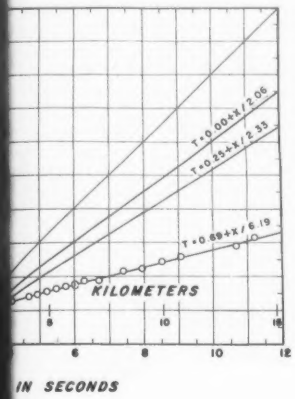

IN SECONDS

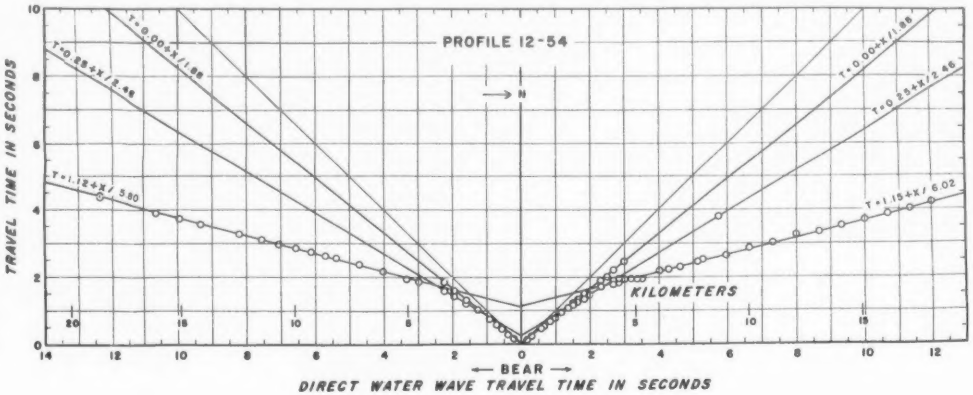

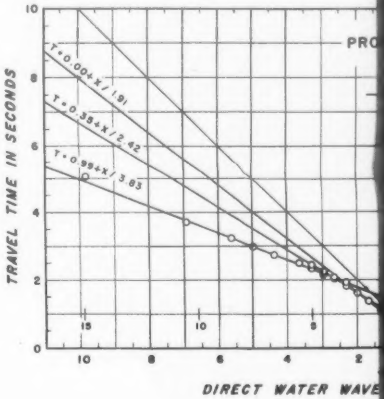

DIRECT WATER WAVE

← VEMA →

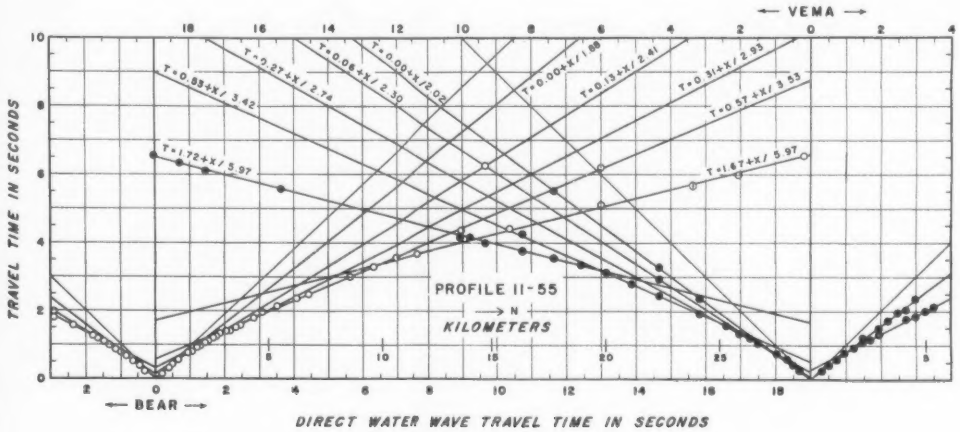

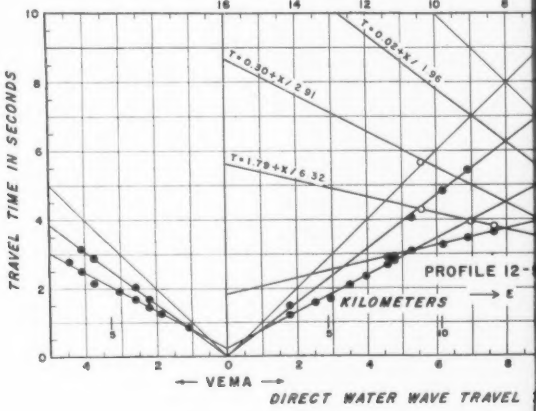

DIRECT WATER WAVE TRAVEL

← BEAR →

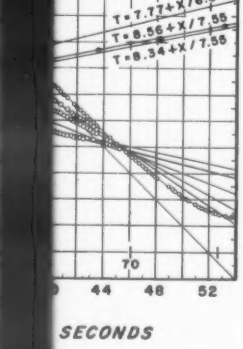
T=7.77+X/6.
T=8.56+X/7.55
T=8.34+X/7.58
70
44
48
52
SECONDS

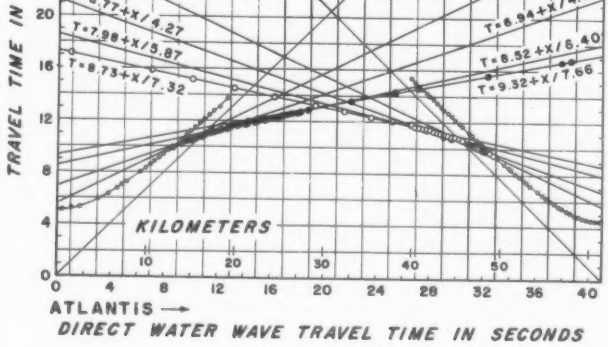
TRAVEL TIME IN
T=7.77+X/4.27
T=7.98+X/5.87
T=8.73+X/7.32
T=8.94+X/
T=8.52+X/6.40
T=9.32+X/7.66
KILOMETERS
0
4
8
12
16
20
24
28
32
36
40
ATLANTIS →
DIRECT WATER WAVE TRAVEL TIME IN SECONDS

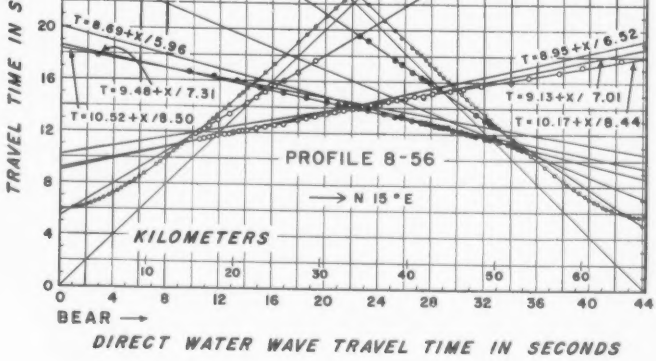
TRAVEL TIME IN S
T=8.69+X/5.96
T=9.48+X/7.31
T=10.52+X/8.50
T=8.95+X/6.52
T=9.13+X/ 7.01
T=10.17+X/8.44
PROFILE 8-56
→ N 15 °E
KILOMETERS
0
4
8
12
16
20
24
28
32
36
40
44
BEAR →
DIRECT WATER WAVE TRAVEL TIME IN SECONDS

TIME IN SECONDS

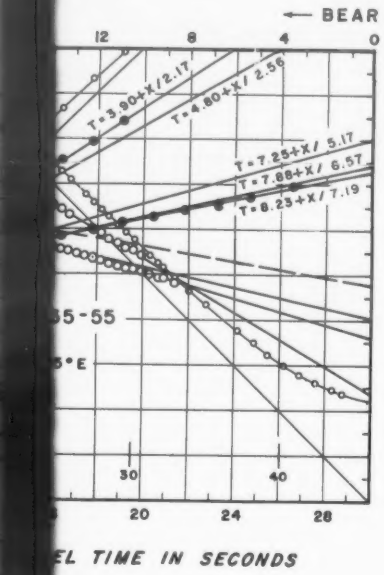

EL TIME IN SECONDS

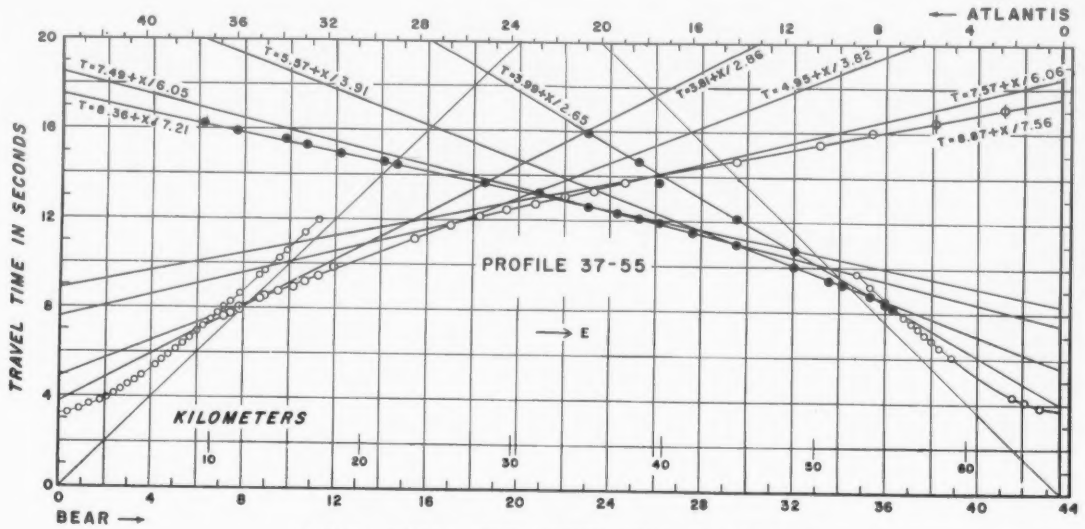

DIRECT WATER WAVE TRAVEL TIME IN SECONDS

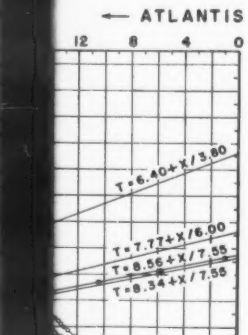

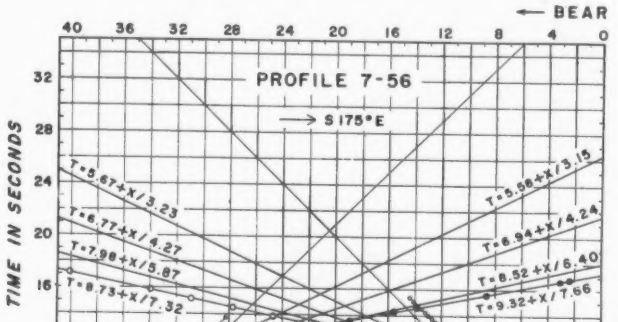

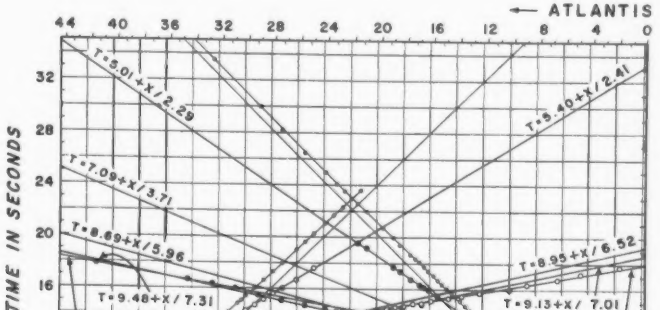

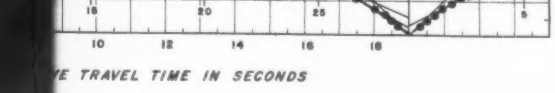

E TRAVEL TIME IN SECONDS

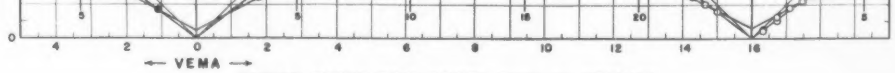

DIRECT WATER WAVE TRAVEL TIME IN SECONDS

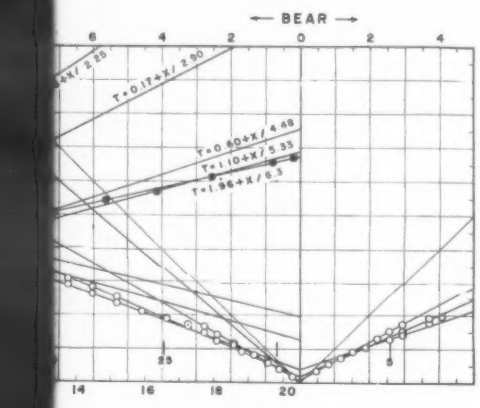

IN SECONDS

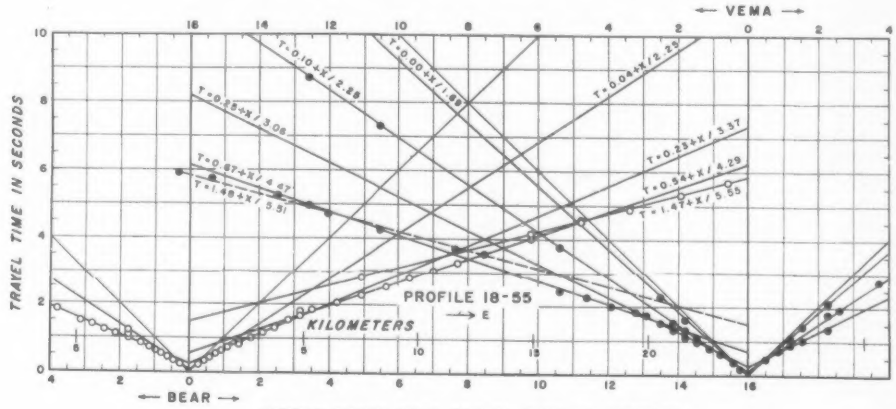

DIRECT WATER WAVE TRAVEL TIME IN SECONDS

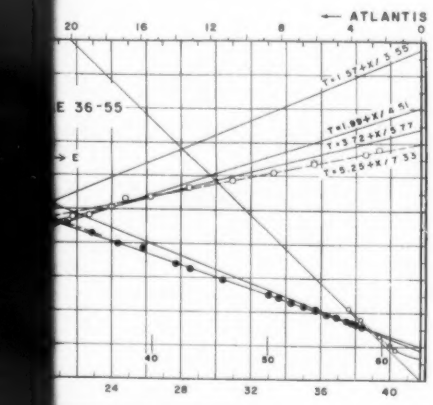

RAVEL TIME IN SECONDS

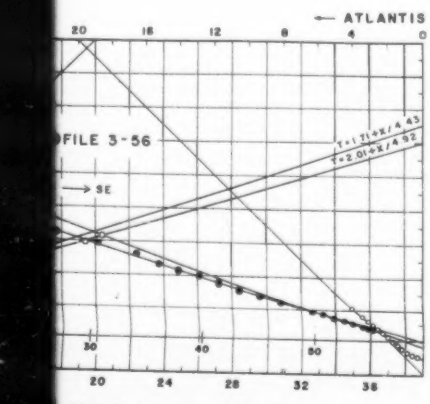

TRAVEL TIME IN SECONDS

← BEAR

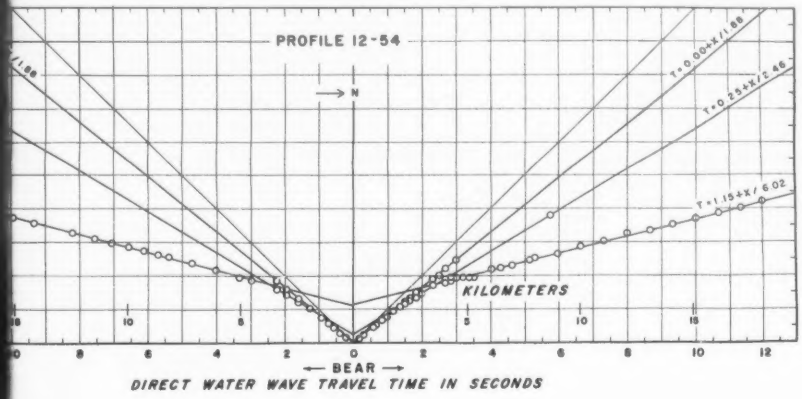
PROFILE 12-54
→ N
T=0.00+X/1.88
T=0.23+X/2.46
T=1.15+X/6.02
KILOMETERS
← BEAR →
DIRECT WATER WAVE TRAVEL TIME IN SECONDS

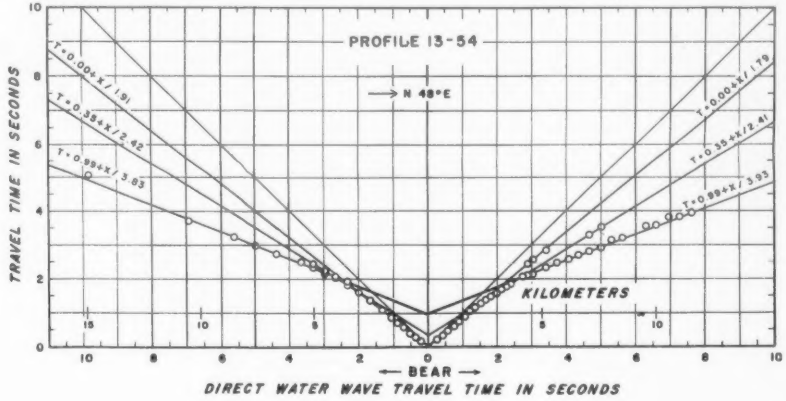
PROFILE 13-54
→ N 48°E
T=0.00+X/1.91
T=0.39+X/2.42
T=0.99+X/3.83
T=0.00+X/1.79
T=0.35+X/2.41
T=0.89+X/3.93
TRAVEL TIME IN SECONDS
KILOMETERS
← BEAR →
DIRECT WATER WAVE TRAVEL TIME IN SECONDS

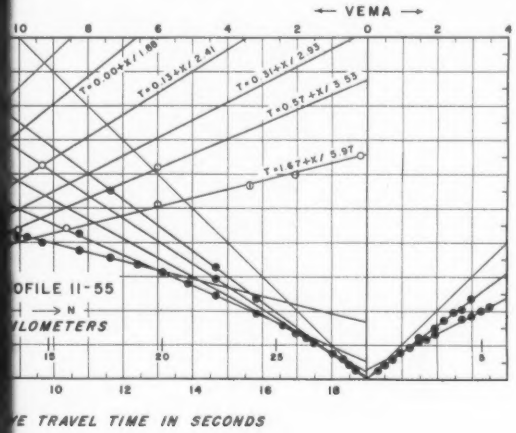
← VEMA →
T=0.00+X/1.88
T=0.13+X/2.41
T=0.31+X/2.93
T=0.57+X/3.53
T=1.67+X/5.97
OFILE 11-55
→ N
ILOMETERS
E TRAVEL TIME IN SECONDS

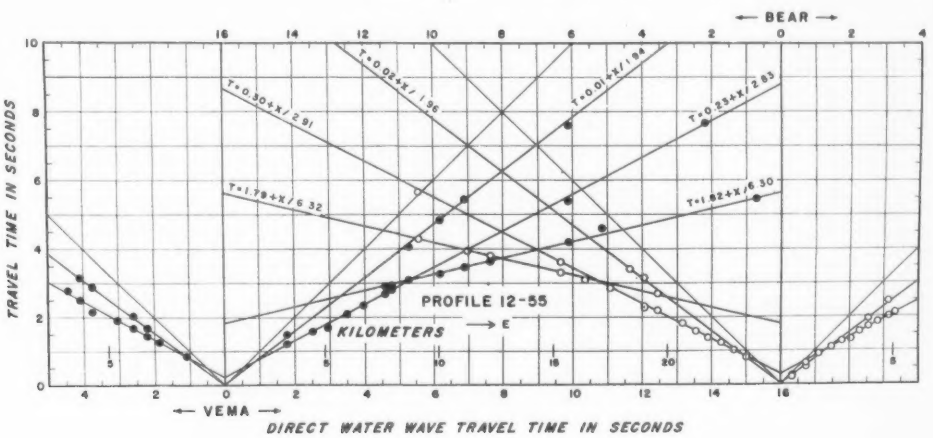
← BEAR →
T=0.02+X/1.96
T=0.01+X/1.94
T=0.30+X/2.91
T=0.23+X/2.83
T=1.79+X/6.32
T=1.62+X/6.30
PROFILE 12-55
KILOMETERS
→ E
TRAVEL TIME IN SECONDS
← VEMA →
DIRECT WATER WAVE TRAVEL TIME IN SECONDS

BULLETIN OF THE GEOLOGICAL SOCIETY OF AMERICA
VOL. 70, PP. 467-508, 20 FIGS., 3 PLS. APRIL 1959

GEOLOGIC EVOLUTION OF THE BEARTOOTH MOUNTAINS, MONTANA AND WYOMING

PART 2. FRACTURE PATTERNS

BY EDGAR WINSTON SPENCER

ABSTRACT

The Beartooth uplift is a large elongate (N.65° W.) range located along the Montana-Wyoming border. The warped Precambrian peneplaned surface is an asymmetric anticlinal fold. Differential uplift of the basement amounting to more than 15,000 feet is greatest along the northern side of the crest. Along the northern and eastern borders of the uplift the crystalline rocks are thrust over Mesozoic sediments. Magnitude of thrusting is variable and is at least 10,000 feet at the northeastern corner where tears have developed in the thrust. The northeastern slope is dissected by glaciation and divided into large valleys and plateaus. The southwestern slope has a relatively uniformly inclined surface. Relief is more than 7000 feet on the northeastern slope and about 2000 feet on the southwestern slope.

Folded granitic gneisses and migmatites are exposed in the core of the range. The folds trend N.-S. to N. 20° E. and plunge southward. Rocks throughout the uplift are complexly fractured. Fracture studies over 700 square miles of the uplift include more than 25,000 fracture measurements made at 250 stations, located to give coverage of all parts of the uplift. The nature of fracturing is considered for the uplift as a whole, for subdivisions of the uplift, and at individual stations. A regional fracture pattern consists of four prominent trends: N. 15° W., N. 45° W., N. 45° E., and N. 65° W. Other trends are at N. 55°-60° E., N. 15°-20°E., N.-S. to N. 5° E., and N. 85° E. to E.-W. All these fractures are nearly vertical. The pattern is consistent and best developed on the southwestern slope. Low-dipping fractures occur in the northeastern part of the uplift and result from more intense deformation in the overthrust parts of the uplift. The inclined fractures do not form a consistent pattern.

Dikes and large fracture zones are shown on aerial photographs of the southwestern slope of the uplift. Fracture trends on photographs have been studied in detail. Photographs alone are not adequate for studies of fracture patterns, but ground measurements can be correlated with photo lineaments.

Five groups of dikes are found in the uplift; all have trends parallel to fractures: (1) Ortho-amphibolite dikes which may be pregranitization are the oldest dikes. (2) Archean metabasaltic dikes, somewhat younger. (3) Unmetamorphosed late Precambrian quartz dolerites. The cycle of metamorphism and granitization is dated at 2.7 billion years. (4) Olivine dolerite dikes, probably Tertiary. (5) Laramide porphyry dikes. Dikes of different ages occupy the same fracture trends; hence the dikes cannot be used to differentiate the fracture patterns. The dikes show that the fracture patterns are Archean.

The major fracture trends indicate that the pattern was formed by warping with relative shortening along the northwest trend, resulting in two sets of tension fractures parallel and perpendicular to maximum shortening. Two sets of conjugate shears also formed at angles of 25°–30° with the direction of maximum shortening. Other fractures appear to have formed in a later deformation when the areas outlined by early major fracture zones were deformed as blocks. These fractures formed with reference to maximum shortening of the blocklike masses. Movements in the core of the uplift in the Laramian were again governed by the pre-existing fractures.

CONTENTS

TEXT

	Page
Introduction	468
Importance of fracture studies	468
Acknowledgments	469
Previous work	469
Regional tectonic setting	469
Introductory statement	469
Structural elements of Bighorn region	472
Structure of Beartooth Mountains	473
Ground measurements	475
Sampling procedures	475

	Page
Analysis of fracture measurements	477
Analysis of mean fracture planes	480
Fracture patterns from aerial photographs	486
Area studied	486
Sources of error	486
Methods of study	487
Observed patterns	488
Divisions of the southwestern slope	492
Summary of results	494
Comparison of ground and aerial-photograph measurements	494
Relations of fractures to other structures	497
Fracture pattern and dikes	497
Fracture pattern and fold structures in granitic gneiss	499
Geologic history of the core of Beartooth uplift	500
Mechanics of deformation	500
Characteristics of fracture patterns	500
Formation of Archean fracture pattern	501
Nature of Laramian deformation	506
References cited	507

ILLUSTRATIONS

Figure	Page
1. Bighorn Basin region	470
2. Major structural features of the Beartooth Mountains	474
3. Variations of point diagrams for fractures measured at a single outcrop	476
4. Examples of departures from isotropic distribution	477
5. Location of fracture stations and foliation measurements	478
6. Fracture concentrations from point diagrams of stations on the southwestern slope of the Beartooth uplift	481
7. Fracture concentrations from summary point diagrams of stations on the northeastern slope of the Beartooth uplift	483
8. Maxima from ground-fracture data on southwestern slope	484
9. Summary of ground measurements in areas of southwestern slope	485
10. Mean fracture planes with dips under 75°	486
11. Fracture patterns at Question Mark Lake	487
12. Histograms of all lineaments identified as fractures on aerial photographs	488
13. Histograms of all lineaments on aerial photographs	489
14. Histograms of long lineaments known to be fractures	489
15. Major fractures on the Beartooth uplift	490
16. Rose diagrams of lineaments in each area on aerial photographs	492
17. Dikes in eastern and central parts of Beartooth uplift	496
18. Fold-fracture relations in the Gardner Lake area	500
19. Origin of fracture trends in Beartooth uplift	503
20. Summary diagrams of fracture data for areas of Beartooth uplift	504

Plate	Facing page
1. Faults and fractures around Granite Lake and fractures east of Beartooth Butte	486
2. Fractures south and north of Jordan Lake	487
3. Fracture patterns on the Beartooth uplift	508

TABLES

Table	Page
1. Regional structural trends	471
2. Fracture trends in eight subdivisions of the southwestern slope	482
3. Fracture trends associated with the northwest trend	493
4. Fracture trends on photographs in divisions of southwestern slope	494
5. Ground measurements compared with photograph measurements	495
6. Trends of dikes	498

Introduction

Importance of Fracture Studies

The exact nature of the process involved when a rock ruptures is not known, but fractures have been used by many geologists to relate stress to strain in rocks. This work has been based largely on Mohr's graphical representation of a state of stress (Nadai, 1950, p. 94) and on experimental results of tension and shear tests on various materials.

Most field studies of fractures are confined to small areas and based on few data. Some workers have used fractures successfully as a means of studying deformation in large areas. Regional studies by Salomon (1911), Wager (1931), Wolk (1937), Parker (1942), and Zwart (1951) show the relation of fractures to deformation in sedimentary rocks. Jolliffe (1942), Wilson (1948), Pincus (1951), and Auden (1954) made regional fracture studies in crystalline rocks.

Fracture studies in tectonically complicated areas in most cases have proved too complex for reliable interpretation. Fracturing in the Beartooth Mountains is extremely complex with great variation in intensity, spacing, and trend of fractures. None the less a fracture study of the uplift is worthwhile for the following reasons: (1) The regional geology

has been studied intensively by members of the Yellowstone-Bighorn Research Association since 1931, and many structural features of the region are known. (2) Detailed structural and petrographic studies are in progress in the crystalline rocks of the uplift as part of a comprehensive research project, the Beartooth project. (3) Outcrops are abundant, and an adequate sample of fractures and coverage of most of the range can be obtained. (4) Aerial photographs that show well-defined fracture patterns on the southwestern slope of the uplift are available, making this region especially suitable to test the relationship between joints measured on the ground and the large fractures seen on aerial photographs. (5) The core of the Beartooth Range is the largest continuous exposure of the basement complex in the Middle Rocky Mountains. Fracture study of the uplift provides an excellent opportunity to study Precambrian deformation and the inferred effects of earlier fracture systems on later deformation.

Acknowledgments

This project received financial support from the Kemp Fund of Columbia University, and the National Science Foundation under grant G-1717 to Prof. Arie Poldervaart of Columbia University. The Yellowstone-Bighorn Research Association provided use of its camp and library facilities at Red Lodge, Montana.

Prof. Marcellus H. Stow, Washington and Lee University, introduced the writer to the interesting problems of this region while doing reconnaissance work in south-central Montana. Prof. W. T. Thom, Jr., of Princeton University, Prof. R. M. Foose of Stanford Research Institute, Dr. F. Donald Eckelmann, Dr. Saurindranath Sen, Dr. Rae L. Harris, and other members of the Yellowstone-Bighorn Research Association have been most helpful through discussions and co-operative field work. Prof. R. M. Foose, Dr. D. U. Wise, and Dr. George Garbarini gave the writer permission to reproduce parts of their map of the border of the Beartooth Range. Profs. Howard Levene, Marshall Kay, and Arthur Strahler of Columbia University made many helpful suggestions on the evaluation of the data.

Messrs. Leroy Hood and Clarence Casella acted as field assistants during the field seasons of 1955 and 1956, respectively.

The writer is especially indebted to Profs. Walter H. Bucher and Arie Poldervaart of Columbia University. Doctor Bucher first recognized the importance of fracture studies in the Beartooth Mountains, through lectures and discussions stimulated the writer's interest, and suggested methods of field investigation and interpretation. Doctor Poldervaart directed the field work, made many valuable suggestions on methods of analysis, and contributed much toward preparation of the script. He also established criteria for recognition of the different groups of dikes and checked their identification.

Previous Work

The Middle Rocky Mountains are being studied under a co-operative plan for investigation of the region by the Yellowstone-Bighorn Research Association. The association was initiated in 1930 by Prof. W. T. Thom, Jr., with the help of Princeton University and the co-operation of geologists from other universities. The abbreviation YBRA is used in all succeeding references to the Yellowstone-Bighorn Research Association.

The YBRA has a field camp at Red Lodge, Montana, and facilities include an excellent library of the region.

Studies of the margins of the Beartooth uplift have been completed recently by a group of students under the direction of Prof. R. M. Foose of Stanford Research Institute. The crystalline core of the uplift is being studied by a group from Columbia University under the direction of Prof. Arie Poldervaart. Parts of the conclusions of this study are based on the findings of this group.

Regional Tectonic Setting

Introductory Statement

Throughout the Paleozoic and Mesozoic, a miogeosyncline (Kay, 1951, p. 7) occupied a broad sinuous zone extending from the Rocky Mountain front in the Yukon, through western Montana and Wyoming, across Utah into southeastern Nevada. This miogeosyncline was separated from the shelf of the craton to the east by a zone of flexure. The geosynclinal trough in the region of southern Montana was either separated or deflected by a westward extension of the craton. During the Paleozoic and Mesozoic, less than 20,000 feet of sediments accumulated in the geosyncline (Nelson and Church, 1943, p. 143).

Folds of the Appalachian type and low-angle thrust faults formed in thick sections of sedi-

ments in the geosyncline in western Wyoming and central Montana in Laramian time. The general trend of these structural elements was N. 45°W. In the foreland east of the geosyncline, in southern Montana and Wyoming, deformation in the Laramian Revolution was strikingly different from that west of the zone of flexure. East of the zone of flexure, separating the geosyncline from the craton, the sedimentary cover was relatively thin, and blocklike uplifts and associated basins formed.

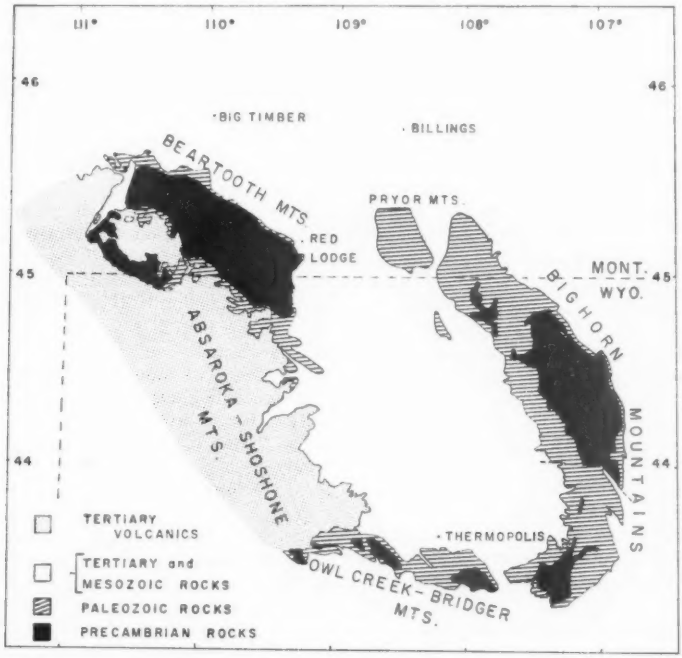

FIGURE 1.—BIGHORN BASIN REGION

These blocklike masses, generally rectangular in shape and exposing broadly warped and tilted peneplaned Precambrian surfaces, make up the Bighorn-Owl Creek-Bridger, Buffalo Fork, Gros Ventre, Beartooth, Wind River, and pre-Tertiary Teton ranges. The ranges are located on the margin of one or more large basins: Bighorn, Wind River, Green River, and Jackson Hole. The major structural elements of ranges which margin the Bighorn Basin are given below. A northern extension of the Bighorn basin, the Crazy Mountain syncline, lies north of the Beartooth Range. The Nye-Bowler fault zone and the Lake Basin fault zone are paralleled by similar fault zones to the north and are also of major structural importance. The Absaroka-Yellowstone volcanic rocks cover a considerable part of the area on the western side of the Bighorn Basin, including the southwestern margin of the Beartooth Uplift.

Figure 1 is an index map of the Bighorn Basin and peripheral mountain ranges. Reference is made to the Tectonic map of the United States (King *et al.*, 1944) and the State geologic maps of Wyoming (1955) and Montana (1955) for details. A summary of trends of major structural elements in the region is found in Table 1.

The ranges are bounded on at least one side by high-angle reverse faults with differential uplift of the basement amounting to thousands of feet. Locally the angle of thrust is low, as at the northeastern corner of the Beartooth Range and in the Bighorn Mountains in the Five Springs Creek area on the western front (Wilson, 1934a) and along the eastern front at Clear Creek (Demorest, 1941). The low-angle thrusts in the last two cases steepen with

TABLE 1.—REGIONAL STRUCTURAL TRENDS

	West	East
Systems recognized in earlier papers:		
Bucher (1953)	N.70°W.	N.5°-15°E.
	N.30°-40°W.	.....
Chamberlin (1945)	E.-W.	N.-S.
Thom (1956)	N.70°W.	N.15°E.
	N.30°W.	N.60°E.
Major structural features:		
Axis of Bighorn Basin	N.40°-45°W.	.....
Axis of Bighorn Mountains	N.30°-40°W.	.....
Cedar Creek anticline	N.30°-35°W.	.....
Axis of Wind River uplift	N.40°-45°W.	.....
Fold and thrust trends in Northern Rocky Mountains	N.40°-45°W.	.....
Axis of Crazy Mountain syncline	N.40°-45°W.	.....
Fold and thrust in Gros Ventre Mountains (Van Dyke, 1956)	N.40°-50°W.	N.-S. to N.10°E.
Faults bounding Pryor Mountains (Blackstone, 1935)	E.-W.	N.-S.
Major faults in Owl Creek Mountains (Masursky, 1952)	N.40°-50°W.	N.65°E.
	N.20°-25°W.	.....
	E.-W.	.....
Nye-Bowler lineament (Wilson, 1936)	N.70°W.	N.55°E.
Lake Basin fault zone	N.70°W.	.....
Cat Creek fault zone	N.70°W.	.....
Border features of the Beartooth Range:		
Northern boundary thrust faults	N.60°-70°W.	.....
Eastern boundary thrust faults	.....	N.5°-15°E.
Western boundary faults	.....	N.30°-35°E.
Gardiner thrust fault	N.60°W.	.....
Rattle Snake Mountain thrust fault	N.45°W.	.....
Cooke City fault line	N.60°-65°W.	.....
Structural trends in the core of the Beartooth Range:		
Faults in the Livingston Peak area (Lammers, 1937)	N.55°-65°W.	.....
	N.30°-35°W.	.....
	E.-W.	.....
Fault and fracture zones in the central Beartooth Uplift (Lammers, 1939, unpublished)	N.15°W.	N.15°E.
	N.45°W.	N.45°E.
	N.75°W.	N.75°E.
Fold axes mapped in the crystalline core (Members of the Beartooth Project)	.....	N.-S. to N.15°E.

depth, probably becoming high-angle reverse faults.

A second important characteristic of the ranges in this region is their asymmetry. In most places one side of the uplift is bounded by a high-angle reverse or thrust fault and the opposite side by a normal fault or by moderate to low monoclinal flexures. Both the Beartooth Range and the Bighorn Range show reversal of asymmetry in parts of the ranges separated by major fault zones which are transverse to the axes of the uplifts. Asymmetry is the same on opposite sides of the same block, both in major and minor folds and faults (Bucher, Chamberlin, and Thom, 1934, p. 175).

Two basically different theories of the mechanics of deformation have been advanced for this region. The wedge-uplift theory postulates that Archean sediments have been intruded by batholithic granites. These granites headed and spread laterally as they rose to the surface, forming wide, shallow, downward-pointing wedges, embedded in metamorphosed and folded sedimentary material. In the Laramian deformation the wedges were arched and intensely compressed. Compression caused

the mountain masses to become warped and resulted in wedge uplifts bordered by overthrusts, underthrusts, or high-angle faults (Thom, 1952, p. 15; 1955, p. 369).

The second theory postulates that in the Laramian blocklike parts of the region were warped and uplifted. Some of the uplifts resembled large folds, and in others movement occurred along earlier faults and was essentially vertical. At corners or sides of the blocks where uplift reached a maximum, overthrust developed. In some cases, as in the Pryor Mountains and the Buffalo Fork area, overturning was minor, but in other areas overthrusting became pronounced, as at the northeastern corner of the Beartooth uplift and in the Five Springs Creek area of the Bighorn Mountains. Scissorlike motions formed tears in the upper plate of Paleozoic and Precambrian rocks at points of maximum overthrusting. Both the Beartooth Mountains and and the Bighorn Mountains were divided by a major transverse zone of faults, and maximum uplift occurred on different sides across these zones. This caused asymmetry to develop in opposite directions on opposite sides of the faults and in the same direction on opposite sides of the same unit (Bucher, 1957, personal communication).

Structural Elements of Bighorn Region

BIGHORN BASIN: This elongated basin, which trends N. 45°W., extends from the Owl Creek-Bridger uplift on the south to the Nye-Bowler fault zone. The Crazy Mountain syncline continues along the same trend to the northwest. The axis of the basin is located on the western side close to the Absaroka volcanic rocks. The northeastern corner of the Beartooth uplift has been thrust out over part of the basin. Paleozoic and Mesozoic sedimentary sections are exposed around the margins of the basin where the Precambrian basement has been uplifted. Tertiary sediments form a thick cover in the center of the basin. The sediments reach a maximum thickness in excess of 15,000 feet along the axis east of the Beartooth uplift. Chamberlin (Bucher, Chamberlin, and Thom, 1933) shows that gravity anomalies confirm these conclusions.

Asymmetrical folds occur on both sides of the Bighorn Basin. All the folds are elongated and trend N. 45°W. Folds along the eastern margin of the basin are asymmetrical toward the east, and those on the western margin are asymmetrical to the west. Some of the larger folds involve the Precambrian basement, *e.g.*, the Rattlesnake Mountain anticline west of Cody, Wyoming. (*See* Dobbin and Erdmann, 1947.)

BIGHORN MOUNTAINS: The Bighorn Range is a broad, asymmetric, anticlinal uplift divisible into three structural units: northern, central, and southern.

The central unit has been warped asymmetrically with steepening on the eastern side, where local overthrusts bounded by tear faults show a maximum displacement of 3 miles eastward (Demorest, 1941, p. 167). The western slope of this unit has a gentle monoclinal dip, well exposed in the Shell Creek Canyon of U. S. Highway 14. Secondary folded structures in the central unit are asymmetrical on the east, and in the northern and southern end they are asymmetrical on the west.

The northern unit is separated from the central segment by the Tongue River fault zone. This unit is asymmetrical and locally overthrust to the west at the Five Springs Creek area (Wilson, 1934a). Two secondary folded structures, which are asymmetrical and thrust westward, interrupt the gentle eastward monoclinal flanks of the unit (Demorest, 1941, p. 171).

The southern unit is separated from the central segment by the well-defined Tensleep fault (Wilson, 1938). Three significant secondary asymmetrical anticlines produced by overthrusting toward the west-southwest have been described by Demorest (1941, p. 169).

OWL CREEK-BRIDGER UPLIFT: Fanshawe (1939) describes the nature of Laramian deformation in the Owl Creek-Bridger uplift, which separates the Bighorn Basin from the Wind River Basin to the south. The Precambrian basement complex has been offset vertically for thousands of feet and locally overthrust along the southern edge of the uplift. The northern slopes are gentle monoclines strikingly shown in the Wind River Canyon. The monoclines are warped and in places consist of a number of small asymmetric flexures (asymmetrical southward). Fanshawe attributes the formation of these structures to regional compression transmitted by the basement complex, causing relative southward movement between the Wind River Basin and the Bighorn Basin.

Masursky (1952) mapped the Western Owl Creek Mountains. His map shows prominent fractures and fault zones similar to those in the Beartooth Mountains. Major trends of the fractures are N. 45°W., N. 65°E., and N.

20°W. Fold axes trend eastward in the northern part of the area and northwestward in the western part of the area.

BUFFALO FORK AREA: The Buffalo Fork area uplift is a westward continuation of the Owl Creek Range. Bengtson (1956, p. 160) describes it as a series of blocklike uplifts bounded on two sides by steep monoclines or high-angle faults. The area consists of two large blocks: South Fork block and North Fork block. South Fork block is a triangular-shaped uplift bounded on the south and west by steep monoclinal flexures, related to high-angle faults in the basement. The strike of the southern monocline is N. 75°W., and its eastern end passes under the Absaroka volcanic rocks. North Fork block is a tilted block elongated northward. The steep western monocline is offset 1½ miles to the west from the corresponding monocline on the southern uplift.

PRYOR MOUNTAINS: The Pryor Mountains consist of four blocks separated by two sets of parallel flexures trending N. 15°W. and E.-W. The northern and eastern sides of the blocks are bounded by steep monoclines and high-angle faults. The southern and western slopes of each block are gentle monoclines. The area is mapped and described by Blackstone (1940). The Pryor Mountains are classic examples of "trapdoor" uplifts (Nelson and Church, 1943, p. 151).

MAJOR FAULT ZONES: Three nearly parallel echelon fault belts with trend N. 65°-75°W. occur north of the Bighorn Basin. In all three the major faults strike northeast, indicating relative eastward movement of the south side.

The Nye-Bowler lineament extends from the Pryor Mountains to the town of Nye, Montana. Asymmetric domes and anticlines along the lineament are cut by two fault systems, one aligned N. 65°-75°W. and a second N. 45°-50°E. Wilson (1936) describes this zone and attributes the formation of the faults to left-handed displacement along a deep-seated basement fault.

The Lake Basine fault zone lies farther north. Asymmetric domes and anticlines along this zone are cut by northeast faults. This zone is similar to the Nye-Bowler lineament (Chamberlin, 1945), and apparently movements along the zone started in the Paleozoic (Thom, 1923).

A similar fault zone occurs between the Judith Mountains and the Porcupine Dome in central Montana. A fourth zone of movement parallel to these echelon fault zones is shown by Dob Lin and Erdmann (1955); the exact nature of this zone is not known.

Structure of Beartooth Mountains

DIVISIONS OF THE UPLIFT: The Beartooth Mountains comprise three units, separated by significant structural features. The largest unit is the central and eastern part, southwest of Red Lodge, Montana, referred to in this paper as the Beartooth uplift. This has the form of a large asymmetric anticline, overturned to the north-northeast and overthrust to the north along the northern border, and to the east along the eastern border. The unit is separated from the North Snowy block to the northwest by a zone of faults, the Mill Creek-Stillwater fault zone. The North Snowy block is asymmetrically folded and thrust southward. The Absaroka-Yellowstone volcanic rocks cover a large area between the South Snowy block and the North Snowy and Beartooth uplifts. The volcanic rocks also cover the southwestern margin of the Beartooth uplift. Major structural features are shown in Figure 2.

Thom (1952, p. 15) considers Rattlesnake Mountain west of Cody, Wyoming, a structural appendage of the Beartooth uplift. The northern end of this mountain is more than 15 miles from the southern end of the Beartooth uplift at Clarks Fork Canyon, Wyoming. A study of this area by D. U. Wise is in preparation. A complex structural pattern of thrusts and normal faults occurs between Rattlesnake Mountain and the Clarks Fork Canyon.

MARGINS OF BEARTOOTH MOUNTAINS: The following outline is taken in part from lectures and discussions at the 1956 YBRA Short Course, particularly from the lecture by Prof. R. M. Foose.

The North Snowy block is bounded on the north between Nye and Livingston, Montana, by a major thrust plane, with subsidiary thrust, dipping northeast (Foote, 1934, unpublished map, YBRA library, Red Lodge, Montana; Vhay, unpublished map, YBRA library, Red Lodge, Montana; Richards, 1954, manuscript on open file, U. S. Geological Survey, Billings, Montana). From the East Boulder River westward, minor thrust planes dip northward; this suggests that large laccolithic masses along this part of the mountain front formed a series of buttresses and caused underthrusting to the north (Rouse *et al.*, 1937). The upper plate of the thrust near Livingston is broken by tear faults along which

the western sides have moved southward (Lammers, 1937; Skeels, 1939).

Basalt flows and agglomerates cover most of the western margin of the North Snowy and South Snowy blocks, making it impossible to determine their exact margins. Sharp flexures with local overturning and thrusting to the southwest are exposed at three localities on the western side of the South Snowy block (Bucher, Chamberlin, and Thom, 1934, p. 174).

Near Gardiner, Montana, a high-angle thrust plane dipping northeast forms the southern margin of the South Snowy block (Wilson, 1934b). Thom (1952, p. 15) suggests that the Gardiner thrust continues southeastward and joins a major vertical fault along the west side of Rattlesnake Mountain west of Cody, Wyoming. This line is covered by volcanic rocks for 60 miles.

The Beartooth uplift is bounded on the southwest by the Clarks Fork-Cooke City trench, a zone of nearly vertical normal faults which strike N. 65°W. The southwestern side dropped 3000–4000 feet at the southeastern end of this zone, which changes northwestward to steep southwest monoclinal dips.

FIGURE 2.—MAJOR STRUCTURAL FEATURES OF THE BEARTOOTH MOUNTAINS
After Geologic Maps of Montana (1955) and Wyoming (1955)

South of Clarks Fork Canyon, where the east side of the Beartooth uplift intersects the Clarks Fork trench, the westward-dipping thrust steepens and becomes a normal fault with 4000 feet displacement. Hughes (1933), Johnson (1934), Pierce (1956, unpublished manuscript, U. S. Geological Survey), and Wise (In preparation) describe parts of the southeastern end of the Beartooth uplift where the Clarks Fork River cuts across the steeply plunging Precambrian surface. North of Clarks Fork Canyon, the east side of the Beartooth uplift is bounded by a thrust that dips to the west (D. U. Wise, personal communication, 1957).

At the sharp bend in the border of the uplift near Red Lodge, Montana, numerous tear

faults are developed in the overthrust mountain front. The Precambrian core of the uplift is thrust out over the axis of the Bighorn Basin at this corner (Fig. 1). Total displacement is unknown, but structural relief of the basement is about 20,000 feet. Tear faults at the northeastern corner of the uplift strike northeast and northwest. Displacements along the tears amount to as much as 10,000 feet. The tears appear to be formed by scissorlike motions displacing the upper thrust plate but not extending great distances into the Precambrian core. Details are given by Perry (1935) and Foose (1956). Westward from Red Lodge to the East Boulder River, the thrust planes dip southwest.

PRECAMBRIAN CORE: The margin of the Precambrian core is made up of metasedimentary rocks and migmatites. Toward the central part of the uplift these rocks grade into granitic gneisses and localized areas of two-mica granites (Cloos and Cloos, 1933; Lammers, 1939, unpublished manuscript, YBRA library, Red Lodge, Montana). Pegmatites are common throughout, and all the rocks are cut by dikes. Mapping by Eckelmann and Poldervaart (1957) and other members of the Beartooth research group indicates a series of relatively open folds trending N.-S. to N. 15°E. and plunging southward at 20°–40°. The folded structures are traced continuously from the migmatite zone at the margins of the uplift into the core of granitic gneiss. The folds are mapped by compositional banding in migmatites and metasediments and foliation in granitic gneisses. The surface of a batholith is probably not extensively exposed anywhere in the central part of the uplift. Work by members of the Beartooth project indicates that the granitic gneisses have been formed by progressive feldspathization of Archean sediments (Poldervaart, in preparation).

Four groups of basaltic dikes and one of prophyry intrusive rocks are found in the uplift. The dikes include Archean, pregranitization ortho-amphibolites; Archean metabasaltic dikes; late Precambrian quartz dolerites, early Laramide porphyry dikes; Tertiary olivine dolerites.

One of the most striking structural features in the uplift is the well-developed fracture pattern. Major fractures form a conspicuous and complex pattern on the southwestern slope of the uplift. Dikes are parallel or subparallel to major fractures. At some outcrops fracturing is simple and consists of three fracture trends, but generally the fracture pattern is extremely complex. Study of these fractures provides one of the most direct lines of approach to the complex deformational history of the uplift. The fractures offer one way of studying the relation between Precambrian and Laramian movements in the core of the uplift. Fractures are clearly shown on aerial photographs of the southwestern slope of the range, and this area is unusually good for study of the relationship between fracture measurements taken from aerial photographs and on the ground.

GROUND MEASUREMENTS

Sampling Procedures

GENERAL CONSIDERATIONS: Field methods for collecting fracture data have been discussed by Pincus (1951) and Muller (1933). The purpose of a fracture study is important in determining location and spacing of stations; nature of rock exposures, intensity of fracturing, and expected number of fracture systems will also influence sampling procedures.

The aims of this study are to determine existing fracture patterns in the crystalline core of the Beartooth Mountains, to trace possible variations in the patterns, and to relate these observations to the regional tectonic pattern.

The following sampling procedures were used:

(1) All fracture stations were located in granitic gneisses.

(2) Stations were spaced to give as detailed coverage of the area as time and accessibility allowed.

(3) Between 100 and 120 fractures were measured at each station used in the regional analysis. Some stations represent fewer measurements, but these have not been used for analysis.

(4) Starting at an arbitrarily chosen point, all fractures in the immediate vicinity of that point were measured. Strike and dip measurements were made on each fracture plane. On the northeastern slope of the uplift, where fracturing was more complicated, 120 measurements were made at each station. This number of fractures in most cases occurred within a circle 10 feet in diameter.

(5) Each fracture was marked with crayon after measurement. This prevented repetition of measurements on prominent fractures and insured sampling of all fractures within the area.

(6) Samples of basaltic dikes were collected when it was possible to determine strike of dikes.

in the analysis. The total area covered was approximately 700 square miles. The writer initially planned to use a grid pattern as basis

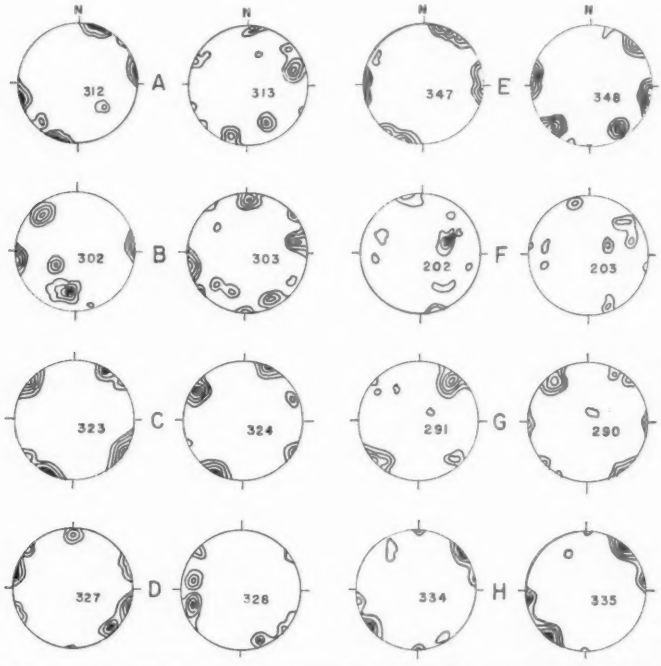

FIGURE 3.—VARIATIONS OF POINT DIAGRAMS FOR FRACTURES MEASURED AT A SINGLE OUTCROP

Each pair of diagrams was obtained by taking two sets of measurements of 100 fractures each at a single outcrop. Measurements are plotted on the upper hemisphere of a Schmidt net. The lowest contour is 4 per cent, and the contour interval is 2 per cent. Number of station is given in each diagram. Similar trends are seen in both diagrams for most of the outcrops.

(7) Stations were not located within fault zones.

(8) Measurements were not made on fractures too irregular to be approximated by a plane.

(9) Strike and dip measurements were made with an estimated accuracy of 3°–5°, depending upon irregularity of fracture surfaces.

(10) Measurements on spacing of fractures were not made.

DISTRIBUTION OF STATIONS: Between the northeastern thrust front of the uplift and the southwestern margin (Fig. 5) 250 stations were located. Of these, 65 were on the northeastern slope of the uplift, 12 were in rock types other than granitic gneiss, and less than 100 measurements were made at 13 stations. The last two groups of stations were not used for location of stations. Physiography and inaccessibility of parts of the area made this impractical.

On the northeastern slope of the asymmetric uplift, glaciers have carved large, U-shaped valleys, separated by flat-topped mountains with summit elevations of 11,000 feet, which correspond to the late Precambrian peneplaned surface. The valleys are filled with glacial debris, talus, and recent stream deposits. The plateau surfaces have a thin cover of vegetation, and all summit outcrops have been disturbed by frost wedging and heaving. Hence, it was necessary to locate stations along margins of the plateaus. These stations are approximately 1 mile apart and are located to facilitate comparison of fracturing at progressively greater distances from

the overthrust front. No stations are located in the area between the western margin of Silver Run Plateau and the plateau east of Mystic Lake, because this area consists of large valleys filled with debris, and rugged, almost inaccessible peaks.

Outcrops are more abundant on the southwestern slope of the uplift, particularly above timber line (10,500 feet). Many areas have as much as 95 per cent exposure, but others are partly covered by glacial debris, lakes, and clogged drainage. Below timber line, forest and more abundant glacial deposits are found.

INVARIABILITY OF MEASUREMENTS: At 11 localities in widely separated parts of the uplift, two stations are located no more than 50 feet apart on a single unfaulted outcrop. Point diagrams of eight of the localities are given in Figure 3. The remaining three localities have relationships identical with those illustrated. Both stations at a single outcrop generally have contoured concentrations centered within 5° of one another. However, the degree of concentration, here defined as the percentage of fractures within 1 per cent of the projection area, does not always correspond. In several cases a fracture direction indicated at one station is not represented at the second station. This type of variation is obvious in the field. Many small fractures in one part of an outcrop may parallel a few large fractures in other parts of the outcrop. Where this relation is found, conclusions should not be based on the degree of concentration, unless length of fractures is considered, as well as their strike, dip, and spacing.

NUMBER OF FRACTURES MEASURED: The number of fractures measured at a station was based on the conclusions of Bucher (1955, personal communication) in the Bighorn Mountains, where he found that no new maxima developed after the first 120 measurements. This study was made in granitic rocks similar to those of the Beartooth Mountains. Pincus (1951, p. 99) determined that there was little change in the pattern of fracture data from the Poundridge, New York, granite and gneiss after 60 points had been measured, though he recommended that at least 100 fractures be measured.

Analysis of Fracture Measurements

REPRESENTATION OF DATA: Strike and dip measurements were projected on the upper hemisphere of a 10 cm Schmidt net. One hundred or more measurements were used for each diagram. A 1 per cent counting circle (Duschatko, 1955), rotated in 5-degree intervals, was used to count the number of points within each area of 1 per cent of the Schmidt net. Figures obtained in this wa were contoured to show areas of concentration. A 2 per cent contour interval was used, and the 4 per cent contour was the lowes drawn on the diagram.

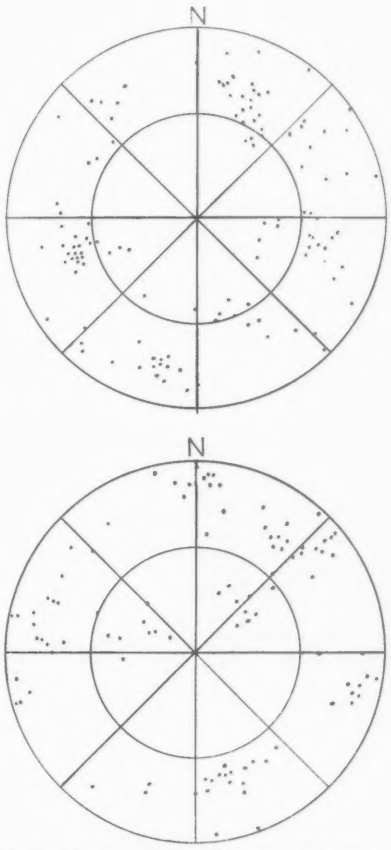

FIGURE 4.—EXAMPLES OF DEPARTURES FROM ISOTROPIC DISTRIBUTION

Division of the Schmidt net used in counting points to determine that the diagrams are departures from isotropic distribution. If as many as 13 points occur within one of the areas, the chances are 1 in 100 that the distribution is the result of chance. The diagrams do not illustrate typical fracture measurements made in this study; they are among those showing the lowest concentration of points.

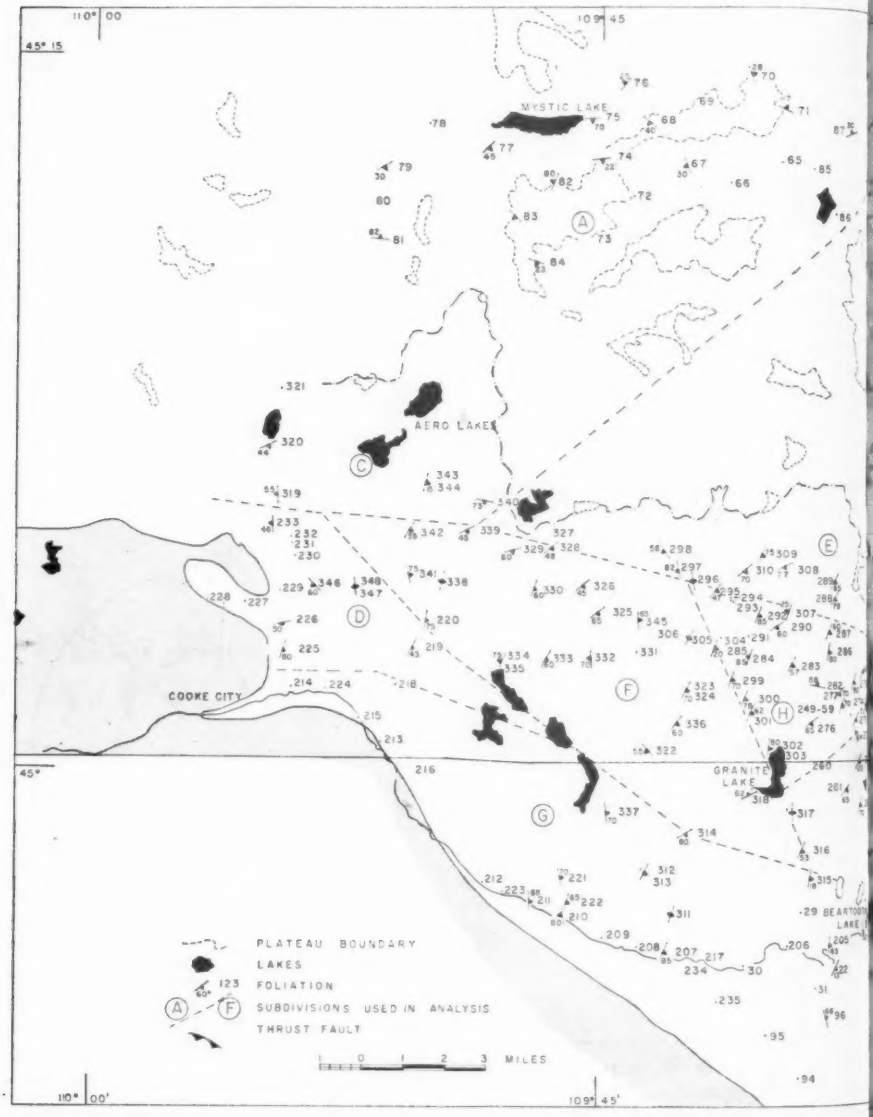

FIGURE 5.—LOCATION OF F

DEPARTURES FROM ISOTROPIC DISTRIBUTION: Pincus (1951, p. 101–105) treated the problem of whether or not the distribution of a given set of fracture measurements is a significant departure from an isotropic distribution. The investigator must choose the level of probability that he will accept as significant. The author has chosen as significant any departure with a probability of 0.01 or less.

The test used by Pincus employs the Poisson exponential binomial limit. For a chosen level of probability, the limit indicates what number of the total measurements must fall within a given area of the plotted diagram to indicate a

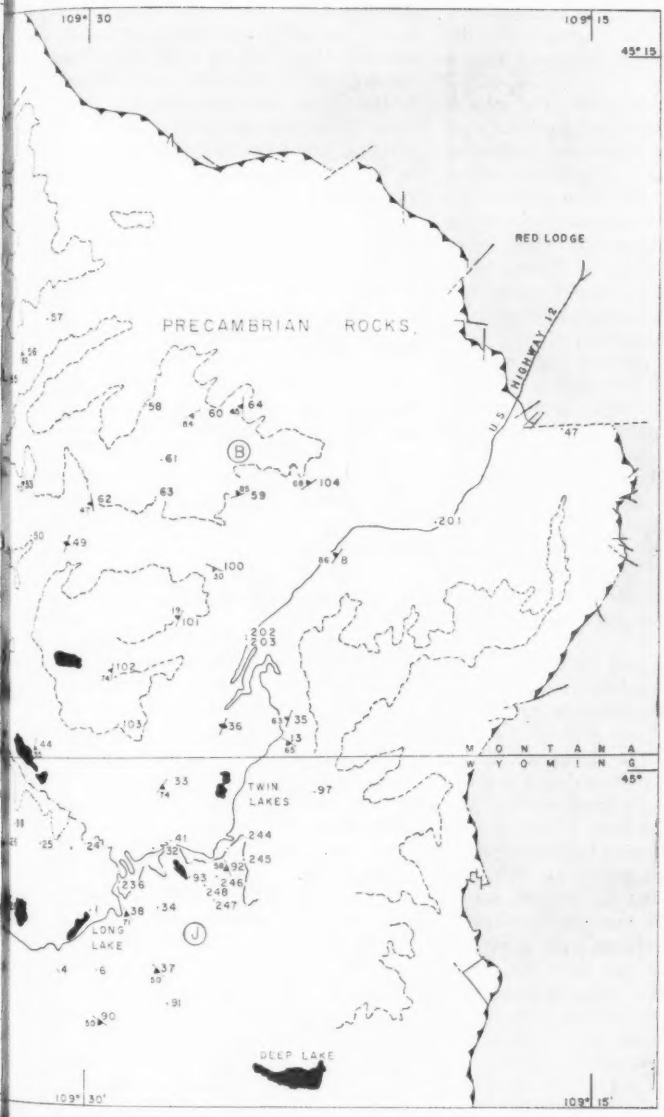

ns and Foliation Measurements

departure from isotropism. The Poisson exponential binomial limit may be evaluated by using the tables prepared by Molina (1947). When 100 measurements have been plotted on a diagram divided into approximately 7 per cent areas, the probability that 13 of the measurements will fall in a single area is 0.01 (1 chance in 100 that the distribution is not a departure from isotropism).

If applied to the fracture data obtained in this study, the test indicates that all the point diagrams are departures from isotropic distribution. Two extreme examples of stations that might appear to lack significant concen-

trations are shown in Figure 4. A fixed counting grid is drawn on the point diagrams, and the number of points falling within each area is indicated.

SIGNIFICANT CONCENTRATIONS: The superiority of more rigid statistical analysis over inspection in selecting significant concentrations on point diagrams is subject to question. Chayes (1949, p. 308–326) demonstrates this by testing six fabric diagrams representing more than 200 measurements each, using the Winchell General Test, the Empty Space Test, and the "r" test of preferred orientation. The diagrams had previously been interpreted by Ingerson, using inspection. Chayes compares results of the statistical tests with results of inspection. All the diagrams are incompatible with an isotropic parent fabric, but by inspection only two are considered indicative of preferred orientations. The Winchell General Test indicates that five of the diagrams do not have significant orientations and that one is questionable. The correlation coefficient "r" leads to conclusions identical with those reached by inspection in five of the six examples, and the sixth diagram is considered questionable both by inspection and by the "r" test.

In the six diagrams that Chayes describes, the concentrations of points are low. Those maxima, or concentrations which he does not consider significant, have highest contours of 4 per cent or less. The significant concentrations have highest contours of 4 per cent or more. In the present fracture study, the co-ordinates of maxima from a large number of contoured point diagrams have been plotted as summary point diagrams to investigate the possibility of a relatively uniform pattern over a large area. If maxima bounded by highest contours of less than 4 per cent are a probable result of chance, then the use of such maxima in a point diagram summarizing the co-ordinates of maxima from a large number of stations would tend to mask patterns of significant maxima.

On the southwestern slope of the Beartooth uplift, fracture measurements indicate a large number of well-defined concentrations. Four point diagrams (Fig. 6) show the concentrations of 4 per cent plus, 6 per cent plus, 9 per cent plus, and 12 per cent plus, which occur on point diagrams for stations located in this part of the uplift. Maxima on the diagrams indicate that the same fracture trends are shown where all maxima (728) of 4 per cent plus are used, as where all maxima (533) of 6 per cent plus or of 9 per cent plus (329) are used. No significant change is found where concentrations of 12 per cent plus (156 maxima) are used. This observation provides confidence in the use of concentrations of 4 per cent or more in comparing results from two or more stations. The 4 per cent level of concentration is used as significant in this paper and has been used in all analyses of ground measurements.

The Poisson exponential binomial limit may be used to give an approximation of the probability of various levels of concentration. A perfectly uniform distribution of the 100 measurements made for each diagram in this study would consist of 1 point in each 1 per cent area. The probability of finding more than the following number of points in any 1 per cent area in a diagram is: 0 points, 1.00; 1 point, 0.63; 2 points, 0.26; 3 points, 0.08; 4 points, 0.02; 5 points, 0.004; 6 points, 0.0006. The chances of having a 4 per cent concentration in a random distribution are therefore approximately 1 in 50.

Analysis of Mean Fracture Planes

SELECTION OF PLANES: Mean fracture planes are here defined as those whose dip and strike co-ordinates lie at the center of the area within the highest contour when lower contours are symmetrically arranged around that maximum. Where the peak is not symmetrically centered, the mean fracture plane is chosen to fall in or on the boundary of the peak contour on the side placing it nearest a symmetrical position with respect to the lower contours.

Aerial photographs of the uplift show fractures within 10°–15° of other fracture trends. To determine whether this characteristic is duplicated in measurements on the ground, care has been taken to measure closely spaced highs on point diagrams as separate maxima, rather than average them to one mean fracture plane. Closely spaced highs separated by a saddle 2 per cent lower than the lowest of the two highs are considered separate fracture planes. Few diagrams have highs spaced within 10°–15°, but apparently unrelated maxima 20° apart are common (Pl. 3).

SUMMARY DIAGRAMS OF THE SOUTHWESTERN SLOPE: Summary point diagrams have been prepared by plotting co-ordinates of each mean fracture plane as a point on a point diagram. The points are then contoured, using a 1 per cent contour interval. The lowest contour is the 2 per cent contour. Four such

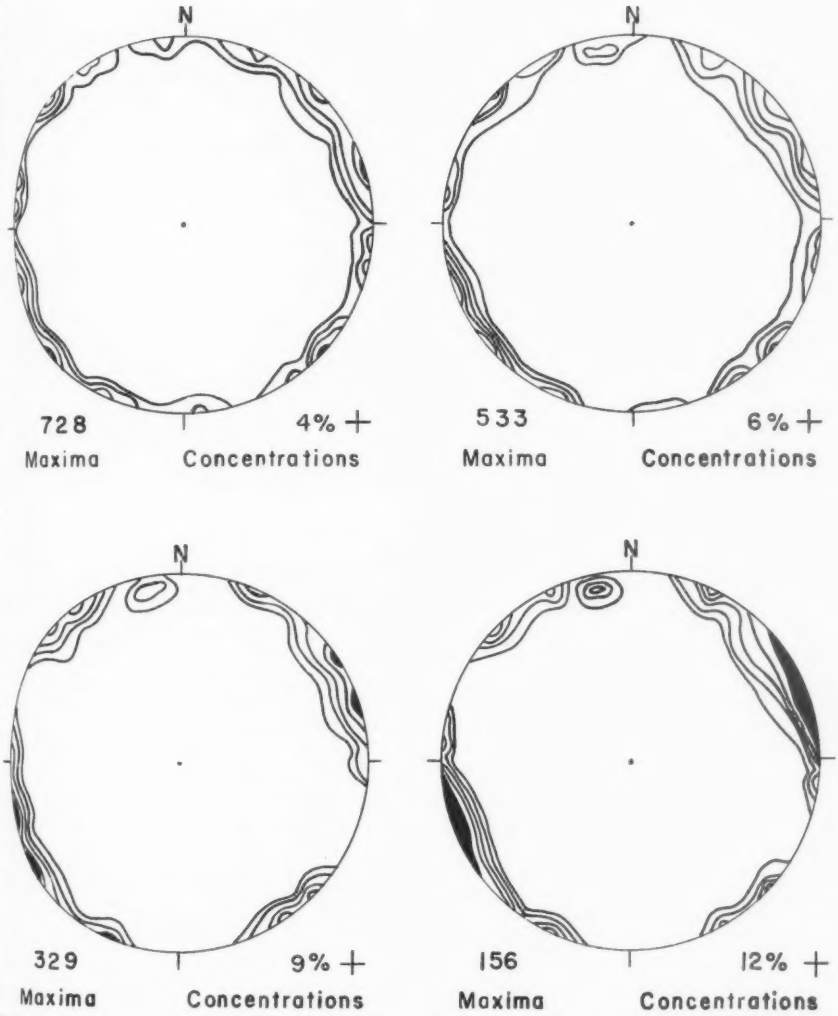

FIGURE 6.—FRACTURE CONCENTRATIONS FROM POINT DIAGRAMS OF STATIONS ON THE SOUTHWESTERN SLOPE OF THE BEARTOOTH UPLIFT

Diagrams were obtained by plotting the concentrations from each point diagram of every station on the southwestern slope of the uplift as points with the co-ordinates of the center of that concentration on a Schmidt net. This was done for all concentrations of 4 per cent or greater, 6 per cent plus, 9 per cent plus, and 12 per cent plus. The number of concentrations, maxima, used for each diagram is given. The lowest contour for each diagram is 2 per cent, and the contour interval is 1 per cent.

diagrams have been prepared for data collected on the southwestern slope. One represents all the mean fracture planes indicated by concentrations of 4 per cent (probability 0.02) or more on all the point diagrams for stations on the southwestern slope. The other three summary diagrams represent all concentrations of 6 per cent plus (probability 0.0006), 9 per cent plus, and 12 per cent plus (Fig. 6). The number of concentrations used in the preparation of each diagram is indicated.

All concentrations on the summary point

diagrams for the southwestern slope of the uplift represent nearly vertical fractures. The 4 per cent plus, 6 per cent plus, and 9 per cent plus summary point diagrams (Fig. 6) have three well-defined concentrations: N. 15°W., N. 45°W., and N. 45°E. Less well-developed concentrations are: N. 65°W., N. 55°-60°E., N. 15°-20°E., N.5-N.5°E., and N. 85°E.-E.W. If concentrations of 12 per cent plus only are considered, the best defined maxima are: N. 15°W., N. 45°W., N. 45°E., and N. 65°W. The N. 45°W. concentration is concealed in a general northwestern high concentration. Concentrations at N. 10°E., N. 60°E., and N. 85°E. are also indicated.

Figure 10 is a point diagram for mean fracture planes dipping at angles less than 75° for all stations on the southwestern slope. Maxima fall along strike directions identical with those of concentrations representing nearly vertical fractures. There are no low-dipping fracture trends on the southwestern slope that can be considered independent of nearly vertical trends. Where low-dipping fractures are found they must be attributed to local tilting or local strain.

The mean fracture planes of stations on the southwestern slope are also summarized in histograms of frequency against strike direction (in 5-degree intervals). The two histograms in Figure 8 are for dips of 55°–79° and 80°–90°. No significant change in the position of peaks indicated by the vertical fractures would occur if the two histograms were grouped together. A similar diagram for the northeastern slope is not used, because many of the mean fracture planes dip at low angles (less than 60°).

The histogram of concentrations of nearly vertical mean fracture planes (Fig. 8) has a number of peaks. The most prominent are N. 20°W., N. 40°W., and N. 40°E., with lesser peaks represented by 18 or more mean fracture planes at N. 70°W., N. 60°E., N. 10°E., and E.-W. The probability that these peaks may be the results of chance is indicated. Between 18 and 19 points must fall within a single interval for a probability of 0.05 (1 chance in 20 that the peak is part of a random distribution). All seven trends have probabilities of 0.05 or less. On the basis of this summary diagram the southwestern slope has a well-defined anisotropic fracture pattern.

TABLE 2.—PROMINENT FRACTURE TRENDS IN EIGHT SUBDIVISIONS OF THE SOUTHWESTERN SLOPE

Area	Directions						
C	85°E.*	65°W.	45°W.	20°W.	10°E.	35°E.	65°E.
D	.....	70°W.*	50°W.*	18°W.	5°E.	38°E.	60°E.
E	85°W.	70°W.	40°W.*	20°W.*	10°E.	45°E.	65°E.
F	E.-W.*	65°W.*	40°W.	15°W.*	20°E.?	38°E.*	60°E.
G	88°E.*	65°W.	40°W.*	15°W.*	20°E.	45°E.*	60°E.
H	86°W.?	55°W.	40°W.*	15°W.	10°E.	40°E.*	60°E.?
I	82°E.	60°W.?	40°W.*	20°W.*-5°W.	12°E.	40°E.*	60°E.?
J	82°E.	65°W.*	47°W.*	15°W.	10°E.	40°E.*	60°E.

* indicates strong well-defined trends
? indicates questionable trends

DIVISION OF SOUTHWESTERN SLOPE OF UPLIFT: The summary point diagrams and histograms indicate the existence of regional preferred orientations, which pose the following questions:

(1) Are certain maxima confined to particular parts of the uplift, or do all the trends occur throughout the uplift?

(2) Is there a systematic change in direction of fractures toward the borders of the uplift?

(3) Have the big blocklike areas seen on aerial photographs of the southwestern slope been rotated or tilted?

(4) What is the nature of fracturing at individual outcrops?

To answer the first three questions, the uplift has been divided into 10 areas, *A*–*J* (Pl. 3). Summary point diagrams of mean fracture planes at stations within each of the areas are shown in Figure 20. Where possible, natural boundaries of probable structural significance have been chosen for the areas. The northeastern slope has no major structural features which can be used to subdivide it

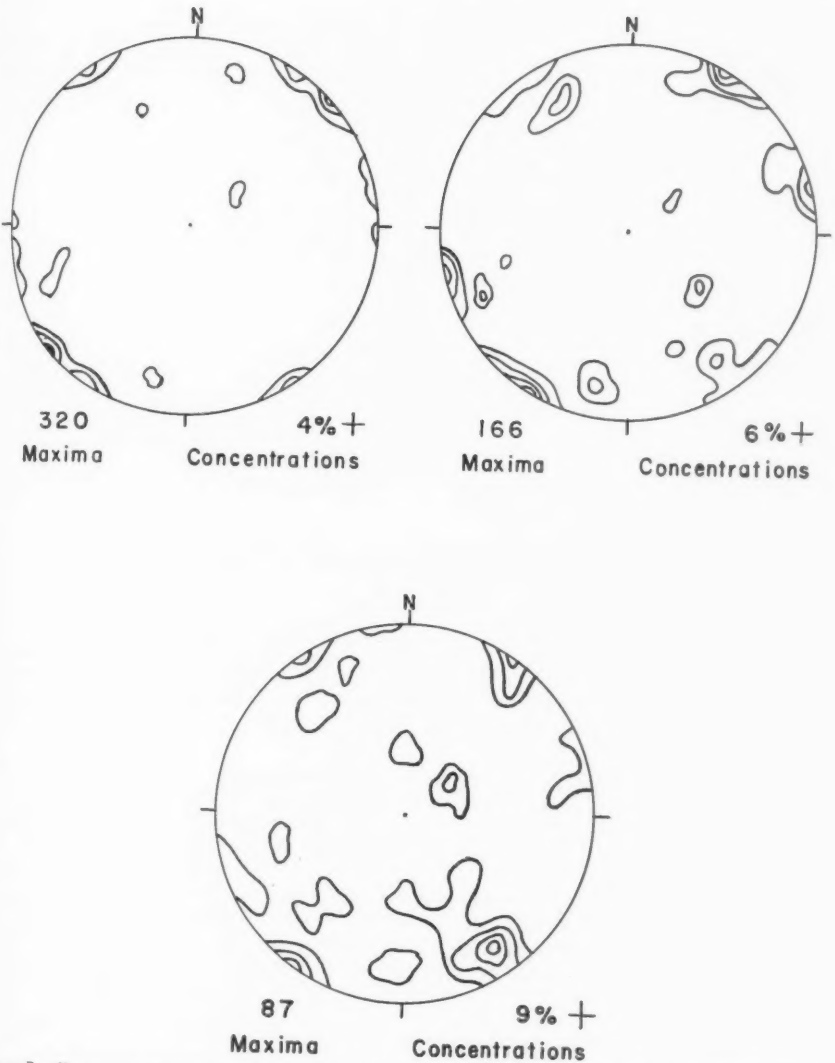

FIGURE 7.—FRACTURE CONCENTRATIONS FROM POINT DIAGRAMS OF STATIONS ON THE NORTHEASTERN SLOPE OF THE UPLIFT

The method of plotting is the same as that used for Figure 5. The nearly vertical fracture sets are the same found on the southwestern slope, but several additional sets of inclined fractures appear in this part of the uplift.

The glaciated valley occupied by the East Rosebud River, which flows northward almost at right angles to the mountain front, has been selected as the natural boundary dividing this slope of the uplift into two areas (*A* and *B*).

The southwestern slope is divided by many large fractures and dikes, which are used as boundaries for the eight areas located on this part of the uplift. An effort has been made to select as boundaries fractures that appear to

have been displaced or show as long continuous trends on the aerial photographs. Boundaries have also been chosen to provide approximately uniformly sized samples of fracture

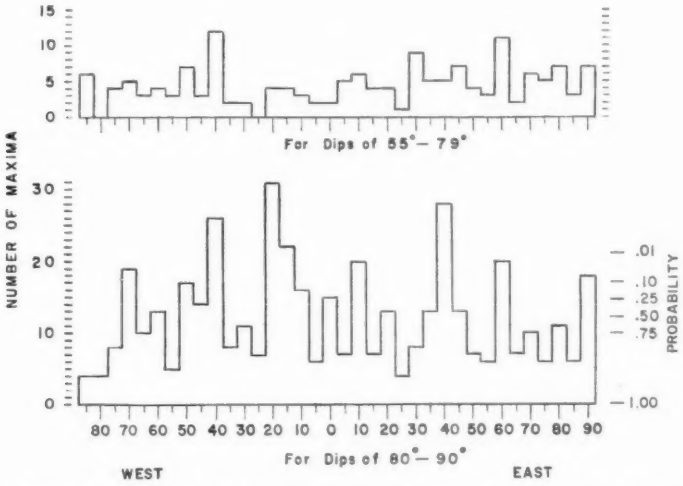

FIGURE 8.—MAXIMA FROM GROUND-FRACTURE DATA ON SOUTHWESTERN SLOPE

These histograms are based on the data used in Figure 5 for concentrations with dip co-ordinates of 55°–79° and 80°–90°. Molina's tables of the Poisson exponential binomial limit were used to evaluate the probability of having various numbers of maxima in a single class interval. The probabilities are based on variations from a uniform distribution.

measurements in each area, and a distribution of areas that makes it possible to compare central parts of the uplift with the margins.

Figure 9 shows histograms of mean fracture planes with dips more than 60° from all stations within each division of the southwestern slope; Figure 20 shows the same data on contoured point diagrams. The probability of finding various numbers of mean fracture planes within 1 of 36 5-degree intervals is indicated for each area. The actual probability is lower than indicated because the intervals are not independent. Where a single interval contains a large number of points, fewer points are available for other intervals. This reduces the probability that a second or third interval will have a large number of points. For this reason one should hesitate to consider as significant only concentrations above some arbitrarily selected level of probability.

Several areas have maxima that correspond to inclined mean fracture planes. Area *D* has N.45°E.-40°NW. and N.75°E.-60°NW.; area *E* has N. 76°W.-60°NE.; area *F* has N. 60°E.-60°NW.; area *I* has N. 78°W-50°SW. and N. 80°W.-60°NE.; area *J* has N. 55°E.-30°NW., N. 30°E.-60°NW., and N. 68°W.-50°NE. In areas *I* and *J* fractures with mean strikes between N. 40°W. and N. 20°E. tend to dip to the west and southwest. Since these directions ordinarily are vertical fracture trends, the block apparently has tilted down on the southwestern side. This is borne out by the presence of a known fault striking N. 40°W. along which the middle Cambrian Flathead sandstone has been vertically displaced more than 500 feet. This fault forms a prominent feature on the western side of areas *I* and *J*.

NORTHEASTERN SLOPE OF UPLIFT: Three summary point diagrams have been prepared for the northeastern slope, using mean fracture planes of all concentrations of 4 per cent plus, 6 per cent plus, and 9 per cent plus (Fig. 7). Few concentrations exceed 9 per cent at stations on the northeastern slope.

Most of the fracture trends on the southwestern slope are weakly developed on the northeastern slope. Directions indicated on the summary point diagrams (Fig. 7) of 4 per cent plus concentrations are in order of development: N. 45°W., N. 55°-60°E., N. 60°W., N. 10°-20°W. All these fractures are

nearly vertical. Inclined fracture concentrations appear at: N. 75°W.-75°NE., N. 80°W.-70°SW., N. 40°W.-25°NE., N. 25°W.-75°SW.,

Area *B* has no high maxima, but a number of poorly developed concentrations are apparent, including N.-S., N.10°W.-90°, N. 55°W.-

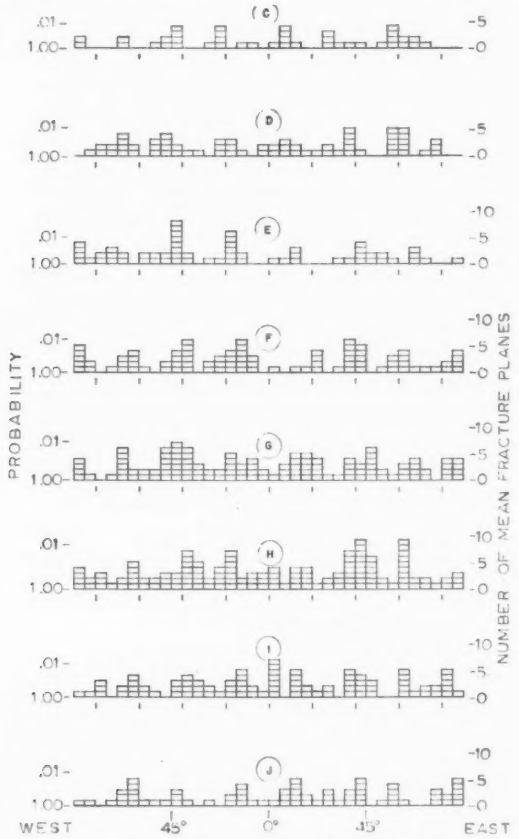

FIGURE 9.—SUMMARY OF GROUND MEASUREMENTS IN AREAS OF SOUTHWESTERN SLOPE

These histograms are based on the same data shown as contoured point diagrams on Figure 20. The probability of chance occurrence of concentrations of mean fracture planes in a class interval is indicated. The probability statement is based on variations from a uniform distribution and was evaluated by Molina's tables of the Poisson exponential binomial limit.

and N. 65°E.-60°NW. Concentrations above 9 per cent provide a simpler pattern, which consists of strong trends at: N. 60°E.-83°SE., N. 55°W.-90°, N. 40°W.-25°NE., and much weaker trends at N. 20°W.-90°, N. 85°W.-90°, N. 58°E.-66°NW., N. 13°W.-60°W., and E.-W.-30°S.

Area *A*, the western division of the northern slope, has four well-developed maxima: N. 69°W.-90°, N. 60°E.-90°, N. 10°E.-90°, and N. 20°W.-90°, and poorly defined maxima at N. 45°W.-70°NE., E.-W.-70°S., N. 40°E.-40°SE., and N. 20°E.-20°NW.

15°NE., N. 85°W.-60°NE., N. 60°E.-55°SE., N. 25°W.-70°SW., and other weaker directions.

SUMMARY OF RESULTS: Comparison of summary point diagrams and histograms (Figs. 6, 8) with summary diagrams for each of the 10 subdivisions of the uplift (Figs. 9, 20) reveals the existence of a remarkably uniform fracture pattern on the southwestern slope of the range. The best-defined trends are N. 15°-20°W., N. 40°-45°W., N. 40°-45°E., and N. 60°-70°W. A similar fracture pattern, but weakly developed and accompanied by low-dipping fractures, is found on the northeastern

slope. Individual outcrops have complex fracture patterns similar to the summary point diagrams for the uplift. A single station may have indications of as few as three, or as many as seven fracture trends. No preferred grouping

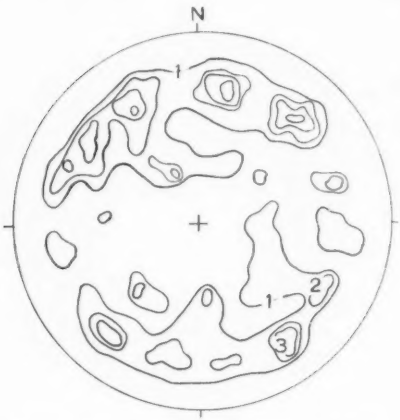

FIGURE 10.—MEAN FRACTURE PLANES WITH DIPS UNDER 75°

This point diagram represents 220 mean fracture planes plotted on the upper hemisphere of a Schmidt net. Contours are for 1, 2, 3, and 4 per cent. All the concentrations fall along strike directions of vertical fracture trends.

of trends is evident at individual outcrops. At Question Mark Lake, fracturing on each block separated by the intersection of major fracture zones is variable. Variations between stations on the same block are as great as variations between stations on different blocks.

FRACTURE PATTERNS FROM AERIAL PHOTOGRAPHS

Area Studied

Aerial photographs of the Beartooth Mountains reveal two strikingly different physiographic parts: a northern and eastern part characterized by deep U-shaped glacial valleys, separated by extensive featureless plateaus representing the Precambrian peneplaned surface, and a southern and western portion characterized by prominent fractures and shear zones, accentuated by glaciation and stream erosion. The two areas are separated by the Continental Divide. No fracture pattern is clearly shown on photographs of the northeastern slope. Therefore, photographs of the southwestern slope only are used. A study of the patterns of deformation on the northeastern slope is in progress.

Sources of Error

The following are possible sources of error in a study of linear features on aerial photographs:

(1) Errors in taking and enlarging photographs. Tilt of camera or enlarger causes distortion of linear features. Distortion is accentuated toward margins of photographs, particularly in areas of high relief. Relief of the southwestern slope is more than 4000 feet in areas covered by some photographs.

(2) Errors in location of north-south lines. If mistakes are made in the location of this line, all trends determined with respect to the line are wrong.

(3) Errors in recognition and selection of fractures. All the fracture zones have been weathered and eroded. In many places where two or more of these zones intersect at small angles, a flat swampy area is found (Pl. 1, 2). Errors might be made in matching features on opposite sides of the valleys. Linear features that might be misinterpreted as fractures include glacial markings, weathering along foliation that trends N.-S.-N. 15°E. throughout most of the uplift, and consequent stream valleys.

(4) Errors in measurement of fractures. Short fractures are difficult to measure accurately and are likely to represent inclined

---

PLATE 1.—FAULTS AND FRACTURES AROUND GRANITE LAKE AND FRACTURES EAST OF BEARTOOTH BUTTE

FIGURE 1.—Faults and fractures around Granite Lake. A number of major shear zones are shown. The southern corner of one of the large blocklike areas which have been tilted is located at the northern end of of Granite Lake.

FIGURE 2.—Fractures east of Beartooth Butte. A comparison of ground measurements at two stations with fractures from aerial photographs of the same area. Point diagrams represent 100 measurements each plotted on the upper hemisphere. The point diagrams are contoured on poles perpendicular to the fracture planes.

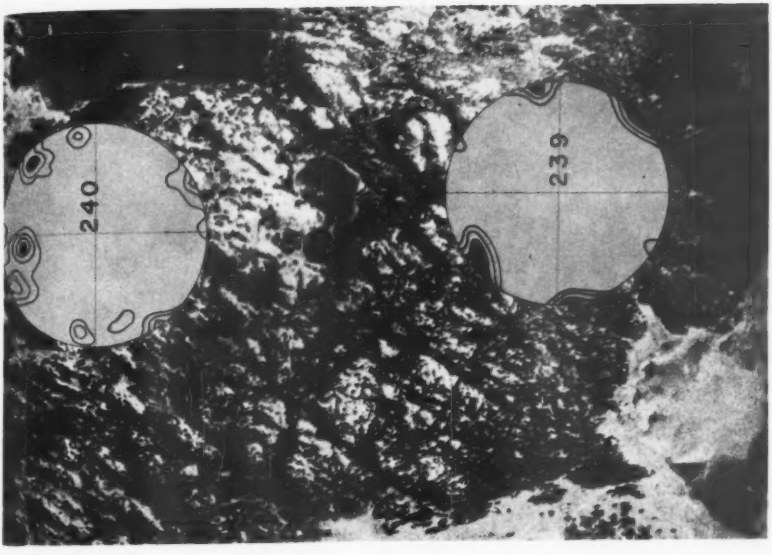

FIGURE 2

N

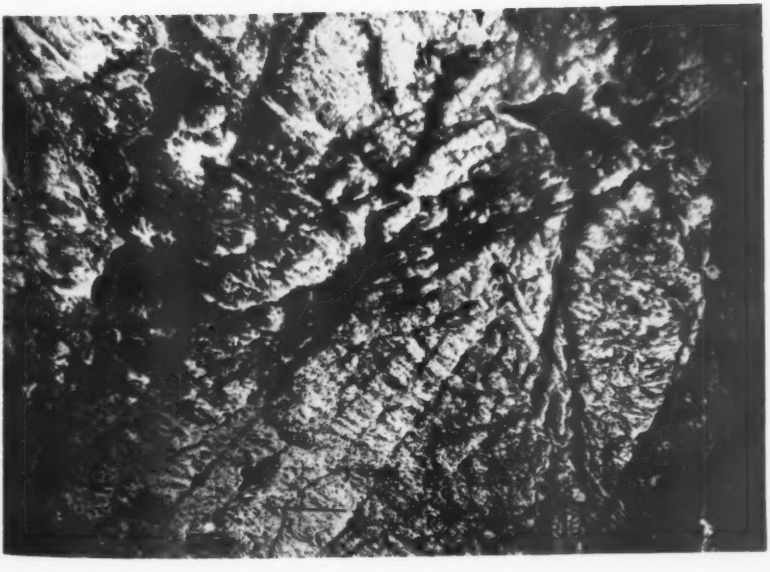

FIGURE 1

FAULTS AND FRACTURES AROUND GRANITE LAKE
AND FRACTURES EAST OF BEARTOOTH BUTTE

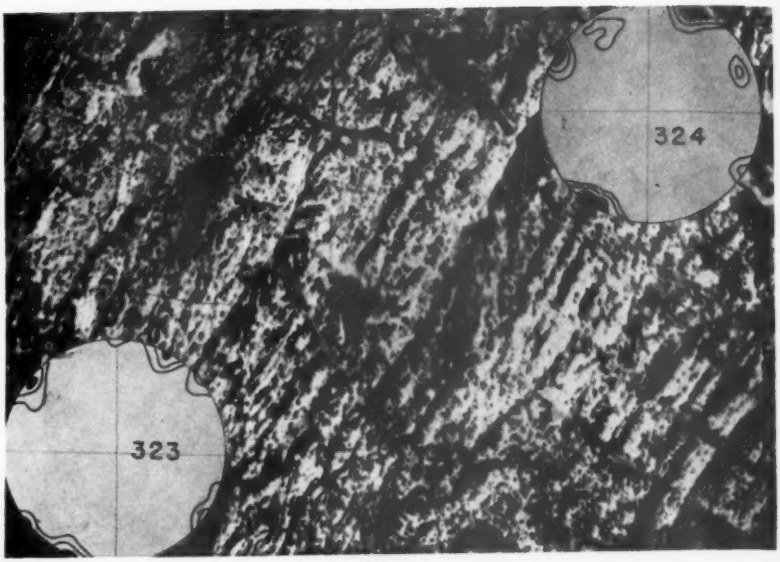

FIGURE 1

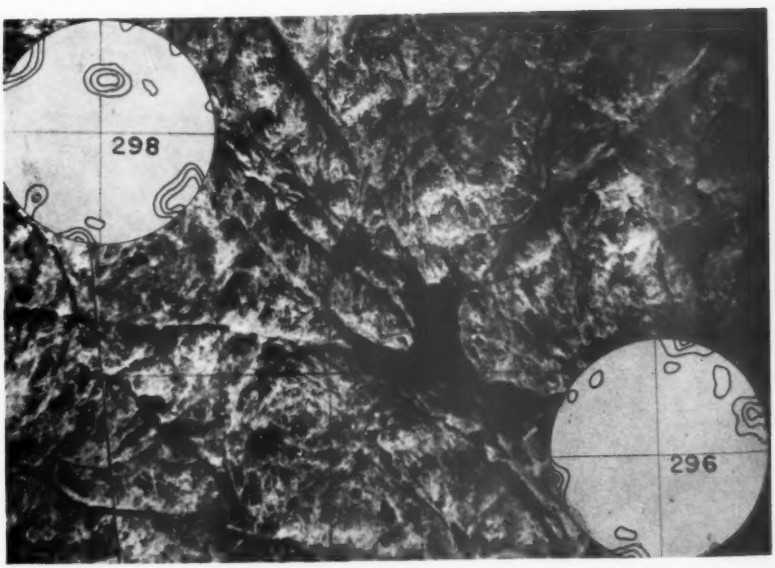

FIGURE 2

FRACTURES SOUTH AND NORTH OF JORDAN LAKE

fractures, exposed on sloping surfaces. Probably the greatest source of error in the measurements lies in differences in strike of inclined fractures, caused by irregular relief. Slightly curved, long fractures must be considered either as series of shorter, straight fractures, or a general trend must be measured. Since many long, irregular fractures are found to consist of many shorter fractures, they have been measured as series of shorter, straight lines. The data have been weighted according to length in most plots; therefore, breaking a long fracture into shorter ones does not create false maxima.

(5) Insufficient data. An insufficient number of fractures may have been measured. In this study an attempt has been made to measure all lineaments that might be fractures. A total of 3560 lineaments was measured. It is estimated that 2000 measurements would have been adequate for this study.

(6) Effects of erosion. Fractures shown on aerial photographs owe their prominence to weathering and erosion. Fractures that are oriented in the direction of glacier movement or strike downslope will appear more prominent on aerial photographs.

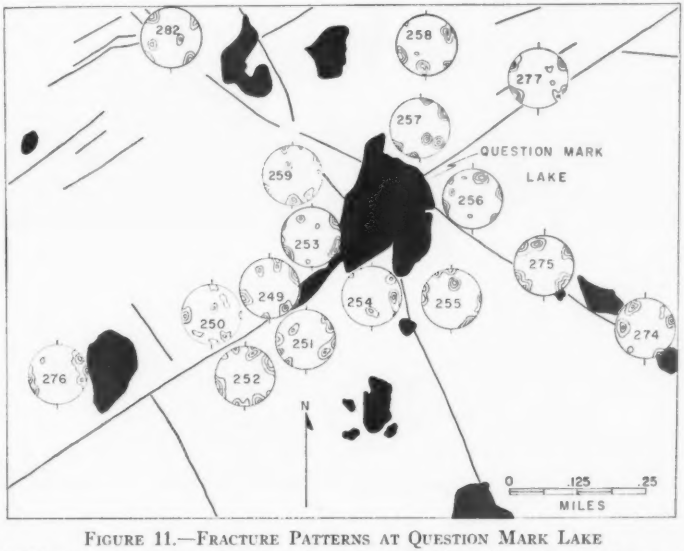

FIGURE 11.—FRACTURE PATTERNS AT QUESTION MARK LAKE

A total of 100 measurements are plotted on the upper hemisphere for each point diagram. The lowest contour is 4 per cent, and the contour interval above that level is 2 per cent. Major fracture zones are indicated by solid lines.

Methods of Study

For this study aerial photographs taken by the U. S. Geological Survey were enlarged to a scale of approximately 1:7800. The photographs were checked for marginal distortions by placing a transparent acetate overlay in the center of one photograph from which fractures were traced. The overlay was then transferred to the adjacent photograph, oriented

PLATE 2.—FRACTURES SOUTH AND NORTH OF JORDAN LAKE

FIGURE 1.—Fractures south of Jordan Lake. A comparison of ground measurements at two stations with fractures from aerial photographs of the same area. One hundred measurements are plotted on the upper hemisphere in each point diagram. The lowest contour is 4 per cent.

FIGURE 2.—Fractures north of Jordan Lake. A comparison of ground measurements at two stations with fractures from aerial photographs of the same area. Point diagrams are contoured on 100 measurements plotted on the upper hemisphere. The lowest contour is 4 per cent and the contour interval is 2 per cent.

using the north-south line, and the same fractures again traced on the overlay. This allowed direct comparison of the same area with minimum and maximum distortion. Most

every lineament more than an eighth of a mile long was measured. A total of 3560 lineaments was measured, and their average length was five-sixteenths of a mile. The second set of

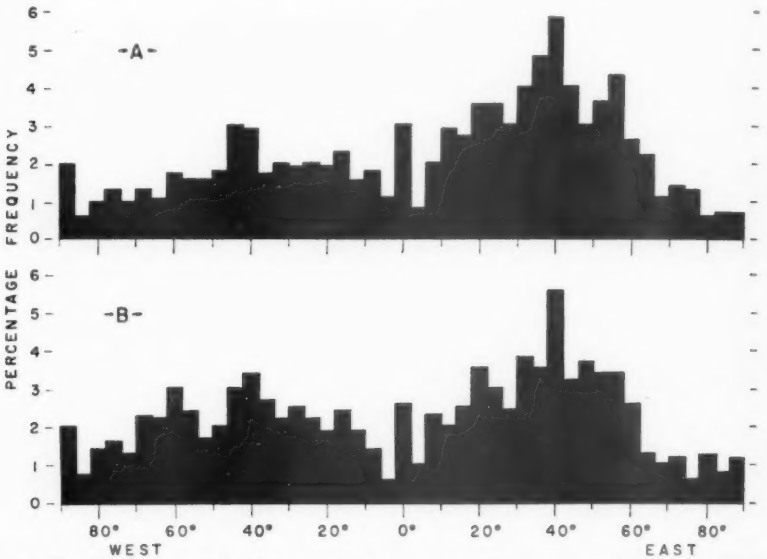

FIGURE 12.—HISTOGRAMS OF ALL LINEAMENTS IDENTIFIED AS FRACTURES ON AERIAL PHOTOGRAPHS

A, a total of 2100 fractures ⅛ mile long or longer are plotted in 4-degree intervals. B, a histogram of the same data weighted according to the length of each fracture. Each fracture is assigned a value equal to its length in ⅛-mile units.

directions of fractures were the same within 2°–3°, but in areas of high relief distortion increased to 5°–10°. No attempt has been made to allow for this distortion. However, fewer measurements were made in areas of high relief (more than 2000 feet), because fractures are not clearly indicated in such areas.

North-south lines were located on the photographs, using U. S. Geological Survey preliminary topographic maps of the Nye, Crandall 1, and Crandall 2 sheets. Several determinations of north were made for each photograph by taking the azimuths of features in different parts of the photographs and using the average value obtained for north. Generally, features at approximately the same elevation were chosen for north-south azimuth determinations.

Two sets of measurements of lineaments on the aerial photographs were made. For the first set of measurements the southwestern slope was divided into areas (the same areas used in analyzing ground measurements), and measurements included only lineaments that had been identified as fractures or faults. A total of 2100 such fractures an eighth of a mile long or longer were measured.

Both sets of data are plotted as histograms showing the percentage frequency of the total number of lineaments falling in each class interval irrespective of length, and a percentage frequency of the total number of lineaments weighted according to length (Figs. 12, 13). Since special structural significance may be attached to long fractures or faults, histograms have been prepared showing the number of fractures half a mile and 1 mile long or longer (Fig. 14). The data for the long fractures is part of the second set of measurements.

Observed Patterns

The following observations may be made from a visual comparison of the histograms in Figures 12, 13, and 14.

(1) The strongest developed direction on

photographs for both long and short fractures is a general northeast trend, centered at N. 40°-45°E.

directions among the shorter fractures (Figs. 12, 13) and is well indicated in the longer ones (Fig. 14) but at a lower concentration.

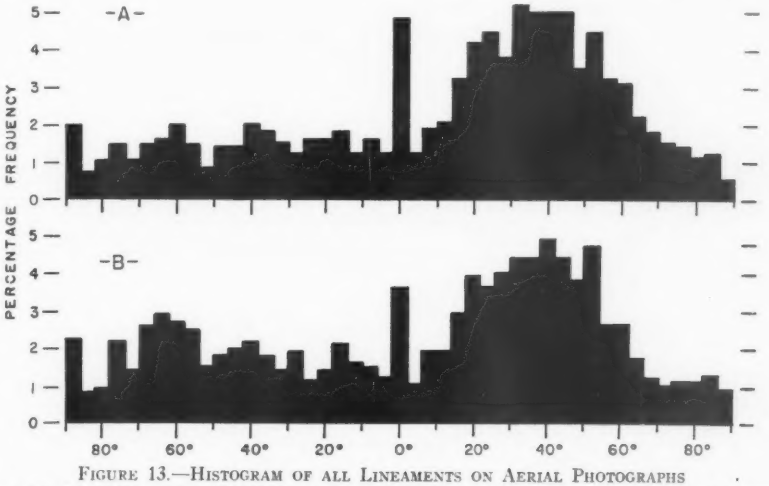

FIGURE 13.—HISTOGRAM OF ALL LINEAMENTS ON AERIAL PHOTOGRAPHS

A, a total of 3560 lineaments ⅛ mile long or longer are plotted in 4-degree intervals. B, a histogram of the same data weighted according to the length of each fracture. Each fracture is assigned a value equal to its length in ⅛-mile units.

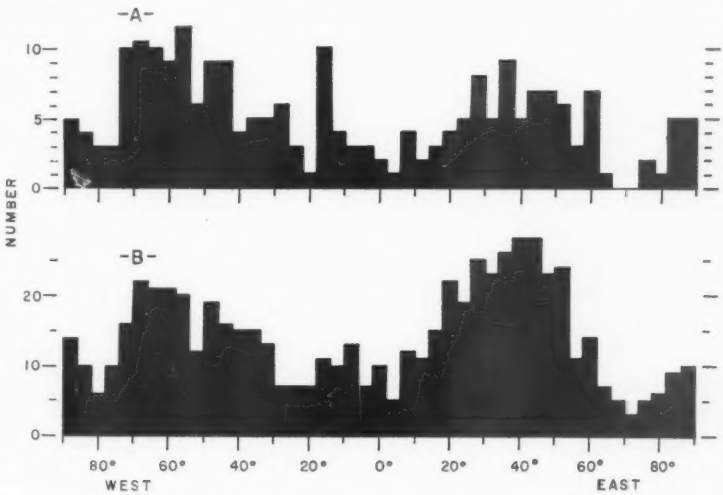

FIGURE 14.—HISTOGRAMS OF LONG LINEAMENTS KNOWN TO BE FRACTURES

A, the number of fractures 1 mile or more long is plotted in 4-degree class intervals. B, the number of fractures half a mile or more long is plotted in 4-degree intervals.

(2) The second most prominent direction is at N. 60°-70°W. This trend is more pronounced in the longer fractures (Fig. 14) than in the shorter ones (Fig. 13).

(3) N. 40°-45°W. is one of the best-developed

(4) A consistent E.-W. trend is shown by both long and short fractures. It is not represented by unusually high peaks but stands well above the saddles on either side.

(5) N. 15°W. is a high, well-defined peak

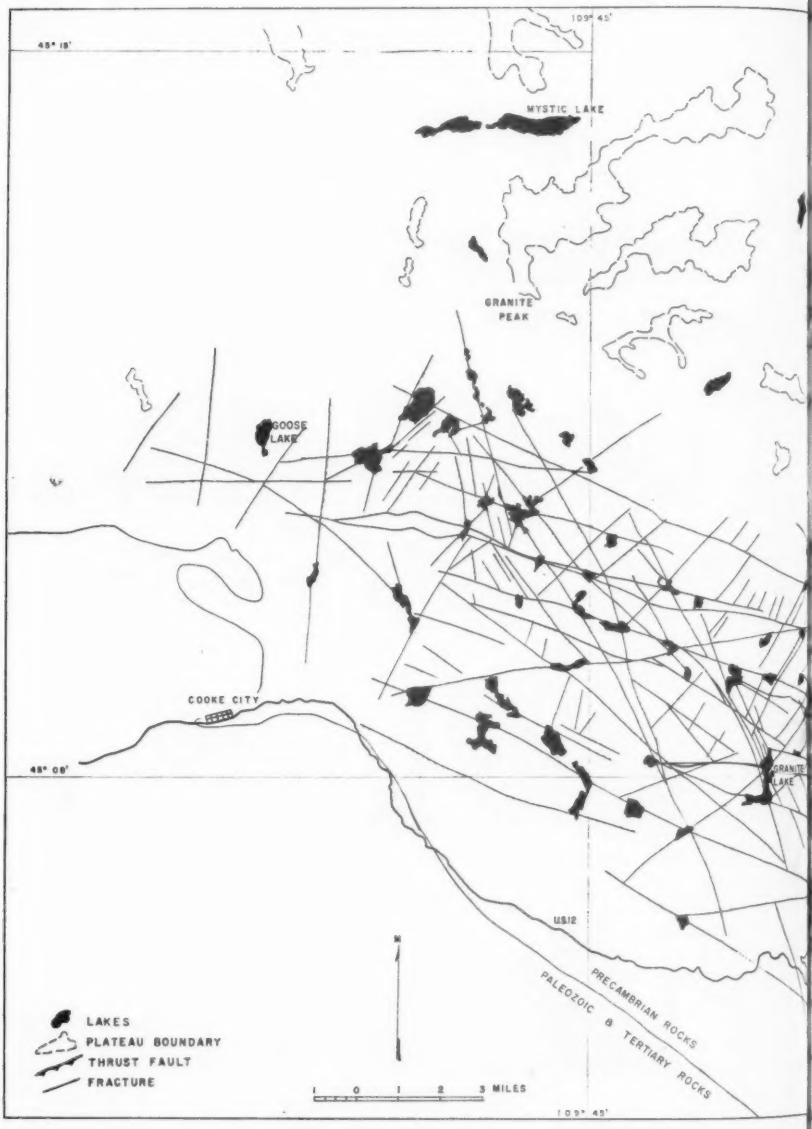

FIGURE 15.—MAJOR FRAC

for the longest fractures (Fig. 14) and is clearly outlined in the weighted data of all lineaments (Fig. 13). It is weakly indicated and surrounded by smaller peaks on the frequency diagrams.

(6) N. 15°-20°E. appears to be a separate high on the side of the major northeast trend and is well defined in studies of the short fractures and those half a mile long; it is not shown when only long fractures are considered.

(7) N. 50°-60°E. is fairly well defined among the longer fractures (Fig. 14). On histograms of all lineaments a high is located at N. 55°E.,

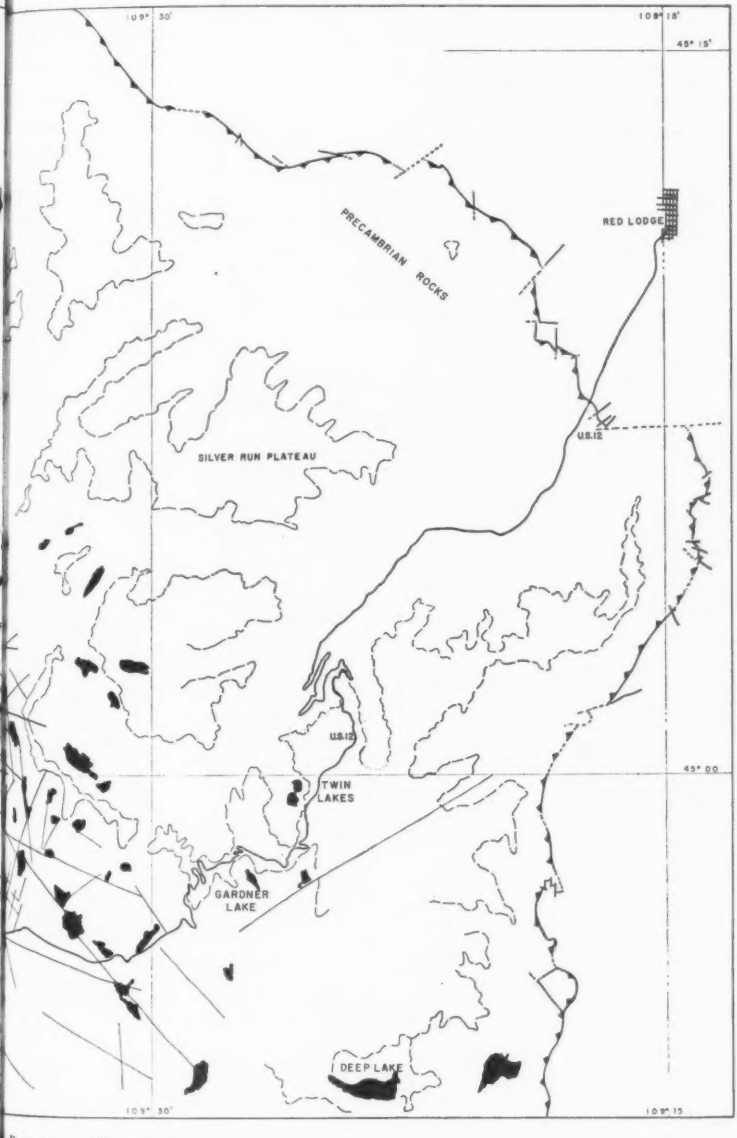

BEARTOOTH UPLIFT

separated from the general northeast trend by a saddle. On the frequency histogram of definite fractures this direction is well shown and is separated by a deep saddle from N. 40°E.

(8) A N.-S. trend is the last important direction. It is one of the highest peaks on the histogram of all lineaments (Fig. 13) and the graph of definite fractures (Fig. 12) but is a very weak peak when long fractures only are considered.

Divisions of the Southwestern Slope

Figure 16 shows a series of rose diagrams of all lineations measured for six of the eight areas, weighted according to lengths of lineaments. The weighting is done by counting as a unit each ⅛-mile length of a fracture. These diagrams are characterized by: the presence of two or more strong peaks, lack of uniformity in development of the same direction in different areas, and many small irregularities. The lack of uniformity in development of trends may be partly due to differences in size of samples, which is determined by how clearly fractures show on the photographs. Area *G* is below timber line, and smaller fractures are not apparent on the photographs. Area *F* is partly timbered, but the other areas are above timber line. The effects of glaciation and drainage in etching out fracture zones are hard to evaluate. The general movement of ice was toward the south-southwest over most of the southwestern slope, but there were local variations, as at Beartooth Butte. Another possible explanation for differences in development of the trends is that well-developed directions are those along which repeated deformation has been most intense. This would result in zones of weakness that would weather out

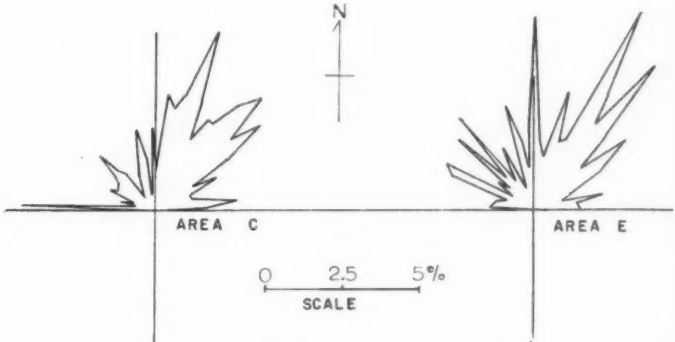

FIGURE 16.—ROSE DIAGRAMS OF LINEAMENTS IN EACH AREA ON AERIAL PHOTOGRAPHS

All lineaments over ⅛ mile long are represented. Each lineament is weighted according to length in ⅛-mile units. Percentages of all measurements within each area are plotted on a radial linear scale. Total number of units for each area is: *C*, 2070; *E*, 1250; *F*, 3225; *G*, 640; *H*, 1110; and *I*, 1400.

TABLE 3.—FRACTURE TRENDS ASSOCIATED WITH THE NORTHWEST TREND

Station Number	Directions						
201	85°W.	70°W.	.....	.....	.....	45°E.	.....
204	.....	.....	20°W.	.....	.....	45°E.	75°E.
205	85°E.	.....	.....	.....	20°E.	.....	.....
208	.....	.....	.....	.....	.....	.....	60°E.
210	.....	65°W.	.....	.....	10°E.	.....	70°E.
211	.....	.....	20°W.	.....	.....	.....	70°E.
215	E.W.	.....	.....	.....	15°E.	.....	75°E.
216	80°W.	.....	25°W.	5°E.	.....	45°E.	60°E.
220	E.W.	70°W.	15°W.	.....	10°E.	.....	.....
227	.....	60°W.	10°W.	.....	20°E.	40°E.	60°E.
229	.....	70°W.	.....	.....	10°E.	45°E.	.....
234	.....	60°W.	20°W.	.....	.....	.....	60°E.
235	.....	.....	20°W.	.....	10°E.	45°E.	.....
240	80°E.	.....	15°W.	.....	10°E.	.....	.....
242	E.W.	.....	.....	.....	.....	.....	.....
243	85°W.	.....	15°W.	.....	.....	35°E.	60°E.
245	.....	65°W.	.....	.....	.....	30°E.	.....
246	.....	.....	.....	.....	.....	35°E.	.....
251	.....	.....	20°W.	5°E.	.....	35°E.	.....
254	80°E.	.....	.....	5°E.	.....	30°E.	.....
257	.....	70°W.	.....	.....	10°E.	35°E.	.....
261	.....	60°W.	20°W.	N.S.	.....	45°E.	70°E.
268	.....	.....	.....	.....	.....	30°E.	.....
271	85°E.	70°W.	20°W.	N.S.	.....	40°E.	.....
273	E.W.	.....	.....	N.S.	.....	30°E.	.....
274	.....	.....	20°W.	N.S.	.....	.....	60°E.
288	.....	60°W.	.....	N.S.	.....	45°E.	.....
289	.....	70°W.	20°W.	.....	.....	30°E.	.....
290	.....	60°W.	.....	N.S.	.....	.....	.....
291	.....	.....	.....	.....	.....	40°E.	.....
293	.....	75°W.	20°W.	.....	.....	35°E.	70°E.
295	E.W.	.....	.....	.....	.....	45°E.	60°E.
296	.....	75°W.	15°W.	.....	.....	45°E.	.....
297	.....	.....	20°W.	.....	10°E.	35°E.	.....
298	80°W.	.....	15°W.	.....	.....	40°E.	.....
300	85°E.	.....	.....	.....	.....	30°E.	.....
303	E.W.	70°W.	15°W.	.....	.....	40°E.	60°E.
307	E.W.	60°W.	20°W.	.....	15°E.	.....	.....
312	E.W.	70°W.	15°W.	.....	.....	40°E.	.....
313	80°E.	70°W.	20°W.	.....	20°E.	.....	65°E.
314	80°E.	70°W.	.....	.....	15°E.	.....	.....
315	85°E.	.....	10°W.	.....	.....	40°E.	.....
316	80°E.	60°W.	10°W.	.....	.....	.....	60°E.
317	.....	.....	15°W.	.....	.....	.....	60°E.
318	85°E.	.....	20°W.	5°E.	.....	30°E.	55°E.
319	E.W.	.....	.....	.....	10°E.	35°E.	60°E.
323	.....	65°W.	.....	.....	.....	40°E.	.....
326	E.W.	.....	.....	.....	20°E.	.....	.....
330	85°W.	.....	.....	.....	20°E.	.....	60°E.
332	E.W.	.....	20°W.	.....	.....	45°E.	.....
334	E.W.	.....	10°W.	.....	.....	.....	60°E.
339	E.W.	.....	20°W.	.....	.....	.....	70°E.
340	.....	70°W.	.....	5°E.	.....	.....	70°E.
341	.....	.....	10°W.	.....	.....	40°E.	60°E.
343	.....	.....	.....	.....	10°E.	35°E.	70°E.
345	85°E.	70°W.	15°W.	.....	20°E.	.....	.....
346	.....	65°W.	20°W.	.....	.....	.....	60°E.

more rapidly. Probably a combination of these causes is responsible for the observed variations.

Small irregularities in each diagram pose a serious problem to the interpretation of fractures from aerial photographs. Two peaks are in many cases within 10° of one another; yet, the 160 fracture stations located on the ground do not indicate the presence of two unrelated maxima within 10° of one another, and only a few stations have maxima within 15°. The lower peaks cannot be disregarded, because many correspond to well-defined maxima shown by ground measurements. Most of these irregularities are thought to result from measuring fractures with dips less than 80° which cut across sloping topography. The more prominent trends for each of the six areas (Table 4) are characterized by high peaks, symmetrical development, or both.

TABLE 4.—PROMINENT TRENDS ON PHOTOGRAPHS IN DIVISIONS OF SOUTHWESTERN SLOPE

Fracture trends are indicated by peaks on the rose diagrams (Fig. 16) for six of the divisions of the southwestern slope. Areas C-I are shown in Plate 3. Areas on the northeastern slope are not considered because few fractures are indicated on photographs of those areas. Two areas of the southwestern slope have been omitted because the samples are not of comparable size.

Area	Directions						
C	E.-W.	.....	45°W.	10°-20°W.	20°E.*	40°-50°E.*	.....
E	.....	.....	.....	.....	N.-S.*	30°-40°E.*	.....
F	.....	55°-60°W.*	.....	.....	.....	30°-40°E*	.....
G	E.-W.*	55°-60°W.*	.....	10°W.*	N.-S.*	30°-50°E.	.....
H	.....	65°W.*	30°-40°W.	.....	.....	35°E.*	65°E.*
I	.....	65°W.*	30°-40°W.*	.....	.....	45°E.	.....

* represents a high peak

Summary of Results

Comparison of the subdivisions of the southwestern slope shows that recognition of all the nearly vertical fracture directions indicated by aerial photographs alone would lead to indefinite conclusions. The evidence does, however, corroborate findings of ground measurements. The most prominent fracture trends are N. 15°-20° W., N. 45° W., N. 45° E., and N. 60°-70° W. Other less consistent trends are at E.-W.-N. 85° E., N. 60° E., N.-S.-N. 10°E., and N. 15°-25° E.

COMPARISON OF GROUND AND AERIAL-PHOTOGRAPH MEASUREMENTS

GENERAL STATEMENT: Among the shortcomings of using only ground measurements are inability to distinguish major from minor joints and widely spaced from closely spaced joints. Sets of data from aerial photographs and ground measurements may be correlated in three ways:

(1) Fracture trends at a single outcrop may be compared with fractures or lineaments on aerial photographs of the area around the outcrop.

(2) Summary diagrams of the two sets of data may be compared for subdivisions of the entire area.

(3) Summary diagrams of the two sets of data for the entire area may be compared.

As the size of the area considered increases, not only does the size of the sample increase but also the chances of including more divergent structures.

INDIVIDUAL STATIONS COMPARED WITH AERIAL PHOTOGRAPHS: Three widely separated areas containing two fracture stations within a quarter of a mile have been selected to compare individual stations with photograph lineaments. The areas selected have well-developed fracture patterns (Pls. 1, 2). The areas are just east of Beartooth Butte, several miles northwest of Beartooth Butte near Jordan Lake and farther north.

All three of these areas have fracture patterns that appear as uniformly developed lineaments on the aerial photographs. The pattern consists of three or four obvious directions and several more faintly indicated trends. A remarkably good correlation is found between ground measurements and fractures on photographs in the immediate vicinity of the station. Generally only one or two parallel major lineaments occur for a single direction within a short distance of a station. Thus, the

size of the sample available for comparison is small.

If other lineaments not in the immediate vicinity of the station are included, 10°–15° deviations from initially measured trends are common.

Other trends indicated are N. 55°-60° E., N. 85° E-E.W, and N.S-N. 20°E. which is the trend of foliation and the direction of ice movements over most of the area.

TABLE 5.—GROUND MEASUREMENTS COMPARED WITH PHOTOGRAPH MEASUREMENTS

Plate 3 shows location of areas and summaries of ground data. *See* Figures 6, 7, 9 for photograph measurements. The sample of photograph measurements in areas D and J is small, and these areas have not been considered here.

Area	Directions							
C	85°E.	65°W.?	45°W.*	20°W.*	10°E.	35°E.	65°E.*	ground
	E.-W.*	.....	45°W.*	15°W.*	20°E.*	45°E.*	65°E.	photographs
E	85°W.	70°W.	40°W.*	20°W.*	10°E.	45°E.*	65°E.	ground
	.....	65°W.*	45°W.	15°W.	10°E.*	35°E.*	60°E.	photographs
F	E.-W.*	65°W.*	40°W.*	15°W.*	20°E.?	40°E.*	55°E.	ground
	E.-W.	65°W.*	35°W.	18°W.	20°E.*	40°E.*	55°E.	photographs
G	88°E.*	65°W.	40°W.*	15°W.*	20°E.	45°E.*	60°E.	ground
	E.-W.*	60°W.*	30°W.?	10°W.?	15°E.	35°E.*	50°E.	photographs
H	86°W.?	55°W.	40°W.*	15°W.*	10°E.	40°E.*	60°E.?	ground
	E.-W.	65°W.*	35°W.*	20°W.?	N.-S. to 20°E.*	35°E.*	60°E.*	photographs
I	82°E.	60°W.?	40°W.	20°W. *	5°W.-10°E.	40°E.*	60°E.	ground
	85°W.*	65°W.*	35°W.*	15°W.?	20°E.*	40°E.	60°E.	photographs

* Well-defined trends
? Questionable trends

COMPARISON OF AREAS ON SOUTHWESTERN SLOPE: The results of comparison of peaks on the rose diagrams for photograph measurements with mean fracture planes from the summary point diagrams for each subdivision of the southwestern slope are tabulated in Table 5.

Degree of development of trends as shown on the rose diagrams is so irregular that no consistency in fracture patterns from one area to another would be suspected if an interpretation were based solely on them. Most directions that are strongly developed on the ground are well developed on the aerial photographs. In no case does a trend represented strongly on either the photographs or the ground fail to appear in the other set of data.

COMPARISON OF SUMMARY DIAGRAMS: A summary histogram of ground fracture measurements (Fig. 8) indicates three very well-developed trends: N. 15°-20° W., N. 40°-50° W., and N. 40°E. A fourth trend, N. 60°-70° W., is shown in the summary of ground measurements, and its importance as a major trend is confirmed by the photographs, which show that it is the most prominent trend of lineaments more than 1 mile long (Fig. 14).

Histograms summarizing the photo measurements (Figs. 12, 13, 14) have one consistent, high, and well-developed peak, N. 40°-45° E. The best defined peak for long fracture zones is N. 60°-70°W. The third, most consistent, trend is N. 40°-50°W. Other trends indicated on one or more of the histograms as having some possible significance are: E.-W., N. 15°-20°W., N. 20°E., N. 50°-60°E., and N.-S.

USE OF AERIAL PHOTOGRAPHS: Fracture measurement in the field is a time-consuming and tedious task; if aerial photographs revealed the same fracture patterns as ground measurements, much time and effort could be saved. The following conclusions of this study related to this question are:

(1) Only fractures with steep dips give reliable results on aerial photographs, unless dip of fractures can be accurately determined.

(2) In detail, photograph measurements of large fractures give a reliable picture of ground-fracture data for vertical fractures, but the possibility of overlooking on photographs lineaments that are fractures is great. In several cases, lineaments would have been overlooked or would not have been considered evidence of fractures if ground data had not been available.

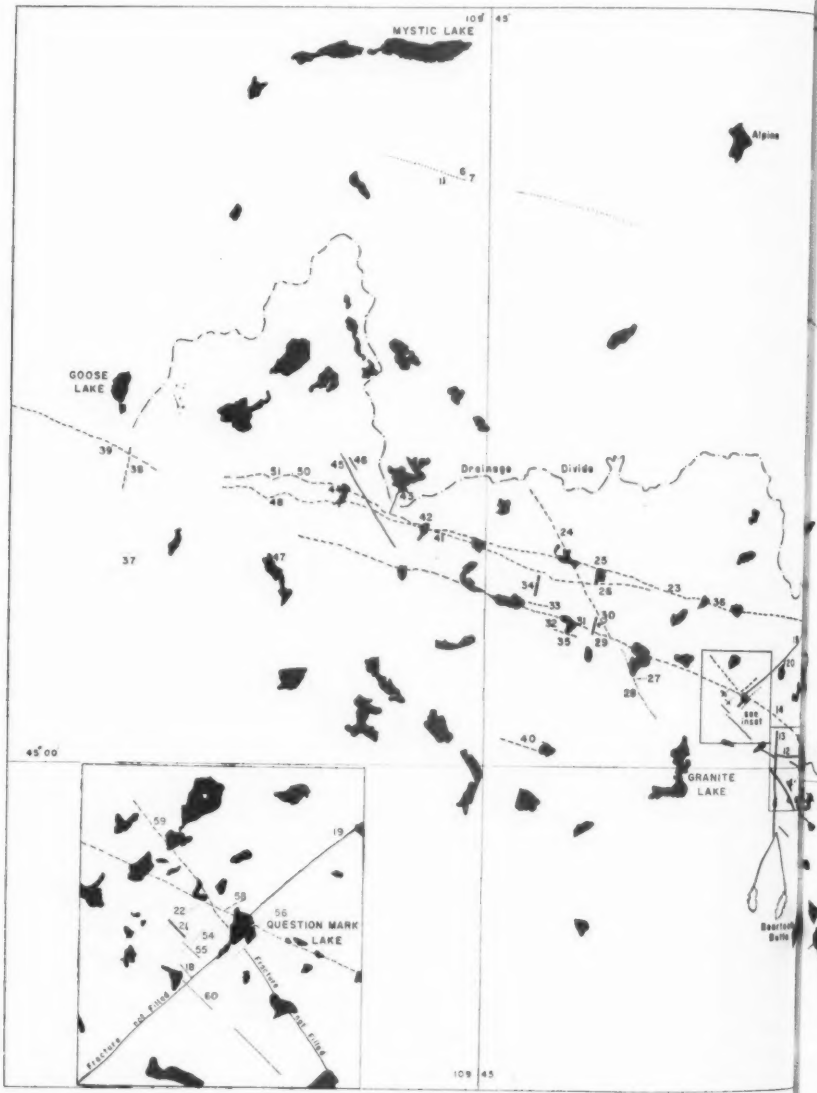

FIGURE 17.—DIKES IN EAST

(3) As the area in which measurements are made is increased, more irregular results are obtained.

(4) Photograph measurements of lineaments indicate approximately the same directions, whether length is taken into account or not; however, special geologic significance may be attached to long fractures. Long fractures are more reliable if the number of measurements is low.

(5) If a large sample of photograph measurements can be made (at least several thousand), irregularities due to error in measurement of trends are minimized, and results more nearly consistent with ground measurements are obtained. The larger sample also

RAL PARTS OF BEARTOOTH UPLIFT

minimizes the effect of irregular fracture trends due to local boundary conditions.

RELATIONS OF FRACTURES TO OTHER STRUCTURES

Fracture Pattern and Dikes

GENERAL STATEMENT: Large dikes are conspicuous on aerial photographs of the southwestern slope of the uplift. A few dikes are continuous for more than 15 miles, and most of the larger dikes can be traced for a mile or more. Rae L. Harris (Personal communication, 1957) mapped several smaller dikes which are disrupted and have irregular outcrops. This may be caused in part by their low dip and the rugged topography. Dikes of different ages are found in the uplift, and trends of the

various groups of dikes provide the best indication of the age of the fracture patterns.

PETROGRAPHIC DESCRIPTIONS AND AGE RELATIONS: Work under the Beartooth project resulted in the recognition of four major groups of basaltic and metabasaltic dikes. A fifth group consists of felsic porphyry dikes.

Criteria for recognition of the different groups of dikes are:

Group 1. Archean, pregranitization orthoamphibolite dikes. These dikes cut the compositional foliation of the granitic gneisses. Principal minerals are plagioclase, hornblende, quartz, and opaque ore. Accessory minerals include biotite, sphene, and epidote. Possibly the dikes have been emplaced before granitization, but more study is needed to establish that they are not highly altered dikes of group 2.

Group 2. Archean metabasaltic dikes, penecontemporaneous with granitization. All the dikes of this group have been metamorphosed, but generally they cut the pegmatites. They include iron-rich metadolerites, metadolerites, olivine-bearing metadolerites, metanorites, and metapicrites. They are distinguished from later dikes by the presence of clouded plagioclase and bronzite, coronas of bronzite around olivine, whereas augite is partly or wholly recrystallized to granular aggregates of hypersthene, hornblende, diopside, or salite.

Group 3. Late Precambrian quartz dolerite. Main constituents are plagioclase, pigeonite, augite, opaque ore, and interstitial quartz and micropegmatite. Hornblende and biotite are accessories.

Group 4. Tertiary olivine dolerites. Principal minerals are plagioclase, olivine, purple titanaugite, opaque ore, and mesostasis. The rocks are remarkably fresh.

LARAMIDE FELSIC PORPHYRY DIKES: These have been described in detail by Rouse *et al.* (1937). The dikes cut Mesozoic sediments along the northern margin of the Beartooth uplift. Many are more than 50 feet thick and several miles long. The felsic porphyry intrusions coincide with zones of greatest Laramian deformation; they are most common along the overthrust margins of the uplift and on the northeastern slope but rare on the southwestern slope. However, north of Cooke City, Montana, Laramian and Tertiary intrusives are abundant (Lovering, 1929).

The minimum age of groups 1, 2, and 3 is established by an erosional unconformity that truncates dikes belonging to these groups and is overlain by middle Cambrian Flathead sandstone. The age of group 4 dikes has not been established. They cut dikes of the first three groups but have not yet been found cutting Paleozoic strata. The writer found cross-cutting relationships that confirm earlier groupings.

TABLE 6.—TRENDS OF DIKES

Group	No. of dikes	Approximate lengths (miles)	Trend
1	3	<1	E.-W. to N. 85°E.
	1	Several	N. 75°W.
	1	2	N. 30°W.
	3	<1	N. 40°-45°E.
2	3	<1	N. 65°-70°W.
	2	>12	N. 60°-70°W.
	1	3	N. 60°W.
	2	1	E.-W. to N. 85°E.
	3	2	N. 60°-65°E.
	1	1	N. 60°E.
	5	Several	N. 30°-45°W.
	1	1	N. 20°W.
	1	1	N. 10°E.
	1	1	N. 45°E.
3	1	2	N. 80°W.
	6	1–3	N. 60°-70°W.
	1	1	N. 50°W.
	8	1–3	N. 30°-45°W.
	1	3	N.-S.
	3	1	N. 30°-35°E.
	1	3	N. 50°E.
	1	1	N. 60°E.
4	2	1	N. 10°E.
	1	1	N. 60°W.
	1	1	N. 45°W.

DIKE TRENDS: All the dikes appear to have been intruded along pre-existing fractures. Larger dikes parallel major fracture trends, and small offshoots conform to fractures in the granitic gneiss.

Eckelmann and Poldervaart (1957) took 89 measurements on mafic dikes in the Quad Creek area. Concentrations of vertical dikes are found at N. 45°-50°W. and N. 20°E. Two other concentrations are at N. 5°E-80°W. and N. 65°E.-75°SE. A plot of 89 readings shows a concentration of vertical dikes at N. 15°–20°W., and three maxima for inclined dikes at N.

40°E-50°NW., N. 15°W.–40°NE., and N. 25°E.–60°SE. The larger and longer porphyry dikes trend N. 60°W.

Dikes studied by the writer are shown on Figure 17. Locations of specimens are indicated by numbers. Most of the dikes are more than 1 mile long. Table 6 gives the number of dikes; approximate lengths and trends for each group of mafic dikes are shown in Figure 17.

Group 1 dikes trend E.-W., N. 75°W., N. 30°W., and N. 40°E. Group 2 dikes trend E.-W., N. 65°W., N. 30°-45°W., N. 20°W., N. 10°E., N. 45°E., and N. 60°E. Group 3 dikes trend N. 80°W., N. 60°-70°W., N. 30°-45°W., N.-S., N. 30°-40°E., and N. 60°E. Group 4 dikes trend N. 60°W., N. 45°W., and N. 10°E.

The existence of dikes that are penecontemporaneous with, if not older than, granitization and have four of the predominant structural trends found in the Beartooth uplift and throughout the Middle Rocky Mountains indicates that structures in this region have been largely controlled by lines of weakness established in the Archean. Insufficient data are available for the group 1 dikes to give a true indication of all the trends of the earliest fracture pattern.

Dikes of groups 1 and 2 trend parallel to all the major fracture directions in the Beartooth Range. Later dikes have been intruded along fractures parallel to these earlier dikes. This relationship makes it impossible to establish the relative ages of different fracture patterns.

Fracture Pattern and Fold Structures in Granitic Gneiss

NATURE OF FOLDS: The granitic gneisses in the eastern part of the Beartooth uplift are folded into broad, open anticlines and synclines which trend N.-S. to N. 15°E. and plunge 20°–40° to the south. Detailed measurements of foliation and elongated migmatites are used to map the folds. Distinct lithologic units continuous over a large area have not been found. A single large syncline has been mapped in the Quad Creek area (Eckelmann and Poldervaart, 1957). This syncline trends N. 5°-10°E. and plunges southward at 30°. Possibly it is continuous with a syncline in the Gardner Lake area to the south (Rae L. Harris, 1957, personal communication). There are three synclines in the Gardner Lake area. Between the synclinal structures foliation is vertical. An anticlinal structure is found east of the Quad Creek area and is parallel to the syncline. A syncline continuous with the one located in the Gardner Lake area has been mapped farther southward (Donald U. Wise, 1957, personal communication). Other folds with N.-S. to N. 20°E. trends are indicated by mapping east of Beartooth Butte.

FRACTURES ON FOLDS: When it became evident that the granitic gneisses were folded, the possibility arose that the fracture pattern might be related to the folded structures. This has been investigated in the Gardner Lake area. The location of the fold axes and point diagrams of 13 fracture stations in the area are shown in Figure 18

The following observations on the fold-fracture relationships may be made:

(1) No consistent relationship is found between folds and fractures with dips less than 70°.

(2) Stations nos. 350, 34, 348, 344, and 38 have two sets of vertical fractures making angles of approximately 30° with the normal to the fold axes. These might be interpreted as conjugate shears related to folding under nearly horizontal compression.

(3) Stations nos. 350, 41, 34, 93, 247, and 349 have concentrations oriented parallel to the crest of the folds; they might correspond to tension fractures along the fold crest. Stations nos. 41, 247, 92, 349, 93, and 246 have concentrations at right angles to the fold axes and might represent a second set of tension fractures.

(4) Stations nos. 41, 349, 93, 247, 350, and 34 have two of these three concentrations.

(5) None of the stations have concentrations corresponding to both conjugate shears and two sets of tension fractures.

(6) Five of the stations, nos. 236, 34, 246, 93, and 92, have well-defined maxima which do not fall into any of these patterns. The larger concentrations are N. 30°-45°E. and N. 30°-45°W.

These observations suggest the possibility of a fold-fracture relationship, but results obtained at different stations are not consistent. No single diagram shows both sets of tension and shear fractures oriented with respect to the fold, but nine of the diagrams indicate one of the two sets.

Two fracture stations in this area are located near faults. The northeast fault south of Christmas Lake displaced the fold axis of the syncline located near the lake. The offset is to the left, and this zone of movement continues to the mountain front (Fig. 15). Station no. 247 is within 500 feet of the zone and shows evidence of shearing. Station no. 38 is within 100 feet of

a second major fracture zone along which some movement has taken place. The diagram of this station also indicates complex shearing. Several of the other diagrams (nos. 92, 244, and 349) have two or more concentrations which are not consistent with fracture patterns previously described. They could result from local movements.

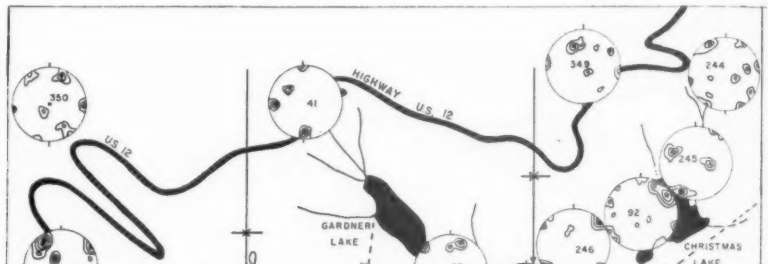

FIGURE 18.—FOLD-FRACTURE RELATIONS IN THE GARDNER LAKE AREA

The contoured point diagrams were plotted on a Schmidt net projection. Each diagram represents 100 fracture measurements. The lowest contour shown is the 4-per cent contour, and the contour interval above 4 per cent is 2 per cent. The fold axes are mapped on the basis of foliation and elongated migmatites in granitic gneisses.

In the opinion of the writer a detailed study using a large number of closely spaced stations is needed to clarify the relationship between folds in the granitic gneisses and the fracture patterns. The present data do not prove that a relationship exists.

Geologic History of the Core of the Beartooth Uplift

The following outline of the geologic history of the crystalline core of the uplift is based on work of the group from Columbia University. (1) Original deposition of a thick sedimentary sequence. (2) Cycle of folding with fold axes striking north-northeast, with emplacement of ultramafic and gabbroidal intrusive rocks before folding. (3) Cycle of regional metamorphism and feldspathization that produced a core of autochthonous to parautochthonous granitic gneiss, elongated northwest, and flanked by migmatites and metasediments. This cycle culminated with the formation of pegmatites, but a few metanorite intrusives were emplaced before the pegmatites. The age of the pegmatites and of the granitization has been determined at the Lamont Geological Observatory (Paul Gast, 1957, personal communication) to be 2.7±0.1 billion years. Ages were determined by the potassium-argon and rubidium-strontium methods, using microcline, muscovite, and biotite. (4) Emplacement of a metabasaltic dikeswarm of metapicrite, metanorite, metadolerite, and iron-rich metadolerite. The dikes cut the pegmatites but are metamorphosed. (5) Emplacement of younger Precambrian dikes of quartz dolerite that cut the metabasaltic dikes and are not metamorphosed. (6) Peneplanation and deposition of Paleozoic and young sediments. (7) Laramian uplift and thrusting with early emplacement of felsic porphyries, primarily along the margins of the uplift. (8) Intrusion of Tertiary olivine-basaltic dikes, primarily in the southwestern part of the uplift.

MECHANICS OF DEFORMATION

Characteristics of Fracture Patterns

PATTERNS AT INDIVIDUAL OUTCROPS: The multiplicity of fracture directions might be

due to rotations during a later deformation of small blocks that had a uniform and simple pattern when originally formed. If rotations were systematic, summaries of a large number of stations located on separate blocks would bring about a superposition of patterns, giving a large number of different trends. To investigate this possibility, each of the 160 stations on the southwestern slope of the uplift was examined to see if generalizations could be made as to frequency of occurrence of two or more trends at the same station. Mean fracture planes of all nearly vertical fractures at each station having a concentration at N. 40°-45°W. were tabulated (Table 3).

Every recognized fracture trend in the uplift occurs at several stations with the N. 40°-45°W. trend. Fracture trends of N. 15°-20°W., N. 35°-45°E., N. 60°-70°W., and N. 60°-70°E. are generally found with N. 45°W. These trends also have the greatest frequency of occurrence in the uplift as a whole. It appears that the frequency of occurrence of a given trend with any other trend is no greater than the frequency of occurrence of the two trends in the uplift as a whole. Thus frequency of occurrence of trends together does not indicate which trends formed together.

To test further the nature of fracturing on adjacent blocks, an area has been selected at Question Mark Lake where several major fracture zones intersect. Sixteen fracture stations are located around the lake, with at least three stations on each block separated by major fracture zones (Fig. 11). Variations within a block bounded by major fractures are as great as variations between the blocks. A systematic rotation of an originally simple fracture pattern does not account for the multiplicity of fracture directions. The above result is expected, since some stations have well-defined though low concentrations corresponding to all the fracture trends, and a large number of stations have as many as six trends.

Other explanations for the erratic nature of patterns at individual stations may be the heterogeneity of the rocks, or the almost certain lack of a perfectly uniform stress field. Fracture measurements have been made only in granitic rocks. This should minimize the effect of extreme variations in rock composition. Lack of perfect uniformity in the stress field appears the most likely explanation. Two stations located not more than 50 feet apart in many cases have the same trends, but the degree of development of a given trend is highly variable from one part of the outcrop to another. In many cases, one station does not have distinct maxima along one or even two fracture directions present at the other station. This is not surprising considering results obtained in compression or tension tests on wax, clay, and engineering materials in laboratories. Samples large enough to develop a well-defined pattern under compression or tension show a pattern that appears uniform over the area as a whole but is only partly indicated at a given point within the area, even if the area considered is far removed from boundaries. Fine illustrations of this phenomemon are given by Nadai (1950, p. 175–371).

PATTERNS FOR THE ENTIRE UPLIFT: Where concentrations of joints from a large number of stations are combined a simple pattern results which consists of four principal vertical joint trends, N. 15°-20°W., N. 40°-45°W., N. 40°-45°E., and N. 65°-70°W. These trends form striking fracture patterns on aerial photographs of the area, but they are not equally developed. The weakest of joint trends, N. 65°-70°W., is the strongest trend among the longest fractures. These fractures tend to be widely spaced. The best-developed joint trend, N. 15°-20°E., is not strikingly developed on the photographs. Both 40°-45°E. and N. 40°-45°W. are well developed among joints and major fractures.

Formation of Archean Fracture Pattern

LIMITATIONS OF THE DATA: Unique solutions to the problem of the nature of stress fields responsible for the formation of fractures are rarely found. Such problems are greatly increased in dealing with complex patterns such as found in the Beartooth uplift. No attempt is made here to determine a unique stress field to account for the strains evidenced by the fractures. Four major fracture trends have been outlined, and at least three other, less-pronounced trends are present. Studies by the Columbia University group and by earlier investigators in the Beartooth Mountains have not yet made it possible to subdivide the regional patterns into two or more sets of contemporaneous fractures, nor has it been possible to establish a definite age relationship for the trends. All the trends appear to be early Precambrian. The multiplicity of trends makes it possible to postulate many stress-strain combinations.

The possible relationship between folds in the granitic gneisses and the formation of fractures has been pointed out. The folds that are presently mapped are confined to the eastern margin of the southwestern slope. If the fractures are related to the folding, lines of weak-

ness must be preserved in the rocks during granitization, just as original bedding is preserved as banding or foliation. Folded bands with different physical properties might influence the formation of later fractures, but compositional bands are not continuous over large areas in the Beartooth uplift and are rare in the core of the range. A second argument against relating the fractures to the folds is the relative size of these features. The folds are broad and open with limbs several miles apart. Some of the fractures are continuous for distances of 15 miles or more, and many extend for 5 or more miles.

PATTERN FORMED BY DOMINANT FRACTURE TRENDS: The nature and intensity of fracturing leads to several observations. The four most prominent fracture trends (Fig. 19*A*) form a striking pattern. Two trends are approximately at right angles, N. 40°-45°W. and N. 40°-45°E., and the other two trends, N. 65°W. and N. 15°W., are about 50° apart. Bucher (1920; 1921; 1954) described the mechanics of formation of patterns similar to these. These patterns would be expected if the area had been shortened along a northwest-southeast line, with tension fractures forming along and at right angles to maximum shortening and two conjugate shears forming at angles of 20°-30° with the direction of maximum shortening. These directions stand out prominently in Figures 15 and 17. Many of these fractures extend for miles across the uplift and outline major blocks on the southwestern slope. The Beartooth uplift has been subjected to several periods of deformation, and some of the fractures are probably older than others. If the stress field applied during the second or third deformation acts along a different line from the first, some of the first-formed fractures would provide lines of weakness along which new movements could occur. However, few slickensides were observed, and no systematic study has been made. New fractures would probably form only at large angles to pre-existing fractures.

The point diagrams of fractures measured at each station in this study were examined to see how close concentrations occurred to one another. Frequently a maximum would be broken into two concentrations within about 10°. These were not separated by distinct saddles and were considered parts of the same maximum throughout the analysis. Other maxima were unrelated but rarely occurred less than 20° apart.

MECHANICS OF FORMATION OF LESS PROMINENT FRACTURES: Perhaps the most important effect of having pre-existing fractures subjected to either increasing stress along the initial line of action, or of having the pattern subjected to a second stress field acting along a different trend, would be the formation of fractures as a result of couples produced locally by boundary conditions. The formation of tensional and compressional fractures in a Mead device (Mead, 1920) would approximate this condition (Fig. 19*B*). The sides of the device would correspond to major early formed fractures. If the block of material bounded by these fractures were compressed or rotated by a couple in such a way that the length of one of the diagonals was reduced, warping would occur, and tension fractures would be expected along and normal to that diagonal; conjugate shears would form at approximately 30° to that diagonal. The orientation of the fractures within the boundaries would not necessarily bear any relation to the stress field applied to the mountain range as a whole.

Figure 19*C* is a diagrammatic representation of tension and shear fractures expected if maximum shortening occurs along a northwest-southeast line (conditions postulated for the Beartooth uplift). Conjugate shear fractures generally form at approximately 60° to one another. In Figure 19*C* the fractures are shown evenly spaced. If the area should be subjected to a second period of deformation in which the stress field acted along a different line, the first-formed fracture pattern would be slightly deformed, and new fractures would be formed within the boundaries of the blocks outlined by the larger of the early fractures. Some of the shear and tension fractures that might be expected are seen in Figure 19*D*. The new tension fractures would form at 90-degree angles, and the new conjugate shear fractures would form at approximately 60-degree angles. The fracture pattern formed in this manner is similar to that of the Beartooth uplift. The four major trends are the result of the earliest deformation. These trends are found within the major blocks outlined by the larger fractures of this set. Some of the fractures formed during the second deformation are nearly parallel to the earlier fractures, but new fractures are formed where no pre-existing fracture is available to take up the new movement.

Two factors would be of importance in determining angular relations between old and new fractures. First is the amount of shortening necessary in the second period of deformation to form new fractures. If the first-formed frac-

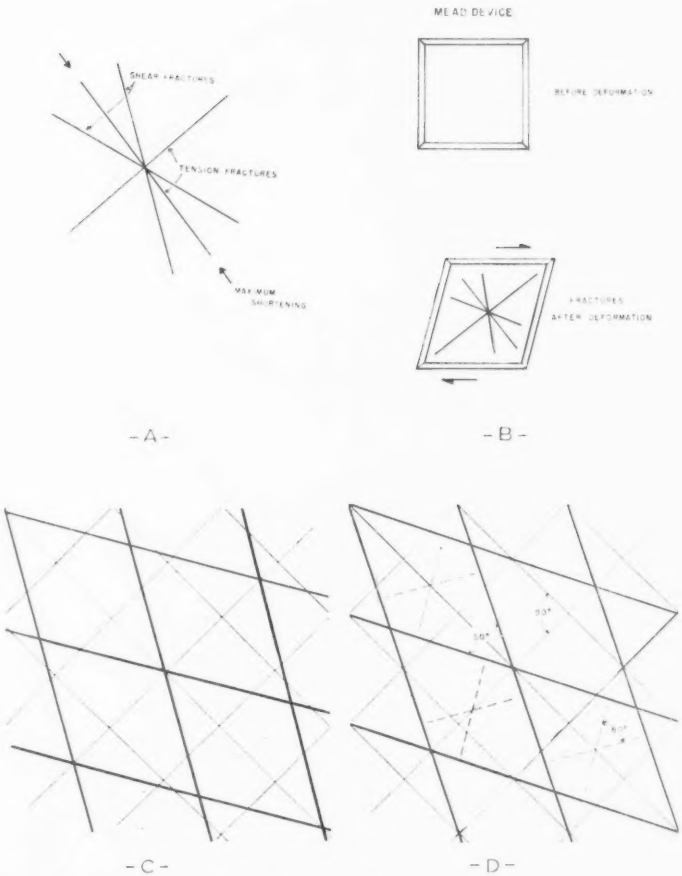

FIGURE 19.—ORIGIN OF FRACTURE TRENDS IN BEARTOOTH UPLIFT

A. Major fracture trends in Beartooth uplift. The four most prominent fracture trends in the uplift are shown. This pattern would be predicted for maximum shortening along a northwest-southeast line. Two sets of tension fractures form parallel and perpendicular to the shortening, and shear fractures form at 25°–30° to the shortening.

B. Fractures formed in the Mead device. The hinged iron frame is shown before and after deformation of the material held within the frame. Tension and shear fractures form in the material. The attitude of the fractures depends upon the shape and amount of deformation. Such a mechanism is probably responsible for the formation of some of the fractures in the Beartooth Mountains. Early major fracture zones behave as the frame in the Mead device. During a second period of deformation new fractures form within the blocklike area bounded by the pre-existing fractures.

C. Blocklike areas bounded by major fractures. The blocklike areas shown have the trends postulated for the early formed fractures in the Beartooth uplift, but the spacing is hypothetical.

D. Fracture pattern after the second deformation. The solid lines have the orientations of the most prominent fractures in the Beartooth Mountains. The heavy solid lines are the postulated early shear fractures; the light solid lines are the postulated early tension fractures. The dashed lines are shear fractures formed if maximum shortening in a second deformation occurs along a northeast-southwest line. These correspond to fracture trends found in the Beartooth uplift.

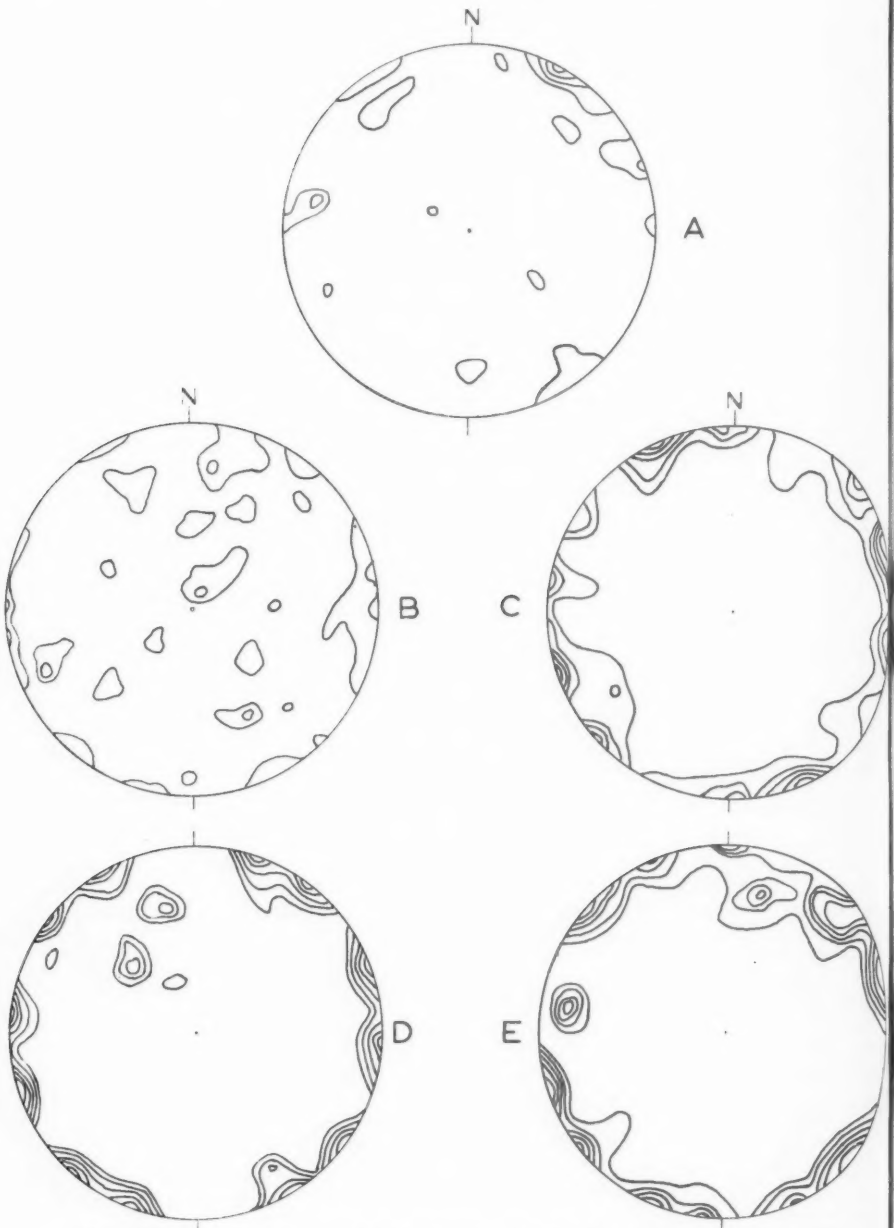

FIGURE 20.—SUMMARY DIAGRAMS OF FRACTURE DATA FOR AREAS OF BEARTOOTH UPLIFT

Each point diagram is based on the maxima from fracture stations in the area represented by it. The limits of the areas are marked on Plate 3. The lowest contour is 2 per cent, and the contour interval above

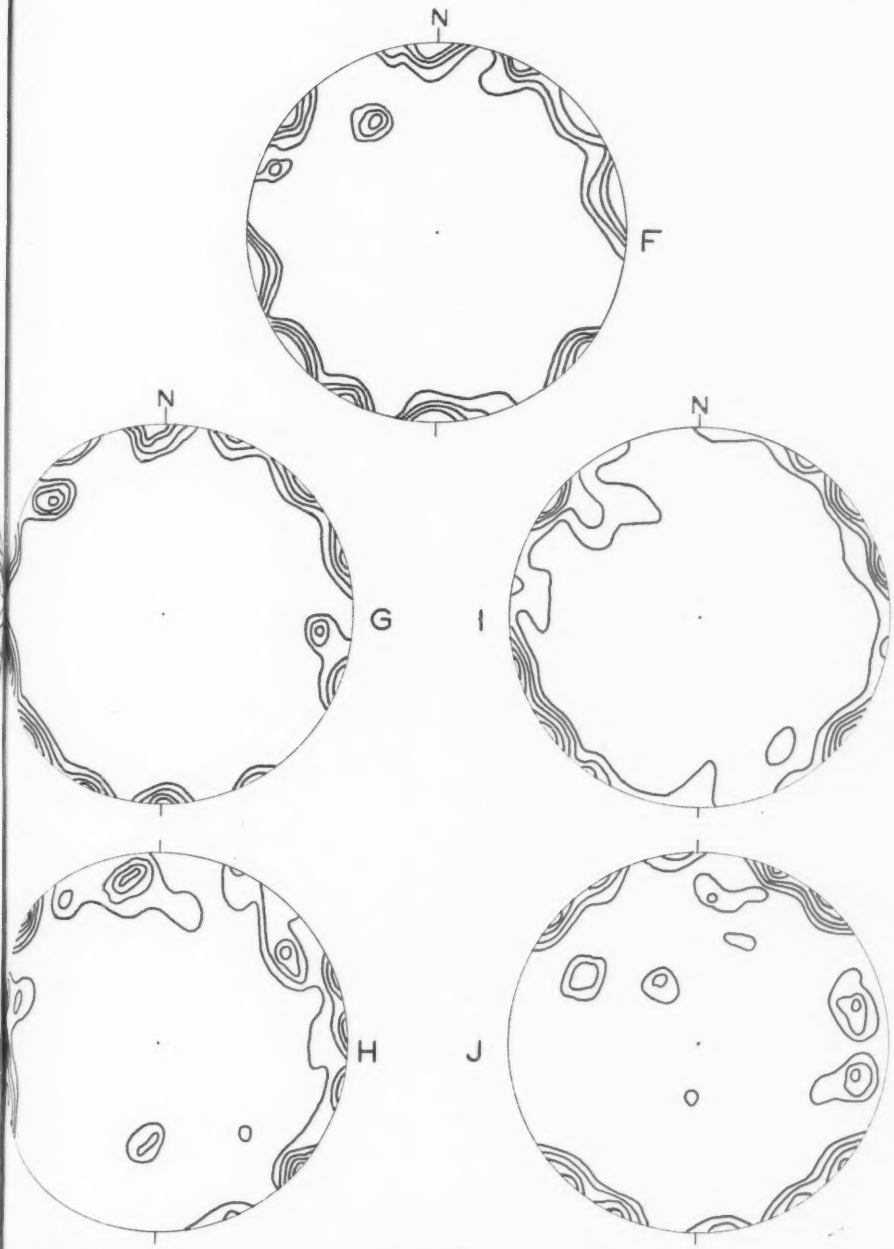

FIGURE 20

that is 1 per cent. Maxima represented in each diagram are: *A*, 190; *B*, 150; *C*, 36; *D*, 69; *E*, 63; *F*, 80; *G*, 120; *H*, 93; *I*, 142; *J*, 67.

tures in the Beartooth uplift are as postulated (Fig. 19*A*), and if they initially formed at angles of 60° and 90°, then they have been rotated through approximately 10°. The second factor is the spacing between major parallel fractures. The shape of this block is determined by the angles between the two sets of lines and the spacing between each pair of lines. The position of the diagonals of the block is determined by the shape of the block. If the block is subjected to a second period of deformation, maximum shortening occurs along one of the diagonals. Tension fractures are formed parallel to and at right angles to the direction of maximum shortening. Shear fractures form approximately at 30-degree angles with the direction of maximum shortening. As the spacing of major fractures changes, the shape of the blocks and the trends of later fractures formed within the blocks are also changed.

VARIATIONS IN FRACTURE PATTERN TOWARD OVERTHRUST FRONT: Fracture patterns on the southwestern slope are different from those on the northeastern part of the uplift. The most striking difference is the appearance of low-dipping fracture concentrations in both areas *A* and *B*. In area *A*, near Mystic Lake, the highest concentration is a vertical N. 60°W. trend. In order of concentration, other nearly vertical fractures are N. 20°W., N. 10°E., and N. 60°E. In spite of overthrusting at the front, many of the fracture trends found on the southwestern slope are present.

Inclined fractures at N. 44°W.-70°NE, E.-W.-70°S., N. 40°E.-40°SE., and N. 20°E.-20°NW. all have concentrations of 2 per cent on the summary diagrams. The low-dipping fractures may be shears formed during Laramian overthrusting. The generalization that fracturing is more complex and the pattern less well defined toward the front is possible, but more closely spaced stations would be required to indicate the nature of the changes.

Area *B* has an even more complex deformational history than area *A*. This area includes the northeastern corner of the uplift which has been thrust northward, northeastward, and eastward. These directions of overthrusting are separated by tear faults which extend into the Precambrian core. The only vertical fracture trend indicated here is a diffuse high between N. -S. and N. 10°W. Most other fractures dip between 60° and 80°. One low-dipping set of fractures is indicated: N. 55°W. dipping 15° NE. It may have formed as echelon tension fractures inclined in the direction of the overthrust as the uplift was thrust out during Laramian deformation (Bucher, 1957, personal communication).

Nature of Laramian Deformation

The consistency of the fracture patterns on the southwestern slope demonstrates that the central core of the Beartooth uplift has behaved very much as a single block since the Precambrian fracture pattern was first formed. Aerial photographs of the southwestern slope show hundreds of major shear or fracture zones. Figure 15 shows the relative magnitude of the major fracture trends, the consistency of these trends, and also indicates that there has been little horizontal displacement of one set of major fractures along a second set. Horizontal movements which do appear are on the order of a few hundred feet. Vertical movements are much more striking.

Post-Paleozoic faulting has been demonstrated along several faults. A nearly vertical displacement of 400 feet has occurred along a fault trending N. 45°W. just east of Beartooth Butte, where middle Cambrian Flathead sandstone has been dropped down on the northeastern side of the fault. A second major fault is indicated on the map of Beartooth Butte (Scheufler, 1954, M.S. thesis, Wayne State Univ., Detroit, Michigan). This fault has slight horizontal displacement, cuts into Clay Butte, strikes N. 65°-70°W., and can be traced on the aerial photographs, but no detailed mapping has been done across them (Pl. 1). Fracture station no. 318 is located on the side of one of these scarps and shows the effects of intense shearing. Most of the faults trend N. 60°-70°W., and judging from the relief on aerial photographs, the northeastern side has gone down in most cases. The scarps cannot be attributed to erosion because glacial striations and grooves indicate a southwestward direction of movement for the ice sheets. One east-west fault scarp is seen on the photographs at Granite Lake (Pl. 1, fig. 1). Here the north side appears to have moved down.

The attitude of the late Precambrian peneplaned surface shows that the Beartooth Range in gross aspect is a large asymmetrical anticlinal structure, the axis of which trends N. 65°W. with overturning toward the northeast. If all the faults are Laramian, most of the movements on the southwestern slope result from tensional stresses acting along a line perpendicular to the crest of the uplift. The response to this tension has been the formation of step-

faulting, graben and horst structures, and tilted blocks with the movements along pre-existing major fractures.

Step-faulting and graben and horst structures are most common along the extreme southern margin of the southwestern slope. Farther up on the slope, tilting of major blocks is more obvious. One of these blocks is east of Beartooth Butte, and though not well shown on the aerial photographs, it is bounded on the southwest by a N. 45°W. fault which displaces the Cambrian formations 400 feet. Fracture measurements that have been made in this area (*I*) show that fracture planes striking between E.-W. and N. 40°W. are tilted and inclined to the northeast. A second major block appears on the photographs (Pl. 1, fig. 1) and is outlined by major fractures trending N. 40°W. and N. 40°E., along which intense shearing and movement is apparent. Relief on the southern corner of this block amounts to more than 1000 feet on opposite sides of a major fracture zone.

The greatest uplift occurred on the northeastern side of the uplift, where the Precambrian crystalline rocks are thrust over the Paleozoic and Mesozoic sediments. Along the northeastern and eastern margin of the uplift, tears formed in the thrust front along major fractures in the basement, and horizontal displacements occurred on opposite sides of these fractures. Some of the major faults can be traced several miles into the core of the uplift, but most appear to be local scissor faults near the thrust front.

As a result of horizontal movements in the northern and eastern parts of the uplift, a more complex fracture pattern with many low-dipping fractures was formed.

The southwestern slope of the uplift is characterized by a uniform, well-developed fracture pattern, whereas the northeastern slope has an ill-defined pattern with many low-dipping fractures. The critical zone separating these two slopes is occupied by a large, deep glaciated valley that trends N. 60°-70°W. This valley probably has major structural significance, but no geologic work has been done there.

References Cited

Auden, J. B., 1954, Erosional patterns and fracture zones in peninsular India: Geol. Mag., v. 91, no. 2, p. 89–101

—— 1954, Drainage and fracture patterns in northwest Scotland: Geol. Mag., v. 91, no. 5 p. 337–351

Bengtson, C. A., 1956, Structural geology of the Buffalo Fork area, northwestern Wyoming, and its relation to the regional tectonic setting: 11th Ann. Field Conf., Wyo. Geol. Assoc. Guidebook, p. 158–168

Blackstone, D. L., Jr., 1940, Structure of the Pryor Mountains, Wyoming: Jour. Geology, v. 48, p. 590–618

Bucher, W. H., 1920, The mechanical interpretation of joints: Jour. Geology, v. 28, p. 707–730

—— 1921, The mechanical interpretation of joints: Jour. Geology, v. 29, p. 1–28

—— 1954, Principles of interpretation of fracture patterns: Yellowstone-Bighorn Research Assoc. Short Course, July 19–21, 5 p.

Bucher, W. H., Chamberlin, R. T., and Thom, W. T., Jr., 1933, Results of structural research in Beartooth-Bighorn region, Montana and Wyoming: Am. Assoc. Petroleum Geologists Bull., v. 17, p. 680–693

—— 1934, Geologic problems of the Beartooth-Bighorn region: Geol. Soc. America Bull., v. 45, p. 167–188

Chamberlin, R. T., 1945, Basement control in Rocky Mountain deformation: Am. Jour. Sci., Daly Volume, p. 98–116

Chayes, Felix, 1949, Statistical analysis of two-dimensional fabric diagrams, and statistical analysis of three-dimensional fabric diagrams, p. 297–326 *in* Fairbairn, H. W., Structural petrology of deformed rocks: Cambridge, Mass. Addison-Wesley Press, 344 p.

Cloos, Hans, and Cloos, Ernst, 1933, Pre-Cambrian structure of the Beartooth, the Big Horn, and the Black Hills uplift and its coincidence with Tertiary uplifting (Abstract): Geol. Soc. America Proc., p. 56

Demorest, Max, 1941, Critical structural features of the Bighorn Mountains, Wyoming: Geol. Soc. America Bull., v. 52, p. 161–176

Dobbin, C. E., and Erdmann, C. E., 1947, Structure contour map of the Bighorn Basin, Wyoming and Montana: U. S. Geol. Survey Oil and Gas Inv. Prelim. Map 74, scale 1 inch = 3 miles

—— 1955, Structure contour map of the Montana Plains: U. S. Geol. Survey Oil and Gas Inv. Map O M 178A, scale 1:500,000

Duschatko, Robert, 1955, Mechanical aid for plotting and counting out pole diagrams: Geol. Soc. America Bull., v. 66, p. 1521–1524

Eckelmann, F. D., and Poldervaart, Arie, 1957, Geologic evolution of the Beartooth Mountains, Montana and Wyoming. Part 1. Archean history of the Quad Creek area: Geol. Soc. America Bull., v. 68, p. 1225–1262

Fanshawe, J. R., 1939, Structural geology of the Wind River canyon area, Wyoming: Am. Assoc. Petroleum Geologists Bull., v. 23, p. 1439–1492

Foose, R. M., 1956, Structural features of the perimeter of the Beartooth Mountains: Yellowstone-Bighorn Research Assoc. Short Course, July 18–20, p. 5

Horberg, Leland, Nelson, V. E., and Church, Victor, 1949, Structural trends in central western Wyoming: Geol. Soc. America Bull., v. 62, p. 373–398

Hughes, R. V., 1933, Geology of a part of the Beartooth Mountain front: Nat. Acad. Sci. Proc., v. 19, p. 239–253

Johnson, G. D., 1934, Geology of the mountain

uplift transected by the Shoshone Canyon, Wyoming: Jour. Geology, v. 42, p. 809–838

Jolliffe, A. W., 1942, Structures in the Canadian Shield: Am. Geophys. Union Trans., v. 23, p. 699–707

Kay, Marshall, 1951, North American geosynclines: Geol. Soc. America Mem. 48, 143 p.

King, P. B., *et al.*, 1944, Tectonic Map of the United States. Scale 1:2,500,000: Am. Assoc. Petroleum Geologists, prepared under the direction of the Comm. on Tectonics, Div. Geol. and Geog., Nat. Research Council

Lammers, E. C. H., 1937, The structural geology of the Livingston Peak area, Montana: Jour. Geology, v. 45, p. 268–295

Lovering, T. S., 1929, The New World or Cooke City mining district, Park County, Montana: U. S. Geol. Survey Bull. 811-A 87 p.

Masursky, Harold, 1952, Geology of the Western Owl Creek Mountains: Wyo. Geol. Assoc. 7th Ann. Field Conf. Guidebook, in pocket

Mead, W. J., 1920, Notes on the mechanics of geologic structures: Jour. Geology, v. 28, p. 505–523

Molina, E. C., 1947, The Poisson exponential binomial limit: N. Y., D. Van Nostrand Co., 47 p.

Muller, L., 1933, Untersuchungen uber statistische Kluftmessung: Geol. und Bau. Jahrb. 5, p. 206–234

Nadai, A., 1950, Theory of flow and rupture of solids. Monograph I, Engineering Society: N.Y., McGraw Hill Book Co., 572 p.

Nelson, V. E., and Church, Victor, 1943, Critical structures of the Gros Ventre and Northern Hoback ranges, Wyoming: Jour. Geology, v. 51, p. 143–166

Parker, J. M., 1942, Regional systematic jointing in slightly deformed sedimentary rocks: Geol. Soc. America Bull., v. 53, p. 381–403

Perry, E. L., 1935, Flaws and tear faults: Am. Jour. Sci., v. 229, p. 112–124

Pincus, H. J., 1951, Statistical methods applied to the study of rock fractures: Geol. Soc. America Bull., v. 62, p. 81–128

Rouse, J. T., *et al.*, 1937, Petrology, structure, and relation to tectonics of porphyry intrusions in the Beartooth Mountains, Montana: Jour. Geology, v. 45, p. 717–740

Salomon, W., 1911, Die Bedeutung der Messung und Kartierung von gemeinen Kluften und Harnischen, mit besonderer Berucksichtigung des Rheintal-Grabens: Zeitschr. der Deutsche Geol. Gesell, Band 63, p. 496–521

Skeels, D. C., 1939, Structural geology of the Trail Creek canyon mountain area, Montana: Jour. Geology, v. 47, p. 816–840

Thom, W. T., Jr., 1923, The relation of deep seated faults to the surface structural features of central Montana: Am. Assoc. Petroleum Geologists, v. 7, p. 1–14

—— 1952, Structural features of the Bighorn Basin rim: Wyo. Geol. Assoc. 7th Ann. Field Conf. Guidebook, p. 15–17

—— 1955, Wedge uplifts and their tectonic significance, p. 369–376 *in* Poldervaart, Arie, *Editor*, Crust of the earth: Geol. Soc. America Special Paper 62, 762 p.

Van Dyke, L. H., 1956, Structure of the upper Horse Creek area: Wyo. Geol. Assoc. 11th Ann. Field Conf. Guidebook, p. 184–187

Wager, L. R., 1931, Jointing in the Great Scar limestone of Craven and its relation to the tectonics of the area: Geol. Soc. London Quart. Jour., v. 87, p. 392–424

Wilson, C. R., Jr., 1934a, A study of the jointing in the Five Springs Creek area east of Kane, Wyoming: Jour. Geology, v. 42, p. 498–522

—— 1934b, Geology of the thrust fault near Gardiner, Montana: Jour. Geology, v. 7, p. 816–840

—— 1936, Geology of the Nye-Bowler lineament, Stillwater and Carbon countries, Montana: Am. Assoc. Petroleum Geologists Bull., v. 7, p. 1–13

—— 1938, The Tensleep fault, Johnson and Washakie counties, Wyoming: Jour. Geology, v. 46, p. 868–881

Wilson, J. T., 1948, Some aspects of geophysics in Canada with special reference to structural research in the Canadian Shield: Am. Geophys. Union Trans., v. 29, p. 691–725

Wolk, E., 1937, Zur Klufttektonik des Niederrheinischen Haupt-Braunkohlenflozes: Zeitschr. Deutsch. Geol. Gesell, Band 91, p. 109

Zwart, H. J., 1951, Breuken en Diaklazen en Robin Hood's Bay: Geol. en Mijnb., v. 13, p. 1–4

Dept of Geology, Washington and Lee University, Lexington, Va.

Manuscript Received by the Secretary of the Society, July 24, 1957

110°
00'
45°15'
PRECAMBRIAN ROCKS
228

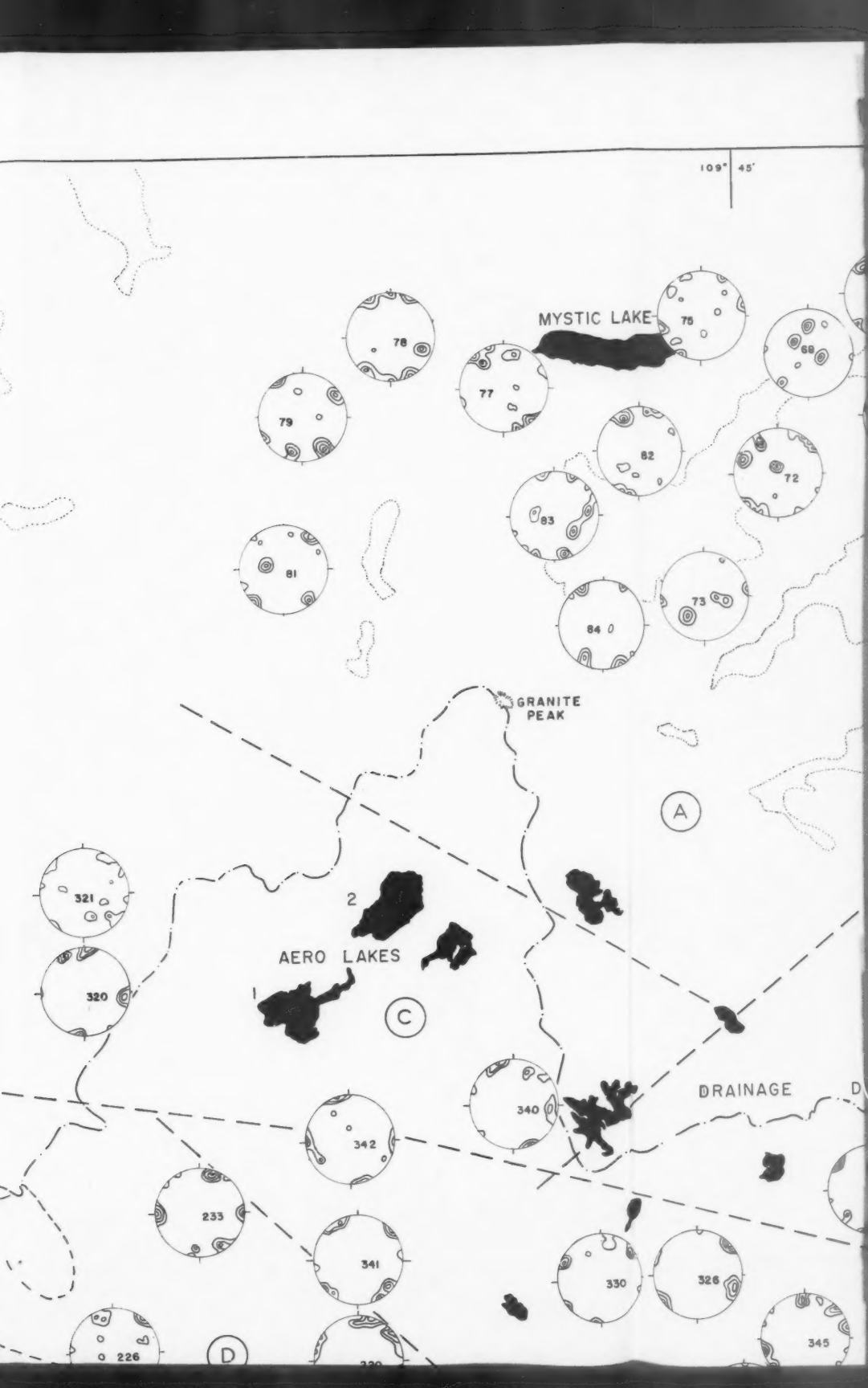
109° 45'
MYSTIC LAKE
78
77
75
69
79
82
72
83
81
73
84
GRANITE PEAK
A
321
2
AERO LAKES
320
1
C
340
DRAINAGE
342
233
341
330
326
345
226
D

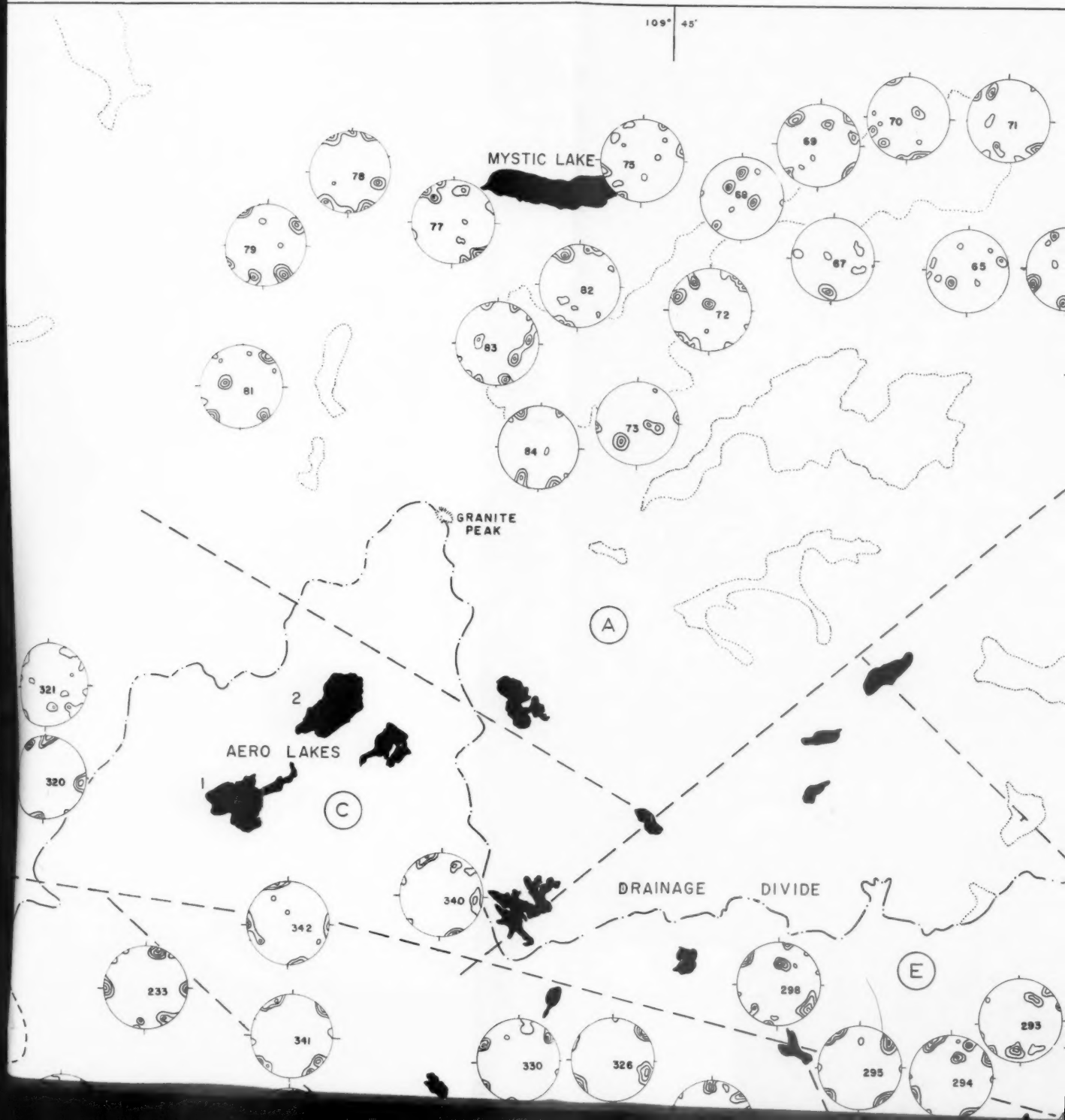
109° 45'
MYSTIC LAKE
78
77
75
79
82
83
81
84
73
72
69
70
71
68
67
65
GRANITE PEAK
A
321
320
2
AERO LAKES
1
C
340
342
233
341
DRAINAGE DIVIDE
E
298
293
330
326
295
294

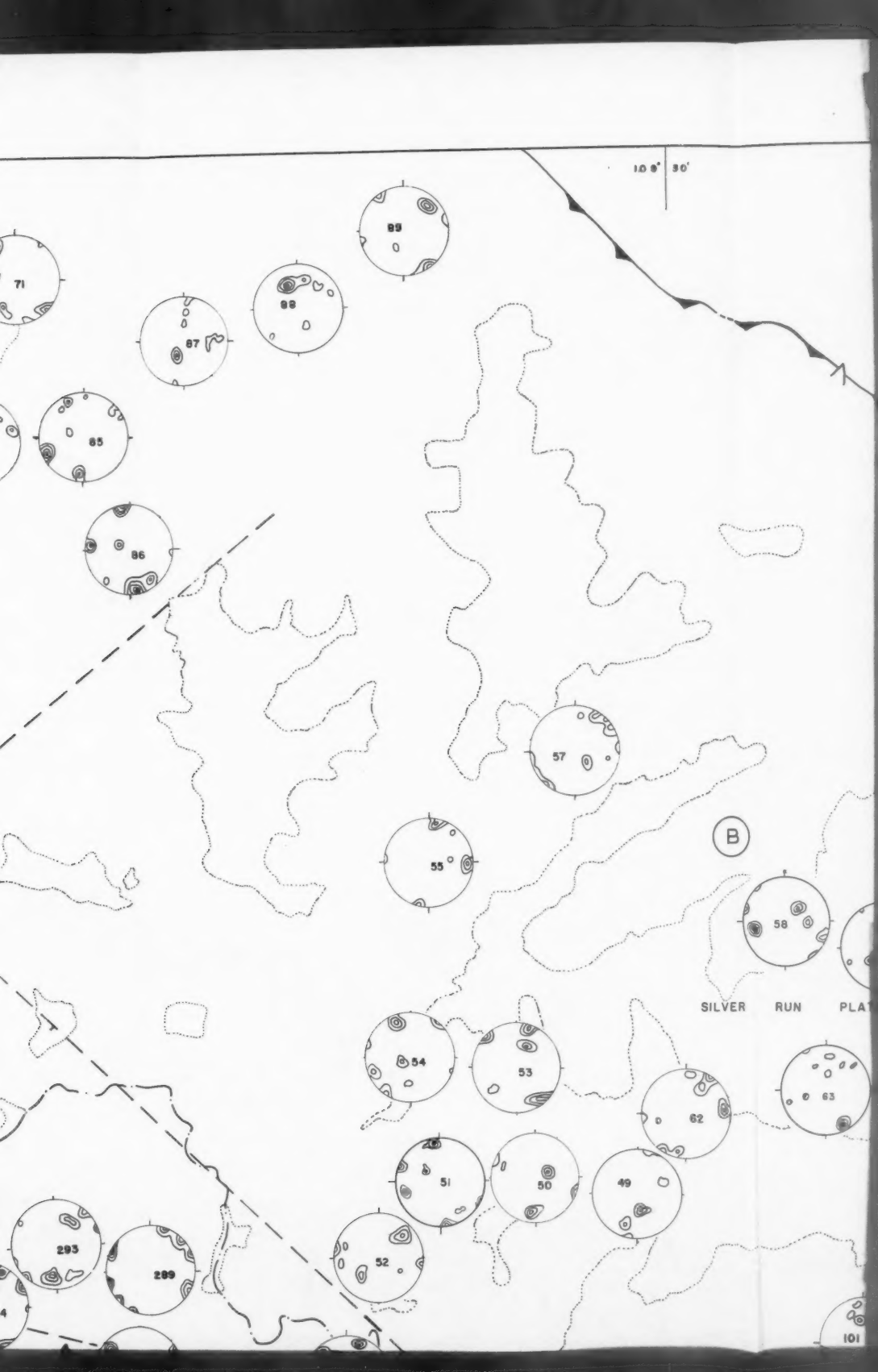
10 8° 30'
99
71
98
87
85
86
57
55
B
58
SILVER
RUN
54
53
63
62
51
50
49
293
289
52
101

10 9° 30'
89
70
71
69
88
87
67
65
85
86
57
55
B
58
60
64
SILVER RUN PLATEAU
54
53
62
63
59
DIVIDE
E
298
293
295
51
50
49
52
100

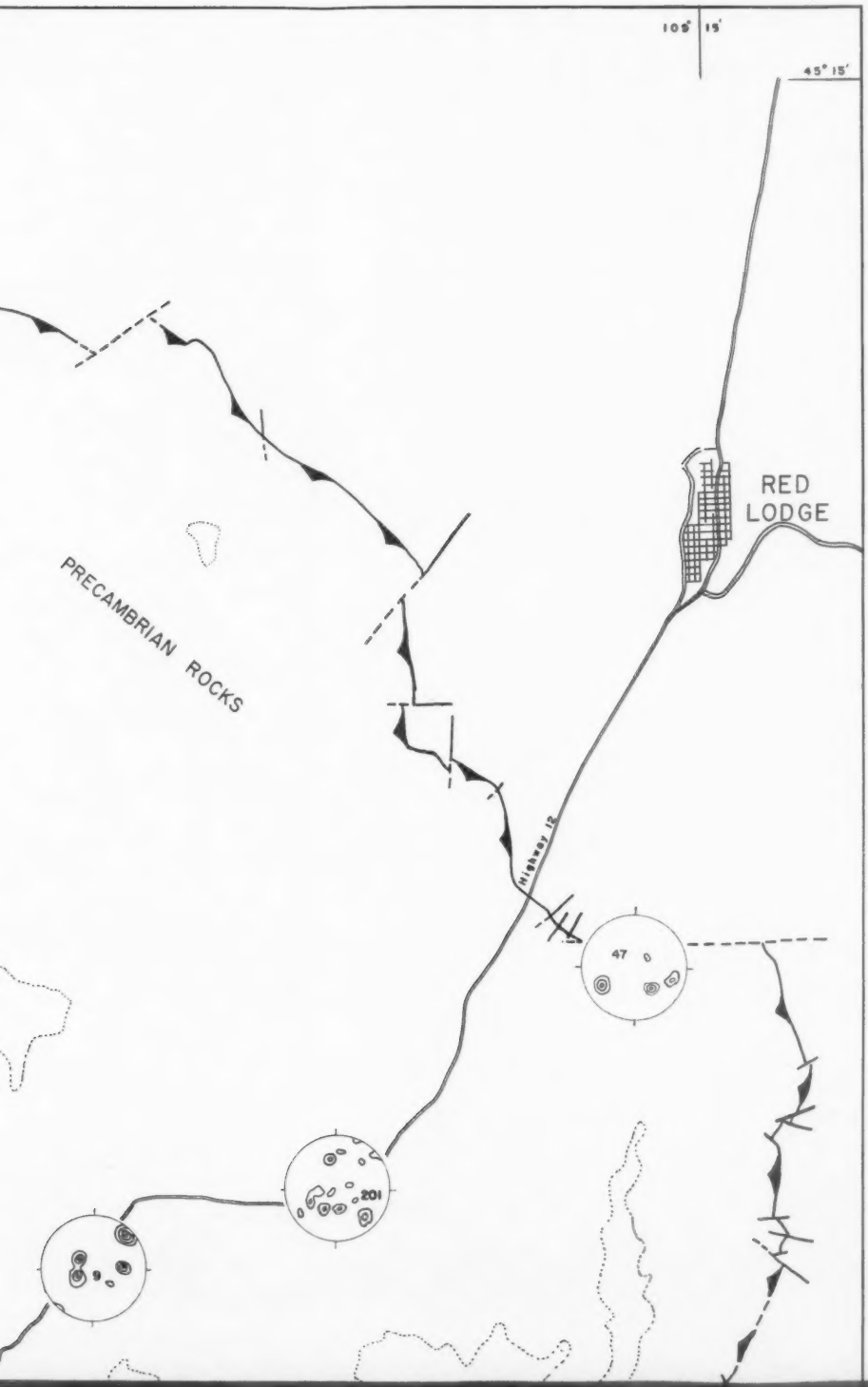
105° 15'
45° 15'
RED LODGE
PRECAMBRIAN ROCKS
HIGHWAY 212
47
201

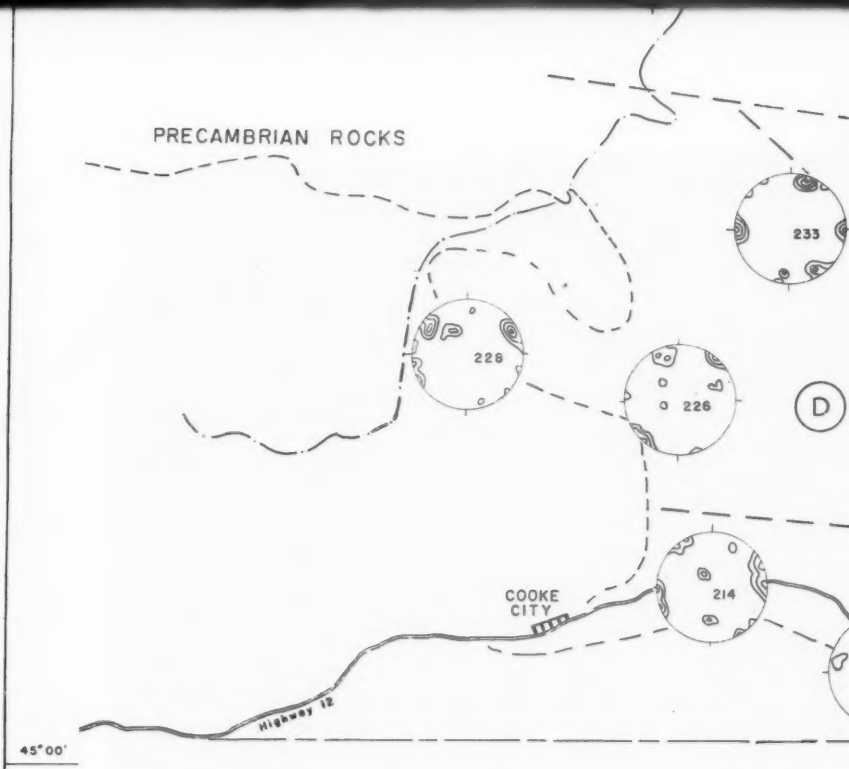

LAKES

PLATEAU BOUNDARY

EACH DIAGRAM REPRESENTS 100 FRACTURE MEASUREMENTS PLOTTE

ON THE UPPER HEMISPHERE OF A SCHMIDT NET

LOWEST CONTOUR 4%

CONTOUR INTERVAL 2% (ABOVE LOWEST CONTOUR

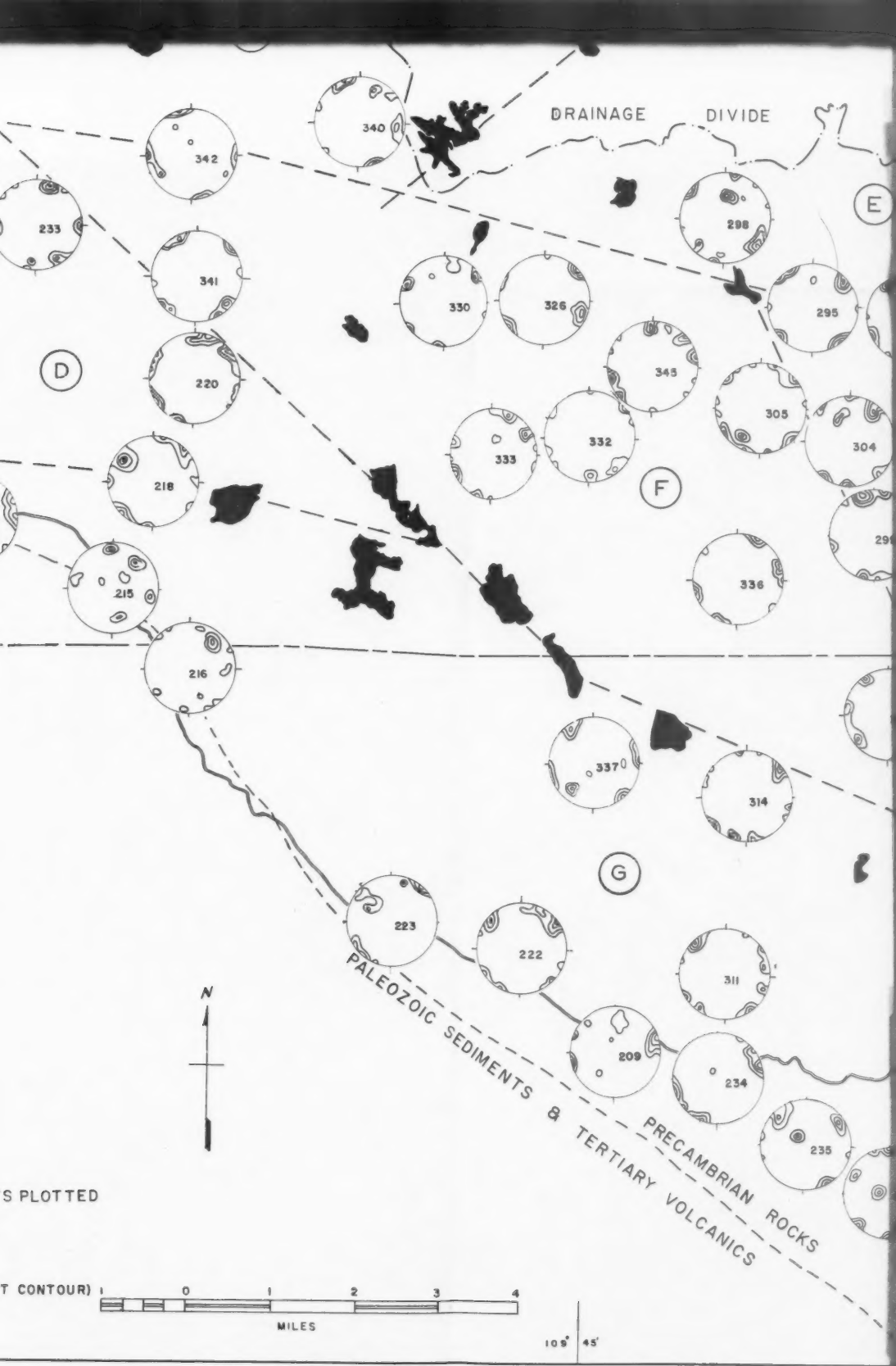

FRACTURE PATTERNS IN TH

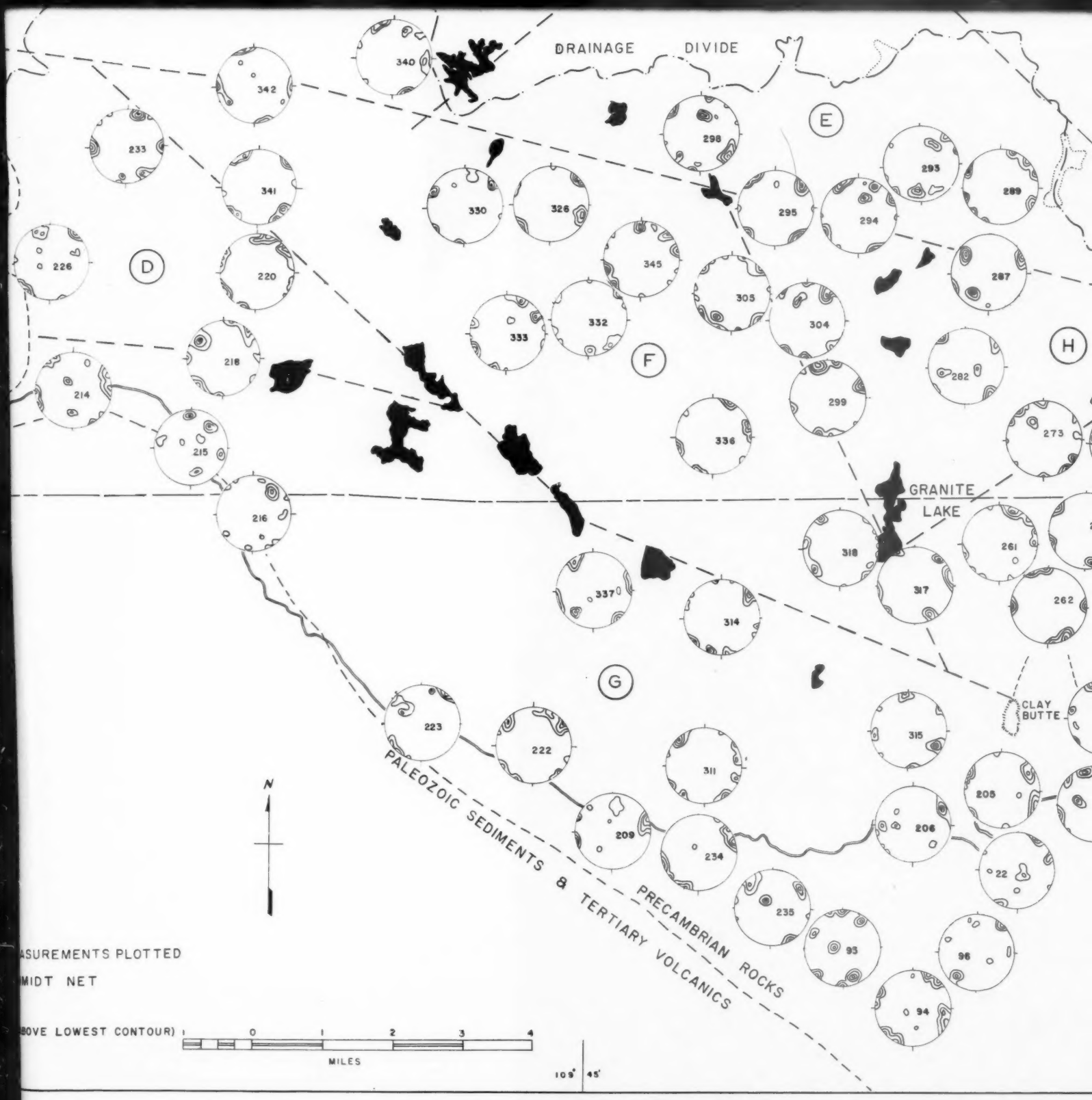

FRACTURE PATTERNS IN THE BEARTOOTH U

Central and east portio

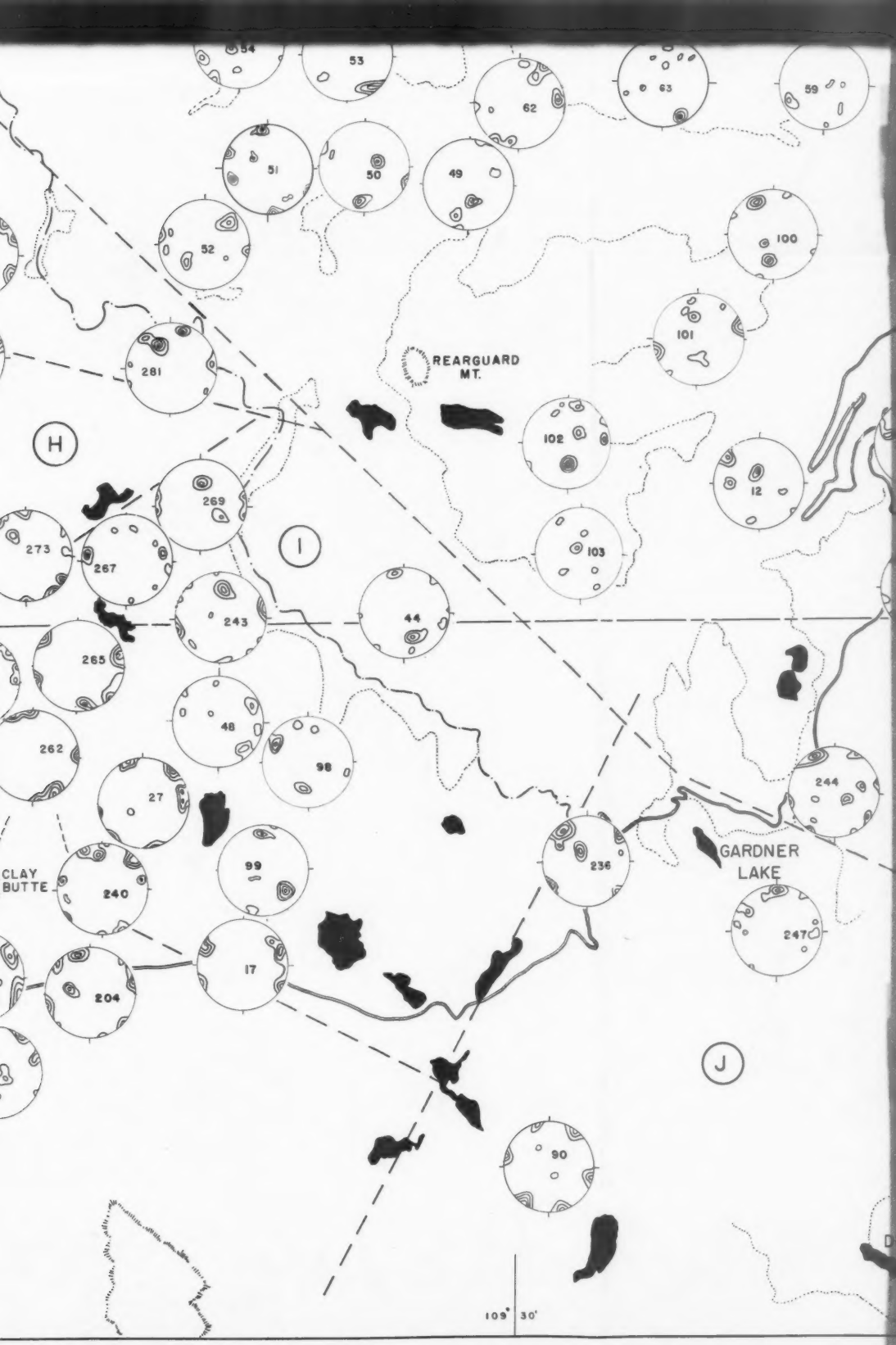

TH UPLIFT, MONTANA AND WYOMING

st portions

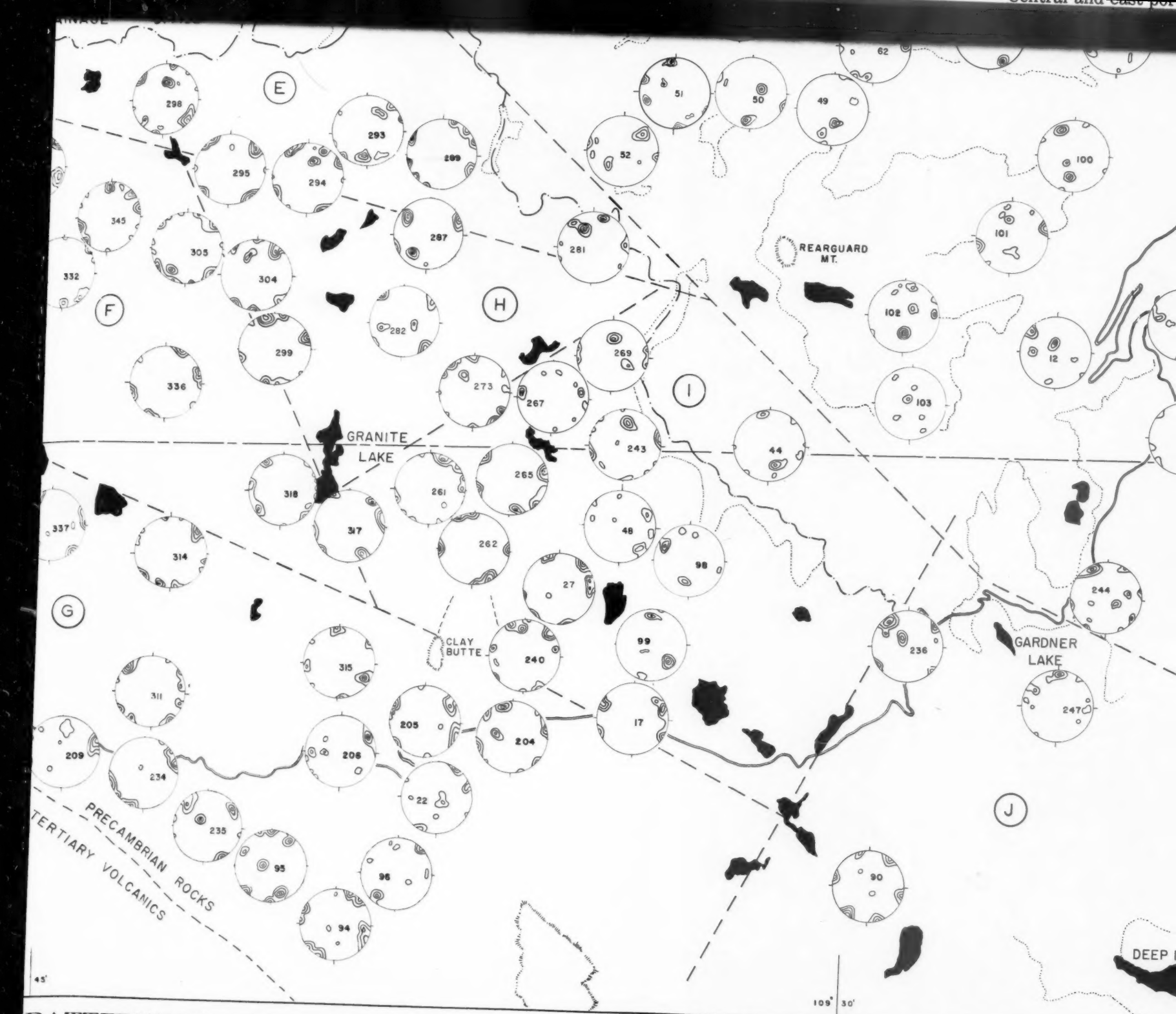

PATTERNS IN THE BEARTOOTH UPLIFT, MONTANA AND WYOMING

Central and east portions

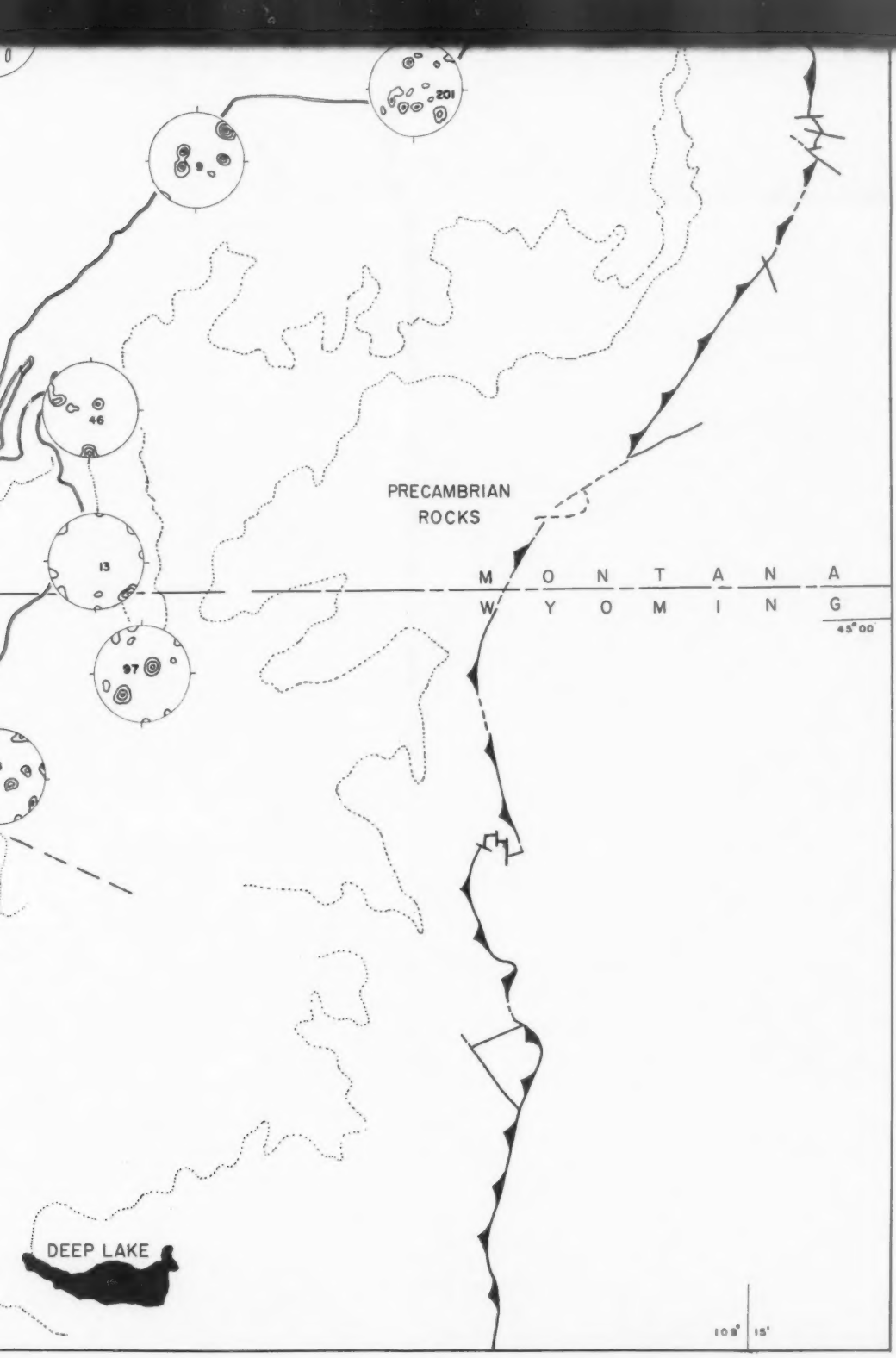
201
46
13
97
PRECAMBRIAN
ROCKS
MONTANA
WYOMING
45°00'
DEEP LAKE
105° 15'

PI

A
Ma
are
Am
rap
the
pin
mu
by
loc
2½
64°
abo
abo
has
abo
Alt
pin
Pre
(W
cat
wa
po
(P
veg
is
of
fra
the
18
of
be
wi
is
on
mo
th
fig
To

Short Notes

BULLETIN OF THE GEOLOGICAL SOCIETY OF AMERICA
VOL. 70, PP. 509-510, 1 PL. APRIL 1959

PINGO IN THE THELON VALLEY, NORTHWEST TERRITORIES; RADIOCARBON AGE AND HISTORICAL SIGNIFICANCE OF THE CONTAINED ORGANIC MATERIAL

BY B. G. CRAIG

Although pingos are common in the Mackenzie Delta, and related smaller features are found elsewhere in northwestern North America (*see* Pihlainen *et al.* 1956, for bibliography), no occurrences have been reported in the interior of the Northwest Territories. A pingo sighted by J. G. Fyles (personal communication) during a flight in 1954 was visited by the writer in 1955. This solitary pingo is located in the District of Mackenzie, about 2½ miles north of the Thelon River at Lat. 64° 19′, Long. 102° 41′.

This feature is a dome-shaped hill rising above an almost flat plain (Pl. 1, fig. 1). It is about 60 feet high and 200 feet in diameter. The base is 395 feet above sea level and 35 feet above the present level of the Thelon River. Although bedrock does not outcrop near the pingo, the area is probably underlain by late Proterozoic sandstone of the Dubawnt Group (Wright, 1957, p. 12–13). Ice-flow features indicate that the direction of last glacier movement was N. 54° W. The pingo occurs in an infilled pond in an old channel of the Thelon River (Pl. 1, fig. 3). The north side is covered with vegetation but the south and southwest side is barren.

The writer was unable to examine the core of the pingo. The top of the feature, however, is fractured and gullied, revealing the structure of the upper few feet (Pl. 1, fig. 2). It comprises 18 inches of structureless silt overlying 3 feet of laminated silt with vegetable remains on the bedding planes and, below, laminated silt without organic remains. The mineral material is mostly of silt size; it contains no sand and only a little clay. It is reddish brown when moist, pinkish buff when dry. From the air this material appears almost white (Pl. 1, fig. 1). Examination of specimens by J. Terasmae of the Geological Survey of Canada revealed that the organic material is largely *Ceratophyllum demersum* L. (Terasmae and Craig, unpublished manuscript) and with a pollen assemblage indicating forest cover, both of which require a warmer climate than that now prevailing in the region. The material has a radiocarbon age of 5500 ± 250 years (L-428).

The age and climatological and ecological significance of the organic material contained in the pingo allow certain conclusions regarding deglaciation of the country between Great Slave Lake and Hudson Bay. Terasmae and Craig state "the presence of *Ceratophyllum* suggests a habitat such as a shallow pond or isolated river channel on a broad flood plain in which silting occurred periodically." The same environment is apparent from observation of the laminated silt and organic layers, which appear to have resulted from repeated spring flooding and burial of the past season's growth, circumstances that prevail at present along the river valley. Deposition probably ceased when the river cut far enough below the level of the channel in which the pingo is situated to prohibit further flooding. The processes resulting in the upheaval of the pingo took place after this.

Neither the pingo nor the silt of which it is composed show any indication of having been overridden by glacial ice. It is located well below the level of the proglacial lake (700 feet above sea level) that occupied the valley of the Thelon River in this region (Craig, *in* Wright, 1957, p. 5; Fyles, *in* Wright, 1955, p. 3). During the final stages of deglaciation the ice damming this lake was in the position of the Keewatin Ice Divide (Lee, Craig, and Fyles, 1957, p. 1760–1761). At this time marine waters from the area of Hudson Bay had submerged much of the land east of the Divide, and along the Baker Lake-Chesterfield Inlet

valley the waters extended inland as far as the Divide. Eventually the remaining ice was breached along this valley, allowing the lake level to drop and marine water to penetrate farther inland. The pingo is only 35 feet above and 60 miles west of a known occurrence of marine shells in the Thelon Valley (Fyles, *in* Wright, 1955, p. 4), and it is possible that the sea extended up to or beyond it. Subsequent lowering of sea level allowed the Thelon River to flow normally, and the conditions for the deposition of the silt and organic material and later the formation of the pingo followed.

It is thus apparent that the area surrounding the pingo was freed of ice considerably more than 5500 years ago, and that the remnant ice along the Keewatin Ice Divide had disappeared or at least shrunken sufficiently by this time to allow the lake in the Thelon Valley to drain. The nature of the organic material associated with the pingo indicates conditions warmer than the present, and its age coincides with that of the postglacial thermal maximum. The formation of the pingo may be due to the marked cooling of climate following this period.

Elsewhere on the mainland of the Northwest Territories organic materials have been found for which radiocarbon ages have been determined (Preston *et al.*, 1955, p. 959), sample Y-261 from the Back River at 4140 ± 150 years, and sample Y-231 from Rankin Inlet at 5220 ± 340 years. At both sites the organic material is reported to be overlain by deposits from subsequent glaciation. This is incompatible with the writer's interpretation of the organic material found in the pingo. These two samples are about the same distance from the Keewatin Ice Divide as is the pingo sample; Y-261 lies northwest of the Divide, and Y-231 southeast. If glacial ice had advanced over one or both of these sites it would almost certainly have dammed the Thelon Valley, flooding the pingo site and probably overriding the area. There is no evidence of such glacial action or lake expansion.

At the Back River locality neither the deposits enclosing the dated peat (Taylor, 1956, p. 949–950, 954) nor the geomorphology of the site as evident in aerial photographs require the presence or proximity of glacial ice following deposition of the peat. Thus, the whole section enclosing the peat may well have resulted from nonglacial fluctuations of the Back River and its tributaries, possibly complicated by ponding by the esker dam a mile downstream, and by blocking of the river by slides of the esker material. There is no need for the silty sands covering the peat-bearing sandy silts to be primary esker deposits nor for the esker to postdate the peat.

With regard to the Rankin Inlet locality Lee (in press) points out that this site was 600 feet under the sea during deglaciation and that the peat "could not have started to form until sometime after the withdrawal of the sea from the vicinity." A glacier readvance of some magnitude would be necessary for deposition of 3–4 feet of till, and Lee found no evidence for such an advance. In explanation he suggests "the position of the till over peat was caused by frost action, with either the till rising and spreading over the peat, or the peat moving downwards or being buried as the whole mass slowly flowed."

References Cited

Lee, H. A., in press, Surficial geology of southern District of Keewatin and the Keewatin Ice Divide, Northwest Territories: Geol. Survey Canada Bull.

Lee, H. A., Craig, B. G., and Fyles, J. G., 1957, Keewatin Ice Divide (Abstract): Geol. Soc. America Bull., v. 68, p. 1760–1761

Pihlainen, J. A., Brown, R. J. E., and Legget, R. F., 1956, Pingo in the Mackenzie Delta, Northwest Territories, Canada: Geol. Soc. America Bull., v. 67, p. 1119–1122

Preston, R. S., Person, Elaine, and Deevey, E. S., 1955, Yale natural radiocarbon measurements II: Science, v. 122, p. 954–960

Taylor, R. S., 1956, Glacial geology of north-central Keewatin, Northwest Territories, Canada: Geol. Soc. America Bull., v. 67, p. 943–956

Wright, G. M., 1955, Geological notes on central District of Keewatin, Northwest Territories: Geol. Survey Canada Paper 55-17, 17 p.

—— 1957, Geological notes on eastern District of Mackenzie, Northwest Territories: Geol. Survey Canada Paper 56-10, 23 p.

Geological Survey of Canada, Ottawa, Ontario, Canada

Manuscript Received by the Secretary of the Society, June 2, 1958

Published by Permission of the Director, Geological Survey of Canada

Plate 1.—PINGO IN THELON VALLEY, NORTHWEST TERRITORIES

Figure 1.—Oblique aerial view of pingo, looking northeast

Figure 2.—Internal structure of upper part of pingo

Figure 3.—Aerial photograph of pingo and surrounding terrain (Department of Mines and Technical Surveys photo A 14908-47)

FIGURE 1

FIGURE 2

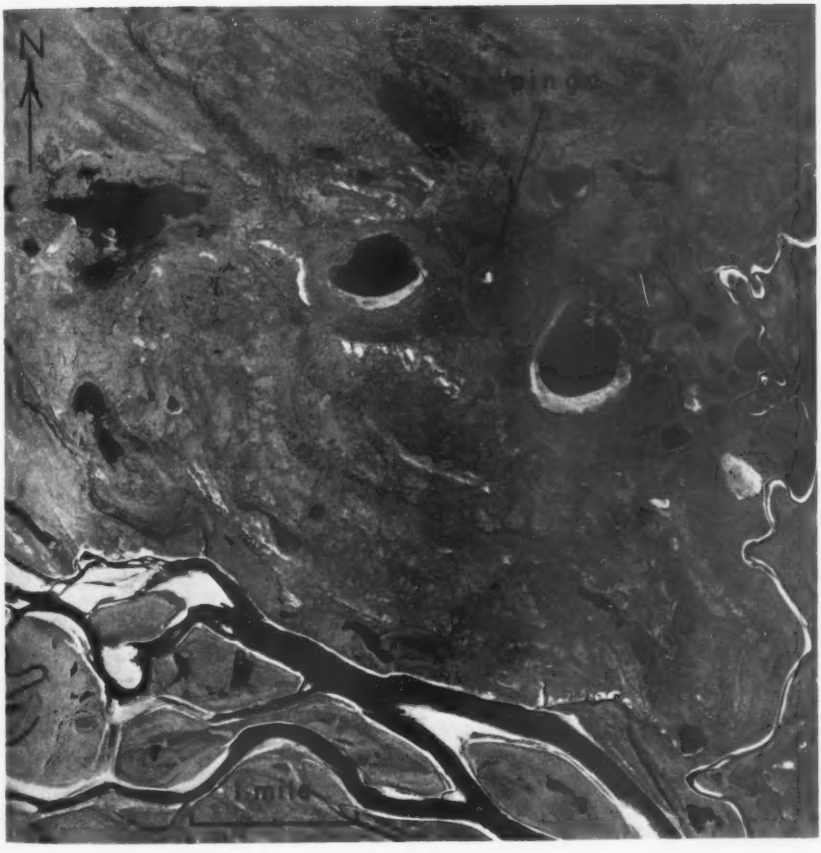

FIGURE 3

PINGO IN THELON VALLEY, NORTHWEST TERRITORIES